Ectopic expression of transcription factors to overcome the lineage barrier between embryonic stem cells and trophoblast stem cells in mouse and human

Dissertation

zur

Erlangung des Doktorgrades (Dr. rer. nat.)

der

Mathematisch-Naturwissenschaftlichen Fakultät

der

Rheinischen Friedrich-Wilhelms-Universität Bonn

vorgelegt von

Franziska Kaiser

aus

Celle

Bonn, 2022

Angefertigt mit Genehmigung der Mathematisch-Naturwissenschaftlichen Fakultät
der Rheinischen Friedrich-Wilhelms-Universität Bonn

Gutachter: Prof. Dr. Hubert Schorle
Gutachterin: Prof. Dr. Marieta Toma

Tag der Promotion: 06.02.2023
Erscheinungsjahr: 2023

Teile dieser Arbeit wurden bereits in folgenden Originalpublikationen veröffentlicht:

Franziska Kaiser, Caroline Kubaczka, Monika Graf, Nina Langer, Jan Langkabel, Lena Arévalo, and Hubert Schorle. “Choice of Factors and Medium Impinge on Success of ESC to TSC Conversion.” Placenta 90, 128-137, 2020, https://doi.org/10.1016/j.placenta.2019.12.017

Franziska Kaiser, Julia Hartweg, Selina Jansky, Natalie Pelusi, Carolina Kubaczka, Neha Sharma, Dominik Nitsche, Jan Langkabel and Hubert Schorle. “Persistent human KIT receptor signaling disposes murine placenta to premature differentiation resulting in severely disrupted placental structure and functionality.” International Journal of Molecular Sciences 21, 5503, 2020, https://doi.org/10.3390/ijms21155503

List of Abbreviations

Abbreviation	
2i	MEK + GSK3β inhibitors
2iL	2i + LIF
5HmC	5-hydroxymethylcytosine 5HmC
5iLAF	MEK, GSK3, ROCK, BRAF, and SRC pathway inhibitors in combination with LIF, Activin and FGF2
5mC	5-methylcytosine
AKT	Protein Kinase B
Ascl2	Achaete-scute complex homolog 2
BAP	BMP4 in combination with inhibitors A83-01 and PD173074 (BMP4/A/P condition)
BCA	Bicinchoninic acid
BMP	Bone morphogenetic protein
bp	Base pair
BRAF	V-raf murine sarcoma viral oncogene homolog B1
BSA	Bovine serum albumin
c-Myc	Cellular myelocytomatosis oncogene
C-TGC	Canal-TGC
cAMP	Cycling adenosine 3',5'-cyclic monophosphate
Cas9	CRISPR associated protein 9
Cdx2	Caudal type homeobox 2
CGI	CpG island
CM	MEF conditioned medium
CpG	Cytosine-phosphate-guanine dinucleotide
Cre	Cre (Causes recombination) recombinase
CRISPR	Clustered Regularly Interspaced Short Palindromic Repeats
Ct	Cycle threshold
CTB	Cytotrophoblast
Ctsq	Cathepsin Q

D816V	Substitution of the aspartic acid position at position 816 with a valine
DEPC	Diethylpyrocarbonate
DiM	(S)-(+)-dimethindene maleate
DMEM	Dulbecco's modified Eagle's medium
DMR	Differentially methylated region
DMSO	Dimethylsulfoxide
DNA	Deoxyribonucleic acid
DNMT	DNA methyltransferase
dNTP	Deoxyribonucleoside triphosphate
dox	Doxycycline
E	Embryonic day
E. coli	*Escherichia coli*
e.g.	For example
EAA	Essential amino acids
EGF	Epidermal growth factor
EGFP	Enhanced green fluorescent protein
Elf5	E74-like factor 5
Eomes	Eomesodermin homolog
EPC	Ectoplacental cone
Epi	Epiblast
EpiSC	Epiblast-derived stem cell
Erk1/2	Extracellular signal-regulated kinase 1⁄2
ESC	Embryonic stem cell (murine)
Esrrb	Estrogen related receptor beta
et al.	And others
EtOH	Ethanol
Ets2	E26 avian leukemia oncogene 2, 3' domain
EVT	Extravillous cytotrophoblast
ExE	Extra-embryonic ectoderm
FACS	Fluorescence activated cell sorting
FBS	Fetal bovine serum
FGF	Fibroblast growth factor
FGFR	Fibroblast growth factor receptor
Gapdh	Glyceraldehyde-3-phosphate dehydrogenase

Gata3	GATA binding protein 3
Gcm1	Glial cells missing homolog 1
gDNA	Genomic DNA
Gjb3	Gap junction beta-3 protein
GlyT	Glycogen trophoblast
GSK3	Glycogen synthase kinase-3
Gö6983	PKC inhibitor
h	Hour(s)
h	Human
Hand1	Heart and neural crest derivatives expressed 1
hCG	human chorionic gonadotropin
hcTSC	Human converted TSC
hEPSC	Human extended hiPSC
hESC	Human ESC
hiPSC	Human induced pluripotent stem cell
hiTSC	Human induced TSC
hNPSC	Human naïve PSC
hPSC	Human pluripotent stem cells
HSC	Hematopoietic stem cells
hTSC	Human TSC
ICM	Inner cell mass
iPSC	Induced pluripotent stem cell
iTSC	Induced trophoblast stem cell
JAK	Janus Kinase
kb	Kilo base pairs
kD	Kilodalton
Klf4	Kruppel-like factor 4
KRT7	Keratin 7
KSR	Knockout Serum Replacement
L-Glu	L-glutamine
LIF	Leukemia inhibitory factor
m	Murine
MAPK	Mitogen-activated protein kinase
MEF	Murine embryonic fibroblast
MEK	MAPK/ERK kinase

MeOH	Methanol
MiH	Minocycline hydrochloride
min	Minute
ml	Milliliter
mm	Millimeter
mRNA	Messenger RNA
NaAc	Sodium acetate
NEAA	Non-essential amino acids
ng	Nanogramm
nM	Nanomolar
Nrg1	Neuregulin 1
ON	Overnight
OSKM	Reprogramming transcription factors Oct4, Sox2, Klf4 and Myc
p	Passage
P-TGC	Parietal-TGC
PBS	Phosphate buffered saline
PBST	Phosphate buffered saline with Tween-20
Pcdh12	Protocadherin 12
PCR	Polymerase chain reaction
PE	Primitive endoderm
Pen/Strep	Penicillin/Streptomycin
PFA	Paraformaldehyde
PGC	Primordial germ cell
Pgk1	Phosphoglycerate kinase 1
PI3K	Phosphoinositide 3-kinase
PKC	Protein kinase C
Pou5f1 (Oct4)	POU domain, class 5, transcription factor 1
Prl2c2/Pfl	Prolactin family 2, subfamily c, member 2
Prl3b1/Pl2	Prolactin family 3, subfamily b, member 1
Prl3d1/Pl1	Prolactin family 3, subfamily d, member 1
PS	Primitive syncytium
RA	Retinoic acid
RAR	Retinoic acid receptor
RIPA	Radio Immuno Precipitation Assay buffer
RNA	Ribonucleic acid

RNAi	RNA-interference
ROCK	Rho kinase
rpm	Rotations per minute
RPMI	Roswell Park Memorial Institute medium
RT	Room temperature
rtTA	Reverse tetracycline transactivator
s	Second
S-TGC	Sinusoidal TGC
SCF	Stem cell factor
Scml2	Scm polycomb group protein like 2
SFCA	Surfactant-free cellulose acetate
SOCS3	Suppressor of cytokine signaling 3
Sox2	SRY-box 2
SpA-TGC	Spiral Artery-TGC
SRY	Sex determining region Y
STAT3	Signal transducers and activators of transcription 3
STB	Syncytiotrophoblast
t2iLGöY	Titrated 2i, LIF, Gö6983, Y-27632
TBS	Tris buffered saline
TBST	Tris buffered saline with Tween-20
TE	Trophectoderm
Tead4	TEA domain family member 4
TET	Ten eleven translocation dioxygenases
TetO	Tet operon
TETRA	Trophectoderm four factors
TF	Transcription factor
Tfap2a	Transcription factor AP-2, alpha
Tfap2c	Transcription factor AP-2, gamma
TGC	Trophoblast giant cell
TGFβ1	Transforming growth factor beta
Tpbpa	Trophoblast specific protein alpha
TSC	Trophoblast stem cell (murine)
TX	Chemically defined TSC medium
V	Volt
Wnt	Wingless/Integrated

WT	Wild type
w/o	without
XEN	Extra-embryonic endoderm stem cells
Y-27632	ROCK inhibitor
YAP	Yes-associated protein 1
γMEFs	Mitotically inactivated murine embryonic fibroblasts by gamma irradiation
ΔCt	Delta cycle threshold; subtraction of Ct (reference gene) from Ct (sample)
µg	Microgramm
µl	Microliter
µM	Micromolar
µm	Micrometer

Table of Contents

List of Figures

List of Tables

1 Summary

The placenta is a transient organ that exhibits various essential functions during pregnancy that allow for proper development of the embryo. Placenta and embryo originate from the first lineage separation in mammalian development when totipotent cells of the zygote differentiate into inner cell mass, trophectoderm and primitive endoderm. The trophectoderm gives rise to the embryonic part of the placenta whereas the inner cell mass will develop into the embryo. This study focuses on the so-called trophoblast stem cells that can be derived from the trophectoderm and are studied as its *in vitro* equivalents. They are strictly separated from embryonic stem cells that can be derived from the inner cell mass. Even though there are several differences between murine and human placental development, which will also be highlighted in the course of this study, the murine prenatal development can be studied as an appropriate approximation to human development.

Here, it is first assessed how murine embryonic stem cells can be fully converted to trophoblast stem cells by ectopically overexpressing trophoblast specific transcription factors which are incorporated into the genome by lentiviral transduction. Obtained induced trophoblast stem cells are indistinguishable from wildtype trophoblast stem cells in terms of morphology, gene expression, cell surface markers and specific epigenetic patterns when transgene expression of *Gata3*, *Eomes*, *Tfap2c*, *Ets2* and *Cdx2* is activated for three days in embryonic stem cells.

After demonstrating a complete cell fate change in murine stem cells, this approach is extended to the respective human system. For ethical reasons, conversion experiments are performed with human induced pluripotent stem cells instead of human embryonic stem cells. Human induced pluripotent stem cells are transduced with different combinations of lentiviruses carrying human trophoblast specific transcription factors. An initial induction of trophoblast fate is detectable, when *TFAP2C*, *TFAP2A*, *GATA2* and *GATA3* are overexpressed in human induced pluripotent stem cells.

Interestingly, trophoblast fate is not only controlled by distinct transcription factor networks but also by important signaling pathways such as KIT receptor signaling. To this end, this study can show that constitutively active KIT signaling results in increased invasive capacity of trophoblast giant cells and irregular differentiation of trophoblast stem cells. In conclusion, it can be demonstrated that placental development is relying on strictly regulated mechanisms, where any errors occurring in development can lead to adverse effects for the unborn fetus.

2 Introduction

The placenta is emerging in parallel to the embryo, with their development starting as early as the beginning of the pregnancy. While the importance of the organ might easily be underestimated due to its transient presence, it is fulfilling an indispensable function during its short period of existence. This highly specialized organ represents the unique source for nourishment of the embryo throughout the pregnancy. It is responsible for preparing the maternal body for implantation and adaption of the maternal immune system. Also, it efficiently keeps harmful substances away from the fetus (Burton and Jauniaux, 2015; Burton et al., 2016; Knöfler et al., 2019). While the organ itself offers a variety of different interesting research fields, this study focuses on the stem cells that can be derived from early stages of the placenta. Stem cell research has been continuously growing, fostering the hope of eventual stem cell-based therapies for various severe diseases or insufficiencies that remain untreatable until now (Yamanaka, 2020).

2.1 First lineage separation in mammalian pre-implantation development

Mammalian development is initiated by the fertilization of an oocyte by a sperm cell. Subsequent cell divisions of the totipotent zygote give rise to uniform blastomeres and ultimately result in formation of the morula at embryonic day (E)2.5 (Figure 1) (Cockburn and Rossant, 2010). At this stage, the inner and outer blastomeres gain diverging characteristics (Cockburn and Rossant, 2010). This development is directed by Hippo signaling which is only activated in inner non-polar cells due to increased cell-cell adhesions. By contrast, it is inactivated in outer polar cells resulting in the initiation of a trophoblast specific transcription factor (TF) network which will be described in detail in the following chapter (Latos and Hemberger, 2013, 2016; Nishioka et al., 2009). This important first separation into different lineages in pre-implantation development is finalized at the early blastocyst stage yielding the inner cell mass (ICM) and trophectoderm (TE) (Figure 1) (Cockburn and Rossant, 2010). The ICM consists of pluripotent cells and gives rise to the epiblast (Epi) which develops to the embryo proper and the primitive endoderm (PE) between E3.5 and E4.5 (Cockburn and Rossant, 2010). The PE later forms the yolk sac tissue. The TE envelops the epiblast and the blastocoel and will later form the embryonic part of the placenta. The epiblast is lined by the PE towards the blastocoel (Cockburn and Rossant, 2010; Latos and Hemberger, 2016). Stem cells can be derived from each of these tissue lineages and cultured *in vitro* indefinitely equivalent to their respective tissue, representing a useful tool to study early embryonic development. In mice, the ICM gives rise to embryonic stem cells (ESC), trophoblast stem cells (TSC) originate from the TE and extra-embryonic endoderm stem cells (XEN) can be derived from the PE (Evans and Kaufman, 1981; Niakan et al., 2013; Tanaka et al., 1998).

ESCs, TSCs and XEN cells exhibit stem cell characteristics such as indefinite self-renewal, proliferation and they can differentiate along their cell lineage *in vitro* (Evans and Kaufman, 1981; Niakan et al., 2013; Tanaka et al., 1998). These stem cell lineages are maintained by distinct epigenetic and transcription factor-controlled mechanisms thereby establishing the so-called lineage barrier which strictly prevents spontaneous differentiation between emerged lineages to maintain proper development of respective tissues (Hemberger et al., 2009; Ng et al., 2008; Rugg-Gunn et al., 2010; Senner et al., 2012). In murine development, the blastocyst implantation occurs on E4.5 and on E7-9 in human development (Hemberger et al., 2020). All three parts of this study revolve around murine and human TSCs which will therefore be presented in detail in the following paragraphs.

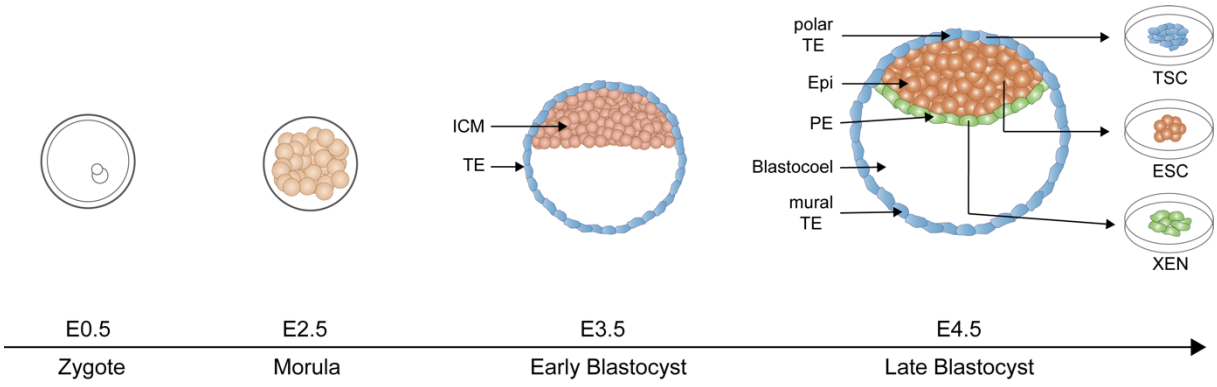

Figure 1: Murine preimplantation development from zygote to blastocyst
After fertilization of the oocyte, several subsequent cell divisions result in formation of the morula which further develops into the blastocyst at E3.5 in murine and at E5 in human development. It represents the first separation into three different lineages: trophectoderm (blue), epiblast (orange) and extra-embryonic ectoderm (green). Self-renewing stem cell lines can be derived from all three tissues: ICM gives rise to ESCs, primitive endoderm to XEN cells and polar TE to TSCs. TE=trophectoderm, PE=primitive endoderm, ICM=inner cell mass, Epi=epiblast, TSC=trophoblast stem cell, ESC=embryonic stem cell, XEN cell=extraembryonic endoderm stem cell. Modified from Cockburn and Rossant, 2010 and Kubaczka et al., 2016.

2.2 Post-implantation development of murine and human placentas

The placenta is a transient organ which is unique to mammals. It is best studied in mice as ethical limitations restrict research on early human placentas (Lee et al., 2016). In general, placental functions include attachment of the developing embryo to the uterine wall by invading into maternal tissue, remodeling maternal vasculature to supply the embryo with gases and nutrients in exchange for fetal waste products as well as hormone and cytokine secretion (Burton and Jauniaux, 2015; Knöfler et al., 2019). Thus, the placenta establishes maternal adaptation to pregnancy, protects the embryo from an immune reaction of the mother and ensures the essential interaction between mother and fetus. Correct placental development is vital for successful upbringing of the fetus (Burton and Fowden, 2015; Burton et al., 2016). Aberrant placental development or function results in severe pregnancy complications such as fetal growth restriction, pre-eclampsia, preterm birth or even intrauterine death and miscarriage

(Hemberger et al., 2020; Knöfler et al., 2019). The placenta is made up of highly specialized cell types, each of which is undertaking coordinated and specific parts of placental function (Simmons and Cross, 2005; Simmons et al., 2007). Mice and humans exhibit a hemochorial placental structure which is characterized by trophoblast villi that are in direct contact with maternal blood. Even though they harbor differences in morphology and development, murine placental development remains the best approximation to human development (Hemberger et al., 2020).

In murine placental development, the late blastocyst at E4.5 consists of the three distinct lineages Epi, TE and PE (Figure 1 and Figure 2). TE cells overlying the ICM are called polar TE, while the mural TE surrounds the blastocoel (Latos and Hemberger, 2016). The mural trophectoderm ceases proliferation and starts to endoreduplicate, thereby giving rise to the primary population of TGCs (Rossant and Cross, 2001; Simmons and Cross, 2005). In a TGC mediated process, the blastocyst implants to the uterine wall around E4.5-E5.5. At the same time, hormone mediated decidualization of maternal endometrial stromal cells takes place (Latos and Hemberger, 2016; McDole et al., 2011). The polar trophectoderm which is directly in contact with the ICM continues proliferating and forms the extra-embryonic ectoderm (ExE) around E6.5 and the ectoplacental cone (EPC) (Figure 2) (Hemberger et al., 2020). At this timepoint, TSCs can be found in the ExE and polar trophectoderm (Hemberger et al., 2020). Gastrulation starts at E6.5 resulting in formation of chorion, allantois, and amnion. The epiblast gives rise to the extra-embryonic mesoderm – allantois as well as mesodermal layers of amnion and chorion are formed thereof (Hemberger et al., 2020).

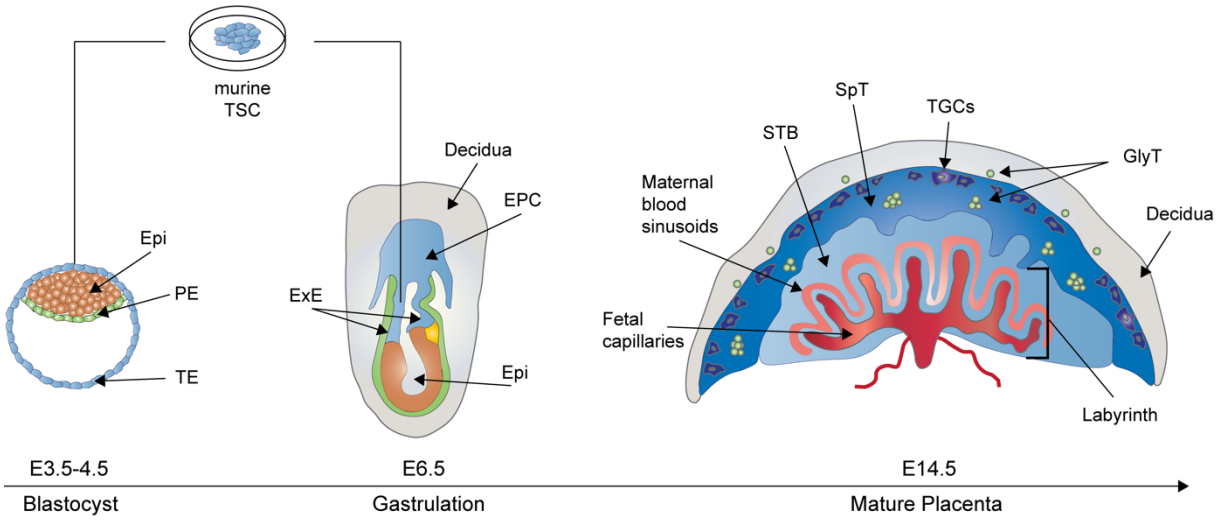

Figure 2: Structural development of the murine placenta
At the late blastocyst stage, the ICM already developed into epiblast and primitive endoderm. During the following days, polar trophectoderm develops into EPC and ExE. Murine TSC can be derived from the blastocyst or the ExE of the conceptus around E6.5. The mature placenta at E14.5 is characterized by fetal blood capillaries that are bathing in maternal blood sinusoids in the labyrinth which also comprises the STB. The labyrinthine structure is surrounded by a SpT layer which is lined by TGCs towards the maternal decidua. GlyT cells can be found in the SpT and the decidua close to the placenta. Epi=epiblast, PE=primitive endoderm, TE=trophectoderm, TSC=trophoblast stem cells, EPC=ectoplacental cone, ExE= extraembryonic ectoderm, STB=syncytiotrophoblast, SpT=spongiotrophoblast, TGC=trophoblast giant cells, GlyT=glycogen trophoblast cells. Modified from Hemberger et al., 2020.

Around E8.5, the chorioallantoic fusion takes place when allantois and chorion are attaching, thereby building the early placenta (Hemberger et al., 2020). Fetal blood vessels expanding from allantois into chorionic layer and subsequent villous branching yield the placental labyrinth (Hemberger et al., 2020; Latos and Hemberger, 2016). The labyrinth develops further from E10 to E14.5 and eventually consists of two layers of syncytiotrophoblast which result from fusion of chorionic trophoblast cells. Syncytiotrophoblasts represent the greatest area for exchange between maternal and fetal blood (Hemberger et al., 2020; Latos and Hemberger, 2016). The spongiotrophoblast derives from the ectoplacental cone, consists of non-syncytial cells, and is situated between labyrinth and giant cells (Rossant and Cross, 2001). The maternal blood flows through the spongiotrophoblast to the labyrinthine spaces. There, trophoblast villi end in the maternal blood for exchange of nutrients, gases, and waste (Rossant and Cross, 2001). The embryo is then nurtured by the enriched fetal blood through the umbilical cord (Hemberger et al., 2020; Rossant and Cross, 2001). Ultimately, at E14.5, the mature placenta can be distinguished in three layers which comprise the labyrinth, the junctional zone, and the parietal (P-) TGC layer in order from embryo to mother (Latos and Hemberger, 2016). The P-TGC layer stretches along the implantation site and is in direct contact with the decidua (Hemberger et al., 2020; Latos and Hemberger, 2016). The labyrinth itself comprises three different cell types: sinusoidal TGCs (S-TGC) are lining the maternal blood sinusoids, followed by syncytiotrophoblast I and syncytiotrophoblast II layers (Latos and Hemberger, 2016). Finally, there is the fetal vasculature consisting of endothelial cells facing the fetal blood (Simmons and Cross, 2005). The junctional zone represents the middle layer and provides structural support to the labyrinth (Simmons and Cross, 2005). It is made up of spongiotrophoblast and glycogen cells. Importantly, these two cell types in combination with TGCs fulfil the endocrine function of the placenta (Hemberger et al., 2020). Glycogen trophoblast cells share characteristics with TGCs and spongiotrophoblast while still being a unique cell type (Simmons and Cross, 2005).

Development of the human placenta was researched in animal models as well as by studying the Boyd Collection (Centre of Trophoblast Research, Cambridge) and the Carnegie Collection (Human Developmental Anatomy Center, Washington DC) which consist of conserved hysterectomy samples including early implantation sites (Hamilton and Boyd, 1960; Hertig et al., 1956; Knöfler et al., 2019). While morphology of the early development in mouse and human is very comparable until the blastocyst stage, differences start arising with implantation (Hemberger et al., 2020). In human placental development, the TE develops four to five days post fertilization. In contrast to the mouse, it is the polar TE and not the mural TE that gets into contact with maternal tissue and implants in uterine epithelium on E6-E7 (Hemberger et al., 2020; Knöfler et al., 2019). Next, early cytotrophoblasts (CTB) surrounded by multinucleated

primitive syncytium (PS) arise (Figure 3). Importantly, the PS represents the first human invasive cell type and was shown to secrete enzymes that enable further invasion into the maternal decidua (Hemberger et al., 2020). Ultimately, the human placenta consists of three main trophoblast cell populations that comprise the CTBs, the extravillous cytotrophoblasts (EVT) and the syncytiotrophoblasts (STB) (Hemberger et al., 2020). The placenta specializes into a finger-like structure called chorionic villi which have an epiblast-derived mesenchymal core covered by villous CTB layer and outer STB layer with the tips being made up of CTB cells (Hemberger et al., 2020). The villi extend into the blood-filled intervillous space to bath in maternal blood (Figure 3) (Hemberger et al., 2020). Starting from the tenth to twelfth week of pregnancy, maternal blood flows from maternal arteries through the intervillous space back to maternal vessels whereas the fetal blood arrives via umbilical cord in capillaries of the chorionic villi and travels back through the umbilical veins (Dellschaft et al., 2020; Hemberger et al., 2020; Knöfler et al., 2019).

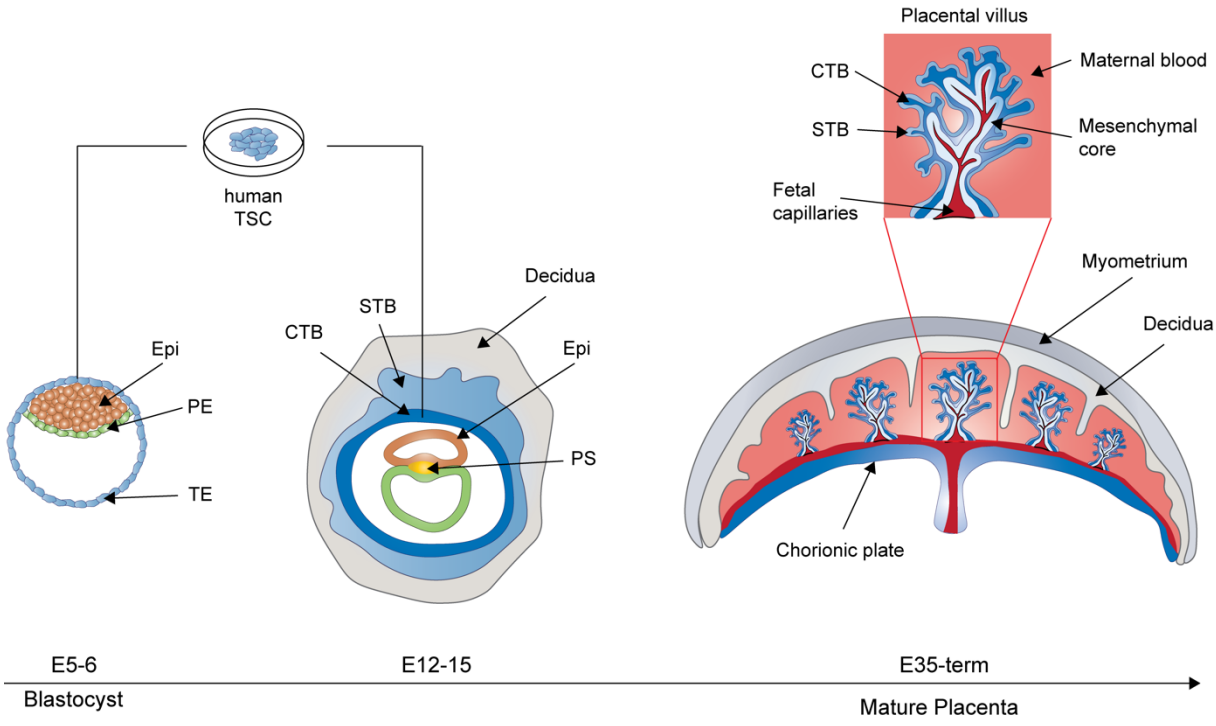

Figure 3: Structural development of the human placenta
After implantation of the blastocyst consisting of Epi, PE, and TE, the outer layer of STB invades into the maternal decidua. An inner layer of CTBs which are proliferating is enclosed by a STB layer around E12. The mature placenta exists from E35 onwards. At that stage, chorionic villi are properly formed. They contain a mesenchymal core that surrounds the fetal blood vessels. The mesenchymal core is encompassed by a layer of CTBs followed by an outer layer of STBs. These villi bath in maternal blood, thereby maintaining exchange of nutrients and gases between maternal and fetal circulation. Human TSC can be derived from the blastocyst or first-trimester placentas (Epi=epiblast, PE=primitive endoderm, TE=trophectoderm, STB=syncytiotrophoblast, CTB=cytotrophoblast, PS=primitive streak, TSC=trophoblast stem cells). Modified from Hemberger et al., 2020.

The CTB is suggested to harbor the human TSC (hTSC) population during the first trimester of pregnancy (Knöfler et al., 2019). The CTB cells proliferate and retain an undifferentiated state, however, hold the capacity to differentiate into EVT and STB (Knöfler et al., 2019). EVT cells can be divided into interstitial EVT and endovascular EVT cells. Interstitial EVT cells invade into the maternal decidua and modulate the maternal immune response to the placenta by interaction with macrophages and uterine natural killer cells (Knöfler et al., 2019). Interstitial EVT cells can differentiate into endovascular EVT cells which are responsible for remodeling of maternal spiral arteries by replacing maternal endothelial cells and inducing apoptosis in smooth muscle cells of the vessel (Knöfler et al., 2019). Fusion, differentiation, and asymmetrical cell division of villous CTB cells results in multinucleated STB cells which are important secretors of placental hormones such as human chorionic gonadotropin (hCG) and placental lactogen. They are in direct contact with maternal blood, thereby providing the surface for exchange of gases and nutrients (Knöfler et al., 2019; Turco and Moffett, 2019).

2.3 Establishment of TSC murine and human transcription factor network

Distinct transcription factor networks consisting of self-reinforcing mechanisms are essential for upholding the stem cell state of ESCs and TSCs (Hemberger et al., 2020; Senner and Hemberger, 2010). These circuits are characterized by a synchronized hierarchy of different transcriptions factors. The presence of these factors depends on the developmental stage, and changes in the course from stem cell maintenance to initiation of differentiation. Both networks are also characterized by comprising antagonistic factors OCT4 or CDX2. Murine and human TSC transcription factor networks will be described in detail in the following paragraph (Hemberger et al., 2020; Kidder and Palmer, 2010; Senner and Hemberger, 2010).

The murine TSC transcription factor network includes the transcription factors ELF5, CDX2, EOMES, GATA3 and ESRRB and is essential for keeping TSCs in an undifferentiated state (Figure 4). Depletion of any of these factors results in developmental abnormalities and even arrest at very early stages indicating the role they play in TSC self-renewal, stem cell maintenance and placental development (Kidder and Palmer, 2010). Interestingly, those transcription factors are not unique to the trophoblast fate, but also play roles in other cell lineages. The combination, however, is unique to the trophoblast (Hemberger et al., 2020).
Due to the previously described HIPPO signaling, localization information is processed and translated into transcriptional adjustments. The transcriptional coactivator yes-associated protein 1 (YAP1) remains in the cytoplasm of inner cells of the morula due to being phosphorylated by HIPPO component LATS1/2 (Nishioka et al., 2009). In polar outer cells, YAP1 is translocated to the nucleus and forms a complex in combination with TEAD/TEF family member TEAD4 resulting in the initiation of the TSC specific transcription factor network

(Home et al., 2012; Nishioka et al., 2008, 2009; Yagi et al., 2007). Knock-down of TEAD4 results in decreased self-renewal of TSCs and affects development of the placenta, TEAD4-/- embryos do not form a blastocoel and die at the pre-implantation stage (Nishioka et al., 2008; Saha et al., 2020). Primarily, the TEAD4/YAP1 complex drives the expression of *Cdx2* (Nishioka et al., 2008; Yagi et al., 2007). CDX2 is regarded as determining factor of trophoblast fate, as it is no longer found in non-TE cells while TEAD4 is still present in all cells at morula stage. Restricted to outer cells of the blastocyst, CDX2 causes downregulation of *Oct4*. In inner, apolar cells without *Cdx2* expression, OCT4 levels and pluripotency remain high (Hemberger et al., 2020). *Cdx2* is expressed in the TSC state, and it is capable of inducing its own expression, but is downregulated with ongoing differentiation. Maternal-zygotic knockout of CDX2 results in cell death and failure of TE development starting already at the morula stage (Jedrusik et al., 2015; Niwa et al., 2005). CDX2 was shown to act upstream of TFAP2C, ETS2 and EOMES in the TF network (Beck et al., 1995; Niwa et al., 2005). Additionally, TEAD4 activates GATA3 which is acting in parallel of CDX2 (Ralston et al., 2010). Interestingly, GATA3 plays an important role in maintaining the stem cell state as well as during differentiation. Depletion of GATA3 causes developmental inhibition at the morula to blastocyst stage (Home et al., 2009). EOMES is detected in the TE starting from E3.5 (McConnell et al., 2005; Russ et al., 2000). Embryos without *Eomes* expression present with a developmental arrest at the blastocyst stage (Russ et al., 2000). EOMES itself goes on to activate the TSC transcription factor TFAP2C. Loss of TFAP2C results in embryonic death around E7-E9 and decreased *Cdx2* expression (Cao et al., 2015; Werling and Schorle, 2002). Both EOMES and TFAP2C were shown to be essential for TSC self-renewal as well as for the expression of TSC enriched genes and can reinforce their own expression in a positive feedback loop by self-promoter binding (Kidder and Palmer, 2010). ELF5 belongs to the ETS-family of transcription factors and is regarded as the TSC fate gatekeeper (Hemberger et al., 2009). In an undifferentiated state, ELF5 builds a complex with EOMES. This transcription factor complex binds to trophoblast self-renewal genes (Figure 4). Once differentiation is induced, TFAP2C levels rise above EOMES levels and ELF5 forms a complex with TFAP2C, now binding to differentiation-promoting genes (Hemberger et al., 2020). SOX2 and ESRRB represent exceptional roles as both factors are essential for ESC and TSC maintenance (Latos et al., 2015a). Placental development of embryos with ESRRB deficiency is distinguished by increased presence of giant cells as well as an irregular chorion layer and embryos die before E10.5 (Latos et al., 2015b; Luo et al., 1997). ESRRB has the capacity to activate TSC specific genes *Elf5*, *Eomes*, *Sox* and *Ets2* (Latos et al., 2015a). ETS2 is also part of the ETS family of transcription factors. Knock-out of ETS2 was shown to cause loss of self-renewal and increase in TSC differentiation. ETS2 is also required for maintaining the expression of *Cdx2* and *Esrrb* (Kidder and Palmer, 2010; Odiatis and Georgiades, 2010; Wen et al., 2007). It also plays an

important role during differentiation. Among others, it is essential for *Hand1* expression and therefore TGC derivation (Odiatis and Georgiades, 2010).

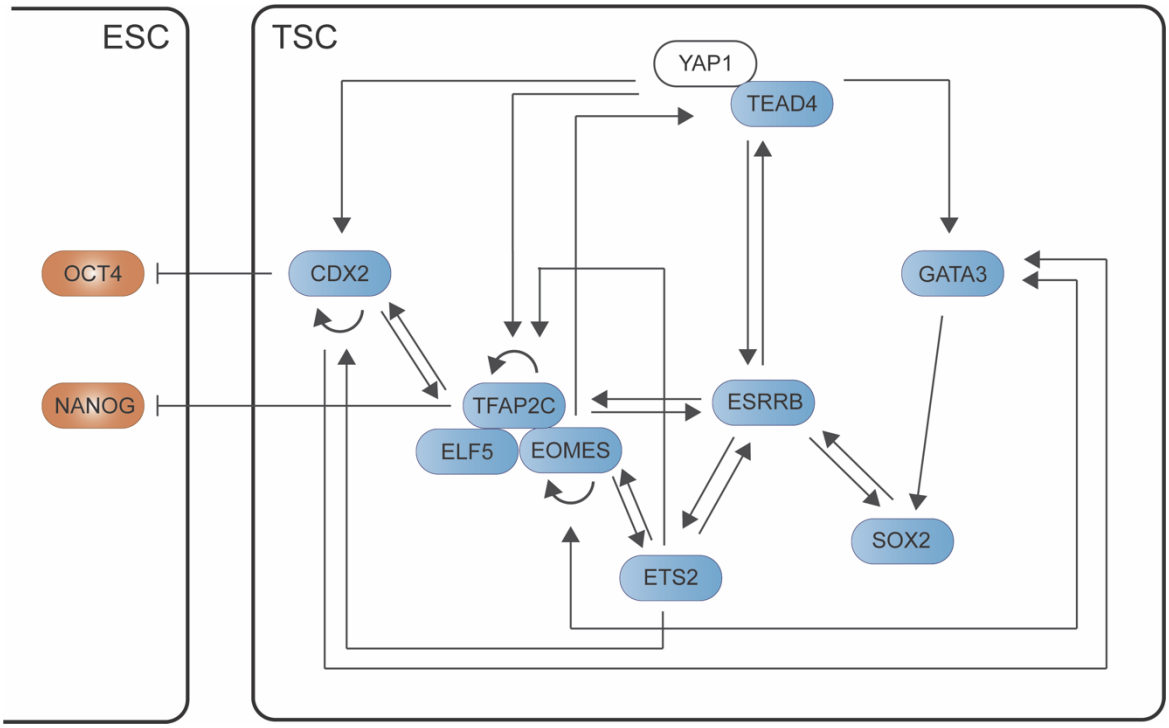

Figure 4: Transcription factor network in undifferentiated murine TSC
Schematic showing transcription factor network in TSC. When TSC are maintained in an undifferentiated state, TEAD4 activates *Cdx2* and *Gata3* expression. ELF5, EOMES and TFAP2C build a complex that is binding to trophoblast renewal genes. This complex is also activated by TEAD4. Downstream of CDX2 and GATA3 also ESRRB, SOX2 and ETS2 are activated. Modified from Hemberger et al., 2020 and Kubaczka et al., 2016.

The transcription factor network in human TE holds several similarities as well as discrepancies to the murine system (Hemberger et al., 2020). Recently, it was successfully shown that the presence of TEAD4 and YAP is essential for proper development comparable to the murine system (Home et al., 2012; Meinhardt et al., 2020; Saha et al., 2020; Soncin and Parast, 2020). It was demonstrated that the TEAD4/YAP1 complex is activating stemness-, proliferation- and cell cycle-genes in primary villous CTBs while at the same time inhibiting genes associated with cell fusion and STB formation (Meinhardt et al., 2020). Of note, a subgroup of hTSCs isolated from placentas of patients suffering from idiopathic recurrent pregnancy losses expressed low levels of TEAD4, showed increased differentiation and reduced proliferation (Saha et al., 2020). By ectopically expressing TEAD4 in these hTSCs, the effect could be rescued, thereby linking adverse TEAD4 expression directly to clinical pathologies (Saha et al., 2020). In early first-trimester placentas, *CDX2* is highly expressed in villous CTB cells, but with ongoing development, its expression decreases quickly with *CDX2* being undetectable with the 20th week of pregnancy (Hemberger et al., 2020). Comparable to murine TE, human TE relies on expression of *CDX2* as a counterpart to *OCT4* expression in the ICM (Hemberger et al., 2020). Also in the human system, TFAP2C is an essential mediator

of trophectoderm development. Interestingly, *TFAP2C* is also expressed in the ICM and epiblast of humans and is involved in maintaining naïve hESC stem cell state which might contribute to lineage plasticity in those cells (Cao et al., 2015; Guo et al., 2021; Pastor et al., 2018). Moreover, GATA2 and GATA3 were identified as core regulators of human TSC fate and *GATA2* mRNA was found to be decreased in women disposed to preeclampsia (Krendl et al., 2017; Whigham et al., 2019). While expression of *TFAP2C*, *ELF5* and *GATA3* is conserved between mice and humans, EOMES is missing from human TE (Deglincerti et al., 2016; Hemberger et al., 2020; Niakan and Eggan, 2013). *ESRRB* and *SOX2* which play important roles in murine trophoblast maintenance are only low expressed in human placentas (Hemberger et al., 2020). A recent publication could shed more light on regulators of human trophoblast fate by making use of a genome-wide CRISPR-Cas9 knockout screen (Dong et al., 2022). While also finding known players such as GATA2 among the essential regulators, they revealed that TEAD1 is responsible for the regulation of many trophoblast factors (Dong et al., 2022). When TEAD1 expression is depleted, hTSCs lose the capacity to differentiate into EVT and STB (Dong et al., 2022).

2.4 Stem cell types arising at the blastocyst stage can be derived and cultured *in vitro*

As previously described, TSCs represent the *in vitro* equivalent of the trophectoderm. If kept under correct culture conditions, TSCs show indefinite self-renewal and possess the ability to differentiate along the trophoblast lineage (Latos and Hemberger, 2013; Tanaka et al., 1998). Even though most known pregnancy disorders usually occur later in development, their origin is often associated with early stages of placental development. Therefore, studies of those initial phases are of importance for understanding placental insufficiencies (Burton et al., 2016; Hemberger et al., 2020; Knöfler et al., 2019). First stable murine TSC lines were derived from the blastocyst at E3.5 or from the extra-embryonic part of the post-implantation conceptus at E6.5 under appropriate medium conditions (Figure 5) (Tanaka et al., 1998). These comprise fetal bovine serum (FBS), fibroblast conditioned medium (CM), fibroblast growth factor (FGF) 4 and heparin (Tanaka et al., 1998). With E8.5, TSCs can no longer be derived from *in vivo* tissue (Simmons and Cross, 2005). As CM as well as FBS contain multiple unknown and variation-underlying factors, a serum free medium was required to limit batch to batch variety and to allow for steady research conditions. Activin and transforming growth factor (TGF) β were found to be secreted by fibroblasts into the CM – factors which both defined media formulations rely on (Kubaczka et al., 2014; Ohinata and Tsukiyama, 2014). The chemically defined TX medium comprises ten chemical components including FGF4, heparin and TGFβ (Kubaczka et al., 2014). Another group developed the CDM/FAXY medium which includes FGF2, activin A, XAV939 and Y27632 and allows for maintenance of TSCs on fibronectin-coated cell culture dishes (Ohinata and Tsukiyama, 2014). Similar to standard TS medium,

TSCs kept under chemically defined conditions in TX medium show proper *de novo* derivation of bona-fide TSC lines and long-term stability (Kubaczka et al., 2014). Of note, TSC colonies under defined conditions exhibit clearer colony morphology and are characterized by decreased differentiation in comparison to cultivation in standard TS medium (Figure 5). TSCs derived in TX medium differentiate into all trophoblast subtypes *in vitro*, contribute to placental chimeras and create lesions when injected subcutaneously into nude mice flanks (Kubaczka et al., 2014).

Human TSCs are thought to be of transient nature, with term placentas now longer being a source for derivation of hTSCs. Even though they were always suspected to reside in blastocysts and in the villous CTB of early first-trimester placenta, successful derivation of human TSC lines was only achieved decades after the establishment of first stable murine TSC lines (Hemberger et al., 2020; Okae et al., 2018; Turco et al., 2018). This was mainly caused by not knowing the correct culture conditions that would support the undifferentiated and proliferating state of hTSCs. In 2018, three publications showed the stable cultivation of hTSCs using distinct culture conditions (Haider et al., 2018; Okae et al., 2018; Turco and Moffett, 2019). While Okae et al. derived hTSCs from blastocysts and first-trimester placentas, Haider et al. and Turco et al. cultivated hTSCs in form of trophoblast organoids (Haider et al., 2018; Okae et al., 2018; Turco and Moffett, 2019). Interestingly, the culture media in all three independently developed studies vary notably from murine TSC medium in terms of signaling cascade activators and inhibitors. They rely on epidermal growth factor (EGF) supplementation, induction of the Wnt pathway as well as inhibition of TGFβ signaling (Haider et al., 2018; Okae et al., 2018; Turco and Moffett, 2019). This contrasts with murine TSCs which require inhibition of Wnt signaling but activation of TGFβ and FGF signaling indicating different roles of Wnt and TGFβ pathways (Latos and Hemberger, 2016; Okae et al., 2018). Remarkably, the identification of the right culture conditions for a self-renewing *in vitro* model of proper hTSCs and trophoblast organoids is already resulting in advanced research and recapitulation of the early human placental development (Soncin and Parast, 2020).

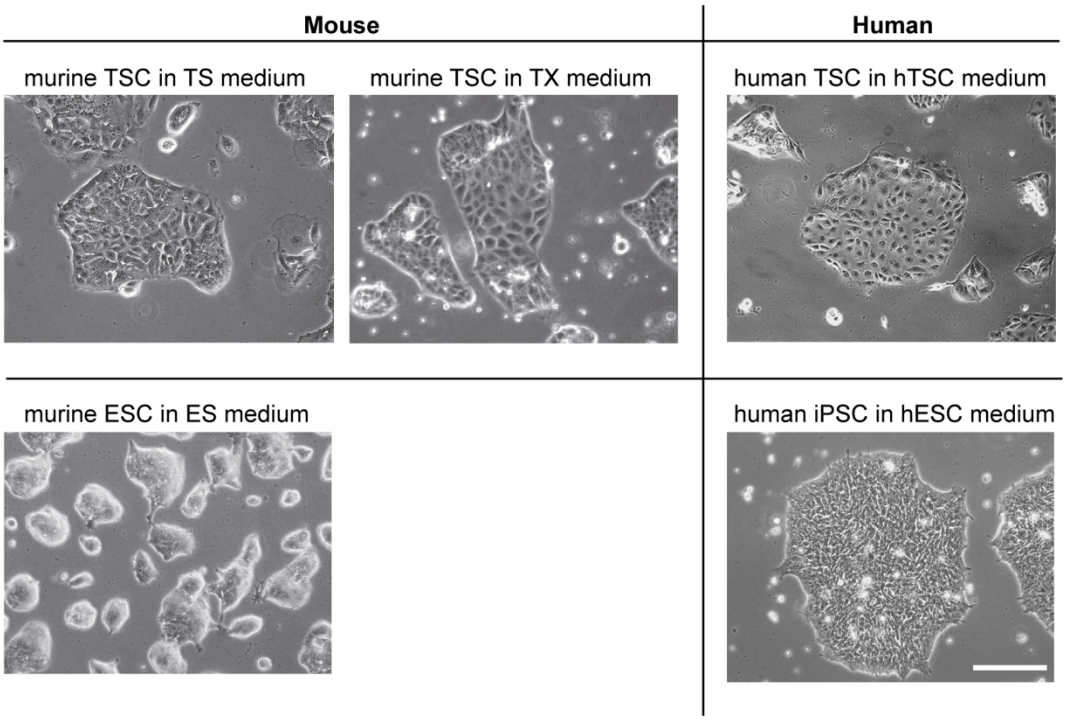

Figure 5: Typical morphology of murine and human ESC/iPSC and TSC *in vitro*
Photomicrographs showing representative morphology of the different stem cells lines cultured *in vitro*. Murine TSC can be cultured in serum containing TS medium or chemically defined TX medium. Scalebar represents 250 µm.

The hTSC lines established by Okae et al. were derived from blastocysts and first-trimester placentas (Figure 5). Obtained hTSC were demonstrated to meet essential criteria for hTSCs including high levels of GATA3 and KRT7 and hypomethylation of *ELF* promoter (Lee et al., 2016; Okae et al., 2018). They are stable in long-term culture and have the potential to differentiate into EVT- and STB-like cells (Okae et al., 2018). EVT cells were obtained by culture on Matrigel with medium containing TGFβ inhibitor A83-01 and decidua derived NRG1, which cause hTSCs to undergo epithelial-mesenchymal transition (Fock et al., 2015; Miller et al., 2005; Okae et al., 2018). Treatment of hTSCs with cyclic adenosine monophosphate (cAMP) agonist forskolin results in aggregation, fusion of cells and formation of syncytia indicating differentiation towards STB (Okae et al., 2018; Strauss et al., 1992). *In vivo* experiments showed invasiveness of derived hTSCs upon injection into immunodeficient mice, cells form lesions and invade into the subcutaneous tissue. Even blood-filled lacunae were detected. Surprisingly, however, hTSCs do not express *CDX2* or show CDX2 or EOMES protein levels. Both trophoblast organoid models were generated from first-trimester cytotrophoblasts, they proliferate continuously and are capable of differentiating to STB and invasive EVT (Haider et al., 2018; Turco and Moffett, 2019).

In both mice and humans, ESCs are the *in vivo* derivatives of the ICM. They are pluripotent and strictly separated epigenetically from TSCs. Standard murine ESC culture requires fibroblast feeder cells and serum containing culture medium supplemented with leukemia

inhibitory factor (LIF) (Figure 5). To allow for chemically defined culture conditions, the 2i medium was developed (Silva et al., 2008). It is supplemented with two inhibitors which are inhibiting the mitogen-activated protein kinase (MAPK)/extracellular signal-regulated kinase (Erk) pathway and glycogen synthase kinase-3 (GSK3) (Silva et al., 2008). Different media compositions result in different states of pluripotency of ESC which can be distinguished in naïve, primed and ground state pluripotency (Ghimire et al., 2018; Sim et al., 2017; Ying et al., 2008). Ghimire et al. could show that naïve stage ESCs can be derived from blastocysts in LIF and serum containing medium on a MEF feeder layer, ground state ESCs can be derived from blastocysts when cultured in either 2i or 2iSB (2i + inhibitor of TGF-β signaling SB431542) medium on gelatin coated dishes. Primed ESCs which were named epiblast stem cells (EpiSCs) can be derived from E6.5 conceptuses on a MEF feeder layer (Ghimire et al., 2018). Human ESCs or iPSCs can be divided into three subtypes which are also depending on different culture conditions: naïve, extended, and primed hESCs/hiPSCs. Primed or conventional hESCs/hiPSCs can be derived from preimplantation blastocysts and are related to the post-implantation epiblast (Thomson et al., 1998). When cultured in serum and FGF2 containing medium, they exhibit an epithelial morphology, high levels of DNA methylation and a transcriptome similar to primed post-implantation epiblast (Nakamura et al., 2016; Nichols and Smith, 2009). For chemically defined conditions, primed ESCs can be cultured in E8 medium (Chen et al., 2011). In contrast, naïve hESCs/hiPSCs (hNPSCs) are related to pre-implantation epiblast and can be cultured in T2iLGöY (titrated 2i, hLIF, Gö6983, Y-27632) or 5iLAF (MEK, GSK3, ROCK, BRAF, and SRC pathway inhibitors in combination with hLIF, Activin and FGF2) medium (Takashima et al., 2014; Theunissen et al., 2014). They show gene expression, which is comparable to early epiblast or late morula, low DNA methylation and resemble murine ESCs more closely than primed hESCs (Theunissen et al., 2014). They might hold the potential to differentiate to TSC-like cells spontaneously as they are TFAP2C positive and YAP proteins show nuclear localization. T2iLGöY- cultured naïve hESCs were also shown to comprise a subpopulation that could neither be allocated to primed nor naïve hESCs but was rather expressing placental markers such as *GATA2* and *GATA3* (Cinkornpumin et al., 2020). Extended hiPSCs (hEPSCs) show contribution to embryonic and extra-embryonic lineages in chimeras *in vivo* and require to be cultured in serum-free N2B27 medium containing LIF, CHIR99021, (S)-(+)-dimethindene maleate (DiM) and minocycline hydrochloride (MiH) (Yang et al., 2017).

2.5 Murine trophoblast giant cells fulfil a wide range of functions

Trophoblast giant cells represent the first terminally differentiated cell type of the murine trophoblast lineage and arise first in the mural trophectoderm (Simmons et al., 2007). TGCs are characterized by polyploidy caused by endoreduplication. Being an invasive cell type, they

play an important role during implantation of the blastocyst into the maternal decidua. Further, they are responsible for the secretion of a range of paracrine and endocrine factors which are essential for the interaction with the maternal immune and blood system (Simmons and Cross, 2005; Simmons et al., 2007). Different specialized subtypes of TGCs have been identified, all of which have distinct origins, undertake specific functions in placental development and maintenance and can be distinguished by distinct gene expression patterns (Figure 6). The TGC diversity is essential for the successful placental formation and function. Analysis of the markers PL1, PL2, PLF and CTSQ allows for the identification of the respective TGC subtype (Simmons et al., 2007).

In general, expression of transcription factor *Hand1* is essential for primary and secondary TGC differentiation and can be detected in all TGC subtypes. Loss of *Hand1* in embryos results in loss of TGC derivation and leads to embryonic death around E7.5 to E8.5 (Riley et al., 1998; Scott et al., 2000; Simmons et al., 2007). Also, upregulation of *Mash2* and *Tpbpa* was detected during the first stages of differentiation towards TGCs before the increase of further, more specified TGC markers (Simmons et al., 2007). However, not all TGCs derive from TPBPA positive precursors (Simmons et al., 2007). Primary TGCs arise for the first time in the mural trophectoderm directly after implantation. Secondary TGCs develop at later stages and are derived from the ectoplacental cone or spongiotrophoblast (Figure 6) (Simmons and Cross, 2005). Parietal (P)-TGCs line the implantation site starting from E6.5, thereby creating a border between the ectoplacental cone and later spongiotrophoblast towards the maternal decidua. They are characterized by being positive for PL1, Pl2 and PLF. They secrete factors directed at decidual cells or maternal natural killer cells (Simmons et al., 2007). Spiral Artery (SpA)-TGCs replace the maternal endothelial cells in the lumen of the spiral arteries, thereby ultimately lining these arteries. They are PLF positive but PL1 and PL2 negative. Also, they are capable of secreting vasodilators and angiogenic factors that facilitate maternal blood flow to the implantation site (Hemberger et al., 2003; Simmons et al., 2007). Canal (C)-TGCs line the canal spaces in the labyrinth which develop due to the fusion of spiral arteries. C-TGCs are PLF and PL2 positive but negative for PL1. Sinusoidal (S)-TGCs are found in the labyrinth layer lining the maternal sinusoids. Due to their proximity to fetal vessels, they are suggested to play a role in secreting hormones or cytokines that access the fetal circulation. *Ctsq* is uniquely expressed in S-TGCs, whereas they also share the marker PL2 but are negative for PL1 (Simmons et al., 2007). Glycogen trophoblasts (GlyT) are unique cells that share TGC but also spongiotrophoblast characteristics (Simmons and Cross, 2005). They arise in the spongiotrophoblast layer past E12.5 and migrate into the decidua (Simmons and Cross, 2005). They can be identified by TPBPA, GJB3 and PCDH12 positivity (Simmons et al., 2007). *In vitro*, the withdrawal of growth factors FGF4, Heparin and TGFβ from the culture medium results in the immediate differentiation of TSCs to TGCs. For this reason, TGC differentiation

is regarded as the default pathway (Simmons et al., 2007). After six days under differentiating conditions, all four markers PLF, PL1, PL2, CTSQ can be detected in cell culture experiments (Simmons et al., 2007). Promotion of PL1 and PLF positive P-TGC differentiation can be achieved by administration of exogenous substances such as retinoic acid (RA) (Hemberger et al., 2004; Simmons et al., 2007; Yan et al., 2001).

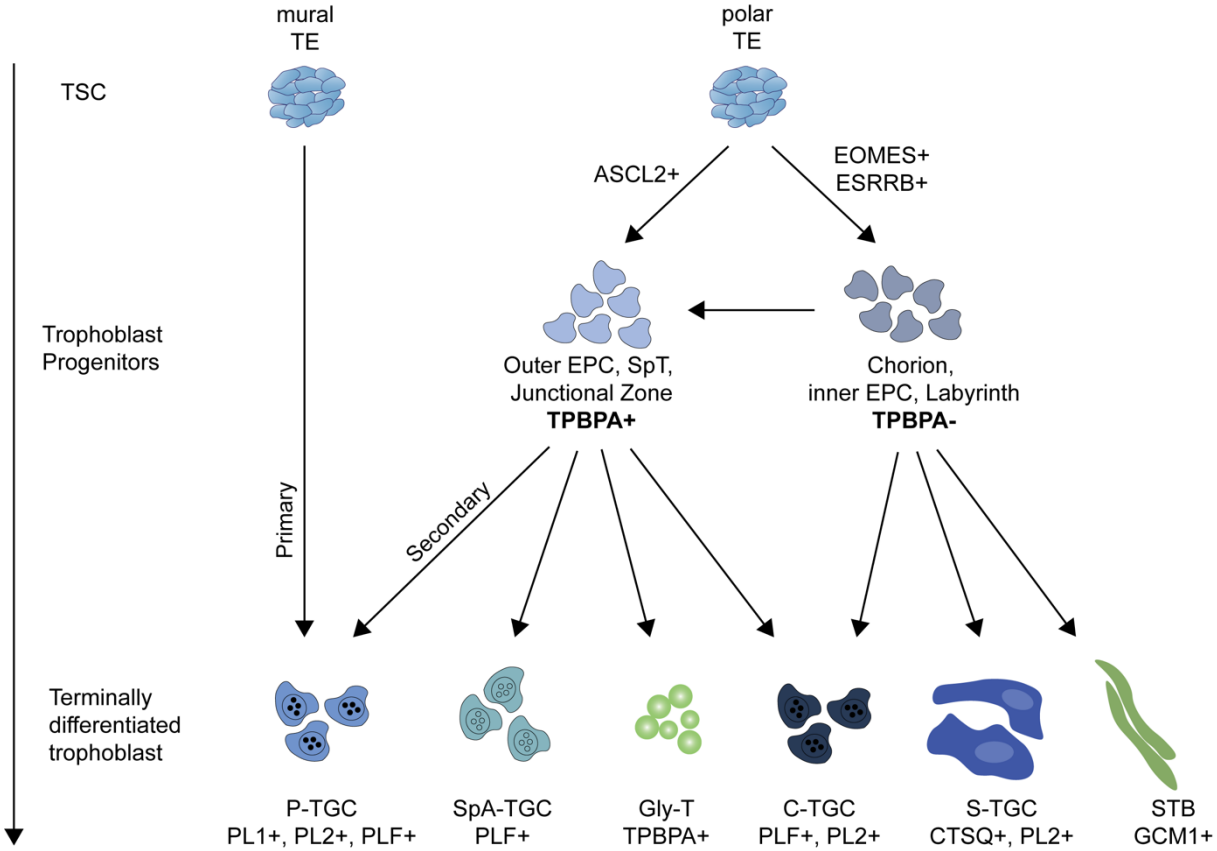

Figure 6: TGC differentiation and marker expression
Differentiation from the TSC state differs between mural and polar TE. Stem cells from mural TE differentiate into P-TGCs in the primary wave of TGC differentiation. Stem cells of polar TE continue to proliferate and give rise to TPBPA positive and negative progenitor cells which in turn continue to differentiate into specialized TGCs such as P-TGC, SpA-TGC, C-TGC an S-TGC as well as GlyT and STB cells. These finally differentiated cells can be distinguished according to their varying marker expression. TE=trophectoderm, EPC=ectoplacental cone, SpT=spongiotrophoblast, TGC=trophoblast giant cells, P-TGC=parietal TGC, SpA-TGC=spiral artery TGC, Gly-T=glycogen trophoblasts, C-TGC=canal TGC, S-TGC=sinusoid TGC, STB=syncytiotrophoblast. Modified from Natale et al., 2017 and Simmons et al., 2007.

2.6 Epigenetic regulation of gene expression

Epigenetic modifications regulate gene expression but they are not laid down in the primary DNA sequence (Waddington, 2012). Those modifications comprise DNA methylation, histone modification and RNA-mediated interference (RNAi) (Allis and Jenuwein, 2016). DNA methylation describes the covalent addition of a methyl group to a cytosine resulting in 5-methylcytosine and is associated with gene repression (Greenberg and Bourc'his, 2019; Hemberger et al., 2009). Most methylated cytosines occur in cytosine-phosphate-guanine

(CpG) dinucleotides of which 60-80% are methylated genome-wide (Parry et al., 2021). CpG-rich regions are called CpG islands (CGI) and are usually unmethylated. About 70% of mammalian promoters are associated with CGIs including promoters of developmental and housekeeping genes (Greenberg and Bourc'his, 2019; Parry et al., 2021). Among others, DNA methylation influences the binding of transcription factors including ELF5 and TFAP2C which prefer binding to non-methylated binding sites (Hemberger et al., 2020). A family of DNA methyltransferases (DNMTs) establishes methylation patterns by transferring a methyl group from the donor – the coenzyme S-adenosyl-L-methionin – onto cytosines (Bestor, 2000; Jeong and Goodell, 2014). DNMT1 mainly maintains methylation patterns after DNA replication whereas DNMT3a and DNMT3b primarily introduce *de novo* methylation onto CpGs (Okano et al., 1999; Parry et al., 2021). DNMT3-like does not harbor the methyltransferase activity but it is able to regulate DNMT3a and DNMT3b (Hata et al., 2002; Suetake et al., 2004). Demethylation of cytosines can take place passively through loss of methylation re-establishment after cell replication and actively by ten eleven translocation (TET) dioxygenases resulting in the break-down product 5-hydroxymethylcytosine (5hmC) (Parry et al., 2021; Schübeler, 2015)

In mammalian development, two genome-wide waves of epigenetic reprogramming occur which result in formation of distinct methylation patterns. The DNA of primordial germ cells undergoes a genome-wide demethylation which allows the establishment of a sex-specific DNA methylation pattern afterwards. Also after fertilization of the oocyte, a wave of demethylation takes place (Reik et al., 2001; Rose et al., 2013). In the post-implantation embryo, DNA methylation is then re-established in embryonic and extraembryonic lineages. This development coincides with increased expression of *de novo* DNMTs DNMT3A, DNMT3B and DNMT3L (Hemberger et al., 2020). Interestingly, apart from imprinted genes, methylation is also retained at CGIs which are associated with genes essential for trophoblast development (Hemberger et al., 2020). Trophoblast DNA exhibits global hypomethylation with 40-50% CpGs being methylated as well as significantly lower levels of 5HmC indicating a higher level of cellular plasticity. In comparison, in embryonic DNA, about 80% of CpGs are methylated (Hemberger et al., 2020). Of note, it was shown that TET1 and 5hmC are required for maintenance of TSC state (Chrysanthou et al., 2018; Senner et al., 2020). Loss of *Tet1* or *Tet2* expression results in induction of differentiation (Hemberger et al., 2020).

2.7 Lineage conversions to and from the murine TSC fate

Embryonic and trophoblast lineages are strictly separated in early mammalian development and spontaneous differentiation in either direction does not occur. A so-called lineage barrier was detected between ESCs and TSCs which is maintained by exclusive and antagonistic expression of *Oct4* and *Cdx2*, distinct transcription factor networks and epigenetic signatures

(Guo et al., 2021; Ng et al., 2008). These epigenetic signatures comprise differentially methylated regions (DMR) in promoter sequences of genes expressed in ESCs or TSCs such as TSC-gatekeeper *Elf5* or pluripotency marker *Oct4* and *Nanog* (Cambuli et al., 2014; Kuckenberg et al., 2011; Ng et al., 2008). A cell fate change between those lineages remains incomplete until those DMR adapt to the new lineage as well. During the past decades, forced conversion from ESCs to TSCs and vice versa has been investigated (Figure 7). ESC fate was successfully induced in TSCs by ectopically expressing four ESC-specific transcription factors: *Oct4*, *Sox2*, *Kfl4* and *c-Myc* (Kuckenberg et al., 2011).

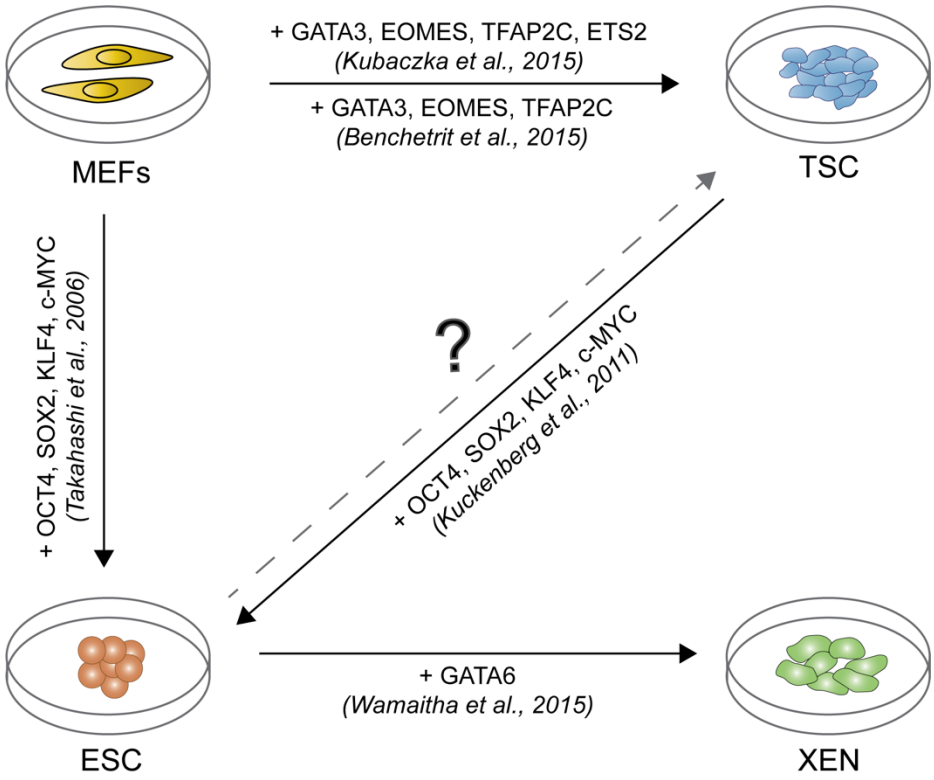

Figure 7: Conversion and reprogramming approaches between murine stem cell types
Ectopic overexpression of transcription factors was implemented for reprogramming of somatic cells to murine ESC or TSC. Similarly, cell fate changes were established from TSC to ESC or ESC to XEN cell fate. The combination of transcription factors sufficient for a complete conversion from ESC to TSC fate was still under investigation. Figure is based on the following publications: Benchetrit et al., 2015; Kubaczka et al., 2015; Kuckenberg et al., 2011; Takahashi et al., 2007 and Wamaitha et al., 2015.

While induction of ESC fate in TSCs was successfully established, the conversion of ESCs to TSCs remained incomplete. Several different combinations of transgene activation and signaling cascade activation were examined (Figure 8). While overexpression of *Tfap2c*, *Gata3*, *Eomes* and *Ets2* in fibroblasts results in completely induced TSCs, this TF combination was shown not to be sufficient in ESC to TSC conversion (Kubaczka et al., 2015). Downregulation of *Oct4*, overexpression of *Gata3*, *Tfap2c* or *Cdx2* yields TSC-like cells, however, bona fide TSC fate is not induced (Cambuli et al., 2014; Kuckenberg et al., 2010; Ralston et al., 2010). Cambuli et al. demonstrated that TSC-like cells obtained from e.g., *Cdx2*

overexpression, *Oct4* downregulation or Ras-Erk1/2 activation in TS medium remain with an epigenetic memory of ESC (Cambuli et al., 2014). In contrast, when using CRISPR/Cas9 mediated activation of *Cdx2* expression in ESC, Wei et al. could show demethylation of the *Elf5* promoter and hypermethylation of the *Oct4* promoter (Wei et al., 2016). Using CRISPR/Cas9 for gene activation holds the advantage of implementing the endogenous *Cdx2* promoter which may yield a physiological level of *Cdx2* (Kubaczka et al., 2016). Importantly, Wei et al. were the first group to use TX medium for this conversion approach (Wei et al., 2014). Apart from overexpression of TSC specific transcription factors, Nosi et al. could demonstrate that ectopic expression of TSC enriched miRNAs is capable of downregulating pluripotency markers in ESCs and inducing a TSC phenotype (Nosi et al., 2017). In another study, it was also shown that the balance of *Esrrb* and *Eomes* expression represents a decisive factor for lineage separation into ESC and TSC fate. High levels of *Eomes* result in TSC fate whereas high levels of *Esrrb* result in ESC fate (Benchetrit et al., 2019).

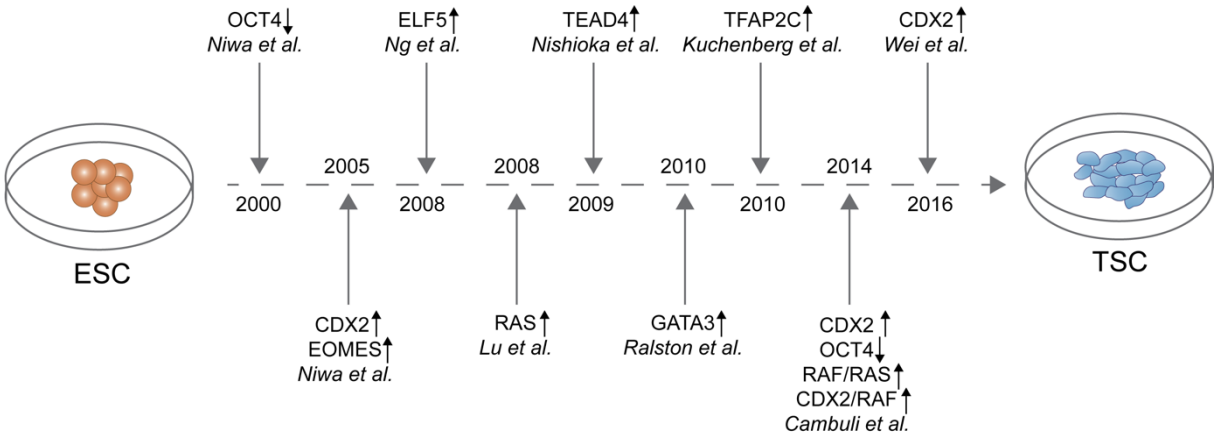

Figure 8: Murine ESC to TSC conversion approaches published during the last decades
For more than 20 years, the conversion from ESC to TSC fate was under investigation. Several groups developed different approaches including overexpression of transcription factors, activation of TSC specific signal cascades or CRISPR/Cas9 mediated gene expression. Respective publications are listed according to their publishing date in combination with the indicated approach. Modified from Kubaczka et al., 2016.

To further study the first lineage separation in mammalian development, organization and crosstalk of stem cells, organoid culture represents a highly valuable tool. Several studies showed spontaneous organization of embryo-like structures by combination of ESCs, TSCs and XEN cells in a 3D co-culture system (Gao et al., 2019; Sozen et al., 2019; Zhang et al., 2019). Even the generation of embryo-like structures was achieved from a co-culture of one unmodified ESC line with two ESC lines which harbor transgenes for induction of TSC or XEN cell fate in ESCs, respectively. Co-culture in combination with transgene activation results in formation of Rosette-to-Lumen-embryoids which allow for modelling the development of different lineage compartments between E4.5 and E5.5 (Langkabel et al., 2021).

2.8 Lineage conversion from hiPSC to hTSC

Over the past years, also the cell fate change from hiPSCs/hESCs to human iTSCs was examined by several groups (Figure 9). These conversion approaches mostly relied on changing or adding components to the culture medium but not on transduction of exogenous factors (Amita et al., 2013; Castel et al., 2020; Cinkornpumin et al., 2020; Dong et al., 2020; Horii et al., 2020; Mischler et al., 2021). Importantly, it soon became clear that primed and naïve ESCs respond differently to those external influences (Castel; Huang, Maruyama and Fan, 2014; Dong et al., 2020). Addition of BMP4 or BMP4 in combination Activin and FGF signaling inhibitors (BAP) to the culture medium of primed hiPSCs was shown to result in TSC-like cells which are rather differentiated trophoblasts but not self-renewing TSCs (Amita et al., 2013; Castel et al., 2020; Cinkornpumin et al., 2020; Dong et al., 2020; Horii et al., 2020; Mischler et al., 2021). The same was observed for hNPSCs and hEPSCs exposed to BAP (Castel et al., 2020). Dong et al., however, showed that also hNPSCs responded to BMP4 treatment – but only if they are cultured in standard hiPSC medium beforehand (Dong et al., 2020). By contrast, Gao et al. showed that hEPSCs but not primed hPSCs or hNPSCs are prone to develop TSC fate due to addition of BMP4 or TGFβ inhibitors (Gao et al., 2019). In 2017, Krendl et al. were closely examining the BMP4-induced conversion from primed hPSCs to hTSCs. The authors discovered that TFAP2C, TFAP2C, GATA2 and GATA3 form a circuit which induces the expression of trophoblast specific markers and suppress the pluripotency network by binding to the first intron of *OCT4*. They could show that GATA3 acts as a pioneer factor in this setting and named the four factors the trophectoderm four (TEtra) factors (Krendl et al., 2017). Krendl et al. could also show that overexpressing GATA3 yields a similar result as BMP4 treatment (Krendl et al., 2017). Nevertheless, it was suggested that all BMP4 based approaches yield differentiated trophoblast cells and not a pure hTSC population (Castel et al., 2020; Dong et al., 2020). Other groups dispute these conclusions and postulate that hiPSCs rather generate mesoderm- or amnion-like cells due to BMP4 (Bernardo et al., 2011; Guo et al., 2021; Io et al., 2021; Roberts et al., 2014). Guo et al. even claim that primed hPSCs have lost the potential to generate hTSCs altogether (Guo et al., 2021). Notably, several groups could show that hNPSCs cultured in t2iLGöY or 5iLAF medium convert to hTSCs once the medium is switched to hTSC medium for 5-10 passages or 10-22 days, respectively (Castel et al., 2020; Cinkornpumin et al., 2020; Dong et al., 2020). The obtained cells were named human converted TSCs (hcTSCs) by Castel et al. (Castel et al., 2020). They lost the expression of pluripotency markers but express *GATA2* and *GATA3*, they were demonstrated to self-renew and propagate unlimited as well as showing typical hTSC morphology (Castel et al., 2020). Also, these cells share expression profiles with hTSCs established by Okae et al. and harbor the potential to differentiate to STB and EVT cells (Castel et al., 2020; Okae et al., 2018). Dong et al. could also demonstrate that global transcriptome and chromatin accessibility was similar

to blastocyst-derived hTSCs (Dong et al., 2020). Medium switch to hTSC medium is not sufficient for hTSC induction in primed hiPSCs (Castel et al., 2020). Interestingly, reprogramming of somatic cells to hiNPSCs using OKSM factors also results in appearance of GATA3 positive cells showing hTSC morphology. When the OSKM reprogramming of fibroblasts is performed in E7 medium from day 7 to day 21 followed by transition to hTSC medium, it results in establishment of hTSC fate – the obtained cells here were called hiTSCs (Castel et al., 2020; Chen et al., 2011; Okae et al., 2018). Like hcTSCs, hiTSCs lost expression of pluripotency markers, self-renew and exhibit differentiation capability to STB and EVT (Castel et al., 2020). Recently, Guo et al. could present data showing that inhibition of ERK and Nodal signaling in hNPSCs yields hTSC fate when cells were cultured in hTSC medium (Guo et al., 2021).

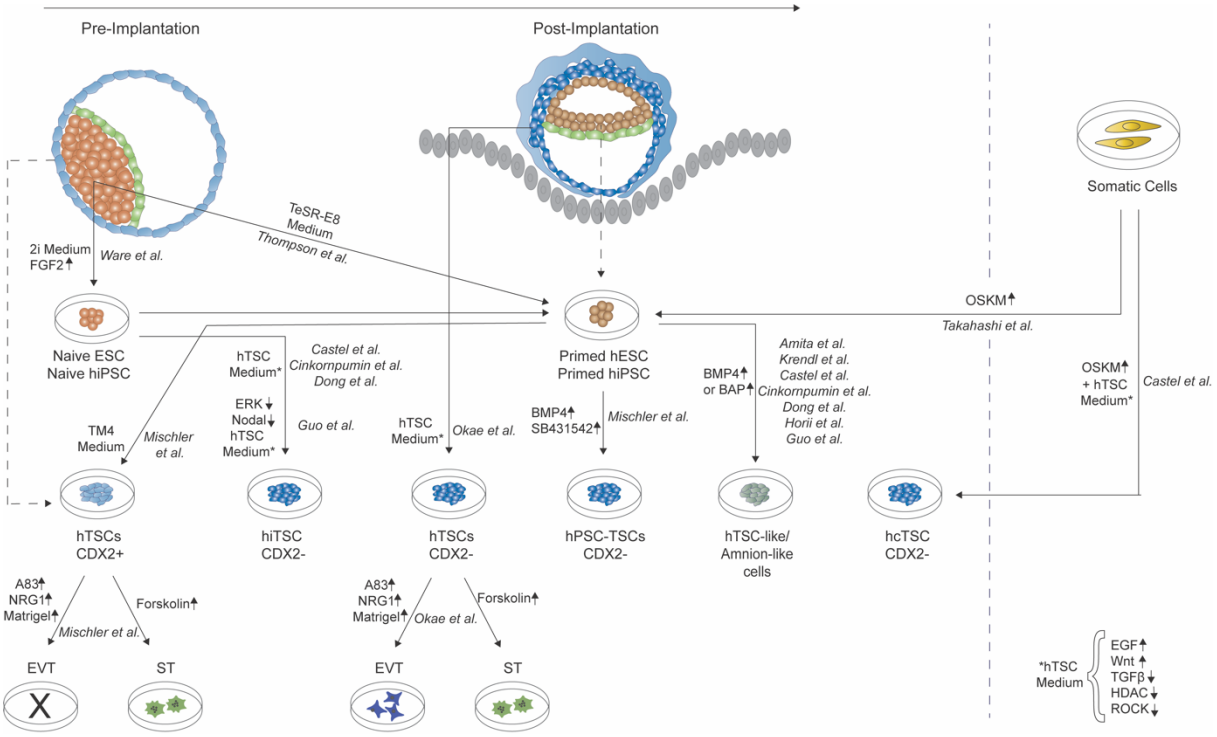

Figure 9: Schematic of conversion and reprogramming approaches in the human system
Several reprogramming approaches have been conducted over the past years trying to establish human TSC fate in human ESC or iPSC. Native hESC/hiPSC represent the pre-implantation stage comparable to CDX2 positive hTSC. Post-implantation stage is represented by primed hESC/hiPSC and CDX2 negative hTSC. TM4 medium contains S1PR3 agonist CYM5541, GSK3β inhibitor CHIR99021, TGFβ inhibitor A83-01, and FGF10. Figure was based on the following publications: Amita et al., 2013; Castel et al., 2020; Cinkornpumin et al., 2020; Dong et al., 2020; Guo et al., 2021; Horii et al., 2020; Krendl et al., 2017; Mischler et al., 2021; Okae et al., 2018; Takahashi et al., 2007; Thomson et al., 1998 and Ware et al., 2014.

In conclusion, hiNPSCs were shown to harbor the greatest potential to convert to hTSCs with further differentiation along the trophoblast lineage. In contrast to murine ESC, they already express transcriptional and epigenomic signatures of trophoblast cells and have therefore been suggested to be predisposed for hTSC fate (Castel et al., 2020; Dong et al., 2020; Guo et al., 2021). The authors can even show that epiblast cells from late human blastocysts have

the capability to regenerate trophectoderm *in vitro* (Guo et al., 2021). Vice versa, it was revealed that human trophectoderm cells from late blastocysts can still regenerate the ICM (De Paepe et al., 2013). Thus, it has been suggested that the lineage separation is less absolute or is acquired later in development in the human system (Guo et al., 2021). The authors postulate that trophectoderm lineage potential is retained in the human ICM even after the blastocyst is formed in contrast to the murine system showing higher developmental plasticity and regulative capacity (Guo et al., 2021).

2.9 KIT receptor plays an important role in placental development

The KIT receptor is a membrane-bound tyrosine kinase that is involved in various inner cell processes such as cell survival, proliferation, differentiation, and adhesion (Ashman, 1999; Kissel et al., 2000). It is abundantly present in hematopoietic stem and progenitor cells and other non-hematopoietic tissue cells (Edling and Hallberg, 2007; Liang et al., 2013). It plays an important role in hematopoiesis, melanogenesis, gametogenesis and fertility (Ashman, 1999; Kissel et al., 2000).

The receptor is activated by binding of the stem cell factor (SCF) ligand. Upon binding, the receptor dimerizes and its tyrosine residues become phosphorylated (Ashman, 1999; Chabot et al., 1988; Copeland et al., 1990). Once the receptor is active, it induces a range of signaling cascades comprising mitogen-activated protein kinase (MAPK), phosphoinositide 3-kinase (PI3K) and janus kinase (JAK)/signal transducers and activators of transcription (STAT) signaling (Pathania et al., 2021). Thereby, the KIT receptor signaling is involved in migration, angiogenesis, proliferation and cell cycle control (Liang et al., 2013; Linnekin, 1999; Roskoski, 2005; Yasuda and Kurosaki, 2008). Mice that carry mutations in *Kit* or *SCF* gene suffer from aberrant proliferation and survival of hematopoietic stem cells, germ cells and melanocytes during embryonic development (Kauma et al., 1996).

Systemic mastocytosis, hematopoietic disorders and tumor diseases are associated with aberrant KIT-signaling (Bodemer et al., 2010; Kemmer et al., 2004; Lasota et al., 1999; Malaise et al., 2009; Miettinen and Lasota, 2005). Several mutations were reported to be causing dysregulation of the human KIT receptor. The substitution of the aspartic acid at position 816 with a valine (D816V) leads to constitutive phosphorylation of the receptor independent of ligand binding and presents the most common activating mutation (Kemmer et al., 2004; Sun et al., 2009; Tian et al., 1999). The successful generation of a humanized KIT^{D816V} mouse model enabled the analysis of this mutation and its effects (Haas et al., 2015). The chimeric KIT receptor is composed of the human intracellular domain including the D816V mutation and murine transmembrane and extracellular domains. It is coupled to a green fluorescent protein (GFP) (Haas et al., 2015; Xiang et al., 2007). The construct is integrated into the ROSA26 locus, thereby being under the control of the endogenous ROSA26 promoter. By Cre-mediated

induction, the gene can be conditionally expressed (Haas et al., 2015; Xiang et al., 2007). Examination of the effect of continuous KIT signaling showed adverse fetal liver erythropoiesis as terminal differentiation of erythroid precursors is repressed. As a result, embryos die after E13.5 (Haas et al., 2015). Also, hematopoiesis is affected in adult animals shown by a polycythemia vera-like myeloproliferative neoplasm in combination with an increased amount of red blood cells and splenomegaly (Pelusi et al., 2017).

The KIT receptor plays an important role during placental development as well. The protein is found in the uterine epithelium of pregnant mice but not in those of unpregnant mice. Further, it is present in the placenta (Horie et al., 1992; Motro et al., 1991; Ottersbach and Dzierzak, 2005). For the first time, KIT and SCF are detected in decidua, trophoblast-chorion and ectoplacental cone at E9 (Motro et al., 1991). Few days later, around E12, KIT is detectable in endothelial cells which line the vessels, in mesenchymal cells of the labyrinth and the chorionic plate and in TGCs (Ottersbach and Dzierzak, 2005). Later in development, at E14.5, KIT and SCF are both found in the labyrinth. Simultaneously, the main presence of KIT is found in the maternal decidua (Motro *et al.*, 1991; Horie *et al.*, 1992, Kauma). At E19, only labyrinthine cells which are in contact with maternal blood are still positive for KIT. At that stage, KIT is undetectable in mesenchymal or endothelial cells (Horie et al., 1992). Hematopoietic development is initiated in the placenta at mid-gestation. Hematopoietic stem cells (HSC) which are detectable starting from E11 are KIT positive. Their population increases until E13, then decreases until they are no longer detectable (Ottersbach and Dzierzak, 2005; Azevedo and Pelajo-Machado, 2018, Sasaki et al., 2010). The stem cell niche consists of endothelial cells which are SCF positive (Ottersbach and Dzierzak, 2005; Sasaki et al., 2010).

In humans, neither SCF nor KIT were found to be expressed in the non-pregnant endometrium (Sharkey et al., 1992, 1994). Only few cells of the myometrium stain positive for SCF (Sharkey et al., 1994). During pregnancy, SCF was shown to be expressed at the maternal-fetal interface – its presence was detected in invasive EVT, fetal fibroblasts within the placental villi, and maternal spiral arteries in the decidua (Kauma et al., 1996; Sharkey et al., 1994). KIT on the other hand was detected in the invading trophoblast, STB, CTB and cells of the decidual stroma (Kauma et al., 1996; Sharkey et al., 1994). Importantly, KIT was found to be expressed by cells of the immune system. It was detected in Hofbauer cells within the chorionic villi, decidual macrophages and in a subset of uterine large granular lymphocytes which represent the main leukocyte population in the decidua during the first trimester. Therefore, the authors suggested that KIT signaling might play a role in regulation of invading EVT as well as its contact to the maternal immune system (Sharkey et al., 1992, 1994).

3 Aim

The aim of this study focused primarily on investigating the conversion from ESC to TSC fate – both in the murine and the human system. In this context, events such as transcription factor interactions during the first lineage separation in mammalian development were sought to be examined more closely.

The first goal was to achieve a complete conversion from murine ESCs to iTSCs by overexpressing TSC specific transcription factors in ESCs while at the same time examining the optimal cell culture conditions for this conversion approach. Transcription factors to be tested included *Gata3*, *Eomes*, *Tfap2c*, *Ets2* and *Cdx2* – in combination and individually. Transgene induction was carried out under serum-containing and serum-free media conditions. Obtained cell clones were only considered to be fully converted if they showed stem cell characteristics and bona fide TSC morphology, marker expression, methylation profile, and *in vivo* functionality. Therefore, a main part of this study targeted the extensive characterization of TSC-like clones after transient, doxycycline mediated transgene expression. After having performed these tests on a molecular and functional level, a final assessment would allow for selection of transcriptions factors and culture medium which are sufficient for a complete conversion.

The knowledge obtained from studying the murine ESC to TSC conversion was then supposed to be transferred onto the human counterpart. Thus, the second objective was to develop an approach on how to induce hTSC fate in hiPSCs based on lentiviral transduction and doxycycline mediated transgene activation. To this end, selection of appropriate hTSC transcription factors was required as well as the final characterization of obtained cells including morphology, marker expression as well as protein levels by immunofluorescent stainings. This study aimed at finding a combination of transcription factors that would result in an initial induction of hTSC fate.

Finally, the autoactivating mutation D816V in the KIT receptor was shown to disrupt proper placental development. Here, the goal was to investigate if marker expression and invasive capacity of KIT^{D816V}-TGCs were affected due to constant KIT receptor signaling.

4 Materials

4.1 Equipment

Table 1: Equipment

Equipment	Manufacturer
Adjustable Pipettes	Eppendorf AG, Hamburg, Germany and Gilson Incorporated, Wisconsin, USA
Agarose gel chamber 40-1214; 40-0911	Peqlab Biotechnologie GmbH, Erlangen, Germany
Bacterial Incubator	Memmert, Schwabach, Germany
Balances BP211S, CP3202P, PT120	Sartorius Lab Instruments GmbH & Co. KG, Göttingen, Germany
Binocular MZ 16 FA	Leica, Wetzlar, Germany
Camera Control Unit DS-U3	Nikon GmbH, Düsseldorf, Germany
Camera Nikon Digital Sight DS-U3 and DS-43	Nikon GmbH, Düsseldorf, Germany
Cameras Leica DM IRB, Leica MZ 16 FA	Leica Camera AG, Wetzlar, Germany
Cell counting chamber, Neubauer Improved	Brand, Wertheim, Germany
Cell culture incubator Heracell™ 240i	Thermo Fisher Scientific Inc., Waltham, USA
Centrifuges 5424; 5417R	Eppendorf AG, Hamburg, Germany
Centrifuges Multifuge 3 S-R; Biofuge Fresco	Thermo Fisher Scientific Inc., Waltham, USA
ChemiDoc™ MP Gel Imaging System	Bio-Rad Laboratories, Inc., Hercules, CA, USA
Electrophoresis Power Supply EV243	PEQLAB Biotechnologie GmbH, Erlangen, Germany
Flow Cytometer FACSCanto™	Beckton Dickinson, Franklin Lakes, NJ, USA
Fluorescent Lamp Ebq 100 Isolated	Leistungselektronik JENA GmbH, Jena, Germany
Gel iX 20 Gel Imaging System	Intas Science Imaging Instruments, Göttingen, Germany
iMark™ Microplate absorbance Reader	Bio-Rad Laboratories, Inc., Hercules, CA, USA
Lab balances DAA/300	Sartorius Lab Instruments GmbH & Co. KG, Göttingen, Germany
Laminar flow cabinet; HERAsafe™	Thermo Fisher Scientific Inc., Waltham, USA
Magnetic Stirrer MR3001	Heidolph Instruments GmbH & Co. KG, Schwabach, Germany
Microscopes Axiovert 40C	Zeiss, Jena, Germany
Microscopes DM IRB	Leica, Wetzlar, Germany
Mini-PROTEAN® Tetra Cell SDS-Page electrophoresis chamber	Bio-Rad Laboratories, Hercules, USA
NanoDrop™1000 Spectrophotometer	Thermo Fisher Scientific Inc., Waltham, USA
Orbital Shaker and Incubator, Innova 4000	New Brunswick Scientific, New Jersey, USA
Orbital Shaker The Belly Button	Dunn Labortechnik GmbH, Asbach, Germany

Pipette controller accu-jet ® Pro	BRAND, Wertheim, Germany
Shaker TL-10	Edmund Bühler GmbH, Bodelshausen, Germany
Thermocycler 2720	Applied Biosystems, Waltham, USA
Thermocycler PTC-200	MJ Research, Waltham, USA
THERMOLAB® Shaking Waterbath	Gesellschaft für Labortechnik mbH, Burgwedel, Germany
ThermoMixer® Thermoblock compact	Eppendorf AG, Hamburg, Germany
Trans-Blot®Turbo™ Transfer System	Bio-Rad Laboratories, Inc., Hercules, CA, USA
ViiA™ 7 Real-Time PCR System	Life Technologies, Carlsbad, CA, USA
Vortex-Genie™ 2	Scientific Industries, New York, USA
Water Bath TW8	Julabo GmbH, Seelbach, Germany

4.2 Consumables

Table 2: Consumables

Consumables	Manufacturer
384-well plate for qPCR	4titude, Surrey, Germany
96-well plates	Becton Dickinson, Franklin Lakes, USA
Blotting Paper	Macherey-Nagel, Düren, Germany
Cell Culture Cryo tubes	Thermo Fisher Scientific Inc., Waltham, USA
Cell Strainer	Becton Dickinson, Franklin Lakes, USA
Centrifuge tubes (15 ml, 50 ml)	Greiner, Kremsmuenster, Austria
FACS tubes	Becton Dickinson, Franklin Lakes, USA
Filter tips	Nerbe plus GmbH, Winsen, Germany
Glass slides	Marienfeld GmbH, Lauda-Königshofen, Germany
Microcentrifuge tubes (1.5 ml, 2 ml)	Sarstedt, Nuembrecht, Germany
Multiwell dishes (6-, 12-, 24-well plates, 10 cm dishes)	TPP, Trasadingen, Switzerland
Parafilm M	Pechiney Plastic Packaging, Chicago, USA
PCR tubes (100 µl)	Axygen, California, USA
Pipette tips – filtered (10, 100, 1000 µl)	Nerbe Plus, Winsen/Luhe, Germany
Pipette tips (10, 100, 1000 µl)	Greiner, Kremsmuenster, Austria
Polyvinylidene difluoride (PVDF) membrane	Roth, Karlsruhe, Germany
Reaction Tubes (5 ml)	Eppendorf AG, Hamburg, Germany
Seals for qPCR plates	4titude, Wotton, United Kingdom
Serological pipettes	Corning Incorporated, Corning, NY, USA

Sterile filter bottles	Merck Milipore, Billerica, MA, USA
Sterile filters (0.2 µm)	Corning Incorporated, Corning, NY, USA
Sterile filters (0.45 µm, surfactant-free cellulose acetate membrane (SFCA))	Corning Incorporated, Corning, NY, USA
TC Flask T75, Standard	Sarstedt, Nürmbrecht, Germany

4.3 Chemicals and reagents

Table 3: Chemicals and reagents

Material	Manufacturer
(RS)-N'-(7-chloroquinolin-4-yl)-N,N-diethyl-pentane-1,4-diamine (Chloroquine)	Sigma-Aldrich, St. Louis, USA
7-Aminoactinomycin D	AppliChem, Darmstadt, Germany
Acetic acid	AppliChem, Darmstadt, Germany
Acrylamide Mix	Roth, Karlsruhe, Germany
Agar	Merck, Darmstadt, Germany
Agarose	Merck, Darmstadt, Germany
Ammonium persulfate (APS)	Roth, Karlsruhe, Germany
Bovine Serum Albumin (BSA)	AppliChem, Darmstadt, Germany
Chloroform	Merck, Darmstadt, Germany
D+Glucose	AppliChem, Darmstadt, Germany
Dimethylsulfoxide (DMSO)	AppliChem, Darmstadt, Germany
dNTPs	Thermo Fisher Scientific Inc., Waltham, USA
Doxycycline	Sigma-Aldrich, St. Louis, USA
Entellan®	Merck, Darmstadt, Germany
Ethanol	VWR International GmbH, Darmstadt, Germany
Ethidium bromide	Sigma-Aldrich, St. Louis, USA
Ethylene diamine tetra acetic acid (EDTA) 0.05 mM (0.02% in DPBS)	Sigma-Aldrich, St. Louis, USA
FACS Clean	Becton Dickinson, Franklin Lakes, USA
FACS Flow	Becton Dickinson, Franklin Lakes, USA
FACS Rinse	Becton Dickinson, Franklin Lakes, USA
Formaldehyde (4%)	Sigma-Aldrich, St. Louis, USA
Geltrex	Thermo Fisher Scientific Inc., Waltham, USA
Gene Ruler 1kb plus, 1kb, 100bp, 100bp plus	Thermo Fisher Scientific Inc., Waltham, USA
Glycin	Merck, Darmstadt, Germany
Hoechst H33342 (1 mg/ml – 100x)	Sigma-Aldrich, St. Louis, USA

Isopropanol (2-Propanol)	VWR International GmbH, Darmstadt, Germany
Knockout Serum Replacement	Thermo Fisher Scientific Inc., Waltham, USA
Loading Dye 6x orange	Thermo Fisher Scientific Inc., Waltham, USA
Methanol	VWR International GmbH, Darmstadt, Germany
MiniComplete Protease Inhibitors	Sigma-Aldrich, St. Louis, USA
Non-fat dried milk powder	AppliChem, Darmstadt, Germany
PageRuler Prestained Protein Ladder	Thermo Fisher Scientific Inc., Waltham, USA
PBS (Tablets)	Sigma-Aldrich, St. Louis, USA
Phosphate buffered saline (PBS) tables	AppliChem, Darmstadt, Germany
Poly-L-Lysine (0.01%)	Sigma-Aldrich, St. Louis, USA
Polybrene	Sigma-Aldrich, St. Louis, USA
Ponceau S	Sigma-Aldrich, St. Louis, USA
Potassium Acetate	AppliChem, Darmstadt, Germany
RIPA (10x)	New England Biolabs GmbH, Frankfurt am Main, Germany
RNAse A	AppliChem, Darmstadt, Germany
Roti® Load (4x) reducing	Roth, Karlsruhe, Germany
Rotiphorese Gel 30	Roth, Karlsruhe, Germany
Sarcosyl	Sigma-Aldrich, St. Louis, USA
Shut Down Solution	Becton Dickinson, Franklin Lakes, USA
Skimmed milk powder	Nestle, Soest, Germany
Sodium acetate	Merck, Darmstadt, Germany
Sodium chloride (NaCl)	Merck, Darmstadt, Germany
Sodium deoxycholate	Sigma-Aldrich, St. Louis, USA
Sodium dodecyl sulfate (SDS)	Sigma-Aldrich, St. Louis, USA
Sodium hydroxide	VWR International GmbH, Darmstadt, Germany
Sodiumchloride	AppliChem, Darmstadt, Germany
TEMED	VWR International GmbH, Darmstadt, Germany
Tetramethylethylenediamine (TEMED)	VWR International GmbH, Darmstadt, Germany
TG-SDS running buffer, 10x liquid concentrate	Amresco, Solon, USA
Tris-(hydroxymethyl)aminomethane	VWR International GmbH, Darmstadt, Germany
Tris-HCl	Roth, Karlsruhe, Germany
Triton X-100	AppliChem, Darmstadt, Germany

TRIzol™ reagent	Sigma-Aldrich, St. Louis, USA
Trypsin Inhibitor, soybean	Thermo Fisher Scientific Inc., Waltham, USA
Tween-20	AppliChem, Darmstadt, Germany
Valproic Acid	European Pharmacopeia Reference
β-Mercaptoethanol (50 mM)	Thermo Fisher Scientific Inc., Waltham, US; Sigma-Aldrich, St. Louis, USA A

4.4 Enzymes

Table 4: Commercially available enzymes

Enzyme	Manufacturer
DNase I (RNase free; 1 U/µl)	Thermo Fisher Scientific Inc., Waltham, USA
DreamTaq DNA Polymerase (5 U/µl)	Thermo Fisher Scientific Inc., Waltham, USA
Fast AP (Thermosensitive Alkaline Phosphatase, 10 U/µl)	Thermo Fisher Scientific Inc., Waltham, USA
Fast Digest™ restriction endonucleases: EcoRI (1 U/µl), EcoRV (1 U/µl), KfI (1U/µl), SalI (1U/µl), XbaI (1U/µl)	Thermo Fisher Scientific Inc., Waltham, USA
Klenow Fragment (10 U/µl)	Thermo Fisher Scientific Inc., Waltham, USA
Maxima™ Hot Start Taq DNA Polymerase	Thermo Fisher Scientific Inc., Waltham, USA
Maxima™ Reverse Transcriptase (200 U/µl)	Thermo Fisher Scientific Inc., Waltham, USA
Platinum™ Taq DNA polymerase (10 U/µl)	Thermo Fisher Scientific Inc., Waltham, USA
Platinum™ Taq high fidelity DNA polymerase (5 U/µl)	Thermo Fisher Scientific Inc., Waltham, USA
Proteinase K	Merck, Darmstadt, Germany
RNase A	Boehringer, Mannheim, Germany
T4 DNA Ligase	Thermo Fisher Scientific Inc., Waltham, USA

4.5 Kits

Table 5: Commercially available kits

Kit	Manufacturer
EZ DNA Methylation-Direct™ Kit	Zymo Research Corporation, Irvine, CA, USA
Human TGF beta Array C2	RayBiotech Life, Inc., Peachtree Corners, USA
Human/Mouse MAPK Phosphorylation Array	RayBiotech Life, Inc., Peachtree Corners, USA
Maxima™ SYBR Green/ROX qPCR master mix	Thermo Fisher Scientific Inc., Waltham, USA
NucleoBond® Xtra Maxi Kit	Macherey Nagel, Dueren, Germany

NucleoSpin™ Gel and PCR Clean-up, Mini kit for gel extraction and PCR clean up	Macherey Nagel, Dueren, Germany
Pierce™ BCA protein assay Kit	Thermo Fisher Scientific Inc., Waltham, USA
ProFection® Mammalian Transfection System	Promega, Madison, WI, USA
Rapid DNA Ligation Kit (T4 Ligase)	Thermo Fisher Scientific Inc., Waltham, USA
RevertAid First Strand cDNA-Synthese-Kit	Thermo Fisher Scientific Inc., Waltham, USA
RNeasy™ Mini Kit	QIAGEN, Hilden, Germany
TA Cloning™ Kit, with pCR™2.1 Vector	Thermo Fisher Scientific Inc., Waltham, USA

4.6 Buffers

Table 6: Self-prepared buffers

Buffer	Composition
Ammonium persulfate (APS) for SDS-PAGE	10% ammonium persulfate in ddH2O
Blocking Buffer for immunofluorescent stainings	2% BSA; 0.1% Triton X-100; PBS
Blocking Buffer for Western Blotting	5% non-fat milk powder; TBST
Cell Lysis Buffer	10 mM NaCl; 10 mM Tris pH 7.5; 10 mM EDTA; 0.5% sarcosyl; 1 mg/ml proteinase K
FACS Buffer	2% FBS in PBS
LB agar	10 g tryptone; 5 g NaCl; 5 g yeast extract; 16 g agar; ad 1 l ddH2O, autoclaved
LB medium (5x)	50 g tryptone; 25 g NaCl; 25 g yeast extract; ad 1 l ddH2O, autoclaved
Mini Prep Buffer 1	50 mM Tris-HCl pH 8.0; 10 mM EDTA; 100 µg/ml RNase A (kept at 4°C once RNase A was added)
Mini Prep Buffer 2	200 mM NaOH; 1% SDS
Mini Prep Buffer 3	3M KAc pH5.5
PBST	1 PBS Tablet, 1000 ml H2O, 1 ml Tween 20
Ponceau S staining solution	0.5 g Ponceau S, 5 ml acetic acid, H2O ad 500 ml
Radio Immuno Precipitation Assay Buffer (RIPA)	10 mM Tris-Cl (pH 8.0), 1 mM EDTA, 1% Triton X- 100, 0.1% sodium deoxycholate, 0.1% SDS, 140 mM NaCl, 1 mM phenylmethylsulfonyl fluoride
Running buffer for SDS-PAGE	25 mM Tris; 192 mM glycine, 1% SDS
SDS Separation Gel (12%)	1.6 ml H2O, 2.0 ml Rotiphorese Gel 30, 1.3 ml 1.5 M Tris (pH 8.8), 50 µl 10% SDS, 50 µl 10% APS, 2 µl TEMED
SDS Stacking Gel	2.1 ml H2O, 500 µl Rotiphorese Gel 30, 380 µl 1.0 M Tris (pH 6.8), 30 µl 10% SDS, 30 µl 10% APS, 3 µl TEMED

TBST	50 mM Tris; 150 mM NaCl; pH 7.5; 0.1% Tween-20
Western blot transfer buffer (10x)	24.2 g Tris base, 144.1 g glycine, 5 ml 20% SDS, H2O ad 1 l
Western blot transfer buffer (1x)	700 ml H2O, 200 ml methanol, 100 ml 10× Western blot transfer buffer

4.7 Cell culture reagents

Table 7: Cell culture reagents

Reagent	Manufacturer
Advanced DMEM	Thermo Fisher Scientific Inc., Waltham, USA
Advanced Dulbecco's Modified Eagle Medium (DMEM) GlutaMAX™	Thermo Fisher Scientific Inc., Waltham, USA
Bovine Serum Albumin (30%)	Biowest, Riverside, USA
Cellbanker® 1	Thermo Fisher Scientific Inc., Waltham, USA
Corning™ Collagen IV, Mouse	Thermo Fisher Scientific Inc., Waltham, USA
DMEM/F12 (without HEPES and L-glutamine)	Thermo Fisher Scientific Inc., Waltham, USA
DMSO	AppliChem, Darmstadt, Germany
Dulbecco's Modified Eagle Medium (DMEM)	Thermo Fisher Scientific Inc., Waltham, USA
Embryonic stem-cell FBS	Thermo Fisher Scientific Inc., Waltham, USA
Fetal bovine serum (FBS)	Sigma-Aldrich, St. Louis, USA
Fibroblast Growth Factor 4 (FGF4), human recombinant	ReliaTech GmbH, Wolfenbüttel, Germany
FluoroBlok™ Cell Culture Inserts	Corning, New York, USA
Gelatin	Sigma-Aldrich, St. Louis, USA
Heparin, sodium salt	Sigma-Aldrich, St. Louis, USA
HEPES buffer	Sigma-Aldrich, St. Louis, USA
Hygromycin (50mg/ml)	Roth, Karlsruhe, Germany
Insulin-Transferrin-Selenium-Ethanolamine (IST-X, 100x)	Thermo Fisher Scientific Inc., Waltham, USA
Insulin, human recombinant	Sigma-Aldrich, St. Louis, USA
Knockout Serum Replacement	Thermo Fisher Scientific Inc., Waltham, USA
L-ascorbic-acid-2-phosphate	Sigma-Aldrich, St. Louis, USA
L-Glutamine	Thermo Fisher Scientific Inc., Waltham, USA
Matrigel	Corning, New York, USA; Sigma-Aldrich, St. Louis, USA
MEM Essential Amino Acids Solution (EAA)	Thermo Fisher Scientific Inc., Waltham, USA

MEM Non-Essential Amino Acids Solution (NEAA)	Thermo Fisher Scientific Inc., Waltham, USA
Penicillin/Streptomycin (P/S)	Thermo Fisher Scientific Inc., Waltham, USA
Phosphate Buffered Saline (PBS)	Thermo Fisher Scientific Inc., Waltham, USA
Poly-l-lysine	Thermo Fisher Scientific Inc., Waltham, USA
Recombinant Human EGF	PeproTech, Rocky Hill, USA
Roswell Park Memorial Institute (RPMI) 1640 Medium	Thermo Fisher Scientific Inc., Waltham, USA
Sodium pyruvate	Sigma-Aldrich, St. Louis, USA
Sodium selenite	Sigma-Aldrich, St. Louis, USA
Sodium-bicarbonate	Sigma-Aldrich, St. Louis, USA
StemMACS™ CHIR99021	Miltenyi Biotec GmbH, Bergisch Gladbach, Germany
StemMACS™ SB431542	Miltenyi Biotec GmbH, Bergisch Gladbach, Germany
StemMACS™ Y27632	Miltenyi Biotec GmbH, Bergisch Gladbach, Germany
Transferrin (holo), human	Sigma-Aldrich, St. Louis, USA
Transforming growth factor β 1 (TGFβ), human recombinant	PeproTech, Rocky Hill, USA
TrypLE™ Express Enzyme (1x), no phenol red	Thermo Fisher Scientific Inc., Waltham, USA
Trypsin inhibitor	Sigma-Aldrich, St. Louis, USA
Valproic acid for system suitability	Sigma-Aldrich, St. Louis, USA
β-Mercaptoethanol	Thermo Fisher Scientific Inc., Waltham, USA
A 83-01	Sigma-Aldrich, St. Louis, USA
Trypsin-EDTA (0.05%)	Thermo Fisher Scientific Inc., Waltham, USA

4.8 Cell culture medium

Table 8: Cell culture medium formulas

Cell Culture Medium	Formula
293T Transfection Medium	Advanced DMEM, 2% FCS, 50 U/ml Pen/Strep, 2 mM L-glutamine, 25µM Chloroquine
293T Virus Production Medium	Advanced DMEM, 5% FCS, 50 U/ml Pen/Strep, 2 mM L-glutamine
CM	Standard TS medium, 70% MEF conditioned TSC medium with freshly added FGF4 (25 ng/ml) and heparin (1 µg/ml)
ESC Medium	DMEM-GlutaMAX™, 15% FCS, 50 U/ml P/S, 2 mM L-glutamine, NEAA (1x), EAA (1x), 0.1 M β-mercaptoethanol; 1000 U/ml LIF
HEK Medium	430 ml DMEM (high glucose); 50 ml FCS; 5 ml NEAA; 5 ml sodium pyruvate; 5 ml L-glutamine; 5 ml P/S

hiPSC Medium	StemMACS™ iPS Brew XF
hTSC Basal Medium	486 ml DMEM/F12; 5 ml BSA (30%); 5 ml ITS-X; 2.5 ml P/S; 900 µl β-mercaptoethanol (55 mM); 250 µl EGF (100 µg/ml); 1 ml FBS; 25 µl L-Ascorbic acid (0.03 g/ml)
hTSC Medium	10 ml hTSC Basal Medium, 5 µl Y27632 (10mM); 1.25 µl VPA; 10 µl Inhibitor Cocktail
hTSC Medium Inhibitor Cocktail	533 µl CHIR99021 (3 mM); 80 µl A83-01 (5 mM); 80 µl SB431542 (10 mM); 107 µl DMSO
MEF Medium	DMEM; 10% FCS; 50 U/ml P/S; 2 mM L-glutamine; NEAA (1x), EAA (1x)
TS Medium	RPMI 1640, 20% FCS, 2 mM L-glutamine, 1 mM sodiumpyruvate, 50 U/ml P/S, 0.1 mM β-mercaptoethanol
TS Freezing Medium (10%)	FCS, 10% DMSO
TX Freezing Medium (10%)	Knockout Serum Replacement, 10% DMSO
TX Medium	DMEM/F12 (without HEPES and L-glutamine), 2 mM L-glutamine, 50 U/ml Pen/Strep, 19.4 mg/ml insulin, 543 mg/l $NaHCO_3$, 64 mg/l l-ascorbic acid-2-phosphate magnesium, 10.7 mg/l holo-transferrin, 14 µg/l sodium selenite, 25 ng/ml human recombinant FGF4, 1 µg/ml heparin, 2 ng/ml human recombinant TGFβ

4.9 Cell lines

Table 9: Cell lines

Cell Line	Description
2102EP	Embryonal carcinoma cell line. Received from Dr. Sina Jostes.
4F ESC (clones 4F1 (E3), 4F2 (F2), 4F3 (H2))	KH2 cells carrying four doxycycline inducible transgenes (Gata3, Eomes, Tfap2c, Ets2). Received from Dr. Caroline Kubaczka. (Kaiser et al., 2020a; Kubaczka et al., 2015).
5F ESC (clones 5F1 (A3), 5F2 (A4), 5F3 (B1))	KH2 cells carrying five doxycycline inducible transgenes (Gata3, Eomes, Tfap2c, Ets2, Cdx2). Received from Dr. Caroline Kubaczka (Kaiser et al., 2020a; Kubaczka et al., 2015).
CT27	Human cytotrophoblast derived TSC line. Received from Hiroaki Okae (Tohoku University Graduate School of Medicine, Sendai, Japan (Okae et al., 2018)).
DR4	Murine embryonic fibroblasts (Tucker et al., 1997)
DT#3	TSC line, double transgenic for KIT^{D816V} mutation. Received from Dr. Caroline Kubaczka (Kaiser et al., 2020a).
DT#4	TSC line, double transgenic for KIT^{D816V} mutation. Received from Dr. Caroline Kubaczka (Kaiser et al., 2020a).
HEK-293T	Human embryonic kidney cell lines.
iCdx2 ESC	KH2 cells carrying Cdx2 as doxycycline inducible transgene. $Gt(ROSA)26Sor^{tm1(rtTA*M2)Jae}$ $Col1a1^{tm2(tetO-Cdx2)}$. Received from Dr. Caroline Kubaczka (Kuckenberg et al., 2010).
iEomes	KH2 cells carrying Eomes as doxycycline inducible transgene. $Gt(ROSA)26Sor^{tm1(rtTA*M2)Jae}$ $Col1a1^{tm2(tetO-Eomes)}$. Generated in this study in cooperation with Nina Langer.

iEts2	KH2 cells carrying Ets2 as doxycycline inducible transgene. Gt(ROSA)26Sor$^{tm1(rtTA*M2)Jae}$ Col1a1$^{tm2(tetO-Ets2)}$. Generated in this study in cooperation with Nina Langer.
iGata3	KH2 cells carrying Gata3 as doxycycline inducible transgene. Gt(ROSA)26Sor$^{tm1(rtTA*M2)Jae}$ Col1a1$^{tm2(tetO-Gata3)}$. Generated in this study in cooperation with Nina Langer.
iLB-C-14ms11	hiPSC line which was reprogrammed using Sendai virus vectors was received from Dr. Michael Peitz (LIFE & BRAIN Center, Bonn, Germany).
iTfap2c ESC	KH2 cells carrying Tfapc2 as doxycycline inducible transgene. Gt(ROSA)26Sor$^{tm1(rtTA*M2)Jae}$ Col1a1$^{tm2(tetO-Tfap2c)}$. Received from Dr. Caroline Kubaczka (Kuckenberg et al., 2010).
KH2 WT ESC	Murine ESC line allowing for integration of transgenes into Col1a1 by Flp-mediated recombination (Beard et al., 2006).
MCF-7	Breast cancer cell line. Received from Dr. Sina Jostes.
R26::M2-rtTA MEFs	Primary MEFs which carry reverse tetracycline-controlled transactivator in the ROSA26 locus. Obtained from embryos at E13.5. Received from Dr. Caroline Kubaczka.
TS-L5	Murine E6.5 derived TSC line from Eomes-EGFP$^{+/-}$conceptus. Mixed background (Swiss Webster/B6). Received from Dr. Caroline Kubaczka.
WT2.1	Wildtype TSC line. Received from Dr. Caroline Kubaczka (Kaiser *et al.*, 2020).
WT2.4	Wildtype TSC line. Received from Dr. Caroline Kubaczka (Kaiser *et al.*, 2020).

4.10 Chemically competent bacteria

Table 10: Chemically competent bacteria

	Genotype	Company
E. cloni® 10G Chemically Competent Cells	F- *mcrA* Δ(*mrr-hsd*RMS-*mcr*BC) *end*A1 *rec*A1 Φ80*dlac*ZΔM15 Δ*lac*X74 *ara*D139 Δ(*ara,leu*)7697 *gal*U *gal*K *rps*L *nup*G λ- *ton*A (StrR)	Lucigen, Wisconsin, USA
One Shot™ TOP10 Chemically Competent E.coli	F-*mcrA* Δ(*mrr-hsd*RMS-*mcr*BC) Φ80*Lac*ZΔM15 Δ *Lac*X74 *rec*A1 *ara*D139 Δ(*araleu*) 7697 *gal*U *gal*K *rps*L (StrR) *end*A1 *nup*G	Thermo Fisher

4.11 Mouse strains

Table 11: Mouse strains

Strain	Description
129S2/Sv	Inbred mouse strain, agouti coat color
C57BL/6J	inbred mouse strain, black coat color
CB6F1	Obtained from crossing BALB/c females with C57BL/6 males, agouti coat color
D2B6F1	Obtained from crossing BA/2 females with C57BL/6 males (hybrid mouse strain)
D2B6F2	Obtained from crossing D2B6F1 mice (2nd generation hybrid mouse strain)

Deleter-Cre	Strain carries Cre recombinase under transcriptional contraol of CMV promoter, 129sv/S2 and C57BL/6 genetic background (Schwenk et al., 1995).
R26-LSL-KIT^{D816V}	Strain carries GFP-2A-cKIT^{D816V} in Rosa26 locus, 129sv/S2 and C57BL/6 genetic background

4.12 Plasmids

Table 12: Plasmids

Plasmid	Source
CMV-CDX2-WT	Addgene, USA (#16553)
FUGW	Addgene, USA (#14883)
pcDNA-GATA2	Addgene, USA (#1287)
pCMX_PL2_AP2γ	provided by Prof. Dr. Anja Boßerhoff (Institute of Biochemistry and Molecular Medicine, FAU, Erlangen-Nürnberg
pCR2.1	Thermo Scientific, Waltham, USA
pLV-tetO-Cdx2	Diploma Thesis Caroline Kubaczka 2011
pLV-tetO-Eomes	Diploma Thesis Caroline Kubaczka 2011
pLV-tetO-Ets2	Diploma Thesis Caroline Kubaczka 2011
pLV-tetO-Gata3	Diploma Thesis Caroline Kubaczka 2011
pLV-tetO-hCdx2	This Thesis
pLV-tetO-hEomes	This Thesis
pLV-tetO-hEts2	This Thesis
pLV-tetO-hGata2	This Thesis
pLV-tetO-hGata3	This Thesis
pLV-tetO-hTead4	This Thesis
pLV-tetO-hTfap2a	This Thesis
pLV-tetO-hTfap2c	This Thesis
pLV-tetO-Oct4	Addgene, USA (#19766)
pLV-tetO-Tfap2c	Diploma Thesis Caroline Kubaczka 2011
pMD2.G; VSV-g	Addgene, USA (#12259)
psPAX2; HIV-GAG	Addgene, USA (#12269)
pUC57-EOMES	Coding sequence of hEOMES was commercially synthesized and integrated in PUC57_BsaI_Free/pBlueScript II SK(+) by General Biosystems, Morrisville, USA

4.13 Antibodies

Table 13: Primary and secondary antibodies

Target Protein	Dilution	Manufacturer
Alexa Fluor™ 488 donkey anti-goat IgG	IF 1:500	Thermo Fisher Scientific Inc., Waltham, USA
Alexa Fluor™ 488 donkey anti-mouse IgG	IF 1:500	Thermo Fisher Scientific Inc., Waltham, USA

Alexa Fluor™ 488 donkey anti-rat IgG	IF 1:500	Thermo Fisher Scientific Inc., Waltham, USA
Alexa Fluor™ 488 goat anti-rabbit IgG	IF 1:500	Thermo Fisher Scientific Inc., Waltham, USA
Alexa Fluor™ 488 rabbit anti-mouse IgG	IF 1:500	Thermo Fisher Scientific Inc., Waltham, USA
Alexa Fluor™ 594 goat anti-rabbit IgG	IF 1:500	Thermo Fisher Scientific Inc., Waltham, USA
Alexa Fluor™ 594 rabbit anti-mouse IgG	IF 1:500	Thermo Fisher Scientific Inc., Waltham, USA
Alexa Fluor™ 647 chicken anti-goat IgG	IF 1:500	Thermo Fisher Scientific Inc., Waltham, USA
Alexa Fluor™ 647 chicken anti-goat IgG	IF 1:500	Thermo Fisher Scientific Inc., Waltham, USA
CD40	Flow Cytometry 1:100	R&D Systems, Minneapolis, USA (AF440)
CDX2	IF 1:200	BioCare Medical LLC, Pacheco, USA (CM226B)
Cytokeratin 7 (RCK 105)	IF 1:100	Santa Cruz Biotechnology Inc., Texas, USA (sc-23876)
ELF5 (C-18)	IF 1:200	Santa Cruz Biotechnology Inc., Texas, USA (sc-9647)
ELF5 (N-20)	IF 1:200	Santa Cruz Biotechnology Inc., Texas, USA (sc-9645)
EOMES	IF 1:500	Abcam, Cambridge, UK (ab23345)
ETS2	IF 1:100-1:200	Santa Cruz Biotechnology Inc., Texas, USA (sc-365666)
GATA2 (H-116)	IF 1:200	Santa Cruz Biotechnology Inc., Texas, USA (sc-9008)
GATA3	IF 1:200	Cell Signaling Technology, Massachusetts USA (D13C9)
GATA3 (HG3-31)	IF 1:300	Santa Cruz Biotechnology Inc., Texas, USA (sc-268)
Goat Anti-Rabbit Immunoglobulins/HRP	WB 1:2000	Agilent Technologies, Inc., Santa Clara, USA (P0448)
NANOG	WB 1:500	Santa Cruz Biotechnology Inc., Texas, USA (sc-134218)
OCT4	WB 1:500 IF 1:200	Santa Cruz Biotechnology Inc., Texas, USA (sc-5279)
PLET1	Flow Cytometry 1:200	Nordic-MUbio, Susteren, The Netherlands (MUB1512P)
Rabbit Anti-Mouse Immunoglobulins/HRP	WB 1:1000	Agilent Technologies, Inc., Santa Clara, USA (P0260)
TEAD4	IF 1:200	Abcam, Cambridge, UK (ab58310)
TFAP2A (C-17)	IF 1:200	Santa Cruz Biotechnology Inc., Texas, USA (sc-6312)
TFAP2C	IF 1:300	Santa Cruz Biotechnology Inc., Texas, USA (sc-8977)
β-ACTIN (AC-15)	WB 1:50000	Sigma-Aldrich, St. Louis, USA (a5441)

4.14 Primers

Primers developed in this study were designed using Primer 3 Plus or NCBI Primer-BLAST. Primers were synthesized by Sigma-Aldrich (Sigma-Aldrich, Taufkirchen, Germany).

Table 14: Genotyping primer sequences

Target Gene	Forward (5'->3')	Reverse (5'->3')
Cdx2 KH2 tg	TTGAGTCCTGTGACCTCCTTG	TAAAGCAGCGTATCCACATAGCG
Cdx2 pLV-tetO tg	TTGAGTCCTGTGACCTCCTTG	TAAAGCAGCGTATCCACATAGCG
Eomes KH2 tg	TCCAAAGGCATGGGGGCTTA	TTATCATGTCTGCTCGAAGCG
Eomes pLV-tetO tg	ACCCCCAGCAATGGAAACTC	AAGCAGCGTATCCACATAGC
Ets2 KH2 tg	CCTGAGCCAGAAGCCGAAT	GCATTCTAGTTGTGGTTTGTCC
Ets2 pLV-tetO tg	GCGTCCAGCCTGATACAGA	AAGCAGCGTATCCACATAGC
Gata3 pLV-tetO tg	TGGTGTCTGCSTTCCAACCA	AAGCAGCGTATCCACATAGC
Gata3 KH2 tg	AGTTCCTCCGACCCCTTCTA	CTCGAAGCGGCCATCGAAT
pCep (pLV-tetO fw) *pLV-tetO common reverse*	AGAGCTCGTTTAGTGAACCG	AAGCAGCGTATCCACATAGC
R26R SA1 as	GACATCATCAAGGAAACCCTGGA	
R26R wt1 as	CCCATTTTCCTTATTTGCCCCTA	
R26R wt1 s	CTCCCAAAGTCGCTCTGAGTTGT	
Tfap2c tg	ACACCGGGACCGATCCAGCCTCC	TGCTCGAGTCGTGGCGATCCTCG

Table 15: qRT-PCR primer sequences

Target Gene	Forward (5'->3')	Reverse (5'->3')
Cdx2	CTTCAACGTTTGTCCCCAGA	CACGGAGCTAGGATACATGC
Ctsq	GAGGCAGTAGTGGTCATCCC	CAGTACTTCTTCCTCCGGACT
Dnmt1	AAGAATGGTGTTGTCTACCGAC	CATCCAGGTTGCTCCCCTTG
Dnmt3a	GAGGGAACTGAGACCCCAC	CTGGAAGGTGAGTCTTGGCA
Dnmt3b	TGCGTCGTTCAGACAGTAGG	GCCCTTGTTGTTGGTGACTT
Elf5	ATTCGCTCGCAAGGTTACTCC	GGATGCCACAGTTCTCTTCAGG
Eomes	CCTGGTGGTGTTTTGTTGTG	TTTAATAGCACCGGGCACTC
Ezrin	CCACCAACCAGCCAAGAT	CCAATCGTCTTTACCACCTGA

Gapdh	ACCACAGTCCATGCCATCAC	TCCACCACCCTGTTGCTGTA
Gata2	CCTCCAGCTTCACCCCTAAG	ACAGGCATTGCACAGGTAGT
Gcm1	CGATGTGAAACTGCCTCAGA	CTTCCTCTGTGGAGCAGTCC
Gjb3	CTCCTCTGCTGTGGGTCTTG	ATGCCGTGGAGTACTGGTT
Hand1	GAACTCAAAAAGACGGATGGTGG	CGCCCAGACTTGCTGAGG
hCDX2	TTCCCATCTGGCTTTTTCTG	AGAGAAGAGCTGGGGAGGAG
hELF5	AGAACATCCGCACACAAGGT	TCACGGGGTATTCTTTGCTC
hEOMES	CGGCCTCTGTGGCTCAAA	AAGGAAACATGCGCCTGC
hGAPDH	TGCCAAATATGATGACATCAAGAA	GGAGTGGGTGTCGCTGTTG
hGATA3	TCTGACCGAGCAGGTCGTA	CCTCGGGTCACCTGGGTAG
hGCM	TGCTGTCTGCTTCTCCGTAA	CACCTATTCGACTCCCCTCA
hHCGα	GTGCAGGATTGCCCAGAAT	CTAGGTGACGTTCTTTTGGA
hKRT7	AAGAACCAGCGTGCCAAGT	TCCAGCTCCTCCTGCTTG
hTEAD4	GATCGGATCCTTGGAGGGCAC GGCCGGCAC	GATCGAATTCTCATTCTTTCACCAG CCTGT
hTFAP2A	TTCCACCCTGACTCGTTACC	GAGGAGAGCCTCACTTTCTGT
hTFAP2C	CCGTGACCCCGATTTTGGAT	GTGGCGATCCTCGCAGTC
LaspA	TGAACTGTCTGGATAAGTACTGGCA	GGTGAAGGACTGCTTGGGAT
Map2k8	CCGACATCTACAGCCTTGGA	GGTGCCTGCTTGTGGATAAT
Mash2	GGTGACTCCTGGTGGACCTA	TCCGGAAGATGGAAGATGTC
Pcdh12	CTCCTGTCCAGCAAATCTCC	TCTGCTTGACCACTAGGCTTG
Pgk1	CTGACTTTGGACAAGCTGGACG	GCAGCCTTGATCCTTTGGTTG
Pl1	TGGAGCCTACATTGTGGTGGA	TGGCAGTTGGTTTGGAGGA
Pl2	CCAACGTGTGATTGTGGTGT	TGCCACCATGTGTTTCAGAG
Plet1	CACTATGGCTAACGTCTCTGG	CTGTCGTCCTCCTTCACTG
Prcl2c	TGCTCCTGGATACTGCTCCTA	GGCTTGTTCTTGTTTTCTGG
Rin3	ATTGGTGCTGTGTGTCCACT	GCCTTCCAGGTACAGTATAGCC
Sh2d3c	CCACATGAAGAGGCGAAGCA	GGATGGGGTAATGAGGTGCTGT

Tead4	TCTAATGCCTTCTTCCTTG TGA	GAGCAGACCTTCGTAGAG CA
Tfap2c	CACCGTGACCCCGATTGT	GAGTAATGGTCGGCGGAC TG
Tinagl	TGATTCCAACGACATCTAC CA	CTTCCATGAGTGCTTGAAC AG
Tpbpa	CCAGCACAGCTTTGGACA TCA	AGCATCCAACTGCGCTTCA

Table 16: Promoter PCR primer sequences

Target Gene	Forward (5'->3')	Reverse (5'->3')
Elf5 A	TTTGTAGTTTGAGTATTTT GGTG	CAATACTTTCACTAACCTT TCCAC
Elf5 B	GTGGAAAGGTTAGTGAAA GTATTG	AAAAAATTCAAACCTAATA TCTA
Nanog	TAGAGATTTTGGTAGTAAG GTTT	CCAACCAAATCAACCTATC TAAA
Oct4	TGGGTTGAAATATTGGGTT TATT	CTAAAACCAAATATCCAAC CATA

4.15 Software

Table 17: Software

Software	Resource
BISMA (Bisulfite sequencing DNA Methylation Analysis)	http://services.ibc.uni-stuttgart.de/BDPC/BISMA/
Adobe Illustrator® (Version CS2)	Adobe, San Jose, USA
Microsoft Office 365®	https://www.microsoft.com/de-de/
Mendeley® Ltd. Reference Manager	https://www.mendeley.com
Ensemble genome browser online tool	https://www.ensembl.org/index.html
NCBI Primer-BLAST	https://www.ncbi.nlm.nih.gov/tools/primer-blast/
Primer3Plus	http://www.bioinformatics.nl/cgi-bin/primer3plus/primer3plus.cgi
ImageJ (Version 1.50i)	https://imagej.nih.gov/ij/
FlowJo™ (Version 10.6.1)	https://www.flowjo.com
Graphpad Prism (Prism 5 for Windows, Version 5.03)	https://www.graphpad.com
Serial Cloner (Version 2-6)	http://serialbasics.free.fr/Serial_Cloner.html

5 Methods

5.1 Cell culture

5.1.1 Cultivation of murine stem cell lines

Murine and human stem cell lines were cultivated on tissue culture plastic (TTP). Murine ESC and TSC were cultured in humidified incubators (Heracell 240i) at 37°C with 7.5% CO_2 while human iPSC and hTSC were cultured in the same incubators at 37°C and 5% CO_2.

Murine TSC lines were kept in 70% standard serum containing TS medium that was conditioned by irradiated murine embryonic fibroblasts (MEF) mixed with 30% unconditioned standard TS medium and was freshly supplemented with 25 ng/ml human recombinant FGF4 and 1 µg/ml heparin (Tanaka et al., 1998). Murine TSC were also cultured in TX medium which was freshly supplemented with 25 ng/ml human recombinant FGF4, 1 µg/ml heparin and 2 ng/ml TGFβ on Geltrex coated wells (Kubaczka et al., 2014). Respective culture medium is indicated by ^{TS} or ^{TX}, respectively. Medium was changed every other day. Murine ESCs were cultured on gelatine coated wells and a feeder layer of irradiated murine embryonic fibroblasts. For gelatine coating, phosphate buffered saline (PBS) containing 0.1% gelatine was incubated on wells for at least 10 min at 37°C. The culture medium for murine ESCs was standard serum containing ES medium (Evans and Kaufman, 1981). ES medium was changed every day. Murine ESCs and TSCs were passaged when the cell culture well was subconfluently covered by stem cell colonies. Therefore, cells were incubated with 0.05% trypsin/EDTA for 5 min at 37°C. Trypsin activity was stopped by addition of serum containing medium or trypsin inhibitor in case cells were cultivated in TX medium. For long-term storage, cells were frozen at -80°C. To this end, cells were harvested using 0.05% trypsin/EDTA and cell pellets were resuspended in 10% DMSO in FBS for standard TS cultured TSCs. TX cultivated cells were resuspended in 10% DMSO in KnockOut Serum Replacement.

5.1.2 Cultivation of human stem cell lines

Human TSC were cultured in hTSC medium described by Okae et al. on wells coated with 5 µg/ml collagen (Col) IV (Okae et al., 2018). For coating, wells were incubated with Col IV diluted in PBS for at least 1.5 h at 37°C. PBS/Col IV mixture was aspirated, wells washed with PBS and hTSC medium was added onto the well and incubated at 37°C for at least 10 min. Next, hTSCs were seeded onto the well. Medium was changed every other day. For passaging, hTSC medium was aspirated and 1 ml TrypLE added onto the cell layer. Plates were incubated for 12-15 min at 37°C. 1 ml of basal hTSC medium was added to stop the reaction. Cells were centrifuged at 380 g for 1 min, resuspended and transferred onto a new well coated with Col IV. For long-term storage, hTSC were frozen in Cellbanker 1 medium according to protocol kindly provided by Hiroaki Okae (Okae et al., 2018). Human iPSCs were

cultured in StemMACS™ iPS-Brew XF on Geltrex coated wells. Medium was changed every day.

5.1.3 Generation of feeder fibroblasts

DR4 MEFs were seeded on cell culture dishes in MEF medium and gradually expanded. Once sufficient 15 cm cell culture dishes showed confluent cell layers, cells were harvested, cell pellets resuspended in MEF medium and pooled in 50 ml tubes. Cell suspensions underwent 9 Gray γ-irradiation to cause mitotic inactivation of fibroblasts. Cells were either re-seeded directly for generation of conditioned TS medium or cryopreserved in MEF medium containing 10% DMSO at -80°C.

5.1.4 Generation of conditioned murine TS medium

Mitotically inactivated DR4 MEFs were seeded on cell culture dishes in MEF Medium. On the next day, medium was changed to standard TS medium. After 72 h, TS medium was harvested, sterile filtered and frozen at 35 ml aliquots in 50 ml tubes at -20°C. This procedure was repeated another two times resulting in three batches of conditioned medium. Batch I and III were pooled whereas Batch II was used individually. After adding 15 ml of unconditioned TS medium to 35 ml conditioned medium, it was ready-to-use.

5.1.5 Ectopic expression of transcription factors using the Tet-On system

For doxycycline-controlled transgene expression, the Tetracycline (Tet)-On system was applied (Figure 10). This system was adapted from gram-negative bacteria that developed a resistance against antibiotic treatment using tetracyclines (Das et al., 2015). In short, the mutant reverse Tet repressor (rTetR) from *Escherichia coli* was fused with a transcriptional activation domain of virion protein 16 (VP16) from herpes simplex virus to create the reverse tetracycline-controlled transactivator (rtTA) (Gossen et al., 1995). If a tetracycline or a tetracycline derivative such as doxycycline is present, it binds to the rtTA which in turn will bind to the tetracycline operator (tetO) and induce expression of the gene of interest (Gossen et al., 1995, Das et al., 2015). The pLV-tetO vector allows for integration of cDNA into an inducible lentiviral vector (Figure 10 C). The gene of interest can be inserted into the vector using EcoRI sites and underlies the control of a doxycycline-controllable promoter (tetOP-CMV) (Stadtfeld 2008).

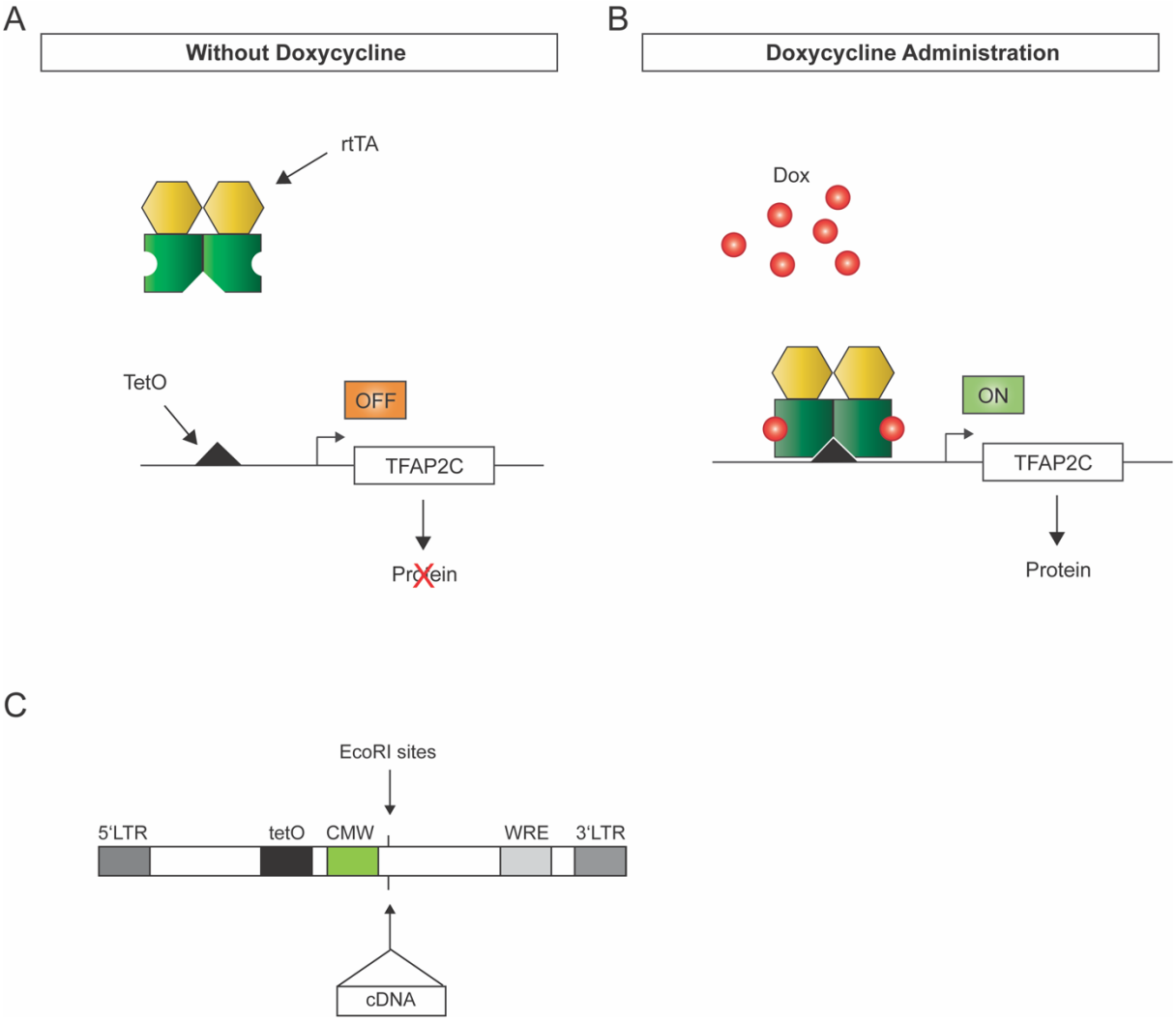

Figure 10: Tet-On system for doxycycline-controlled transgene expression
A.+B. Schematic depicting Tet-On system derived from bacterial resistance against tetracycline treatment. Without the presence of doxycycline, rtTA cannot bind to TetO promoter (**A.**). Once doxycycline is present, it binds to rtTA. rtTA then binds to TetO promoter which causes induction of expression of gene of interest (**B.**). **C.** Schematic of linearized pLV-tetO lentiviral vector that allows for integration of cDNA using EcoRI sites. Gene of interest then underlies transcriptional control of doxycycline-controllable promoter (tetO-CMV). Modified from Das et al. 2015 and Stadtfeld et al., 2008.

5.1.6 Generation of single factor ESC lines

Two types of transgene integration were applied to generate stem cell lines that carry doxycycline inducible transgenes stably integrated into the genome. For single factor murine ESC lines, the KH2 cell line was implemented (Beard et al., 2006). This cell lines allows for site-specific Flp-mediated recombination of target DNA into the Col1a1 locus (Figure 11). Therefore, coding sequences of *Gata3*, *Eomes*, and *Ets2* were cloned into the plasmid pBS31_tetO_promoter/simian virus 40p using EcoRI restriction sites. Plasmid DNA was purified by precipitation and resuspension in TE buffer under sterile conditions. Next, 20 µg of ligated plasmid pBS31_Gata3, pBS31_Eomes or pBS31_Ets2 were electroporated with 10^7 KH2 ESC in combination with 10 µg of a vector encoding for Flp-recombinase (pCAGGS-flpE). Electroporation was performed at 230 V and 500 µF. Coding sequences were integrated into

Col1a1 locus by Flp-mediated recombination now underlying the doxycycline dependent tetO-minimal cytomegalovirus (CMV) promoter. In the ROSA26 locus, KH2 cells also carry the reverse tetracycline transcriptional activator (rtTA) transgene (R26-M2rtTA). After successful integration, an ATG start codon is added to a hygromycin resistance cassette present in the Col1a1 locus allowing for selection of positive clones. For selection, 140 µg/ml hygromycin were added to the culture medium for 10 days. Then, colonies were picked, expanded and their genomic DNA (gDNA) sequenced for proper integration of the open reading frame (ORF) of transgenes. For verification of transgene integration, ESCs were genotyped using primer sequences listed in Table 14.

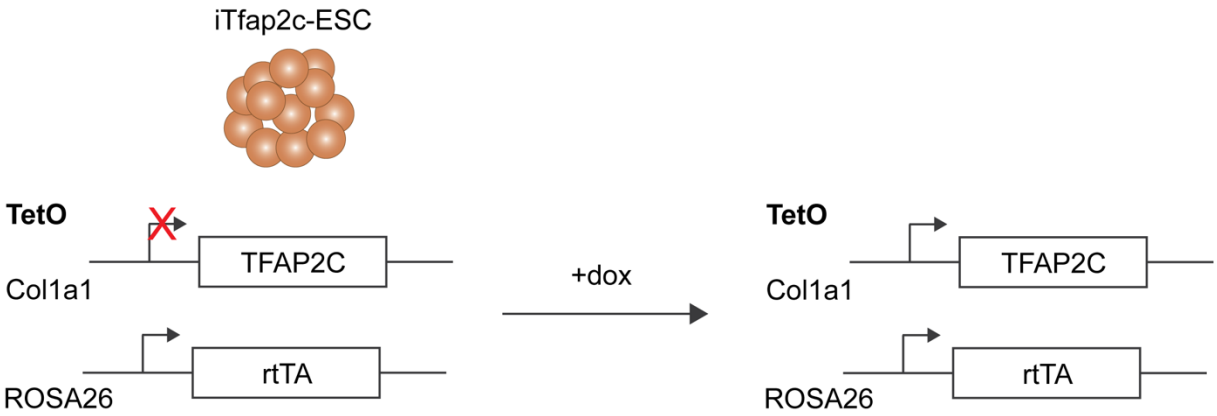

Figure 11: KH2 cell line carrying doxycycline inducible transgene in Col1a1 locus
Due to Flp-mediated recombination, cDNA of gene of interest can be inserted into Col1a1 locus of KH2 ESCs. Upon doxycycline administration, doxycycline molecules can bind to rtTA which then activates TetO promoter. At the same time, KH2 ESC carry the rtTA gene driven off the constitutively active ROSA26 promoter (Beard et al., 2006).

5.1.7 Lentivirus production

Generation of hiPSC cell lines carrying several transgenes was performed by second generation lentiviral transduction as described in Kubaczka et al. (Kubaczka et al., 2015). Coding sequences of hTSC transcription factors *TFAP2C*, *TFAP2A*, *GATA2*, *GATA3*, *TEAD4*, *EOMES* and *CDX2* were cloned into the pLV-tetO (kindly provided by Konrad Hochedlinger, Harvard University) using EcoRI restriction sites. Ligated pLV-tetO plasmids were precipitated and resuspended in 10 mM Tris buffer under sterile conditions. HEK-293T cells were seeded on poly-l-lysine coated 10 cm cell culture plates. HEK-293T cells were transfected using calcium-phosphate precipitation in transfection medium for production of lentiviruses. Calcium-phosphate precipitation mix was prepared using the ProFection Mammalian Transfection System (Table 18).

Table 18: Calcium-phosphate precipitation for lentiviral particle production in 10 cm dish

Reagent	Amount
2 M $CaCl_2$	61.5 µl
Lentiviral Vector DNA (pLV-tetO)	18.5 µg
Helper DNA (psPAX2)	9.25 µg
Envelope DNA (pMD2.g)	9.25 µg
Ad H_2O	600 µl
2x HBS Buffer	600 µl

Before pipetting the transfection mix dropwise onto the HEK-293T cells, it was incubated for 15 min at room temperature (RT). After 5-6 h, the medium was changed to virus production medium. The next morning, medium was replaced by fresh virus production medium. The supernatant containing the lentiviral particles was harvested 72 h and 96 h past transfection. It was sterile-filtered using a surfactant-free cellulose acetate (SFCA) membrane with 0.45 µm pore size. It was aliquoted and stored at -80°C.

5.1.8 Transduction of hiPSC

Next, transduction of hiPSC cells was performed with 50 µl, 100 µl or 150 µl virus supernatant in the presence of 5 µg/ml polybrene overnight. On the next day, supernatant was discarded, cells washed with PBS and culture medium added. After another two days of culture, cells were expanded and frozen at -80°C for further experiments.

5.1.9 Induction of transgene expression

For induction of transgene expression in murine ESC, cells were cultured in supplemented standard serum containing TS medium or supplemented TX medium with doxycycline (2 µg/ml) for three days. Medium supplemented with doxycycline was changed every other day. After three days, cells undergoing conversion were continuously cultivated in respective medium without doxycycline addition. A TSC line derived from a E6.5 conceptus was used as a control cell line (Kubaczka et al., 2014). For transgene induction in hiPSCs, cells were cultured in hTSC medium published by Okae et al. supplemented with doxycycline (2 µg/ml) (Okae et al., 2018). Medium was exchanged every other day.

5.1.10 In vitro differentiation

For induction of *in vitro* differentiation, cells were cultured without growth factor supplementation. TS-Medium cultured cells were cultured without FGF4 and heparin whereas TX cultured cells were cultured without FGF4, heparin and TGFβ for three, six and nine days. At each time point, RNA was isolated from three independent samples.

5.1.11 Invasion Assay

To assess the invasive capacity of TGCs, an invasion assay was developed. Therefore, FluoroBlok™ Cell Culture Inserts with a pore size of 8 µm were placed into a 12-well cell culture plate. Membranes of the inserts were then coated with 0.8 mg/ml Matrigel which was dried at 37°C for 2 h followed by RT incubation overnight. On the next day, Matrigel layer was rehydrated with TS medium. TSC were harvested using 0.05% trypsin/EDTA. They were counted using the Improved Neubauer cell counting chamber and seeded at $2x10^4$ cells per insert. They were kept in differentiation medium – TS medium without CM, FGF4 or heparin – for 5 days. The lower chamber was filled with 700 µl TS medium as well and changed every day. On day five, medium from the lower chamber and Matrigel from the upper chamber were discarded. Filters were washed several times using PBS. Invaded cells on bottom side of the filter were fixed and cell nuclei stained by incubation in methanol containing 1% Hoechst for 10 min at RT. After additional three washing steps with PBS, the quantification of invaded cells was performed by fluorescent microscopy.

5.2 Molecular biological methods

5.2.1 Polymerase chain reaction

Amplification of DNA was achieved by polymerase chain reaction (PCR). PCR was performed for genotyping of transgenic cell lines, amplification of cDNA for generation of lentiviral vectors or amplification of bisulfite converted DNA for methylation analyses. The reaction set ups are given in Table 19, Table 20 and Table 21.

Table 19: Genotyping PCR reaction

	Volume
GreenBuffer (10x)	5 µl
DNA polymerase Dream taq	0.2 µl
Primer forward (10 µM)	1 µl
Primer reverse (10 µM)	1 µl
dNTPs (10mM)	1 µl
DNA template	100 ng gDNA
H_2O (dd)	ad 50 µl
Cycling Protocol	95°C 2 min 95°C 30 s 60°C 30 s 72°C 30 s } 35x 72°C 5 min

Table 20: Amplification of bisulfite converted DNA – PCR reaction

	Volume
Reaction Buffer (10x)	5 µl
DNA polymerase Platinum taq	0.2 µl
Primer forward (10 µM)	1 µl
Primer reverse (10 µM)	1 µl
dNTPs (10mM)	1 µl
$MgCl_2$	1.5 µl
DNA template	1-3 µl converted DNA
H_2O (dd)	ad 50 µl
Cycling Protocol	95°C 2 min 95°C 30 s 61°C 30 s 72°C 45 s } 40x 72°C 5 min

Table 21: Amplification of PCR products for later use in TA cloning – PCR reaction

	Volume
High Fidelity PCR Buffer (10x)	5 µl
DNA polymerase Platinum taq High Fidelity	0.2 µl
Primer forward (10 µM)	1/2 µl
Primer reverse (10 µM)	1/2 µl
dNTPs (10mM)	1 µl
$MgSO_4$ (50mM)	2 µl
DNA template	1 µl
H_2O (dd)	ad 50 µl
Cycling Protocol	94°C 2 min 94°C 30 s 55°C 30 s 68°C 2 min } 30x 68°C 5 min

For purification of PCR reactions, the NucleoSpin Gel and PCR Clean-up kit was used.

5.2.2 Genomic DNA isolation from in vitro cultured stem cells

Cells were harvested using 0.05% trypsin/EDTA. Cell pellet was washed with PBS and resuspended in 400 µl cell lysis buffer containing 40 µl Proteinase K (10 mg/ml). Lysis mix was incubated at 55°C for at least 2 h or overnight. Samples were centrifuged at 13,000 rpm for 10 min. The supernatant was transferred into a fresh tube and 2 volumes EtOH (100%) and 1/10 volume sodium acetate (3M, pH 5.2) were added. The sample was then incubated at -80°C for

30 min for DNA precipitation. Next, sample was centrifuged at 13,000 rpm for 10 min at 4°C and washed twice with EtOH (70%). The pellet was air-dried and resuspended in H_2O. Genomic DNA samples were stored at 4°C until further use.

5.2.3 Cloning techniques

5.2.3.1 Transformation of bacteria

LB agar plates were prepared by heating LB agar in a microwave until liquified, cooling it down until reaching about 50°C, adding appropriate antibiotics and pouring solution into 10 cm petri dishes. Prepared dishes were stored at 4°C after solidifying at RT. Chemically competent bacterial lab strains E.Cloni or TOP10F Escherichia coli (E.coli) were transformed with cDNA of transcription factors. To this end, bacteria were removed from -80°C storage and thawed on ice. Once marginally thawed, 5 µl of ligated vector were pipetted into bacterial solution. Bacteria and vector were incubated on ice for 20 min. Next, heat shock treatment was performed at 42°C for 45 s followed by cooling of the mixture for 3 min on ice. 250 µl LB medium without antibiotics was added and bacteria and medium were incubated shakingly at 37°C for 1 h. Finally, bacteria solution was spread evenly on LB agar plates containing appropriate antibiotics using a cell spreader. Plates were incubated at 37°C overnight. Plasmid DNA was isolated from picked colonies by Miniprep and analyzed by test digests.

5.2.3.2 Plasmid isolation from transformed bacteria - Miniprep

LB Medium (2 ml) containing antibiotics for selection of properly transformed bacteria was inoculated with bacterial colony which was commonly picked from agar plate. Bacterial culture was incubated shakingly overnight at 225 rpm and 37°C. On the next day, bacterial solution was transferred into 2 ml tube and centrifuged at 13,000 rpm for 5 min. The supernatant was removed, and the bacterial pellet resuspended in 150 µl Mini Prep Buffer 1 which was freshly supplemented with RNase A (100 µg/ml). Next, 300 µl of Mini Prep Buffer 2 were added to the solution, mixture was inverted 6 times and incubated at RT for 5 min. 150 µl of Miniprep Buffer 3 were added then, mixed by shaking and followed by centrifugation for 5 min at 13,000 rpm. The pellet was discarded while the supernatant was transferred into a fresh tube filled with 1 ml of EtOH (100%) for precipitation of plasmid DNA. DNA was pelleted after vortexing for 15 Min at 13,000 rpm and 4°C. DNA pellets were washed two times using EtOH (80%). Next, pellets were dried at RT until no residual alcohol was left and resuspended in 40 µl H_2O (dd).

5.2.3.3 Plasmid isolation from transformed bacteria - Maxiprep

For high purification of high amounts of plasmid, 250 ml of LB medium were inoculated with bacterial clone carrying the correct vector. Medium and bacteria were incubated overnight at 37°C shakingly. On the next day, plasmids were isolated by NucleoBond Xtra Maxi Kit following the manufacturer’s instructions.

5.2.3.4 Restriction endonuclease digest

Restriction digests were performed using restriction endonucleases for linearizing plasmids, for separating insert from vector or identification of correct bacterial clones. To identify bacterial clones that successfully incorporated a vector after transformation, plasmid DNA was extracted from bacterial clones using the MiniPrep protocol and analyzed by a test digest. Here, the reaction mix shown in Table 22 was incubated at 37°C for 30 min. The enzyme was inactivated by incubation at 65-85°C for 5 min.

Table 22: Test digest

	Volume
Fast Digest Restriction Enzyme (1 U/µl)	0.5 µl
Fast Digest Green Buffer (10x)	2 µl
DNA	3 µl
H_2O (dd)	ad 20 µl

A preparative digest was performed to obtain large amounts of linearized vector and cut-out insert. The respective reaction mix was incubated at 37°C for 1 h (Table 23). After inactivation of the restriction enzyme, digested samples were loaded onto a 0.7% agarose gel for subsequent electrophoresis. Obtained DNA bands were isolated and purified using the NucleoSpin Gel and PCR Clean-up kit.

Table 23: Preparative digest

	Volume
Fast Digest Restriction Enzyme (1 U/µl)	5 µl
Fast Digest Green Buffer (10x)	5 µl
Plasmid DNA	5-10 µg
H_2O (dd)	ad 50 µl

5.2.3.5 Ligation

Several different techniques were applied for ligating cDNA of transcription factors into the respective vectors. For TA cloning, the TA Cloning Kit along with the vector pCR2.1 was employed. The kit contains a linearized pCR2.1 vector with a T-overhang that allows for binding of PCR products with adenosine overhangs which were added by the Taq-DNA-polymerase during amplification. See reaction setup in Table 24. The reaction was incubated at 16°C overnight.

Table 24: TA cloning setup

	Volume
T4 DNA Ligase (40 U/µl)	1 µl
T4 DNA Ligase Buffer (5x)	2 µl
pCR2.1 (25 ng/µl)	2 µl
Fresh PCR product	3 µl
H_2O (dd)	ad 10 µl

For sticky end ligation, both the vector and the insert had to be digested with the same restriction enzyme which generates sticky ends such as EcoRI. The linearized vector was first dephosphorylated meaning the removal of 3' and 5' phosphate groups from DNA ends to avoid recirculation. Therefore, the vector was treated with alkaline phosphatase for 10 min at 37°C followed by heating the mixture for 5 min at 75°C for enzyme deactivation (Table 25).

Table 25: Dephosphorylation of linearized vectors

	Volume
Fast AP thermosensitive Alkaline Phosphatase	0.5 µl
Reaction buffer for (10x)	1 µl
Linearized vector	100 ng
H_2O (dd)	ad 10 µl

Vector and insert were then incubated at a 1:3 ratio using T4 ligase over night at 16°C (Table 26).

Table 26: Standard ligation setup

	Volume
T4 Ligase (40 U/µl)	1 µl
T4 Ligation Buffer (10x)	2 µl
Dephosphorylated vector	10 µl
Insert	7 µl
H_2O (dd)	ad 10 µl

For blunt cloning, either restriction enzymes generating blunt ends were used or sticky ends were removed by treatment of digested, purified DNA with Klenow fragment which digests 3' overhangs and fills in 3' ends at 5' overhangs (Table 27).

Table 27: Klenow treatment

	Volume
Klenow Fragment	2 µl
Klenow Buffer	5 µl
Insert or linearized vector	30 µl
dNTPs	0.5 µl
H_2O (dd)	ad 50 µl

Next, vector and insert with blunt ends were added at a ratio of 1:1 according to Table 28. The complete reaction was incubated for 25 min at 25°C and stopped by addition of EDTA and additional incubation at 75°C for 20 min.

Table 28: Blunt cloning reaction setup

	Volume
T4 Ligase (40 U/µl)	1 µl
T4 Ligation Buffer (10x)	1 µl
Vector (e.g. pLV-tetO) blunt ends	100 ng
Insert (e.g. Gata2)	1 µl
H_2O (dd)	ad 10 µl

5.2.4 Gene expression analyses

5.2.4.1 RNA isolation and mRNA quantification

Cells were harvested using 0.05% trypsin/EDTA. RNA was isolated from obtained cell pellets using the RNeasy Kit according to the manufacturer's instructions. Concentration and quality of obtained RNA was detected by spectrophotometry using the NanoDrop 1000. Isolated RNA was stored at -80°C until further use. Subsequent DNase digest was performed on 500 ng RNA per sample using Thermo Fisher Scientific DNAse I (Table 29).

Table 29: DNase I digest

	Volume
Buffer + $MgCl_2$ (10x)	1 µl
DNase 1 (10 U/µl)	0.25 µl
RNA	500 ng
H_2O (DEPC)	ad 10 µl

Reaction mix was incubated at 37°C for 30 min. To stop the reaction, 1 µl EDTA (50mM) was added and incubated at 65°C for 10 min. Next, the whole DNase I digest reaction mixture was

implemented in the complementary DNA (cDNA) synthesis using the RevertAid Premium Kit following the manufacturer's instructions.

RNA levels were analyzed by quantitative real-time polymerase chain reaction (qPCR) using Maxima SYBR Green/ROX Master Mix on a ViiA7 instrument (Table 30). Respective primer sequences are given in Table 15. qPCR reactions were performed in triplicates. The expression of target genes analyzed was normalized to the geometric mean of the expression of housekeeping reference genes glyceraldehyde-3-phosphate dehydrogenase (*Gapdh)* and phosphoglycerate kinase (*Pgk1)*.

Table 30: qPCR reaction setup

	Volume
Maxima^{TM} SYBR Green/ROX qPCR master mix (2x)	5 µl
Primer forward (10 µM)	0.25 µl
Primer reverse (10 µM)	0.25 µl
cDNA	1 µl
H_2O (dd)	ad 10 µl

5.2.5 Protein analysis

5.2.5.1 Protein isolation

Cells were harvested using 0.05% trypsin/EDTA. After centrifugation for 5 min at 12,000 rpm, cells were washed with PBS and resuspended in 50 µl RIPA buffer (1x). Cells and buffer were mixed by pipetting. After incubation on ice for 10 min, sample was centrifuged for 10 min at 10,000 rpm and 4°C. The supernatant was kept at -20°C until further analyses, the pellet was discarded.

5.2.5.2 Western Blotting

The Pierce BCA Protein Assay Kit was used to measure protein concentrations on an iMark Microplate Reader. Next, a 12% sodium dodecyl sulfate polyacrylamide gel electrophoresis (SDS-PAGE) was performed. Therefore, 20 µg of protein per sample were mixed with 5 µl Roti-Load (1x) buffer and incubated at 95°C for 5 min on a thermal shaker. PageRuler Prestained Protein Ladder was implemented as protein ladder. Proteins were electrophoresed at 70 V for the first 30 min and 90 V for the rest of the run. A Roti PVDF membrane was activated by 2 min incubation in methanol. Using a Trans-Blot Turbo, proteins were transferred onto the membrane in the Western Blot Transfer Buffer (1x). A ponceau staining was conducted for 5 min shakingly in order to assess complete transfer of proteins. Membrane was rinsed in H_2O (dd) and PBST and blocked for 1 h at RT in WB blocking buffer. Next, first

antibody diluted in WB blocking buffer was incubated with membrane at 4°C overnight. After washing of the membrane with PBST, it was incubated with a HRP-conjugated secondary antibody for 1-2 hours at RT. Membrane was washed with PBST afterwards again. Antibodies and concentrations are listed in Table 13. For detection of proteins, membrane was incubated with Pierce ECL Western Blotting Substrate for 5 min in the dark. Signal was detected on a ChemiDoc MP.

5.2.5.3 Immunofluorescence staining

For immunofluorescence stainings (IF), monolayers of *in vitro* cultured cells were washed with PBS and fixed for 10 min at RT with 4% formalin. Permeabilization of cells was then carried out with 0.5% Triton X-100 in PBS for 10 min. IF blocking buffer (2% bovine serum albumin and 0.1% Triton X-100 in PBS) was incubated on cells for 1 hour at RT. Primary antibody was diluted in IF blocking buffer and incubated on cells at 4°C overnight. After washing with PBS, cells were stained with Alexa-Fluor-conjugated antibodies diluted in IF blocking buffer in the dark for 1 hour at RT. For antibodies and dilutions see Table 13. Hoechst was used to stain cells' nuclei. For negative controls, primary antibody staining was omitted, and cells were only stained with the secondary antibody and Hoechst.

5.2.5.4 FACS analysis

Cells were harvested on day 3 or at passage 5 using 0.05% trypsin/EDTA and filtered through a 35 µm cell strainer to obtain a single cell solution. After washing of cells with fluorescence-activated cell sorting (FACS) buffer (2% FBS in PBS), they were incubated with first antibodies α-CD40 antibody and α-PLET1 antibody for 30 min on ice. Following an additional washing step with FACS buffer, cells were resuspended in Alexa-Fluor-conjugated antibodies diluted in FACS buffer and incubated in the dark for 30 min on ice. For antibodies and dilutions see Table 13. Cells were then washed and resuspended in 7-amino-actino-mycin D (7-AAD; 1% in FACS buffer). The subsequent flow cytometry analysis was then carried out using a FACSCanto. Results were analyzed using FlowJo Software. Three independent samples were at least analyzed per cell line and timepoint.

5.2.5.5 Pathway analysis

Cells were harvested from cell culture plates by incubation with 0.05% trypsin/EDTA. Cells were lysed and protein concentration was measured using the Pierce BCA Protein Assay Kit on an iMark Microplate Reader. Per sample, 350 µg of protein were examined using the Human/Mouse MAPK Phosphorylation Array and Human TGF beta Array C2. The ChemiDoc MP was implemented for signal detection whereas the signal intensities were determined using ImageJ (U.S. National Institutes of Health). Membrane background signal was subtracted from signal densities.

5.2.6 DNA methylation analysis

Genomic DNA was isolated from cells by precipitation-based extraction. Next, 100 ng of gDNA were implemented in bisulfite conversion using the EZ-DNA Methylation-Direct kit. *Elf5*, *Oct4* and *Nanog* promoter sequences were amplified using primers listed in Table 16. PCR products were then ligated into the pCR2.1 vector via TA cloning. Next, vectors were transformed into E.Cloni cells and cultured on LB agar plates overnight. Individual colonies were picked, and DNA extracted by Miniprep. 10-15 randomly picked clones were then sequenced using M13 reverse primers by GENEWIZ Germany GmbH (Leipzig, Germany). The BISMA software was implemented for analysis of CpG methylation. For each cell clone, six representative sequences were shown, the mean value of methylated CpGs was determined based on all successful analyses.

5.3 *In vivo* experiments

5.3.1 Animal studies

All animal studies were performed according to the German law of animal protection and in agreement with the approval of the local institutional animal care committees (Landesamt für Natur, Umwelt und Verbraucherschutz, North Rhine-Westphalia, approval ID number: 84-02.03.2013/A428 approved date: 31 January 2014).

5.3.2 Blastocyst injection

$5F^{TX}$-iTSC were transduced with an EGFP expressing lentiviral vector (FUGW; Addgene plasmid: 14883; (Lois et al., 2002)). For at least three passages, cells were then switched from TX medium to standard TSC medium containing 1,5x FGF4 and 1,5x heparin. D2B6F2 blastocysts were obtained and 7-10 EGFP-iTSCs were injected into each blastocyst. Seven manipulated blastocysts were subsequently transferred into each side of the uteri of pseudo pregnant CB6F1 foster mice. At E12.5, F1 embryos and placenta were extracted and analyzed for EGFP signal. Blastocyst injections and embryo transfer were carried out by Angela Egert.

5.4 Statistical analyses and presentation of obtained data

Statistical analyses and data calculation were performed using GraphPad Prism. Significant differences were determined by applying unpaired *t*-test. Data are presented as mean ± standard error of the mean (SEM). Significant differences were indicated as follows *: $p<0.05$; **: $p<0.01$ and ***: $p<0.001$. Adobe Illustrator was used to create figures.

6 Results I

While fibroblast to murine TSC reprogramming was successfully established previously, it still remained unknown how to achieve complete conversion of ESC to TSC (Kubaczka et al., 2015). Though previous studies have shown that TSC-like fate can be induced by various approaches such as overexpressing *Cdx2* or downregulating *Oct4*, the obtained cells remained with an epigenetic memory of ESCs (Cambuli et al., 2014). Importantly, these studies have been conducted by using standard TS culture medium. Valuable contribution to the current state of research was added by a CRISPR/Cas9 mediated *Cdx2* activation in combination with TX culture which yielded a TSC-like methylation pattern in obtained clones (Wei et al., 2016). However, it is still in question whether this successful outcome was realized because CRISPR/Cas9 mediated gene activation is advantageous compared to overexpression using an episomal expression vector system or due to the different culture medium applied. Hence, this study set out to elucidate which factors and culture medium are sufficient for a complete ESC to TSC conversion.

6.1 Establishment of murine ESC-lines carrying inducible TSC transcription factors

For adjustable transient activation of transgenes, the Tet-On system provides an efficient and convenient method that is applicable using the KH2 ESC line or the pLV-tetO vector combined with second-generation lentiviral transduction (Beard et al., 2006; Stadtfeld et al., 2008). By doxycycline-mediated induction of expression, transgenes are activated. In the absence of doxycycline, transcription of transgenes is discontinued. The KH2 ESC line allows for site specific insertion of transgenes driven by the TetO promoter into the Col1a1 locus using Flp-mediated recombination (Beard et al., 2006). The vital reverse tetracycline transcriptional activator (rtTA) is integrated into the ROSA26 locus. Successful recombination establishes a hygromycin resistance providing a selective marker for generated cell clones.

Candidate TSC transcription factors were chosen to be integrated into murine ESCs as doxycycline-inducible transgenes in order to generate stable transgenic ESC lines. These transcription factors comprised TFAP2C, CDX2, EOMES, GATA3 and ETS2. First, single factor (SF) lines were generated (Figure 12 A). Therefore, cDNA of individual factors was integrated into Col1a1 locus of KH2 ESC line. Shortly, cDNA of e.g., *Tfap2c* was cloned into the vector pBS31_tetO_promoter/simian virus 40p which in combination with a vector encoding for Flp-recombinase (pCAGGS-flpE) was electroporated into KH2 ESCs. Obtained single factor lines were called inducible (i) Tfap2c, iCdx2, iGata3, iEomes, iEts2 (Kuckenberg et al., 2010). Four factor (4F) lines were generated by lentiviral transduction of iTfap2c with pLV-tetO vectors coding for *Gata3*, *Eomes* and *Ets2* (Kubaczka et al., 2015). Three 4F lines were obtained and named 4F1, 4F2 and 4F3 (Figure 12 B). Additional transduction of 4F1 with a pLV-tetO vector harboring coding sequence of *Cdx2* resulted in 5F lines 5F1, 5F2 and 5F3

(Figure 12 C). Throughout the experiments, non-manipulated KH2 cells served as the control for conversion experiments. Generation of different cell lines was performed by Peter Kuckenberg, Tatiana Hesse, Monika Graf, Caroline Kubaczka and Nina Langer with the support of Angela Egert.

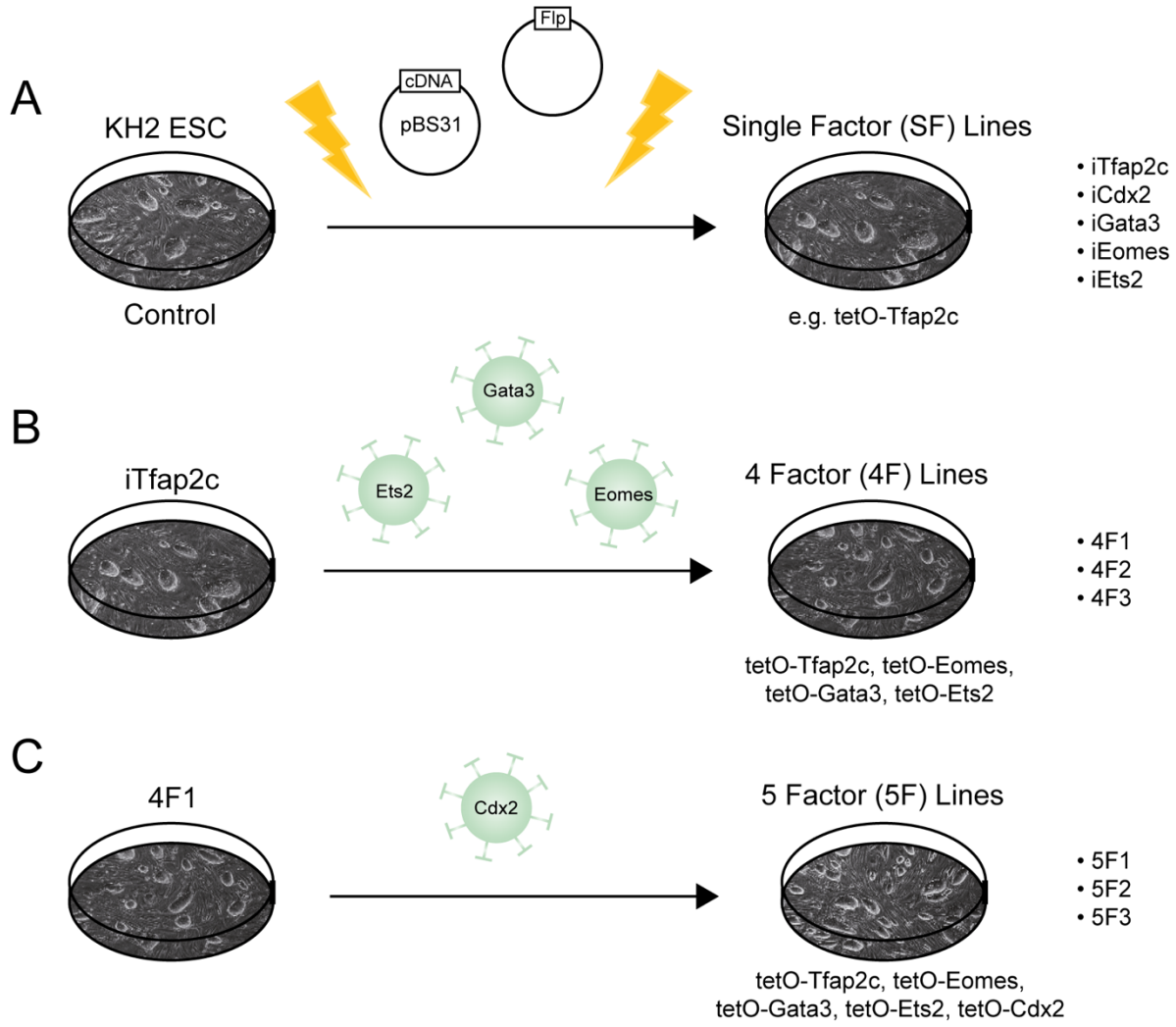

Figure 12: Schematic depicting generation of transgenic ESC lines
A. cDNA of individual transcription factors was introduced into KH2 ESC by electroporation – indicated by yellow lightning – and integrated into Col1a1 locus by Flp-mediated recombination, thereby generating single factor (SF) ESC lines. **B.** Lentiviral transduction of iTfap2c – indicated by schematic viruses – with additional transgenes *Eomes*, *Gata3* and *Ets2* resulted in generation of 4 factor (4F) clones. **C.** Further transduction of 4F1 with lentiviral vector encoding for *Cdx2* established 5 factor (5F) lines.

6.2 Validation of generated transgenic ESC lines

First, generated cell lines were validated concerning integration of the constructs into the genome as well as functionality by translation and transcription of transgenic DNA. To this end, genotyping PCR confirmed insertion of cDNA into the genome of all established cell clones (Figure 13). Single factors were verified for transgene integration into Col1a1 locus. Lentiviral

transduction leads to random integration and transgene primers spanning from vector backbone to cDNA were used for genotyping.

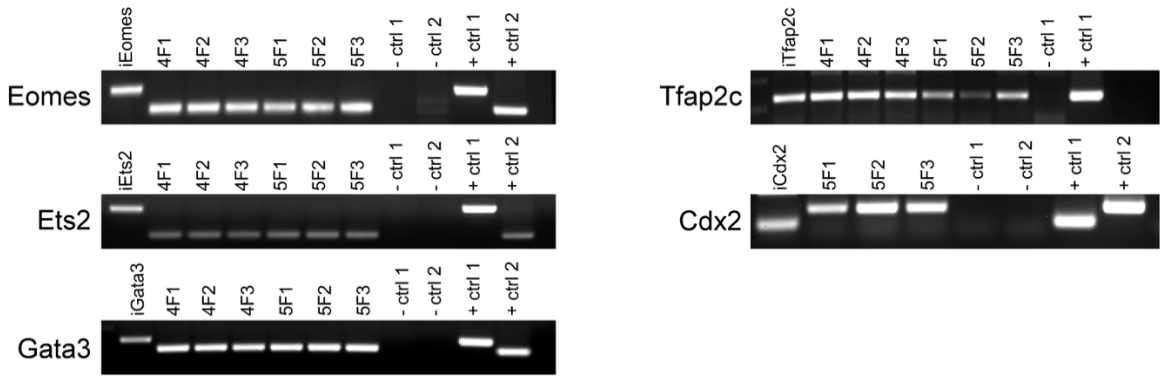

Figure 13: Genotyping PCR shows integration of transgenes in established ESC-lines
By using transgene flanking PCR primers, insertion of transgenes in ESC genome was verified. Modified from Kaiser et al., 2020a.

Induction of transgenes was performed by addition of doxycycline (2 µg/ml) to the culture medium for three days. Suffixes ^{TS} or ^{TX} indicate whether cell clones were cultured in TS medium or TX medium, respectively. After three days of transgene activation, transgene expression was detected using qRT-PCR. Expression was significantly higher for clones cultured with doxycycline than those without doxycycline administration (Figure 14 A-C). Interestingly, transgene expression was heterogenous in between 4F and 5F clones – indicating a varying number of lentiviral vector integrations into the genome or alterations due to transgene silencing (Figure 14 B and C). 4F3 showed lowest transgene expression for all four transgenes examined (Figure 14 B). Also, transgene expression was higher in clones cultured in TX^{+dox} medium than clones in TS^{+dox} medium. Presumably, this results from serum proteins contained in TS medium which were shown to inhibit doxycycline, thus lowering the amount of molecules available for rtTA binding and subsequent transgene activation (Riond and Riviere, 1989; Schmidt et al., 2008). Importantly, controls without doxycycline administration did not show induction of transgenes. Therefore, it can be assumed that once doxycycline is no longer administered to the medium, transgenes are inactivated.

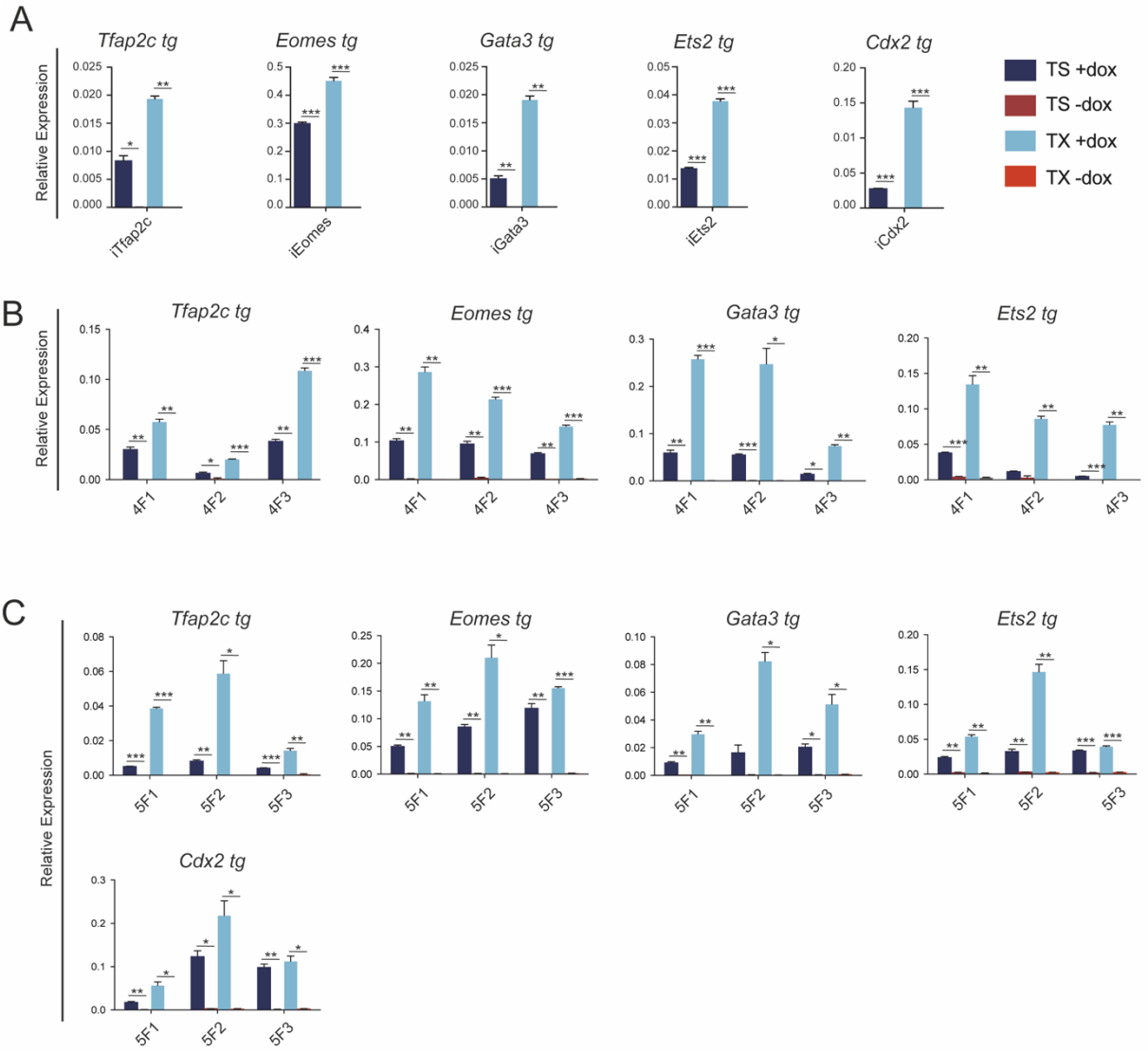

Figure 14: Transgene expression after three days of doxycycline administration
A. Transgene expression of single factors in SF lines iTfap2c, iEomes, iGata3, iEts2 and iCdx2 detected by qRT-PCR after three days of doxycycline administration in comparison to no doxycycline control. Cells were cultured in TS and TX medium. **B.** qRT-PCR analysis of transgene expression of *Tfap2c*, *Eomes*, *Gata3* and *Ets2* in 4F clones after three-day administration of doxycycline compared to no doxycycline control. 4F clones were cultured in TS or TX medium. **C.** qRT-PCR analysis of transgene expression of *Tfap2c*, *Eomes*, *Gata3*, *Ets2* and *Cdx2* in 5F clones after three-day administration of doxycycline compared to no doxycycline control. Again, cells were either cultured in TS or TX medium. RNA was obtained from three independent experiments. Expression was normalized to housekeeping genes *Gapdh* and *Pgk1*. Bars display mean value ± SEM. *p* values were calculated using unpaired *t*-test and are indicated with **p* < 0.05, ***p* < 0.01 and ****p* < 0.001. Modified from Kaiser et al., 2020a.

Finally, it was tested whether transgene induction resulted in an increase of respective protein levels using an immunofluorescence staining. In all clones, proteins levels of all transgenes were detectable after three days of doxycycline supplementation whereas ESCs without transgene activation remained negative for EOMES, GATA3, ETS2 and CDX2 (Figure 15 A-G). It was already shown that also ESC colonies show few TFAP2C positive cells, whereas in TSC colonies, all cells are TFAP2C positive (Kuckenberg et al., 2010). Also, in this study, KH2 cells showed TFAP2C positive cells. After doxycycline administration, a notable increase in TFAP2C positive cells per colony could be detected for all clones expressing transgenic *Tfap2c* (Figure 15 B, F and G).

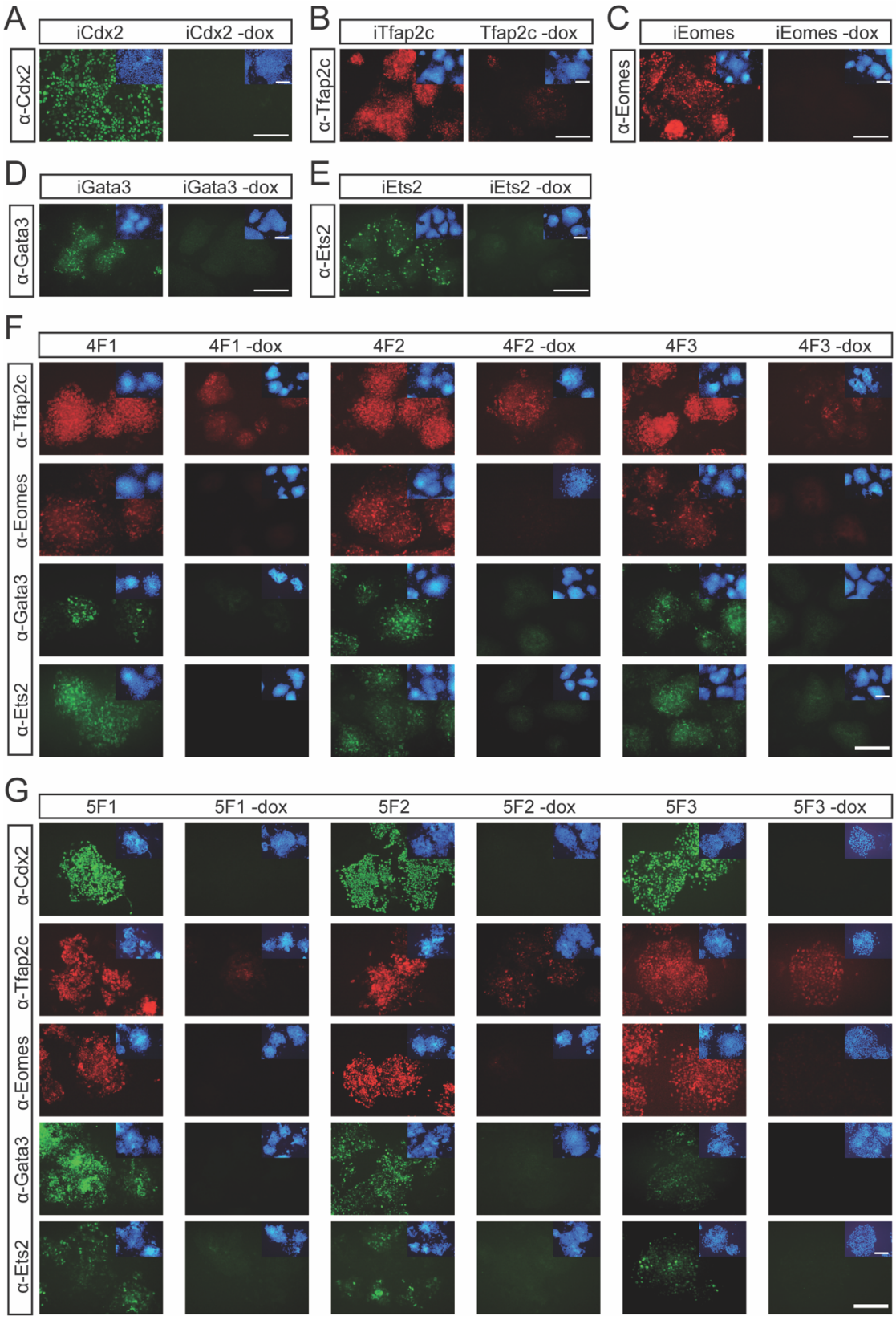

Figure 15: Protein levels after three days of doxycycline mediated transgene activation
A.-E. Immunofluorescence staining against CDX2 in iCdx2 clones (**A.**), against TFAP2C in iTfap2c clones (**B.**), against EOMES in iEomes clones (**C.**), against GATA3 in iGata3 clones (**D.**) and against ETS2 in iEts2 clones (**E.**). **F.** Immunofluorescence staining against TFAP2C, EOMES, GATA3 and ETS2 in 4F1, 4F2 and 4F3 clones. **G.** Immunofluorescence staining against TFAP2C, EOMES, GATA3, ETS2 and CDX2 in 5F1, 5F2 and 5F3 clones. All stainings were performed after three days of doxycycline mediated transgene induction in comparison to no doxycycline control. Insets display corresponding Hoechst staining. Scale bar: 250 µm. Modified from Kaiser et al., 2020a.

6.3 Induction of transgenes for ESC to TSC conversion

After validating the generated cell lines, the main objective was determining the combination of candidate transcription factors sufficient for a complete ESC to TSC conversion. To this end, doxycycline-mediated transgene expression was induced for three days. The corresponding experimental setup is depicted in Figure 16. Conversion approaches were performed in TS as well as in TX medium in order to assess the effect of environmental conditions created by the culture medium. On day -1, ESCs were seeded on gelatin-coated wells in ES medium without MEF feeder layer. On the next day, medium was changed to TS or TX medium supplemented with doxycycline (2 µg/ml). Doxycycline administration was continued for three days, thereafter clones were kept in respective medium without doxycycline and cultured up to passage 5.

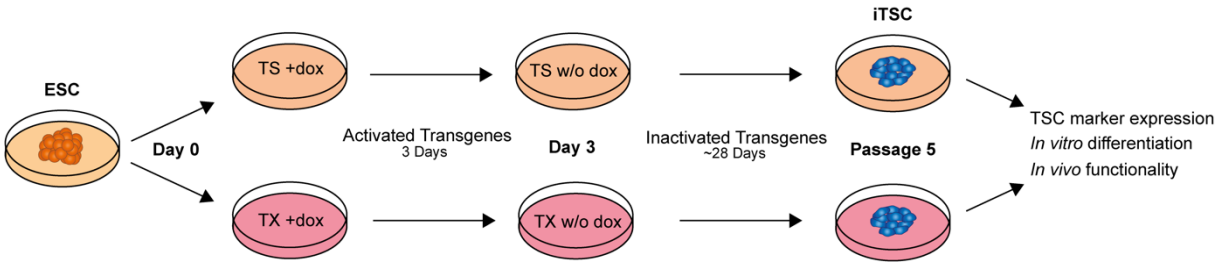

Figure 16: Schematic depicting ESC to TSC conversion protocol
ESCs were cultured feeder-free on gelatin coated wells in defined concentration and ES medium for 24 hours. On the following day, medium was changed for three days to fibroblast conditioned TS medium or chemically defined TX medium supplemented with doxycycline allowing for transgene induction. Starting from day 3, cells were continuously propagated to passage 5 in TS or TX medium without doxycycline administration. Clones were analyzed extensively on day 3 and at passage 5.

Splitting ratio and frequency as well as stable propagation differed between clones and medium condition (Table 31). While most 4F, 5F and iCdx2 induction approaches could be stably cultivated up to passage 5, remaining SF lines proved to be more susceptible to differentiation and apoptosis. Of note, iTfap2c, iGata3, iEomes and iEts2 could not be cultured in TX medium at all, similar to ESC control cells (Table 31). At passage 5, endpoint analyses comprised morphology analyses, detection of TSC surface markers, TSC marker expression, TSC methylation patterns, differentiation assays and an *in vivo* functionality assay (Figure 16).

Table 31: Percentage of clones that could be stably propagated up to passage 5
Modified from Kaiser et al., 2020a.

	4F	5F	iCdx2	iTfap2c	iEomes	iGata3	iEts2	ESC
TS	55	80	85	45	20	40	40	65
TX	80	95	95	0	0	0	0	0

6.4 Morphology of clones changes rapidly after transgene induction

First, morphology of clones undergoing conversion was assessed. After three days of transgene induction, cell clones cultured in TS medium lost the typical ESC appearance and already displayed a rather flat, epithelial like colony formation, which is characteristic of TSC

morphology (Figure 17 A-C). Cells undergoing conversion in TX medium were characterized by a dominant differentiation throughout all colonies independent of the transgene cocktail activated. The colonies seemed flatter and wider in size. However, while they lost the distinct ESC morphology, they were not yet showing TSC morphology. During subsequent passaging, 4F, 5F and iCdx2 clones could be propagated up to at least passage 5 in both culture conditions. At passage 5, $5F^{TS}$, $5F^{TX}$, $iCdx2^{TS}$ and $iCdx2^{TX}$ showed clear TSC morphology in both media conditions (Figure 17 B and C). 4F clones, however, showed TSC morphology in TX medium but reverted to clear ESC-like morphology in TS medium (Figure 17 A).

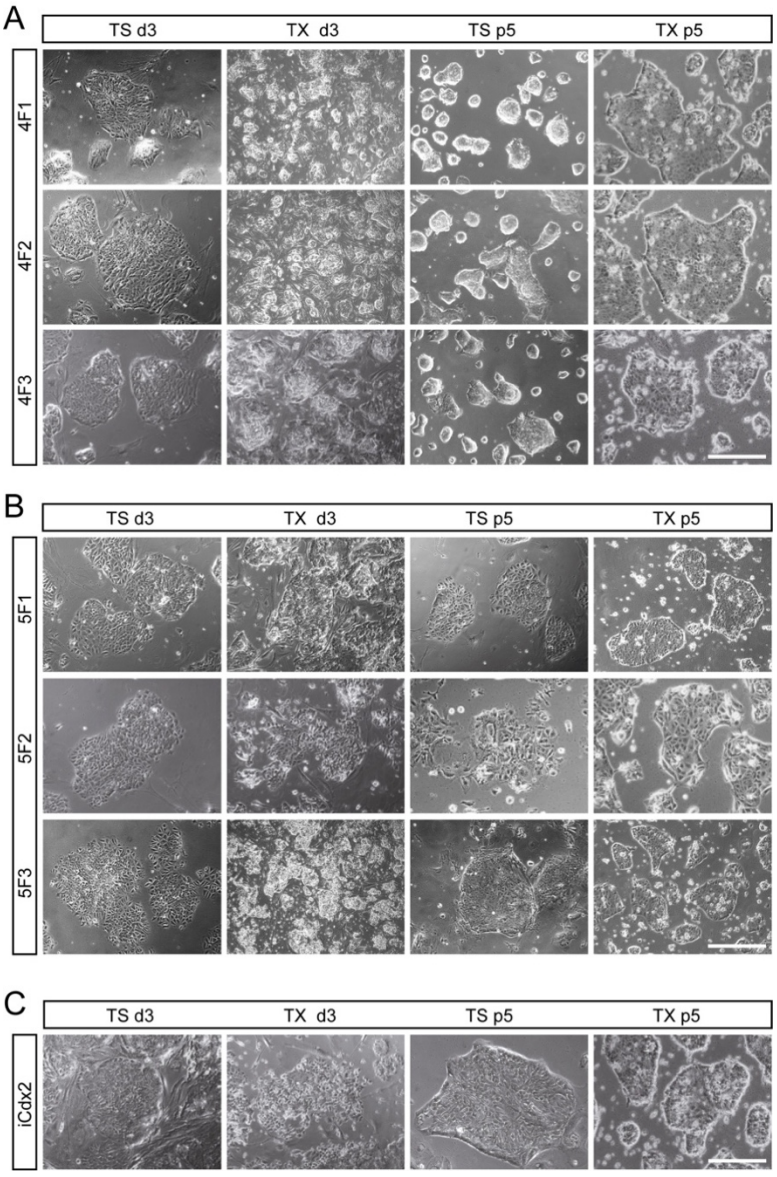

Figure 17: Transgene induction yields changed colony morphology
A. Representative photomicrographs of 4F1, 4F2 and 4F3 colonies after a three-day induction of transgenes and at passage 5 past transgene induction in TS and TX medium. **B.** Representative photomicrographs of 5F1, 5F2 and 5F3 cultured in TS and TX medium. Images depict morphology after three days of transgene induction and at passage 5. **C.** Representative photomicrographs of iCdx2 clones on day 3 and at passage 5. Clones were cultured TS and TX medium. Scale bar: 250 µm. Modified from Kaiser et al., 2020a.

6.5 OCT4 is downregulated fastest in response to transgenic *Cdx2* expression

While ESCs exhibit pluripotency which is maintained by a transcription factor network revolving around OCT4, TSCs are multipotent and OCT4 negative. Consequently, it stands to reason that during ESC to TSC conversion, OCT4 is required to be downregulated. Thus, OCT4 levels were monitored during the first eight days of conversion for 4F3, 5F2 and iCdx2 clones in

comparison to ESC control cells (Figure 18). Clones were cultivated in TS or TX medium containing doxycycline for three days with subsequent culture without doxycycline up to day 8. Proteins were isolated every other day and OCT4 levels detected using Western Blotting.

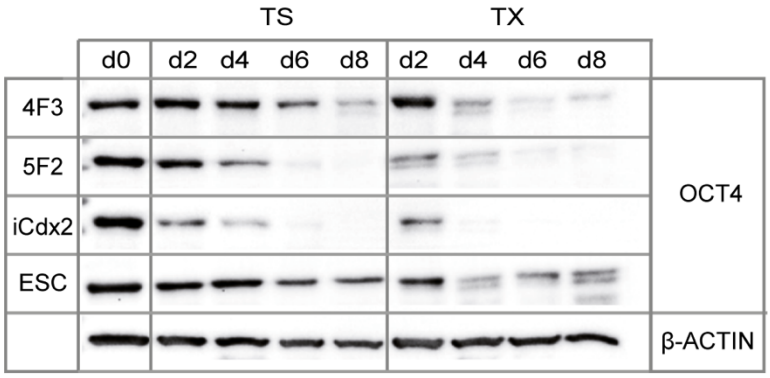

Figure 18: Monitoring of OCT4 levels during first days of conversion
4F3, 5F2, iCdx2 clones as well as control ESCs were cultured in TS/TX medium supplemented with doxycycline followed by a 5-day culture in respective medium w/o doxycycline. Protein was isolated every other day and OCT4 levels were detected by Western Blotting on day 2, day 4, day 6 and day 8 of the conversion in comparison to housekeeping control β-ACTIN. Modified from Kaiser et al., 2020a.

All clones presented with strong OCT4 levels on day 0 when still being cultured in LIF-containing ES medium (Figure 18). A time-dependent decrease of OCT4 levels was detected for all clones examined, however, to differing extent. 4F3 clone showed the slowest downregulation which became apparent on day 6 in TS and on day 4 in TX medium but detectable OCT4 levels were maintained up to day 8 under both conditions. 5F2 clones exhibited diminishing OCT4 levels already on day 4 in TS medium and as early as day 2 in TX medium. The fastest OCT4 downregulation concluding in complete loss of the protein was detected for iCdx2 clones. On day 8 in TS and from day 6 in TX medium, OCT4 protein was undetectable. As CDX2 activity is essential for OCT4 downregulation, transgenic *Cdx2* expression in 5F and iCdx2 clones resulted in quicker downregulation than in 4F clones where endogenous *Cdx2* needed to be induced via the four transgenes first – resulting in a temporal delay of OCT4 repression. Interestingly, culture in TX medium led to a quicker OCT4 downregulation than TS cultivation for all three clones. Control ESCs remained with OCT4 levels up to day 8 under both conditions, yet levels were decreasing from day 6 in TS and from day 4 in TX medium due to the loss of LIF supplementation. It can be assumed that transgene combinations which result in sufficient OCT4 downregulation hold the best chances for a complete ESC to TSC conversion as they counteract the ESC transcription factor network most efficiently. Conversion in 4F clones might take longer as they have to induce endogenous *Cdx2* expression first.

6.6 Cell surface markers CD40 and PLET1 are increasing past transgene induction

Cell surface proteins CD40 and PLET1 were described as TSC specific markers. CD40 was shown to be expressed on TSCs but not on ESCs whereas PLET1 levels are characterized by a biphasic expression pattern in the course of trophoblast differentiation which peaks at the stage of undifferentiated TSCs (Murray et al., 2016; Rugg-Gunn et al., 2012). Levels of both

markers were analyzed on day 3 and at passage 5 for 4F, 5F and iCdx2 clones as well as ESC and TSC control cells (Figure 19). On day 3, transgene induction yielded upregulation of both markers in TS and TX medium in all 4F, 5F and iCdx2 clones (Figure 19 A-C). However, wildtype TSC levels were still significantly higher than in converting clones. Surprisingly, $4F1^{TS}$ and $4F2^{TS}$ showed high levels of double positive cells. Levels were analyzed an additional time after five passages in the respective medium. $4F^{TS}$ clones displayed lower levels than on day 3, now resembling control ESC levels indicating a reversion to ESC state (Figure 19 A). $4F^{TX}$, $5F^{TS}$, $5F^{TX}$ and $iCdx2^{TS}$ and $iCdx2^{TX}$ showed higher levels of double positive cells than on day 3, which were in the range of wildtype TSC levels (Figure 19 A-C). Interestingly, this suggests a continuing conversion past transgene induction. $5F3^{TX}$ and $iCdx2^{TX}$ showed slightly lower levels of double positive cells than remaining $5F1^{TX}$ and $5F2F^{TX}$, however, CD40 positive cells comprised 97% in $5F3^{TX}$ and 99% in $iCdx2^{TX}$ indicating that only PLET1 levels were reduced in comparison to control TSCs.

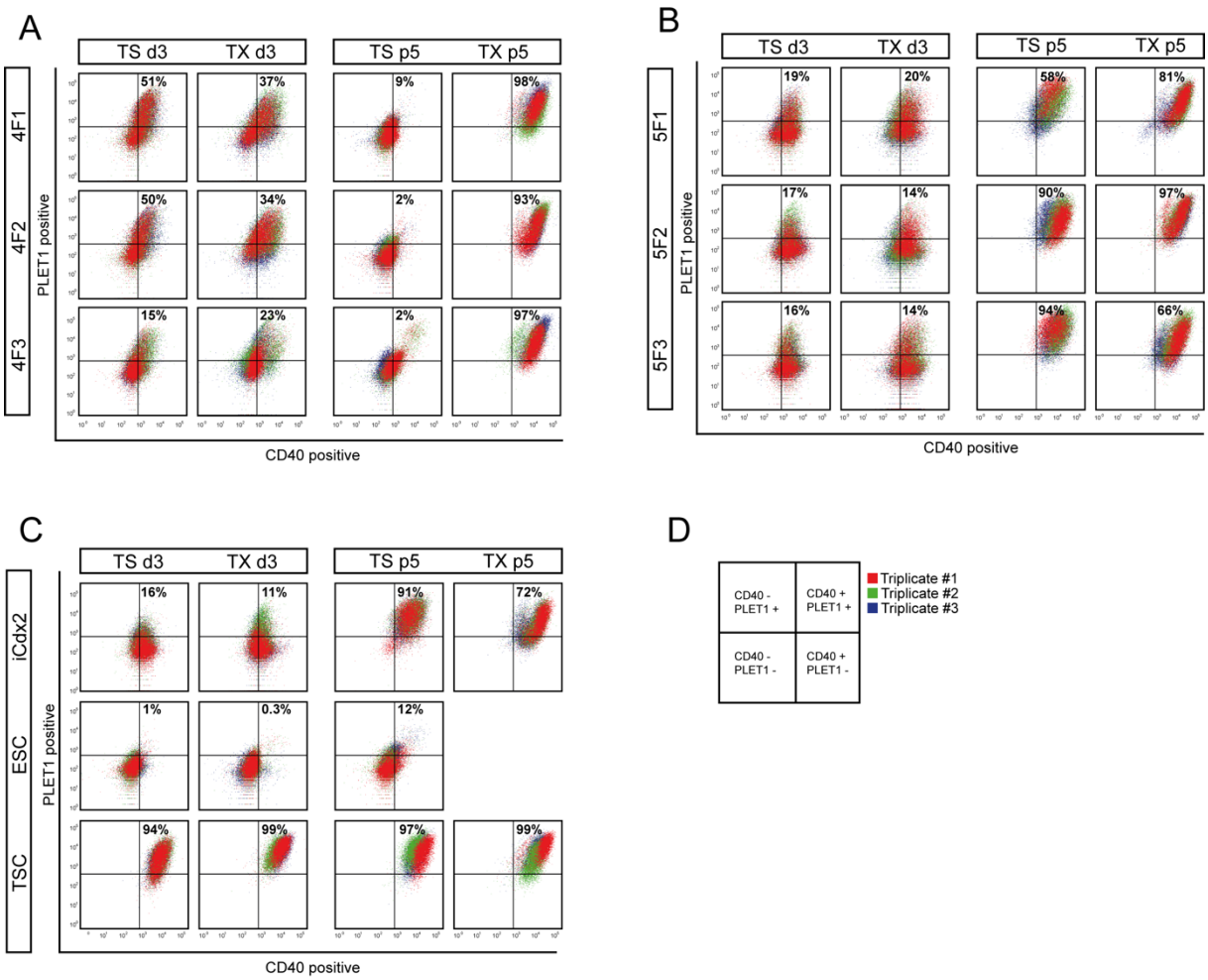

Figure 19: CD40 and PLET1 levels increase with subsequent cultivation
Flow cytometry analysis of TSC surface markers CD40 and PLET1 **A.** Levels of CD40 and PLET1 in 4F clones cultured in TS and TX medium on day 3 and at passage 5. **B.** CD40 and PLET1 levels in 5F clones on day 3 and at passage 5. Clones were cultured in TS or TX medium. **C.** CD40 and PLET1 positive cells in iCdx2, ESC and TSC cells cultured in TS or TX medium on day 3 and at passage 5. **D.** Legend for visualization of flow cytometric data. Percentages indicate CD40 and PLET1 double positive cells. Analysis was performed with samples from three independent experiments. Modified from Kaiser et al., 2020a.

6.7 Endogenous expression of TSC markers higher in TX medium

Key TSC transcription factors include ELF5, CDX2, EOMES and TFAP2C. To further characterize established clones during (day 3) and past conversion (passage 5), the endogenous expression levels of those markers were explored using qRT-PCR. RNA was isolated from all 4F, 5F, iCdx2 and control ESCs as well as TSCs on day 3 and at passage 5. On day 3, all clones examined showed an upregulation of marker expression in comparison to control ESCs. Yet, wildtype TSC expression levels were significantly higher. Of note, expression of *Elf5* and *Eomes* was significantly higher in TX medium than in TS medium cultured clones for all samples (Figure 20). The same could be observed for the expression of *Cdx2* and *Tfap2c* in most clones. Interestingly, at this point it became apparent that the TSC transcription factor network was initiated by expression of transgenes. Even though $4F^{TS}$ and $4F^{TX}$ clones did not include transgenic *Cdx2* expression, they still displayed an equivalent upregulation of endogenous *Cdx2* in comparison to 5F and iCdx2 clones. In iCdx2 clones, endogenous *Elf5*, *Eomes* and *Tfap2c* expression was induced to a similar extent as in 5F clones. This strengthens previous findings that CDX2 is involved upstream of ELF5, TFAP2C and EOMES in the transcription factor network and can activate their expression intrinsically (Beck et al., 1995; Niwa et al., 2005).

As flow cytometry analyses revealed an ongoing conversion past transgene induction, marker expression was again analyzed at passage 5. In comparison to transcript levels on day 3, an upregulation for *Elf5*, *Cdx2* and *Eomes* for clones cultured in TX medium was observed (Figure 20). Levels were now comparable to those of control TSCs. Similar to day 3, expression in TX cultured clones was significantly higher than for respective clones cultured in TS medium. While $4F^{TS}$ displayed no expression of *Elf5*, *Cdx2* and *Eomes*, $5F^{TS}$ and $iCdx2^{TS}$ showed at least low expression levels of respective genes. For all clones, *Cdx2* expression remained below levels detected for bona fide TSCs. It was significantly higher in $4F^{TX}$ than $4F^{TS}$, but equivalent in $5F^{TS}$ and $5F^{TX}$ as well as $iCdx2^{TS}$ and $iCdx2^{TX}$. $5F3^{TS}$ showed significantly higher *Cdx2* expression than $5F3^{TX}$. 4F and iCdx2 clones displayed significantly higher levels of *Tfap2c* when cultured in TX medium which were comparable to wildtype TSC levels. $5F^{TS}$, $5F^{TX}$ and $iCdx2^{TS}$ demonstrated increased *Tfap2c* expression compared to day 3 but levels remained below those of bona fide TSCs. Interestingly, transcript analyses confirm the previous finding of ongoing conversion past transgene induction. In the end, this persistent process results in a TSC-like expression pattern for all clones except for $4F^{TS}$. In conclusion, data obtained from morphology, cell surface protein and gene expression analyses suggest that an induction of TSC fate had taken place in $4F^{TX}$, $5F^{TS}$, $5F^{TX}$, $iCdx2^{TS}$ and $iCdx2^{TX}$. Even though $4F^{TS}$ showed an initial response to transgene activation on day 3, morphology and marker expression relapsed into an ESC-like state at passage 5.

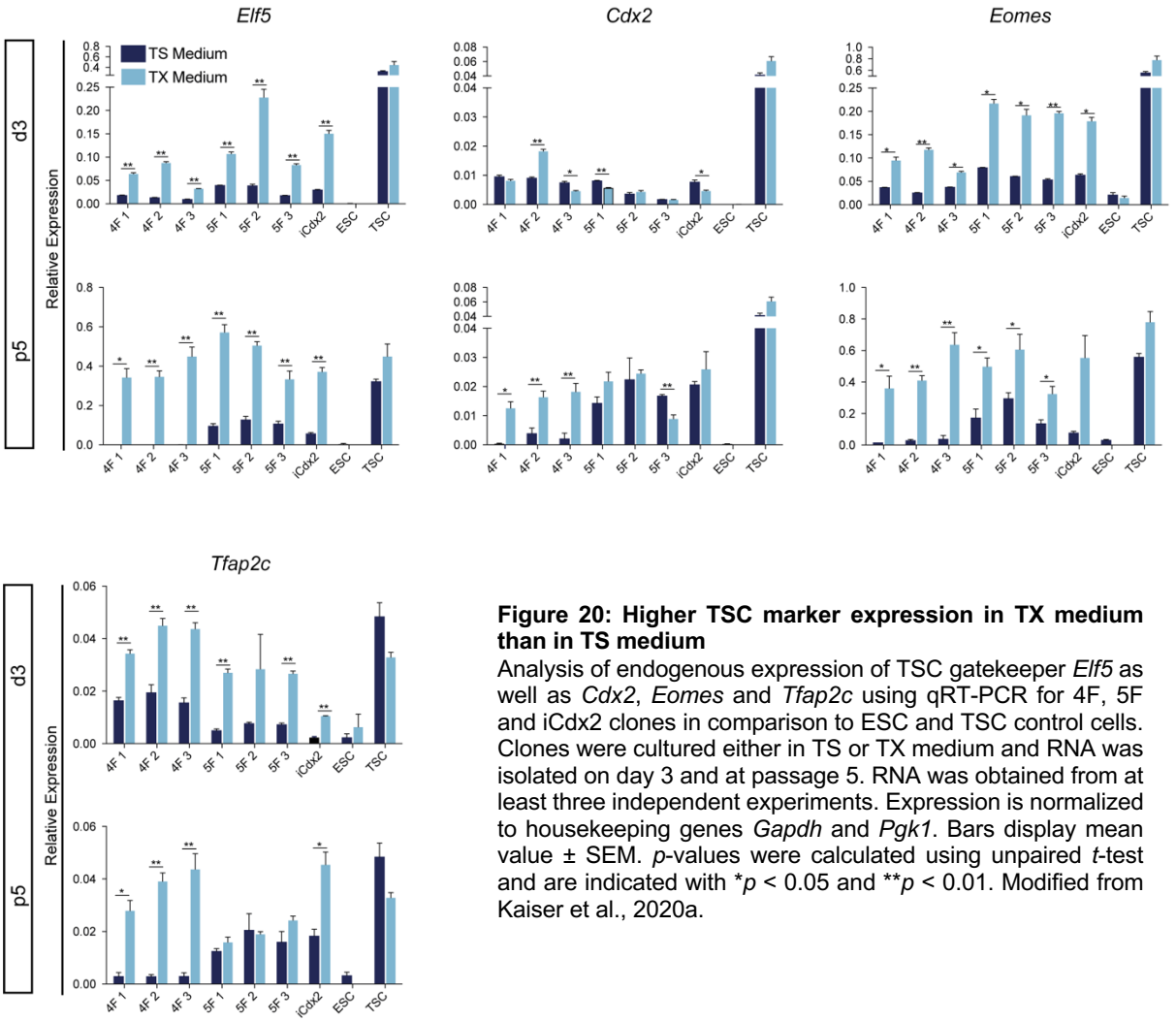

Figure 20: Higher TSC marker expression in TX medium than in TS medium
Analysis of endogenous expression of TSC gatekeeper *Elf5* as well as *Cdx2*, *Eomes* and *Tfap2c* using qRT-PCR for 4F, 5F and iCdx2 clones in comparison to ESC and TSC control cells. Clones were cultured either in TS or TX medium and RNA was isolated on day 3 and at passage 5. RNA was obtained from at least three independent experiments. Expression is normalized to housekeeping genes *Gapdh* and *Pgk1*. Bars display mean value ± SEM. *p*-values were calculated using unpaired *t*-test and are indicated with **p* < 0.05 and ***p* < 0.01. Modified from Kaiser et al., 2020a.

6.8 Activation of remaining single factors does not induce TSC-fate

In contrast to 4F, 5F and iCdx2 clones, the remaining SF clones iEomes, iGata3 and iEts2 did not result in stable induction of TSC fate. On day 3, first analyses revealed morphology of iTfap2c^{TS}, iTfap2c^{TX} and iEomes^{TS} to be comparable to ESC control cells (Figure 21 A). iGata3^{TS} and iGata3^{TX} as well as iEts2^{TS} were characterized by an epithelial-like appearance. iEomes, iEts2 and ESC cultured in TX medium showed occurrence of severe differentiation. At passage 5, SF lines iEomes^{TS} and iEts2^{TS} remained with ESC-like morphology similar to ESC control cells while iTfap2c^{TS} and iGata3^{TS} appearance was neither alike ESCs nor TSCs (Figure 21 A). In TX medium, these SF cell lines could not be stably propagated comparable to control ESCs. Within the first two passages, they differentiated, ceased proliferation, or underwent apoptosis. Also, CD40 and PLET levels detected on day 3 were not increased in iTfap2c, iEomes and iEts2 – neither in TS nor in TX medium (Figure 21 B). Only iGata3 showed an increase in levels of double positive cells. Additionally, SF lines did not show an upregulation in transcript levels of *Elf5*, *Cdx2*, *Eomes* and *Tfap2c* on day 3 (Figure 21 A-C). Preliminary molecular analyses of TS-cultured SF lines at passage 5 revealed that no stable

increase in TSC marker levels was achieved and clones remained ESC-like (data not shown). Taken together these results clearly indicate that a conversion to TSC fate did not occur following a three-day induction of transgenes in SF lines iTfap2c, iEomes, iGata3 and iEts2.

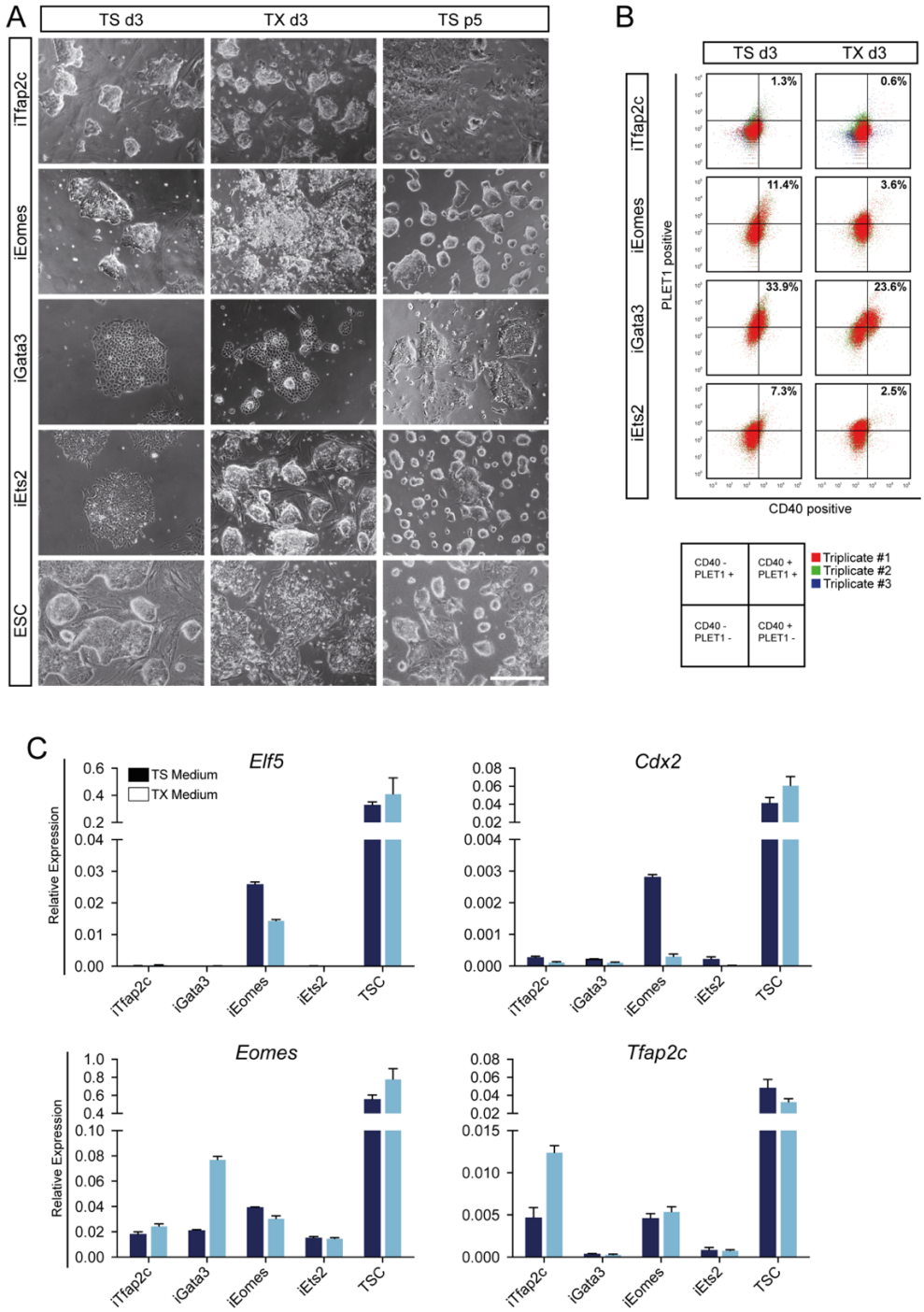

Figure 21: Analysis of conversion approaches using remaining single factor lines
A. Representative photomicrographs of iTfap2c, iGata3, iEomes and iEts2 depicting colony morphology on day 3 in TS or TX medium and at passage 5 in TS medium (Scale bar: 250 µm). **B.** Flow cytometry analysis of CD40 and PLET1 positive cells in iTfap2c, iGata3, iEomes and iEts2 on day 3. Clones were cultured in either TS or TX medium supplemented with doxycycline. Flow cytometry analysis was performed with samples from at least two independent experiments. Percentages indicate CD40 and PLET1 double positive cells within the upper right gate. **C.** qRT-PCR analysis of endogenous expression of TSC marker *Elf5*, *Cdx2*, *Eomes* and *Tfap2c* for iTfap2c, iGata3, iEomes and iEts2 in comparison to TSC control cells on day 3. Clones were cultured either in TS or TX medium supplemented with doxycycline. RNA was obtained from at least three independent experiments. Expression is normalized to housekeeping genes *Gapdh* and *Pgk1*. Bars display mean value ± SEM. Modified from Kaiser et al., 2020a.

6.9 CDX2 and TFAP2C positive colonies in $4F^{TX}$, $5F^{TS}$, $5F^{TX}$, $iCdx2^{TS}$ and $iCdx2^{TX}$

As endogenous expression of *Cdx2* and *Tfap2c* at passage 5 remained low in comparison to wildtype TSCs, immunofluorescence staining against CDX2 and TFAP2C was carried out to verify the presence of the respective proteins within the colonies. $4F^{TX}$, $5F^{TS}$, $5F^{TX}$, $iCdx2^{TS}$ and $iCdx2^{TX}$ unanimously showed colonies positive for CDX2 and TFAP2C that in terms of quality and pattern did not vary from control TSCs (Figure 22 A-F). CDX2 positive cells were scarce in $4F^{TS}$ colonies while TFAP2C positive cells could be found to a similar extent as in control ESC (Figure 22 A and B). This coincides with data obtained from transcript level analyses (Figure 20). Importantly, 4F and ESC control cells remained negative for OCT4 after five passages in TS medium (Figure 22 G).

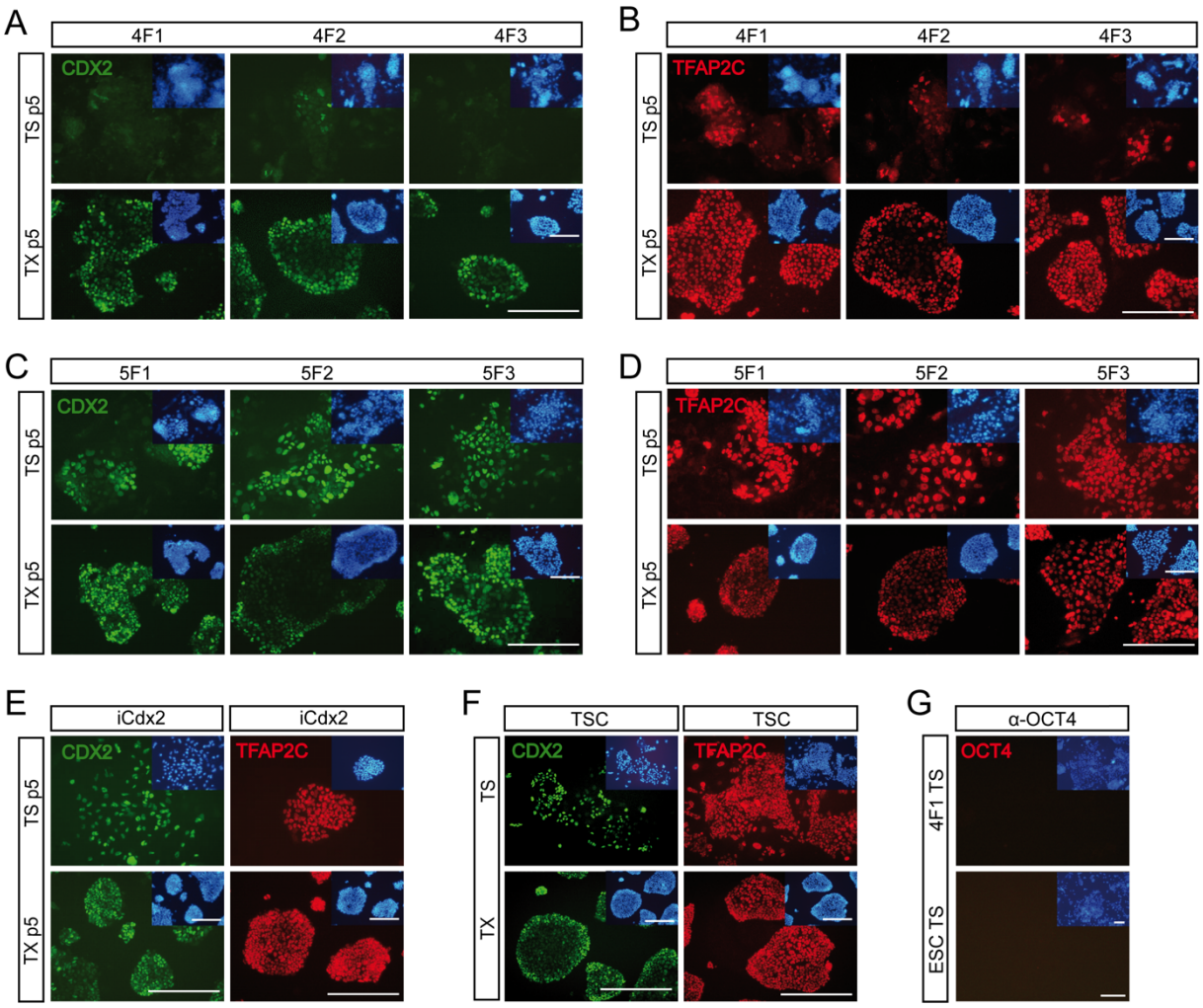

Figure 22: Presence of endogenous CDX2 and TFAP2C in converted clones
A.+B. Immunofluorescence staining against CDX2 (**A.**) and TFAP2C (**B.**) in 4F clones cultured in TS and TX medium at passage 5. **C.+D.** Immunofluorescence staining against CDX2 (**C.**) and TFAP2C (**D.**) in 5F clones cultured in TS and TX medium at passage 5. **E.** Immunofluorescence staining against CDX2 and TFAP2C in iCdx2 clones cultured in TS and TX medium at passage 5. **F.** Immunofluorescence staining against CDX2 and TFAP2C in TSC control cells cultured in TS and TX medium **G.** Immunofluorescence staining against OCT4 in 4F1 clone and ESC control cells at passage 5 cultured in TS medium. Insets in A.-G. display corresponding Hoechst staining, scale bar represents 250 µm. Modified from Kaiser et al., 2020a.

6.10 TSC methylation pattern indicates complete conversion to TSC fate

Next, methylation status of *Elf5, Oct4* and *Nanog* promoter was analyzed. The *Elf5* promoter holds a differentially methylated region that is hypomethylated in TSCs and hypermethylated in ESCs (Ng et al., 2008). Accordingly, *Elf5* is repressed in ESCs and expressed in TSCs. Previously, it was shown that even though TSC markers were upregulated, ESC to TSC conversion remained incomplete due to an epigenetic memory of ESCs in TSC-like cells (Cambuli et al., 2014). Subsequently, *Elf5* promoter methylation was assessed for 4F, 5F and iCdx2 clones at passage 5.

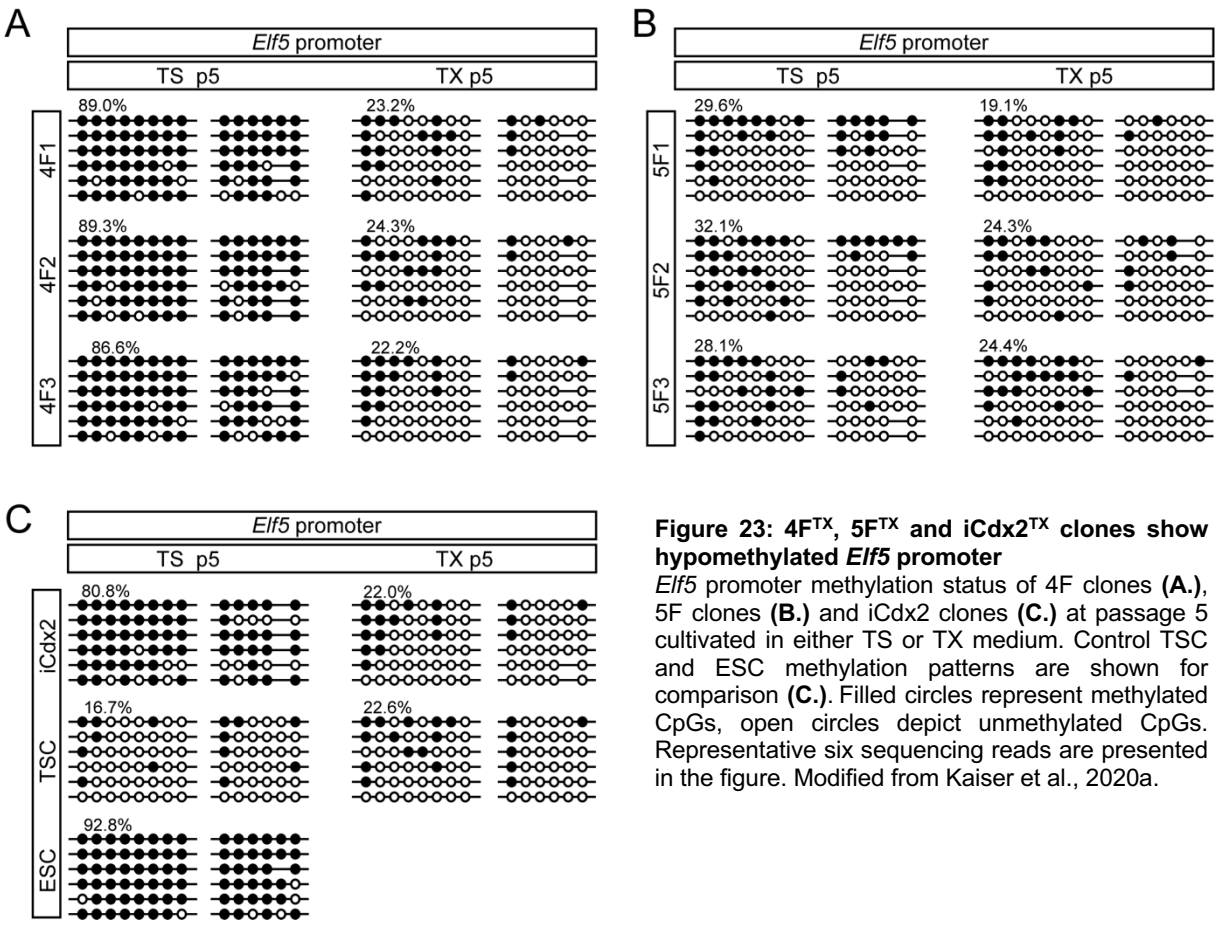

Figure 23: 4F^{TX}, 5F^{TX} and iCdx2^{TX} clones show hypomethylated *Elf5* promoter
Elf5 promoter methylation status of 4F clones **(A.)**, 5F clones **(B.)** and iCdx2 clones **(C.)** at passage 5 cultivated in either TS or TX medium. Control TSC and ESC methylation patterns are shown for comparison **(C.)**. Filled circles represent methylated CpGs, open circles depict unmethylated CpGs. Representative six sequencing reads are presented in the figure. Modified from Kaiser et al., 2020a.

All 4F clones and iCdx2 cultured in TS medium retained an ESC-like methylation pattern as the *Elf5* promoter remained hypermethylated (Figure 23 A and C). The same clones cultured in TX medium displayed a hypomethylated region. Surprisingly, all 5F clones showed a hypomethylated promoter independent of culture conditions (Figure 23 B). Similar to the *Elf5* promoter, *Oct4* promoter and *Nanog* promoter too are differentially methylated in ESCs and TSCs, though, here the respective regions are hypomethylated in ESCs and hypermethylated in TSCs (Kuckenberg et al., 2011). Next, 4F3, 5F2 and iCdx2 clones were analyzed for the methylation status of *Oct4* and *Nanog* promoter. Corresponding to *Elf5* promoter findings, 4F^{TS} and iCdx2^{TS} retained a methylation pattern reminiscent of ESCs – both promoter regions

remained hypomethylated (Figure 24 A and B). $4F^{TX}$, $5F^{TS}$, $5F^{TX}$ and $iCdx2^{TX}$ displayed a hypermethylation of both regions similar to wildtype TSCs further reinforcing the complete conversion taking place in these clones.

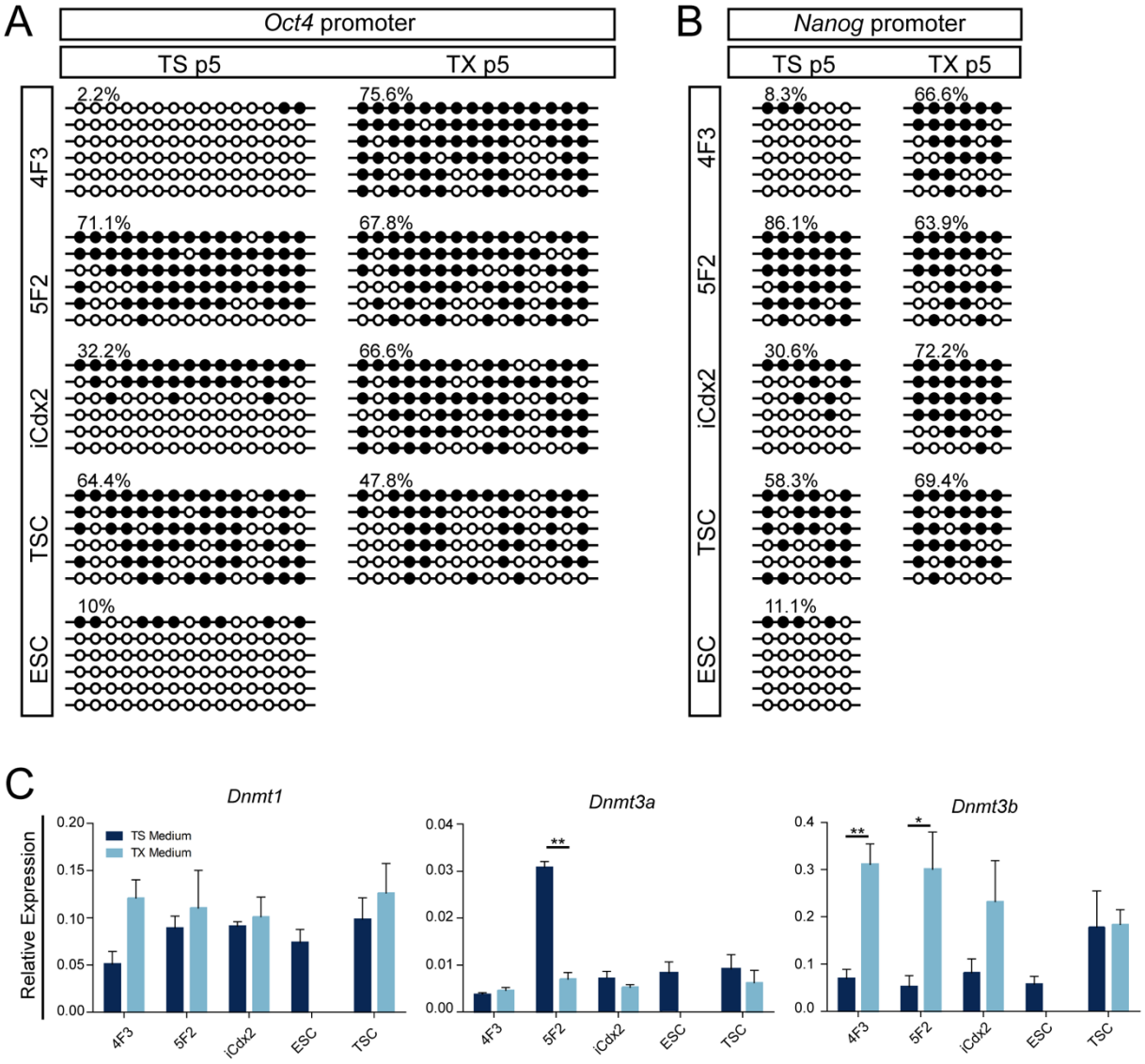

Figure 24: *Oct4* and *Nanog* promoter display TSC methylation in TX clones
A. *Oct4* promoter methylation status of 4F3, 5F2 and iCdx2 cultured in TS and TX medium. **B.** Methylation status of *Nanog* promoter of 4F3, 5F2 and iCdx2 cultured in TS and TX medium. Filled circles represent methylated CpGs, open circles depict unmethylated CpGs. Representative six sequencing reads are presented in the figure. **C.** qRT-PCR analysis of *Dnmt1*, *Dnmt3a* and *Dnmt3b* expression levels of 4F3, 5F2 and iCdx2 clones at passage 5 cultured in TS or TX medium. RNA was obtained from at least three independent experiments. Expression is normalized to housekeeping genes *Gapdh* and *Pgk1*. Bars display mean value ± SEM. *p* values were calculated using unpaired *t*-test and are indicated with **p* < 0.05 and ***p* < 0.01. Modified from Kaiser et al., 2020a.

Of note, these results demonstrated that the DNA was not only demethylated in the course of the conversion, but DNA methylation patterns were newly established. The transfer of methyl groups to cytosines is mediated by DNA methyltransferases (DNMTs). To investigate whether a change in methylation was associated with DNMT transcript levels, expression of *Dnmt1*, *Dnmt3a* and *Dnmt3b* was examined next in 4F3, 5F2 and iCdx2 clones at passage 5 as well

as in control ESCs and TSCs (Figure 24 C). Transcript levels of DNMT1 which ensures the maintenance of methylation patterns were akin – independent of cell lines and culture condition. Interestingly, high expression levels of *Dnmt3a* and *Dnmt3b* which are introducing *de novo* methylation were found in those clones that showed hypermethylation of *Oct4* and *Nanog* promoter at passage 5. *Dnmt3a* was significantly higher expressed in $5F2^{TS}$ than in $5F2^{TX}$ and control TSC. Other clones showed low expression levels comparable to control TSC. $4F3^{TX}$, $5F2^{TX}$ and $iCdx2^{TX}$ showed higher expression of *Dnmt3b* than respective clones cultured in TS medium (Figure 24 C).

Taken together, these results demonstrate that $4F^{TS}$ and $iCdx2^{TS}$ did not completely convert to TSC fate. When cultured in TX medium, however, these clones showed a full conversion, indicating the importance of environmental conditions for reprogramming approaches. 5F clones displayed TSC methylation pattern independent of culture conditions indicating the importance of transgenes activated.

6.11 Upregulation of markers driven by differentially methylated promoters in TX clones

Recently, a study showed that *Elf5*, *Oct4* and *Nanog* promoters do not represent the only differentially methylated loci between ESCs and TSCs (Cambuli et al., 2014). The authors could introduce nine additional genes promoters that are hypermethylated in ESCs but hypomethylated in TSCs. Hence, transcript levels of supplementary markers *Tead4, Ezrin, Hand1, Lasp1, Map3k8, Plet1, Rin3, Sh2d3c* and *Tinagl* were assessed next for 4F, 5F and iCdx2 clones in both culture conditions at passage 5 (Figure 25). Expression was induced extensively for most markers in $4F^{TX}$, $5F^{TS}$, $5F^{TX}$, $iCdx2^{TS}$ and $iCdx2^{TX}$ and levels were comparable to TSC levels. $4F^{TX}$ clones showed significantly higher levels than $4F^{TS}$ clones for all transcripts analyzed except *Hand1*. It can be assumed that the respective promoter regions became hypomethylated during the course of conversion thereby allowing expression of respective genes detected in this experiment.

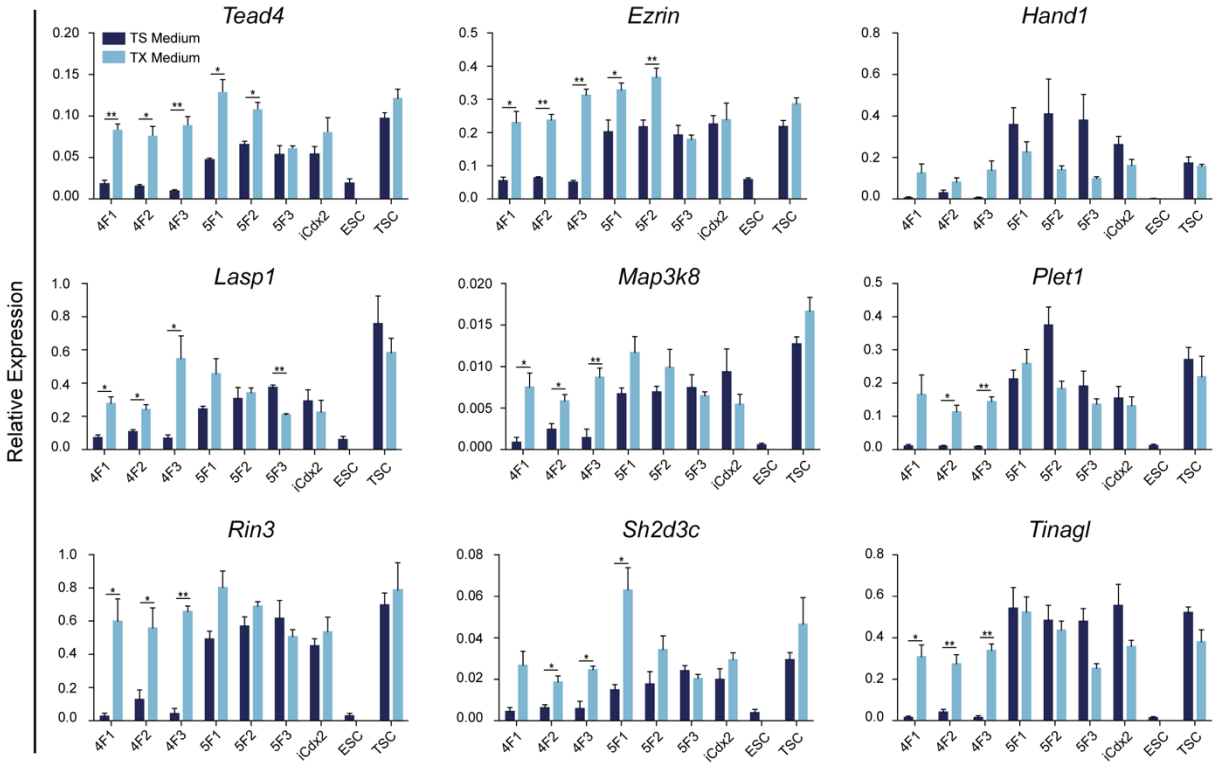

Figure 25: Additional TSC marker show higher expression in TX than in TS medium
qRT-PCR analysis of endogenous expression of TSC marker *Tead4*, *Ezrin*, *Hand1*, *Lasp1*, *Map3k8*, *Plet1*, *Rin3*, *Sh2d3c* and *Tinagl* in 4F, 5F and iCdx2 clones in comparison to ESC and TSC control cells at passage 5. Clones were cultured either in TS or TX medium after three-day induction of transgenes. RNA was obtained from at least three independent experiments. Expression is normalized to housekeeping genes *Gapdh* and *Pgk1*. Bars display mean value ± SEM. Significance was determined by unpaired *t*-test and indicated with $*p < 0.05$ and $**p < 0.01$. Modified from Kaiser et al., 2020a.

6.12 Success of conversion in TX medium is not caused by MAPK or TGFβ signaling

When considering the data obtained as of yet, it is evident that TX medium influenced the ESC to TSC conversion severely, as 4F and iCdx2 clones showed TSC methylation pattern in TX medium only. Presumably, medium components or the concentration thereof in the TX medium could impinge on signaling pathways within the converting cell and thereby promoting TSC fate. On the other hand, unknown factors secreted by fibroblasts in the conditioned medium could inhibit certain TSC pathways. To elucidate this question, two prominent pathways in TSCs, MAPK signaling and TGFβ signaling were examined (Figure 26). Proteins were isolated from cell lysates of iCdx2 cells at passage 8 converted in TS and TX medium as well as TSC control cells from both conditions. Signaling cascades were investigated using a phosphorylation array for MAPK and a protein array for proteins involved in the TGFβ pathway (Figure 26 A and B). However, quantification of signal densities showed no difference between medium conditions regarding phosphorylation in MAPK pathway or protein levels of TGFβ pathway (Figure 26 C and D).

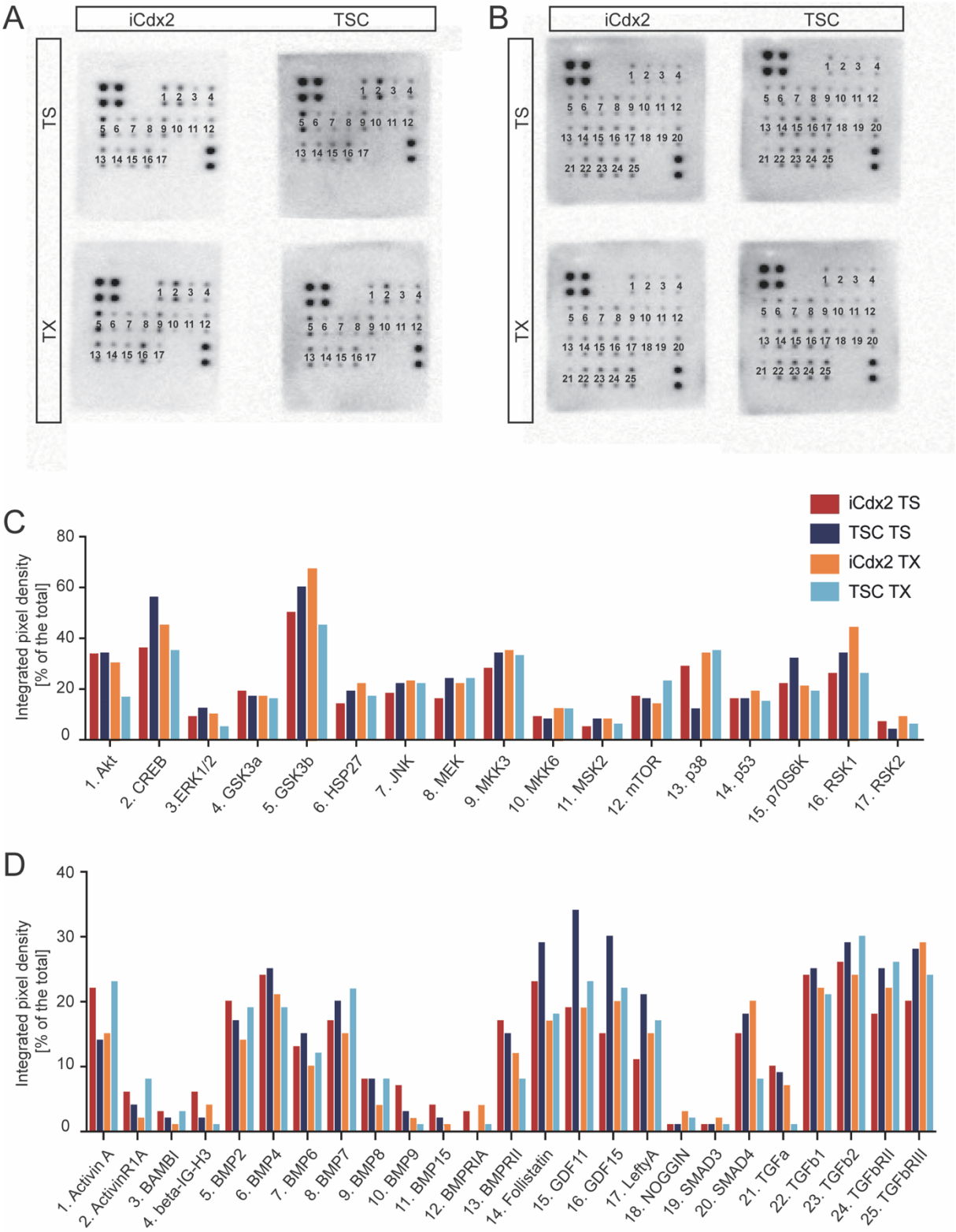

Figure 26: Pathway analysis reveals no difference between TS and TX culture
A. Phosphorylation Array of phosphorylated proteins involved in MAPK pathway in iCdx2^{TS} and iCdx2^{TX} cells compared to wildtype TSC^{TS} and TSC^{TX}. Proteins were analyzed in duplicates. **B.** TGFβ Array of proteins involved in TGFβ pathway in iCdx2^{TS} and iCdx2^{TX} cells compared to wildtype TSC^{TS} and TSC^{TX}. Proteins were analyzed in duplicates. **C.** Signal density quantification of phosphorylated MAPK pathway proteins. **D.** Signal density quantification of TGFβ pathway proteins. Modified from Kaiser et al., 2020a.

6.13 4F3^{TX}, 5F2^{TX} and iCdx2^{TX} self-renew *in vitro*

Important characteristics of stem cells comprise unlimited self-renewal as well as differentiation along their respective lineage. 4F3^{TX}, 5F2^{TX} and iCdx2^{TX} were thus tested for long-term stability and *in vitro* differentiation into trophoblast subtypes. First, long-term stability was assessed by cultivating the clones for about five months up to passage 38 in TX medium. At passage 38, cells were analyzed for morphology, gene expression and protein levels of known TSC markers. The three clones remained with distinct TSC morphology (Figure 27 A). Neither cell proliferation nor level of differentiation altered over the course of time. Also, colonies remained positive for CDX2, EOMES and TFAP2C (Figure 27 A). Gene expression analyses revealed high levels of *Elf5*, *Cdx2*, *Eomes* and *Tfap2c* comparable to levels detected at passage 5 indicating a stable transcription process and showing long-term stability of clones examined (Figure 27 B).

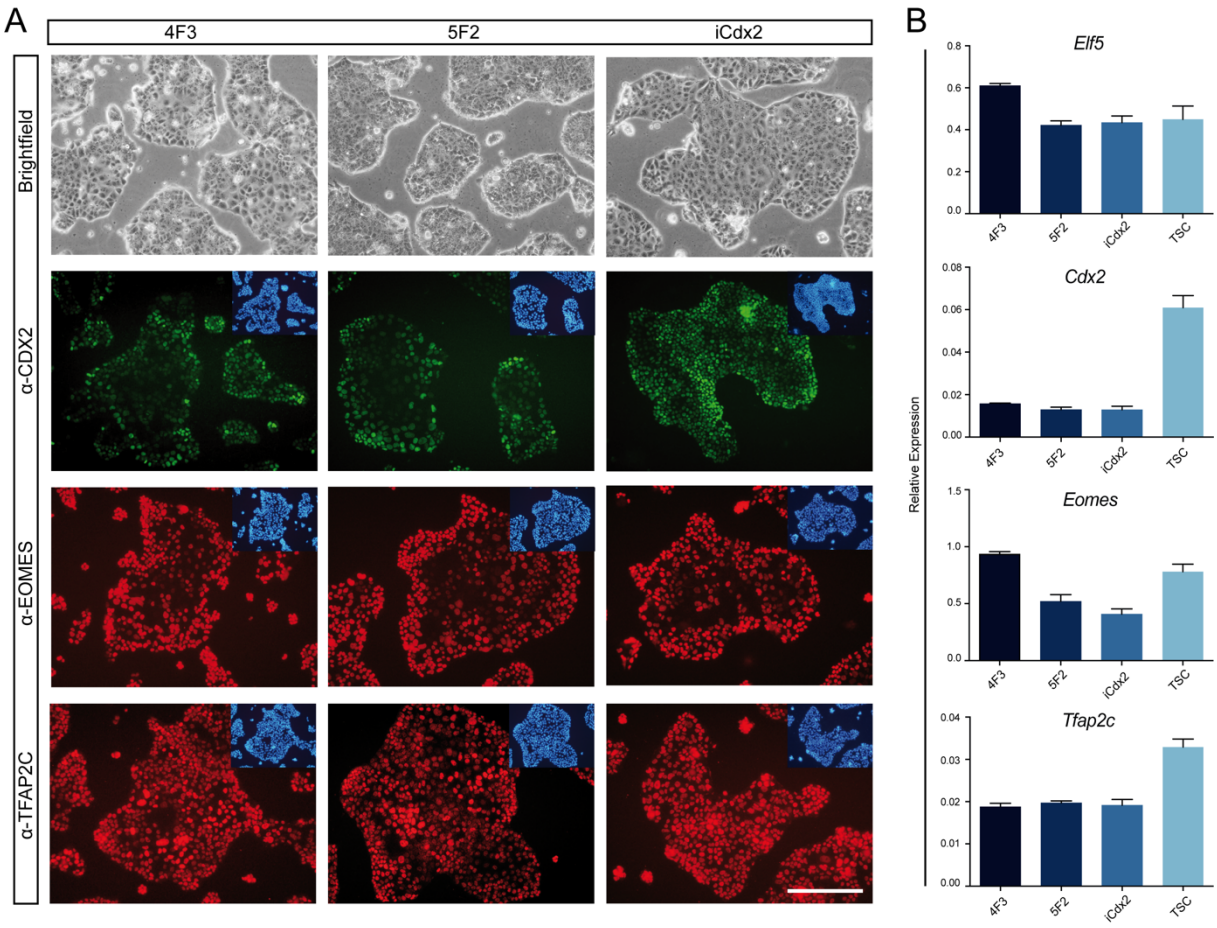

Figure 27: Converted clones cultured in TX medium are stable in long-term culture
A. Representative photomicrographs of 4F3^{TX}, 5F2^{TX} and iCdx2^{TX} at high passage 38 depicting TSC morphology in brightfield images. All clones exhibit CDX2, TFAP2C and EOMES positive colonies as revealed by the immunofluorescence staining. Insets display corresponding Hoechst stainings; Scale bar: 250 µm. **B.** Endogenous expression of TSC markers *Elf5*, *Cdx2*, *Eomes* and *Tfap2c* analyzed in 4F3^{TX}, 5F2^{TX} and iCdx2^{TX} by qRT-PCR at passage 38. Analyses were obtained from three independent RNA isolations, expression is normalized to housekeeping genes *Gapdh* and *Pgk1*, bars display mean value ± SEM. Modified from Kaiser et al., 2020a.

6.14 4F3^{TX}, 5F2^{TX} and iCdx2^{TX} differentiate along the trophoblast lineage *in vitro*

The *in vitro* differentiation potential of 4F3^{TX}, 5F2^{TX} and iCdx2^{TX} was explored by culturing clones in differentiation-inducing medium for nine days (Figure 28). This entailed the withdrawal of growth factors FGF4, heparin and TGFβ from culture conditions. On day 3 of differentiation, TGCs were arising for the first time and increasing in number up to day 9 (Figure 28 A). Every third day, RNA was isolated from differentiating cells in order to assess the expression of several trophoblast differentiation markers. Markers analyzed comprised *Tfap2c*, *Hand2*, *Pl1*, *Pl2*, *Plf1* and *Tpbpa* – all of which are involved in different stages of differentiation. TFAP2C becomes upregulated during differentiation while HAND1 is involved in giant cell differentiation and found in the ectoplacental cone. PL1, PL2 and PLF1 are markers for P-TGCs while TPBPA is a spongiotrophoblast marker (Simmons et al., 2007). For all clones, withdrawal of growth factors yielded an upregulation from day 0 to day 9 for all markers indicating a proper differentiation to diverse placental subtypes (Figure 28 B). However, the increase in expression was most profound in 5F2^{TX}.

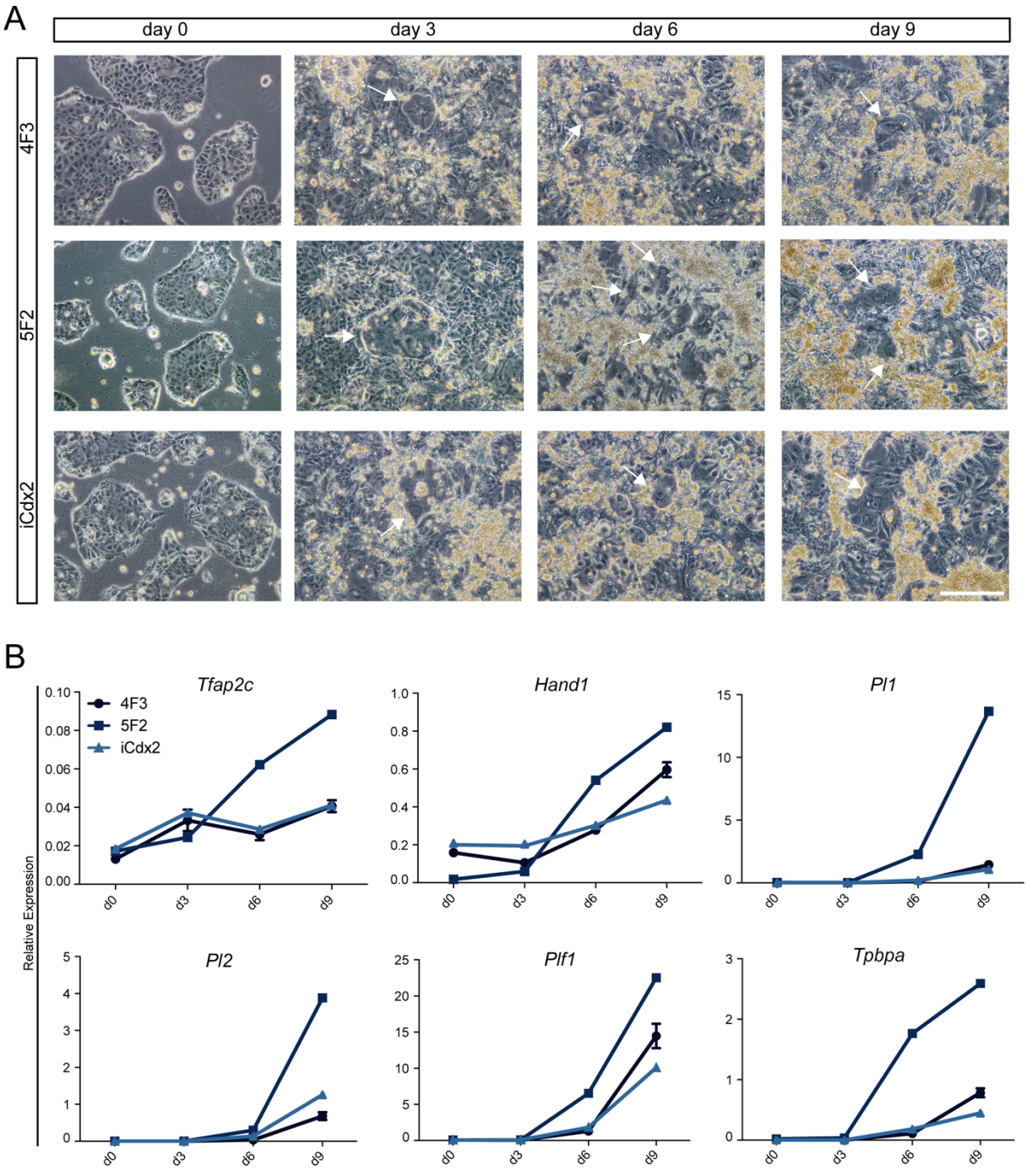

Figure 28: 4F^{TX}, 5F^{TX} and iCdx2^{TX} differentiate *in vitro* upon growth factor withdrawal
A. Representative photomicrographs demonstrating morphology of 4F3^{TX}, 5F2^{TX} and iCdx2^{TX} undergoing *in vitro* differentiation for 0, 3, 6 and 9 days caused by growth factor withdrawal from culture medium. White arrows indicate trophoblast giant cells. Scale bar: 250 µm. **B.** Analysis of TSC differentiation markers *Tfap2c*, *Hand1*, *Pl1*, *Pl2, Plf1* and *Tpbpa* in 4F3^{TX}, 5F2^{TX} and iCdx2^{TX} during differentiation using qRT-PCR. Cells were kept under differentiation inducing conditions for 3, 6 and 9 days. RNA was obtained from three independent experiments. Expression was normalized to housekeeping genes *Gapdh* and *Pgk1*. Data is represented by mean value ± SEM. Modified from Kaiser et al., 2020a.

6.15 5F2^{TX} cells contribute to placental tissue upon blastocyst injection

While the *in vitro* data consistently indicated a conversion to bona fide TSC fate in 5F^{TX} clones, *in vivo* functionality and multipotency were yet to prove. Even though Cambuli et al. showed that also incompletely converted TSC-like cells contribute to placental tissue, blastocyst

injections remain an important tool in TSC research to show a clone's full potential. Hence, the *in vivo* differentiation potential of 5F2^{TX} cells was assessed next. Clones 5F2^{TX} and 5F3^{TX} at passage 5 were transduced with the lentiviral vector FUGW which is carrying EGFP driven by the ubiquitin C promoter. As EGFP intensity differed between colonies, single green fluorescent colonies were picked. Subclones were expanded until showing a confluent and homogeneous EGFP positive population followed by a flow cytometric analysis to determine the amount of EGFP positive cells.

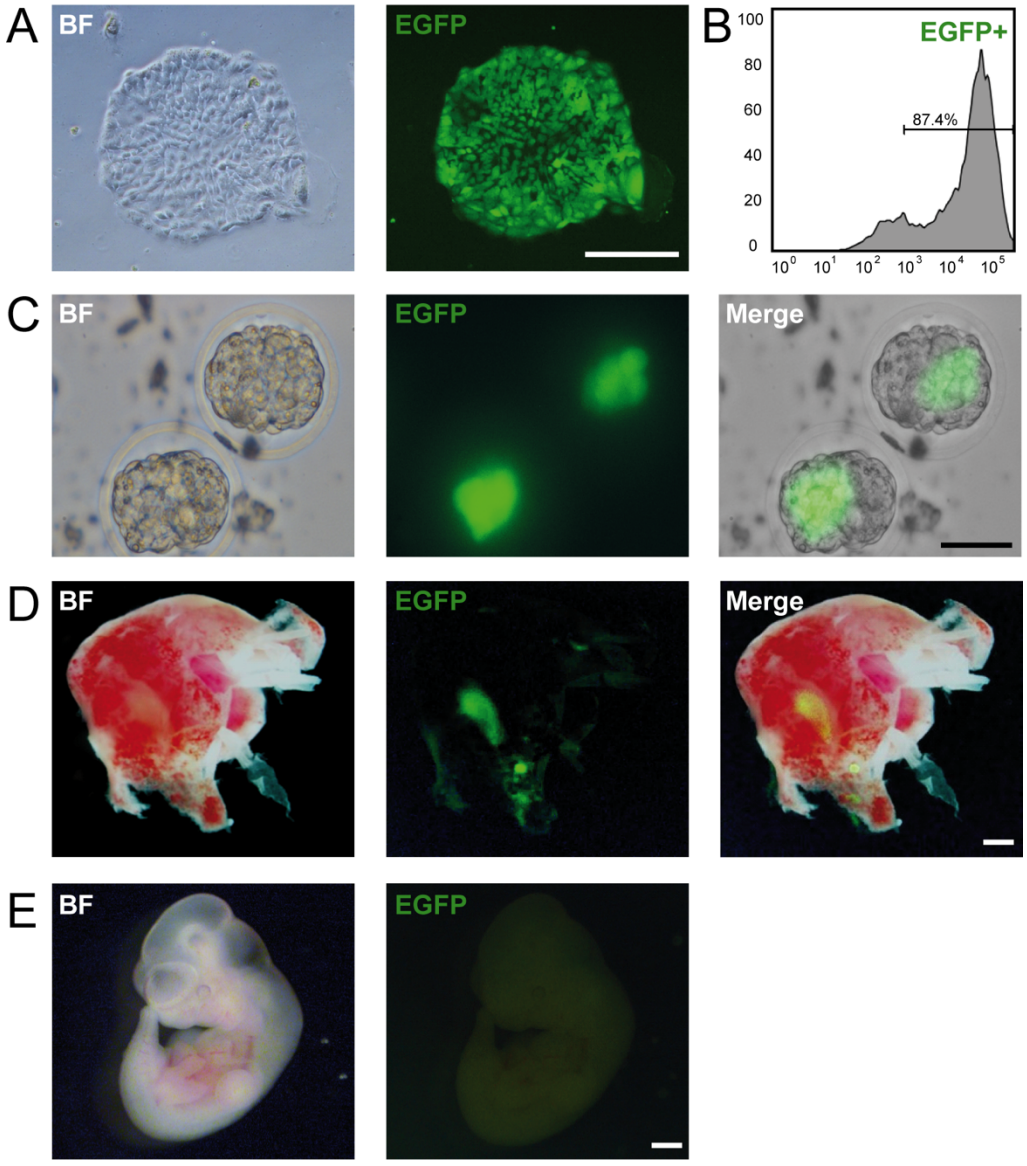

Figure 29: Placenta chimerization of 5F2^{TX} upon blastocyst injection
A. Representative photomicrograph depicting EGFP-positive cells of 5F2^{TX} subclone K. Scale bar: 250 µm. **B.** 87.4% of the cells of transduced 5F2^{TX} subclone K were detected to be EGFP-positive using flow cytometry. **C.** Micrographs depicting manipulated E3.5 blastocysts after injection of EGFP-positive 5F2^{TX} subclone K. Scale bar: 50 µm. **D.** Dissected placenta on day E12.5 after blastocyst injection demonstrating chimerization of 5F2^{TX}. Scale bar: 1mm. **E.** Associated embryo is not showing integration of EGFP-positive 5F2^{TX}-cells. Scale bar: 1mm. Modified from Kaiser et al., 2020a.

Based on the amount of EGFP positive cells and stability in culture, 5F2^{TX} subclone K with 87.4% EGFP-positive cells was chosen for blastocyst injections (Figure 29 A and B). Prior to injection, medium was switched from TX culture to TS medium with 1.5x FGF4 and heparin. 7-10 EGFP-positive 5F2^{TX}-iTSCs were injected into E3.5 blastocysts (Figure 29 C). Manipulated blastocysts were transferred into uteri of pseudo-pregnant foster mice. On E12.5, embryos and placentas were analyzed for contribution of injected cells. EGFP positive cells could be found in the placental tissue but not in the embryo (Figure 29 D and E). Overall contribution rate was determined as 18.2% which is in line with contribution rates previously established.

In summary, clone 5F2^{TX} was extensively analyzed and demonstrated full TSC potential in terms of morphology, gene expression, methylation status and multipotency *in vitro and in vivo*. Therefore, going forward, these 5F^{TX} cells as well as 4F^{TX}, 5F^{TS} and iCdx2^{TX} were considered as completely induced TSC.

6.16 TSC fate is not induced by TX medium culture alone

Having conducted the comprehensive molecular analyses described in the previous chapter, some questions had yet to be addressed. While 4F^{TX} and iCdx2^{TX} clones achieved a full conversion, 4F^{TS} and iCdx2^{TS} did not. As transgene combination, duration of transgene induction as well as doxycycline concentration remained constant, the culture medium represented the decisive factor. TX medium was suggested to mimic the *in vivo* environment more closely than standard TS medium (Kubaczka et al., 2014). Also, TX medium was shown to be strictly selective for bona fide TSCs (Kubaczka et al., 2014). This finding was supported in this study as control ESCs and incompletely converted cells iTfap2c^{TX}, iGata3^{TX}, iEomes^{TX} and iEts2^{TX} could not be cultured in TX medium and were lost within two passages. However, the reason as to why TX medium promotes ESC to TSC conversion still needed to be investigated.

As other studies could show that altered environmental conditions can affect cell fate decisions, it was first excluded that withdrawal of LIF and TX culture alone was sufficient to induce TSC fate in ESCs. Thus, control ESCs were subjected to different TSC culture conditions (Figure 30). As already shown before, ESCs can be cultivated in TS medium, lose OCT4 positivity but remain with ESC-like methylation pattern at passage 5. When changing ES medium to TX medium, ESC control cells cannot be propagated. As the apoptosis observed in those ESCs could also result from abrupt serum loss, ESCs were switched gradually from ES to TX medium culture next. To this end, the percentage of TX medium in ES medium was increased daily from 25% to 50% to 75% until reaching 100% TX culture medium on day 4. However, also this stepwise medium change led to loss of proliferation,

increase in differentiation and apoptosis in ESC within two passages past medium change. Finally, ESC^{TS} at passage 5 were further cultured in TS medium up to passage 12 or switched gradually to TX medium ($ESC^{TS \rightarrow TX}$) resulting in ESC-like colonies in TS medium but loss of cells in TX medium (Figure 30).

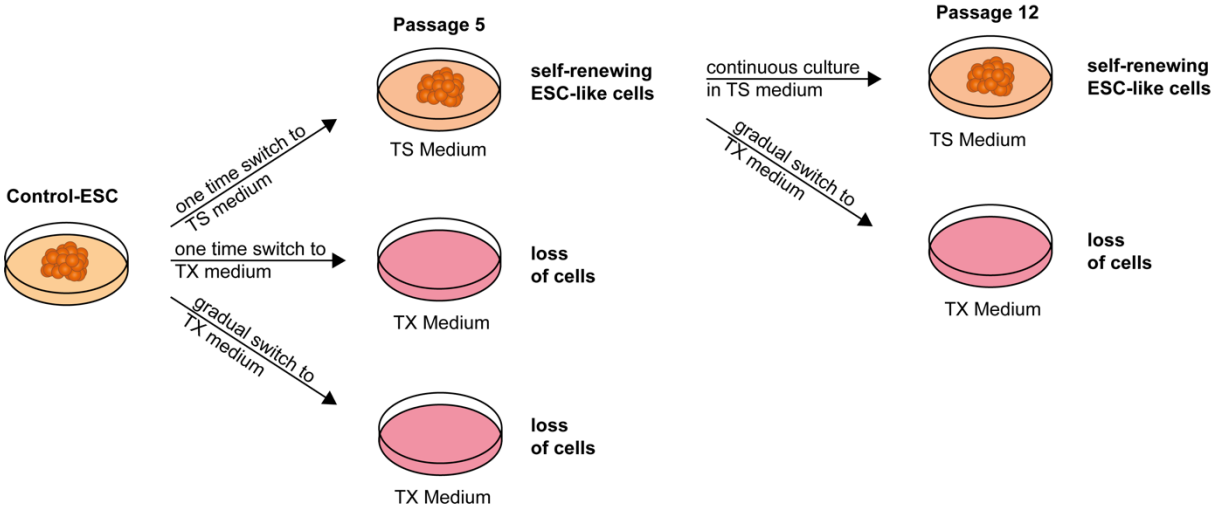

Figure 30: TSC culture conditions alone do not result in TSC fate in ESCs
ESC control cells were switched from ES medium to TS or TX medium. Medium switch to TX medium was also performed stepwise – every day medium was adjusted from 25% TX to 50% TX to 75% TX to finally 100% TX medium. After both switches to TX medium, cells could not be propagated for more than two passages. Cells ceased proliferation, differentiated, and underwent apoptosis. In TS medium, cells lost OCT4 positivity but continued self-renewing and proliferating until passage 5. At passage 5, ESCs were either kept in TS medium until passage 12 or switched stepwise to TX medium again. Cells remained unharmed in TS medium but could not be cultured in TX medium.

Thus, TSC culture conditions alone did not result in induction of TSC fate in ESC control cells under the different settings evaluated demonstrating the necessity of transgene induction.

6.17 Additional culture in TX medium induces TSC fate in $4F^{TS}$ and $iCdx2^{TS}$

Next, $4F3^{TS}$ and $iCdx2^{TS}$ clones were examined further. Morphological analyses and FACS analyses showed a homogenous population for both clones. $4F3^{TS}$ colonies remained with ESC-like morphology whereas $iCdx2^{TS}$ closely resembled TSC morphology. Correspondingly, FACS analyses demonstrated that merely 2% of $4F3^{TS}$ cells were double positive for CD40 and PLET1 while 91% of $iCdx2^{TS}$ cells at passage 5 were positive for both markers. Yet, both clones did not show TSC methylation patterns. Yet again, cells were also negative for OCT4. Interestingly, even though both clones showed neither distinct ESC nor TSC characteristics, they continued proliferating in TS medium without undergoing apoptosis. Further analyses, such as single-cell RNA-sequencing, could help evaluating the state of these cell populations in depth. Here, in a first attempt, $4F3^{TS}$ and $iCdx2^{TS}$ at passage 5 were switched to TX medium and named $4F3^{TS \rightarrow TX}$ and $iCdx2^{TS \rightarrow TX}$. As TX was shown to be strictly selective for bona fide

TSCs, these incompletely converted cell clones were assumed not be stable in TX medium. Unexpectedly, in contrast to ESCs, they did not undergo apoptosis, differentiate or stop proliferating. Thus, development of these clones in TX medium was monitored further. During this additional setup, $4F^{TS}$ and $iCdx2^{TS}$ clones were converted and cultured up to passage 5 in TS medium reaching a stage of incomplete conversion. At this timepoint, clones were switched gradually from TS to TX medium culture in order to exclude effects of abrupt serum loss on cell survival, proliferation and differentiation (Figure 31). $4F^{TS}$ and $iCdx2^{TS}$ control cells were kept in TS medium. During gradual medium switch from 25% to 100% TX medium, cells were continuously observed for increased differentiation or apoptosis (Figure 32). This experiment was performed with cell clones originating from three independent conversion attempts.

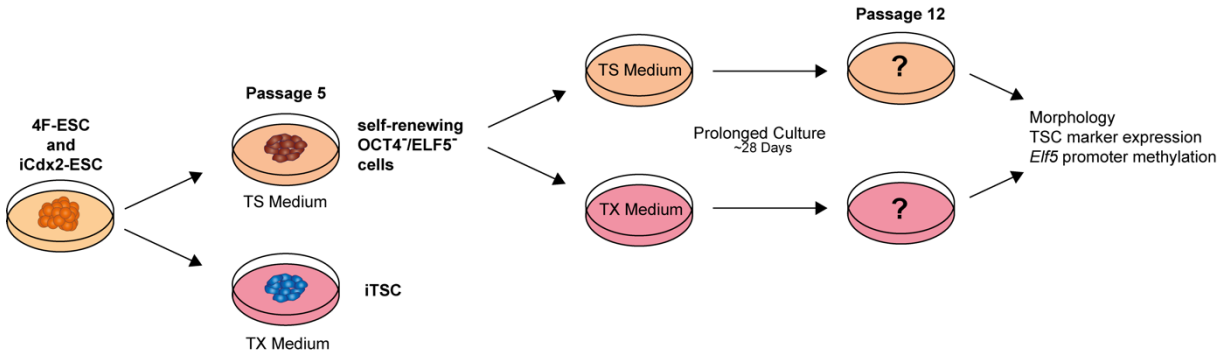

Figure 31: Schematic depicting switch to TX medium for $4F^{TS}$ and $iCdx2^{TS}$ at passage 5
After culturing 4F3 and iCdx2 clones in TS medium to passage 5 in TS medium, culture medium was switched to TX medium gradually or cultivation was continued in TS medium for further passages. At passage 12, cells were again analyzed for cell surface marker levels, gene expression and methylation status of *Elf5* promoter in comparison to clones continuously cultured in TS medium.

Under 75% TX medium culture, differences in morphology became apparent (Figure 32). While $iCdx2^{TS}$ and $iCdx2^{TS\rightarrow TX}$ were not affected by medium change, $4F^{TS\rightarrow TX}$ cells displayed increased differentiation. Surprisingly, in $4F^{TS\rightarrow TX}$ clones on day 4 of medium switch, TSC-like colonies could be detected amidst differentiating areas. Starting from passage 7, clear TSC colonies were emerging in $4F^{TS\rightarrow TX}$ and $iCdx2^{TS\rightarrow TX}$ clones without the presence of increased differentiation or apoptosis. As described before, $ESC^{TS\rightarrow TX}$ were lost within two passages.

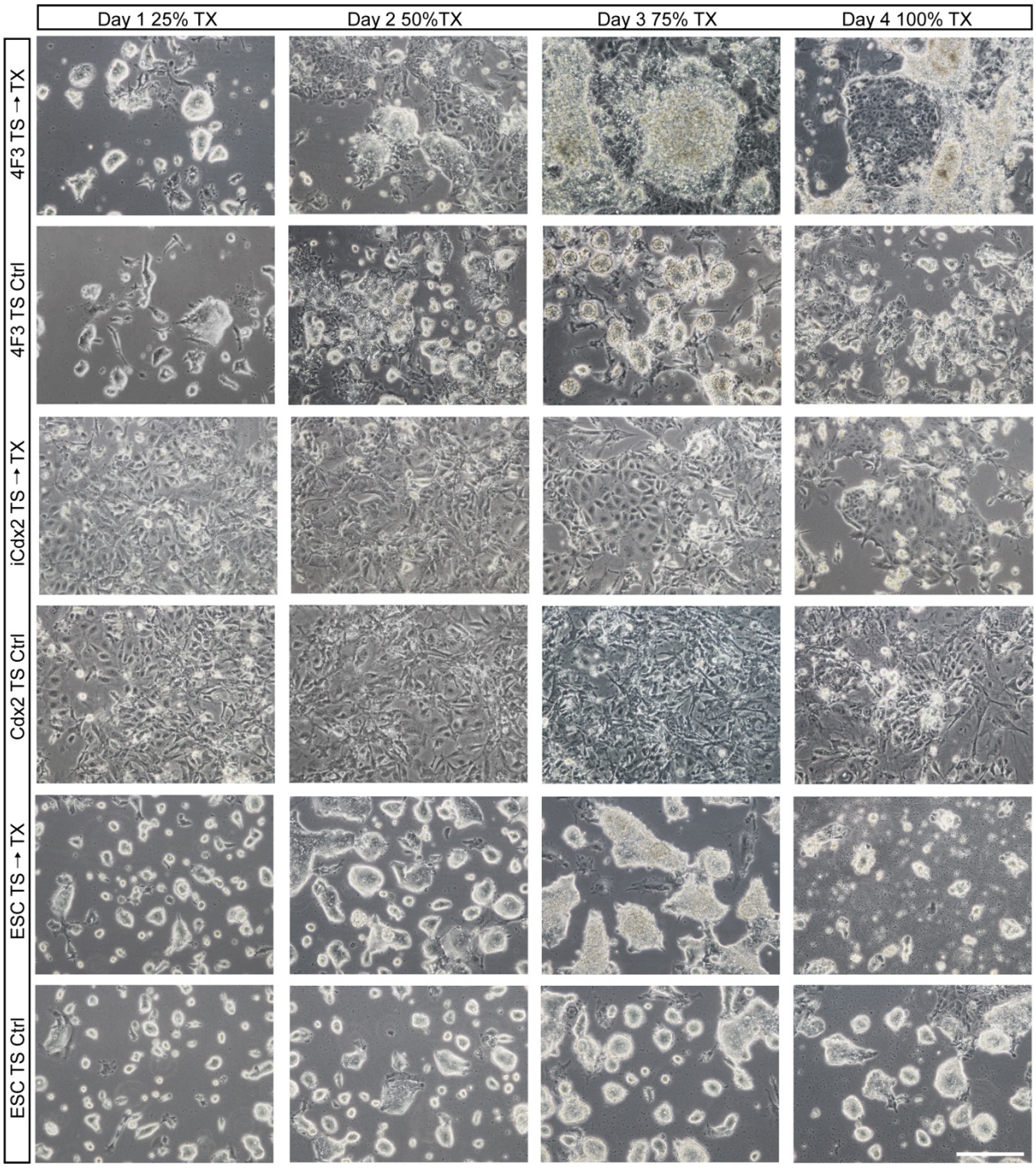

Figure 32: Switch of TS to TX culture of 4F^{TS} and iCdx2^{TS} at passage 5
Representative photomicrographs depicting change in morphology upon medium switch in 4F3^{TS}, iCdx2^{TS} and ESC^{TS} to TX medium at passage 5 in comparison to same clones continuously cultured in TS medium. Scale bar represents 250 µm.

Next, cells were continuously propagated to passage 12 in TS or TX medium. At passage 12, 4F3$^{TS→TX}$ and iCdx2$^{TS→TX}$ clones were cultured in TS medium for five passages followed by an additional cultivation in TX medium. At this time point, obtained clones were re-examined for colony morphology, levels of cell surface markers CD40 and PLET1, marker expression of *Elf5*, *Cdx2*, *Eomes* and *Tfap2c* and methylation status of *Elf5* promoter region.

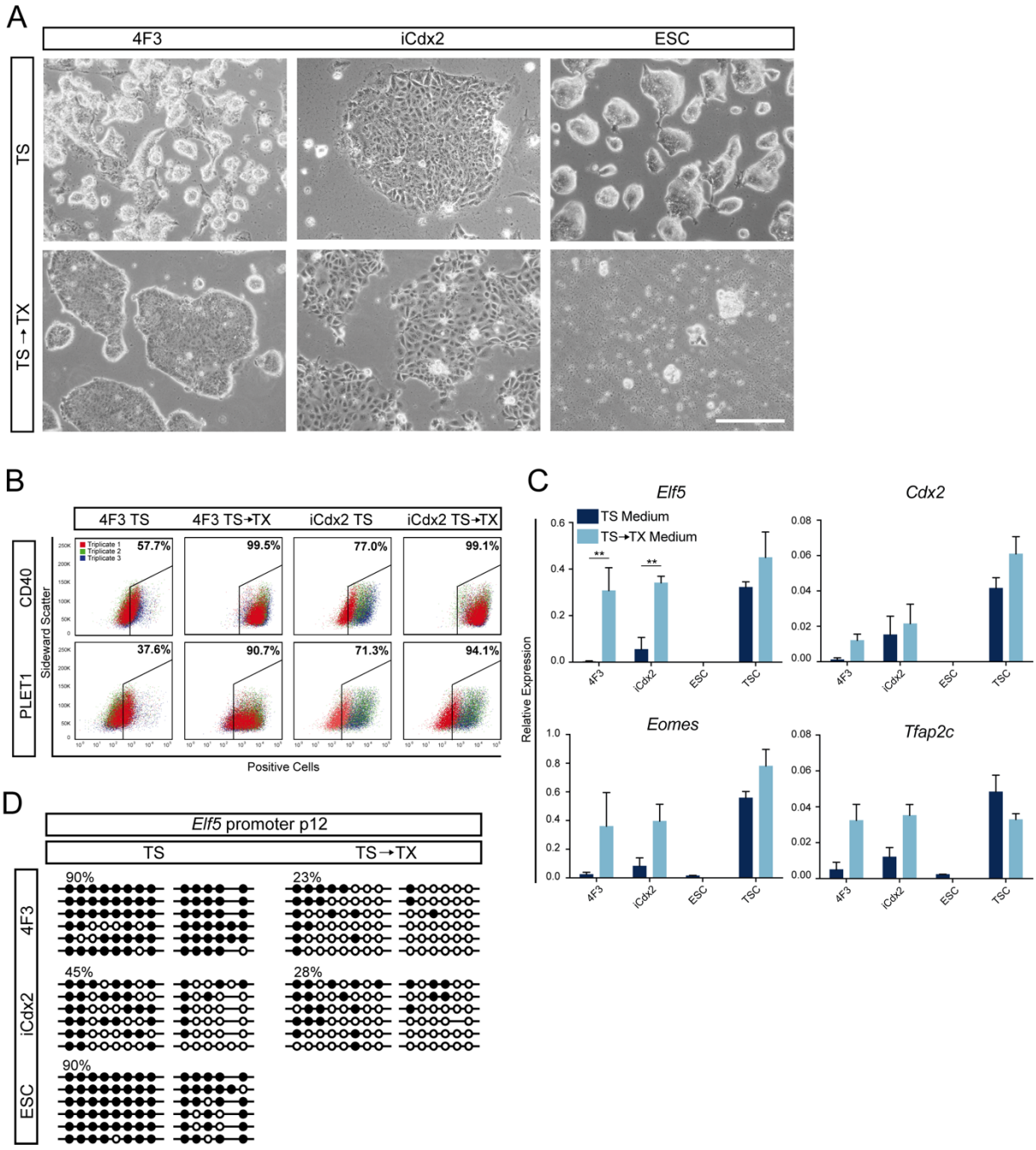

Figure 33: Analysis of 4F^{TS} and iCdx2^{TS} at passage 12
A. Representative photomicrographs of 4F3, iCdx2 and ESC control cells depicting colony morphology at passage 12 in TS or TX medium. Scale bar represents 250 µm. **B.** Flow cytometry analysis of CD40 and PLET1 positive cells in 4F3, iCdx2 and ESC control cells at passage 12. Clones were cultured in either TS or TX medium starting from 4F3^{TS}, iCdx2^{TS} and ESC^{TS} at passage 5. Flow cytometry analysis was performed with samples from three independent experiments. Percentages indicate CD40 and PLET1 positive cells within the gate. **C.** qRT-PCR analysis of endogenous expression of TSC marker *Elf5*, *Cdx2*, *Eomes* and *Tfap2c* for 4F3, iCdx2 and ESC control cells at passage 12 in comparison to TSC control cells. Clones were cultured in either TS or TX medium starting from 4F3^{TS}, iCdx2^{TS} and ESC^{TS} at passage 5. RNA was obtained from three independent experiments. Expression is normalized to housekeeping genes *Gapdh* and *Pgk1*. Bars display mean value ± SEM. Significance was determined by unpaired *t*-test and indicated with $^{**}p < 0.01$. **D.** *Elf5* promoter methylation status of 4F3, iCdx2 and ESC control cells at passage 12 cultivated in either TS or TX medium starting from 4F3^{TS}, iCdx2^{TS} and ESC^{TS} at passage 5. Filled circles represent methylated CpGs, open circles depict unmethylated CpGs. Representative six sequencing reads are presented in this figure.

After being cultured in TS medium for 12 passages past transgene induction, $4F3^{TS}$ still remained with an ESC-resembling morphology (Figure 33 A). However, colonies appeared decomposed and were characterized by decreased proliferation. Interestingly, $4F3^{TS→TX}$ showed clear TSC morphology, as did $iCdx2^{TS}$ and $iCdx2^{TS→TX}$ clones. ESC^{TS} retained typical ESC morphology. As described before, $ESC^{TS→TX}$ could not be propagated up to passage 12 (Figure 33 A). Cell surface protein levels of CD40 and PLET1 levels were low in $4F3^{TS}$ (Figure 33 B). While $iCdx2^{TS}$ showed higher percentage of CD40 and PLET1 positive cells, only $4F3^{TS→TX}$ and $iCdx2^{TS→TX}$ exhibited levels of more than 90% of CD40 and PLET1 positive cells, indicating TSC-like cell surface protein levels. *Elf5* expression was significantly higher in clones cultured in TX medium than in clones cultured in TS medium (Figure 33 C). $4F3^{TS→TX}$ and $iCdx2^{TS→TX}$ *Elf5* expression was equivalent to bona fide TSCs. Also, *Cdx2*, *Eomes* and *Tfap2c* expression was higher in clones switched to TX medium than of respective clones continuously cultured in TS medium. *Tfap2c* levels reached TSC wildtype levels for both clones in TX medium. Analysis of the *Elf5* promoter methylation at passage 12 revealed that $4F3^{TS}$ remained with ESC methylation pattern (Figure 33 D). Interestingly, $iCdx2^{TS}$ demonstrated an intermediate state of methylation pattern which was neither hypo- nor hypermethylated. $4F3^{TS→TX}$ and $iCdx2^{TS→TX}$, however, showed clear demethylation of the differentially methylated region indicating a complete conversion at passage 12.

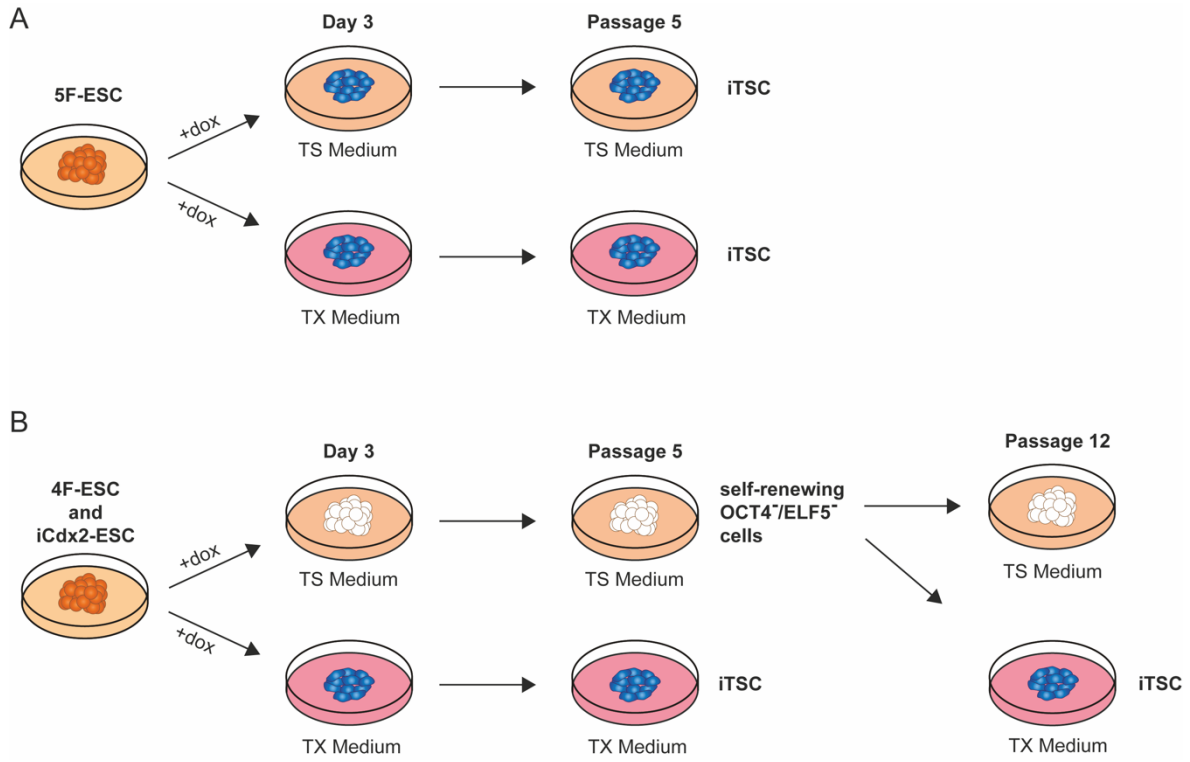

Figure 34: Summary of successful ESC to TSC conversion approaches of this study
A. 5F-ESC convert to bona fide iTSC after three days of transgene induction under both culture conditions. **B.** 4F-ESC and iCdx2-ESC convert to iTSC after three days of transgene induction and culture in TX medium only. When culturing 4F-ESC and iCdx2-ESC for 5 passages after three-day transgene induction in TS medium followed by additional passages in TX medium, these clones also indicated a complete conversion to TSC fate.

In conclusion, $4F3^{TS}$ and $iCdx2^{TS}$ clones seem to harbor the potential to fully convert to TSC fate (Figure 34). However, under environmental conditions created by standard TS medium this potential had not been fully tapped. In TX culture only, these clones convert completely.

Parts of this chapter have been published in:

Franziska Kaiser, Caroline Kubaczka, Monika Graf, Nina Langer, Jan Langkabel, Lena Arévalo, and Hubert Schorle. “Choice of Factors and Medium Impinge on Success of ESC to TSC Conversion.” Placenta 90, 2020.

7 Results II

As presented in the previous chapter, murine ESC to TSC conversion was now intensively analyzed. In the human system, however, theoretical knowledge and culture experience of hTSCs remains limited. Only recently, the first stable hTSC lines were derived which self-renewed *in vitro* and fulfilled most established hTSC criteria such as expression of *GATA3*, demethylation of the *ELF5* promoter and *in vitro* differentiation into EVT- and STB-like cells (Lee et al., 2016; Okae et al., 2018). While *TFAP2C* expression was demonstrated, presence of TFAP2C protein was not detected. Moreover, all obtained lines remained CDX2 negative (Okae et al., 2018). In contrast to murine TSC cultivation, the newly developed human culture medium relies on inhibition of TGFβ pathway, activation of the Wnt signaling and supplementation of epidermal growth factor (EGF). A similar growth medium was used by two groups establishing organoid based hTSC culture (Haider et al., 2018; Turco et al., 2018). In terms of conversion to the human trophoblast fate, it was repeatedly shown that exposure to BMP4 results in induction of hTSC fate in hiPSC cells (Amita et al., 2013; Dong et al., 2020; Horii et al., 2020). However, it was not established yet, if overexpression of hTSC specific transcription factors yields TSC fate in hiPSCs as well. Hence, the second part of this thesis aimed at further examining published hTSC lines and providing preliminary data on elucidating the conversion from hiPSCs to hTSCs.

7.1 Characterization of human TSCs

In the aforementioned study, human TSCs were derived from human blastocysts or cytotrophoblast of the first trimester (Okae et al., 2018). Three cytotrophoblast (CT) and three blastocyst (bTS) cell lines were received from the authors for the following experiments. First, cell lines CT27 at passage 11 and bTS4 at passage 14 were taken into culture and expanded according to the published procedure (Okae et al., 2018). Colony morphology of both lines displayed a monolayer of epithelial-like cells (Figure 35 A). After several passages, qRT-PCR analysis and immunofluorescence staining were conducted to assess CT27 cells for expression of previously described hTSC marker. Gene expression analyses showed that CT27 expressed *KRT7*, *HCG* and low levels of *GATA3* (Figure 35 B). TFAP2C and GATA3 were detectable in CT27 colonies, however, CDX2, EOMES and ETS2 could not be detected (Figure 35 C).

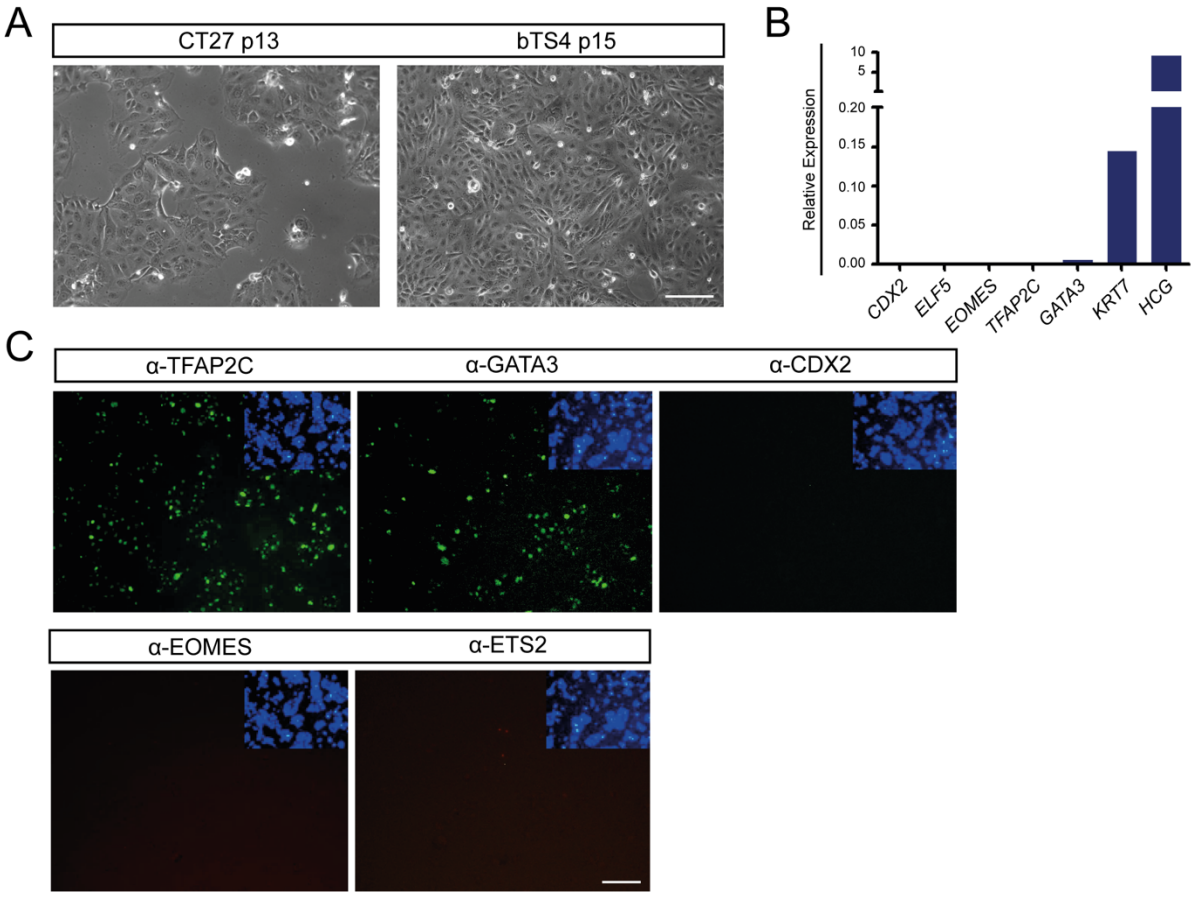

Figure 35: Characterization of hTSC lines
A. Brightfield images depicting colony morphology of hTSC lines CT27 and bTS4 cultured in hTSC medium. Scale bar: 250 µm. **B.** qRT-PCR analysis of expression of *CDX2*, *ELF5*, *EOMES*, *TFAP2C*, *GATA3*, *KRT7* and *HCG* in CT27 at p13. **C.** Immunofluorescence staining of CT27 at p14 against TFAP2C, GATA3, CDX2, EOMES and ETS2. Insets display corresponding Hoechst stainings; scale bar: 250 µm.

7.2 Candidate transcription factors for hiPSC to hTSC conversion approaches

First, suitable candidate genes for induction of human TSC fate were selected. These were supposed to include CDX2 as well as GATA3, EOMES, TFAP2C and ETS2 (GETE) factors which proved successful in murine ESC to TSC conversion (Kubaczka et al., 2015). It was also reported that the so-called “TEtra" factors comprising TFAP2A, TFAP2C, GATA2 and GATA3 are of importance in initiating the hTSC transcription factor network in human pluripotent stem cells (Krendl et al., 2017). Additionally, TEAD4 was repeatedly demonstrated to play an important role in human trophoblast development (Home et al., 2012; Lee et al., 2016; Okae et al., 2018). Thus, first analyses were conducted with the following eight hTSC transcription factors: TFAP2A, TFAP2C, GATA2, GATA3, EOMES, CDX2, TEAD4 and ETS2.

After choosing adequate transcription factors, their cDNA was cloned into the lentiviral vector pLV-tetO for subsequent transduction of hiPSCs. To this end, plasmid pLV-tetO-Oct4 (Addgene: #19766) was obtained and linearized by excision of *Oct4* cDNA using EcoRI digest. The origin of transcription factor cDNAs varied and three different cloning strategies were

applied including sticky-end ligation, blunt-end ligation and integration of PCR products via TA cloning. In short, coding sequence of hGATA2 was obtained from pcDNA plasmid (Addgene: #1287) and coding sequence of hEOMES was commercially synthesized and integrated in PUC57_BsaI_Free/pBlueScript II SK(+) by General Biosystems (Morrisville, USA). In their respective vector of origin, cDNAs were flanked by two EcoRI restriction sites. Thus, cDNA was separated from vector backbone by preparative digest using EcoRI and subsequently inserted into the target vector pLV-tetO using its sole EcoRI site. TFAP2C cDNA was obtained from plasmid pCMX_PL2 provided by Prof. Dr. Anja Boßerhoff (Institute of Biochemistry and Molecular Medicine, FAU, Erlangen-Nürnberg). Coding sequence of TFAP2C was released from the vector by EcoRV digest yielding blunt ends. CDX2 cDNA was isolated from CMV-CDX2-WT (Addgene: #16553) by double digest with restriction enzymes SalI and XbaI. Obtained fragments and linearized pLV-tetO backbone were treated with Klenow fragment to prepare ends for blunt cloning. Using T4 ligase, *TFAP2C* cDNA as well as *CDX2* cDNA were inserted into the pLV-tetO vector. Finally, *ETS2* is expressed in human peripheral blood monocytes (PBMC), the MCF-7 cell line expresses *TFAP2A* and *TEAD4* is found in the 2102EP cell line. Therefore, cDNA from these three cell types was used to generate cDNA of *ETS2*, *TFAP2A* and *TEAD4* by PCR. *GATA3* was amplified from plasmid pENTR/Dtopo Ty1-TEV-GATA3. Amplified coding sequences were ligated into pCR2.1 vector via TA cloning. Inserts in pCR2.1 were flanked by EcoRI restriction sites which were used to isolate cDNAs by restriction digest and for subsequent ligation into the pLV-tetO backbone. Dominik Nitsche performed generation of tetO-TFAP2A and tetO-TEAD4 as well as identification of the right clone for tetO-TFAP2C, tetO-GATA2, tetO-GATA3 by applying test digests. Restriction digest of eight obtained pLV-tetO vectors using EcoRI showed successful insertion of all candidate cDNAs into the vector (Figure 36). Next, all vectors were verified by Sanger sequencing to ensure that no mutations had been introduced in the coding sequence throughout amplification and cloning steps. Further, correct orientation of insert was confirmed.

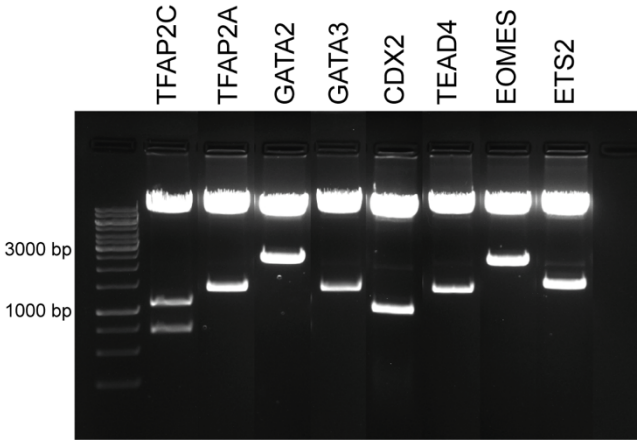

Figure 36: Human candidate transcription factor cDNA integrated into pLV-tetO vectors
Photograph depicting restriction digest of pLV-tetO vectors and integrated cDNA of *TFAP2C*, *TFAP2A*, *GATA2*, *GATA3*, *CDX2*, *TEAD4*, *EOMES* and *ETS2* using EcoRI. As coding sequence of *TFAP2C* itself contains an EcoRI restriction site, three fragments were obtained. 1kb DNA ladder was used as reference.

Second generation lentivirus production was performed in 293T HEK cells using transfer vector pLV-tetO as well as a helper (psPAX2) and an envelope plasmid (pMD2.G). Completed virus particles were harvested in the supernatant on two subsequent days. Obtained lentiviruses were first tested on murine R26::M2-rtTA MEFs to verify efficient protein synthesis of transgenic transcription factors. These rtTA-MEFs carry the rtTA cDNA integrated in the ROSA26 locus, expression thereof is driven by endogenous ROSA26 promoter. Dose-dependent transduction was tested in order to establish the appropriate volume for sufficient transgenic protein levels after 24 hours of transgene induction. Therefore, 50 µl, 100 µl and 150 µl of virus solution were applied as exemplarily shown by pLV-tetO-GATA3 transduction (Figure 37). Cells were cultured in MEF medium and transgene expression induced by doxycycline administration. Higher virus concentration was associated with higher levels of GATA3 positive cells whereas transduced cells without doxycycline administration remained without detectable GATA3. As addition of 50 µl virus containing supernatant yielded overall increased GATA3 levels, this volume was implemented for further investigations.

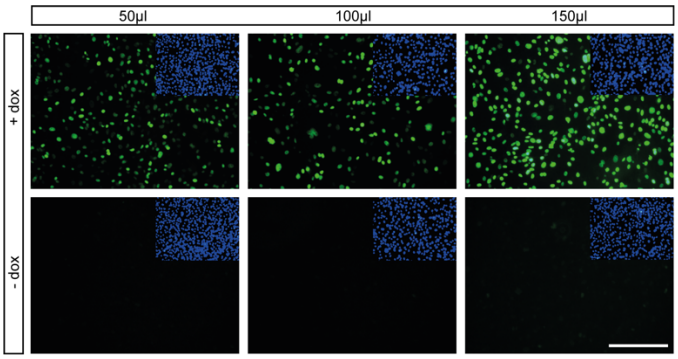

Figure 37: Transduction of rtTA MEFs with a lentiviral vector encoding for *hGATA3*
R26::M2-rtTA MEFs were transduced with pLV-tetO-GATA3 lentiviruses and cultured with doxycycline for 24 hours. Corresponding photomicrographs depict detection of GATA3 in comparison to no doxycycline control cells. Insets display corresponding Hoechst stainings; scale bar: 250 µm.

Next, the presence of remaining transgenic proteins was verified after 24 hours of transgene induction, here shown for R26::M2-rtTA MEFs transduced with 50 µl harvested virus supernatant (Figure 38). GATA2, ETS2 and CDX2 levels remained low after transduction and could not be increased by higher volumes of virus containing medium. Also, repeated lentivirus production of pLV-tetO-GATA2 and pLV-tetO-CDX2 showed a similar result. In the future, prolonged doxycycline administration could be tested as well as different antibodies to increase presence and detection of respective proteins.

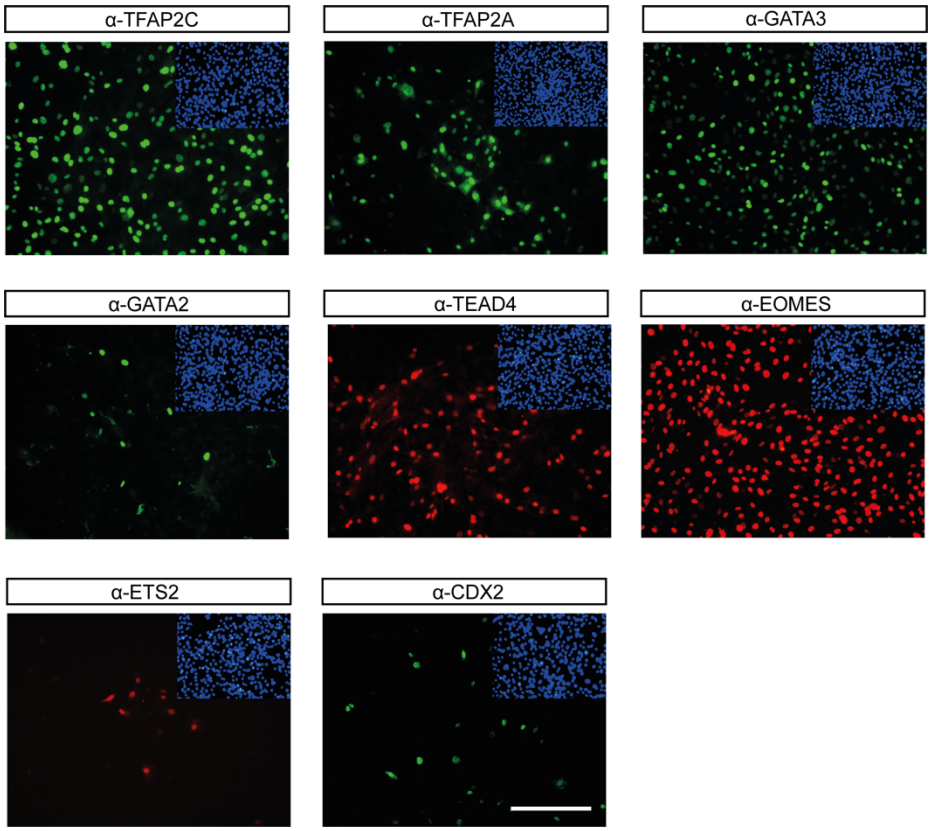

Figure 38: Transgenic protein levels after 24 hours of transgene induction
Immunofluorescence staining against TFAP2C, TFAP2A, GATA3, GATA2, TEAD4, EOMES, ETS2 and CDX2 after transduction of R26::M2-rtTA MEFs with lentiviral vectors pLV-tetO-TFAP2C, pLV-tetO-TFAP2A, pLV-tetO-GATA3, pLV-tetO-GATA2, pLV-tetO-TEAD4, pLV-tetO-EOMES, pLV-tetO-ETS2 or pLV-tetO-CDX2 and doxycycline mediated transgene induction for 24 hours. Insets display corresponding Hoechst stainings. Scale bar: 250 µm.

7.3 Transduction of hiPSCs with viral vectors encoding for hTSC transcription factors

Next, hiPSCs were transduced overnight with six different combinations of generated lentiviral vectors (Table 32). The hiPSC iLB-C-14ms11 cell line which was reprogrammed from somatic cells using Sendai virus vectors, was received from Dr. Michael Peitz (LIFE & BRAIN Center, Bonn) and served as the starting cell population for the following investigations. Each approach was conducted with 50 µl lentiviral solution of each transgene in combination with a lentiviral vector encoding for rtTA and in the presence of polybrene (5 µg/ml).

Table 32: First-time establishment of transgenic hiPSC lines

Clone	Transgenes
iTFAP2C	tetO-TFAP2C
iCDX2	tetO-CDX2
iTETRA	tetO-TFAP2A, tetO-TFAP2C, tetO-GATA2, tetO-GATA3
iGETE	tetO-GATA3, tetO-EOMES, tetO-TFAP2C, tetO-ETS2
iGETT	tetO-GATA3, tetO-EOMES, tetO-TFAP2C, tetO-TEAD4
i7F	tetO-TFAP2A, tetO-TFAP2C, tetO-GATA2, tetO-GATA3, tetO-EOMES, tetO-TEAD4, tetO-ETS2

24 hours after transduction of hiPSCs and prior to transgene induction, colonies remained with unchanged hiPSC-like morphology as well as unaltered amount of differentiation and apoptosis indicating that respective virus load was tolerated by cells (Figure 39).

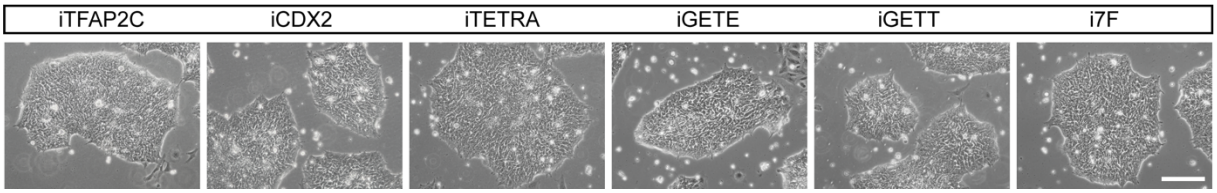

Figure 39: Morphology of transduced hiPSCs prior to transgene induction
Representative photomicrographs of different transgenic hiPSC lines 24 hours past transduction. hiPSCs were transduced with lentiviral vectors encoding for (1) TFAP2C, (2) CDX2, (3) TFAP2A, TFAP2C, GATA2, GATA3 (4) GATA3, EOMES, TFAP2C, ETS2 (5) GATA3, EOMES, TFAP2C, TEAD4 and (6) TFAP2A, TFAP2C, GATA2, GATA3, EOMES, TEAD4 and ETS2. Scale bar represents 250 µm.

Past transduction, cells were expanded in hiPSC medium in preparation for transgene induction. Then, cell culture medium was changed to hTSC medium published by Okae et al. and supplemented with doxycycline (2 µg/µl) for 30 days (Okae et al., 2018). Analyses were performed after 10 days, 20 days and 30 days of doxycycline mediated transgene induction.

7.4 iPSC transduction results in initial hTSC fate induction in iTETRA clones

After 10 days of doxycycline mediated activation of transgenes, iTETRA clones showed formation of colony-like structures due to transgene activation. No morphological differences were detectable for iCDX2, iTFAP2C, iGETE, iGETT and i7F in comparison to clones cultured without doxycycline (Figure 40 A). However, distinct iPSC colony formation was lost. Interestingly, proliferation rate seemed to be increased in cells cultivated with doxycycline

administration. RNA expression analyses revealed that iTETRA clones showed slight increase in levels of *CDX2*, *TFAP2C*, *GATA3*, *HCG* and *KRT7* in comparison to respective clone cultivated without doxycycline (Figure 40 B). However, all transcript levels remained very low, therefore, no interpretation of data on day 10 was not possible. For technical reasons, iCDX2 had to be excluded from transcript analyses.

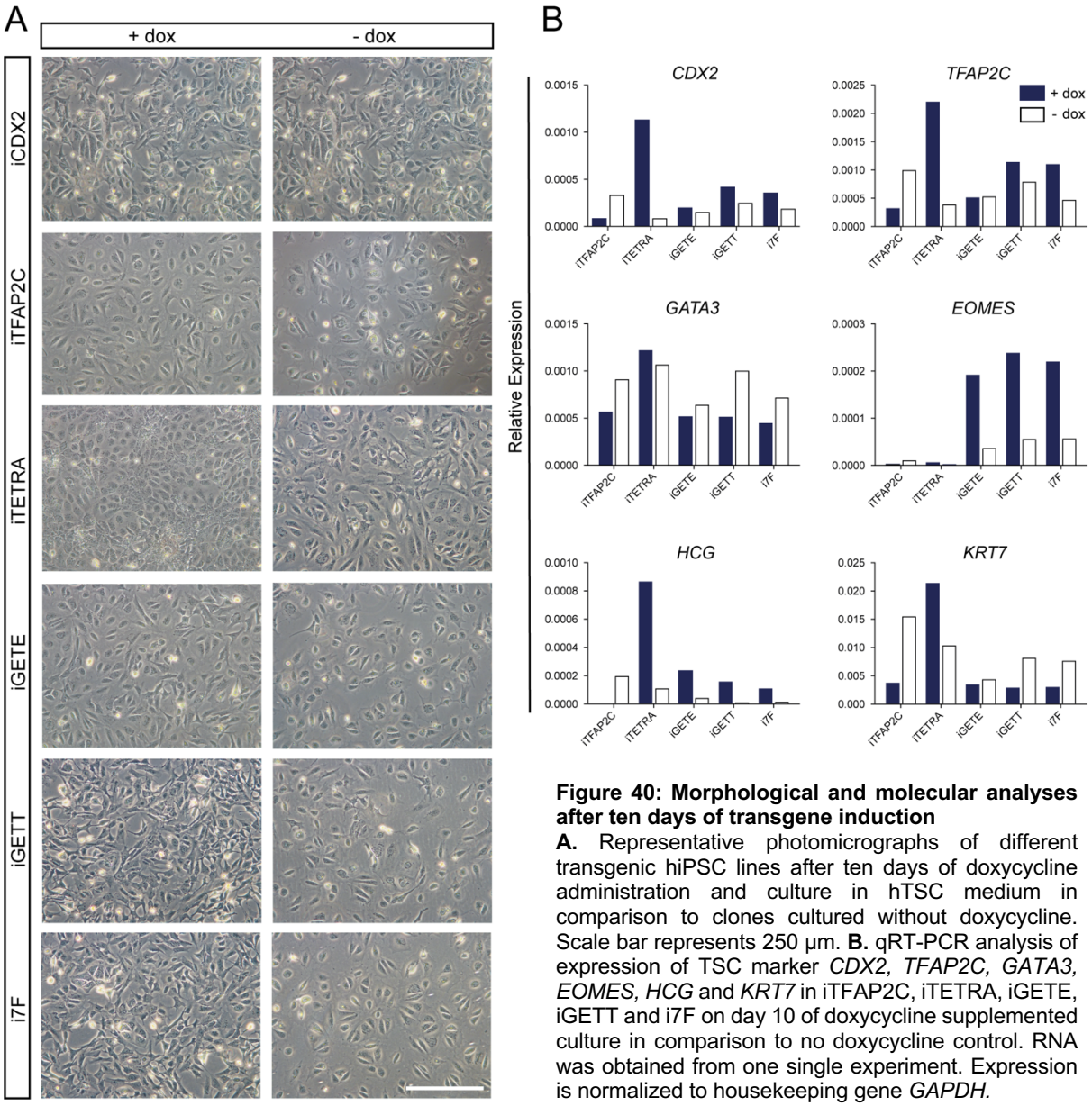

Figure 40: Morphological and molecular analyses after ten days of transgene induction
A. Representative photomicrographs of different transgenic hiPSC lines after ten days of doxycycline administration and culture in hTSC medium in comparison to clones cultured without doxycycline. Scale bar represents 250 µm. **B.** qRT-PCR analysis of expression of TSC marker *CDX2, TFAP2C, GATA3, EOMES, HCG* and *KRT7* in iTFAP2C, iTETRA, iGETE, iGETT and i7F on day 10 of doxycycline supplemented culture in comparison to no doxycycline control. RNA was obtained from one single experiment. Expression is normalized to housekeeping gene *GAPDH.*

All clones were further explored for protein levels of hTSC markers GATA3, TFAP2C, EOMES, ETS2 and CDX2 on day 10. Interestingly, iTETRA showed presence of few GATA3, TFAP2C and CDX2 positive colonies (Figure 41 A). Moreover, as mentioned before, morphological analyses of iTETRA revealed formation of distinct colonies in a confluent cell layer (Figure 41 B). These defined colonies coincide with GATA3-, TFAP2C- and CDX2-positive cells and

are further characterized by a widespread organization of cell nuclei in comparison to surrounding cells as depicted in Hoechst staining of analyzed colonies.

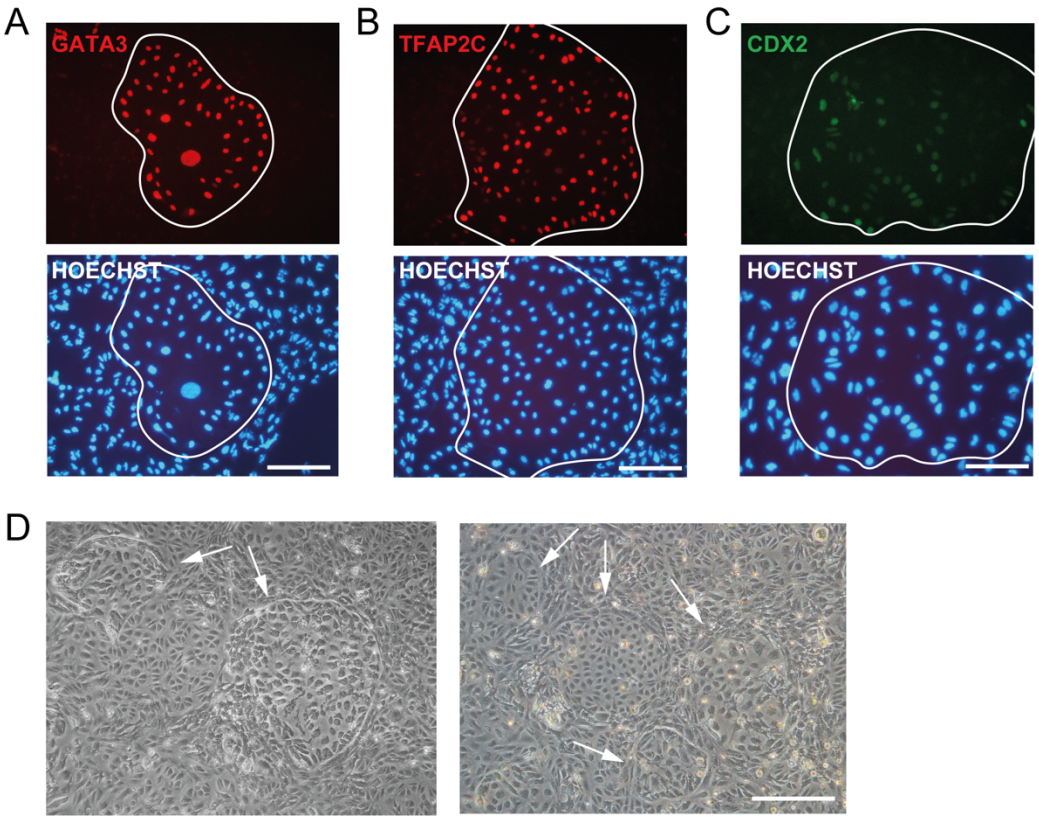

Figure 41: iTETRA colonies are GATA3, TFAP2C and CDX2 positive on day 10
A.-C. Immunofluorescence staining against GATA3 (**A.**), TFAP2C (**B**.) and CDX2 (**C.**) in iTETRA clones after ten days of transgene induction. Scale bar represents 250 µm. **D.** Representative brightfield photomicrographs of iTETRA clone after ten days of doxycycline administration. Scale bar represents 250 µm.

Under constant doxycycline supplementation, transgenic clones were further cultured up to day 20 and day 30. Continuous passaging resulted in formation of distinct colonies for remaining clones as well. However, this development remained most pronounced in iTETRA clones (Figure 42 A). On day 30, expression of *CDX2*, *TFAP2C*, *GATA3*, *EOMES*, *HCG* and *KRT7* was again analyzed in comparison to levels of wildtype hTSC line CT27 (Figure 42 B).

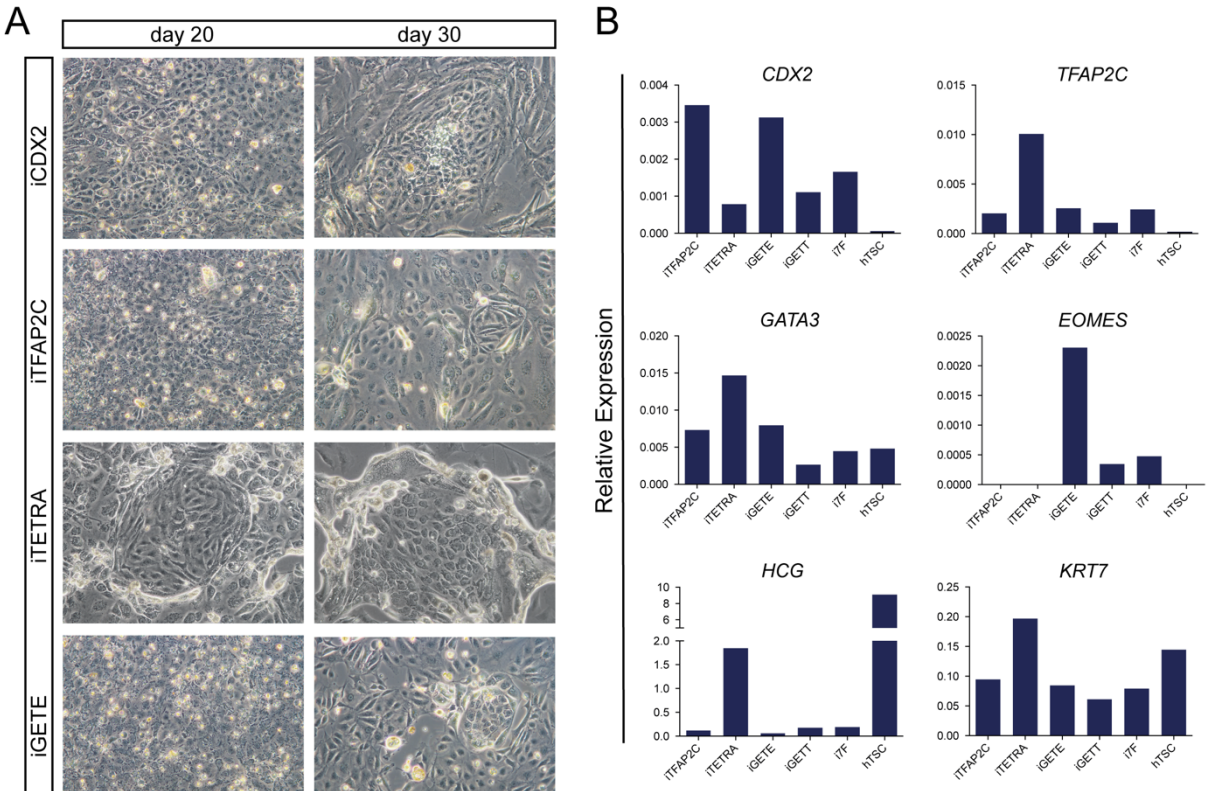

Figure 42: iTETRA show increased levels of hTSC markers on day 30
A. Representative photomicrographs of different transgenic hiPSC lines after 20 and 30 days of doxycycline administration and culture in hTSC medium. Scale bar represents 250 µm. **B.** qRT-PCR analysis of expression of TSC marker *CDX2, TFAP2C, GATA3, EOMES, HCG* and *KRT7* in iTFAP2C, iTETRA, iGETE, iGETT and i7F on day 30 of doxycycline supplemented culture in comparison to wildtype CT27 hTSC. RNA was obtained from one single experiment. Expression is normalized to housekeeping gene *GAPDH.*

Due to limited data available, interpretation of transcript levels was difficult. Shortly, *TFAP2C*, *GATA3*, *HCG* and *KRT7* expression was highest in iTETRA clones in comparison to remaining transgenic clones but only low levels of *CDX2* and *EOMES* were detected in iTETRA. Surprisingly, with further passaging, iTETRA clones showed selection for distinct structures observed on day 10. On day 30, only colonies highly resembling hTSC colonies remained in culture (Figure 43 A).

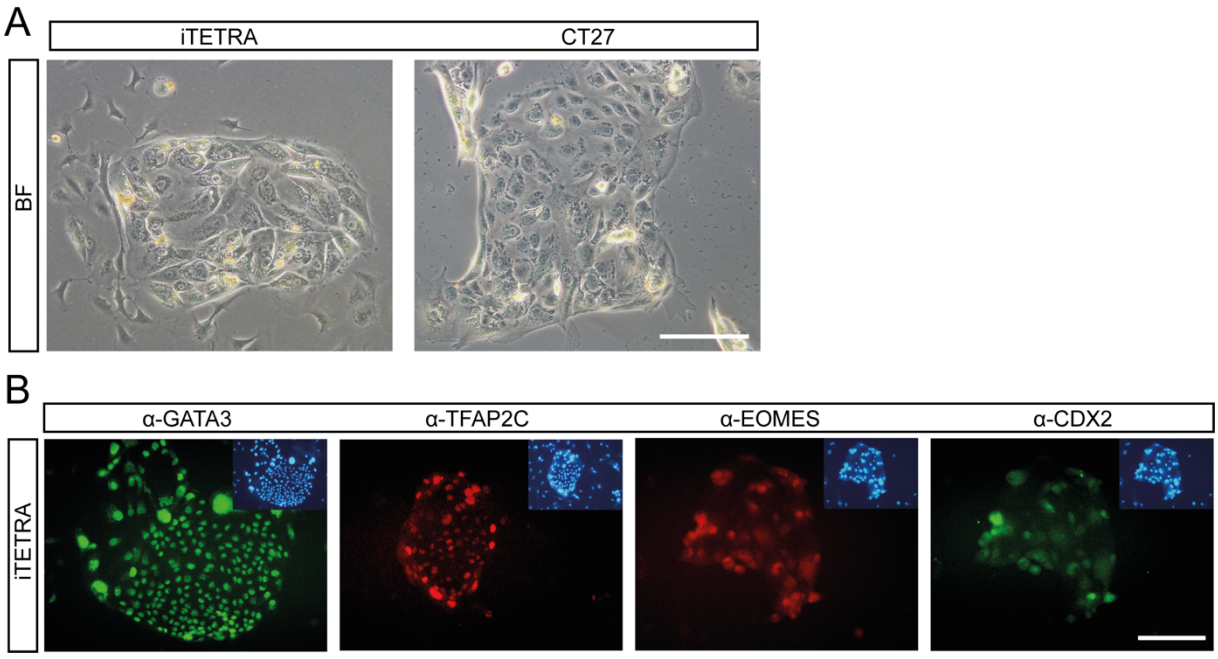

Figure 43: iTETRA show hTSC morphology on day 30
A. Brightfield images of iTETRA clone on day 30 in comparison to wildtype hTSC line CT27. Scale bar represents 250 µm. **B.** Immunofluorescence staining against GATA3, TFAP2C, EOMES and CDX2 in iTETRA clones on day 30 showing positive colonies for all proteins investigated. Insets display corresponding Hoechst stainings. Scale bar represents 250 µm.

These colonies were found to be GATA3, TFAP2C, EOMES and CDX2 positive. While most of the colonies were GATA3 positive, only 5% of all the colonies analyzed showed CDX2 positive cells indicating an induction of hTSC fate in these colonies (Figure 43 B; Table 33). Moreover, representative micrographs in Figure 43 shows a colony that is both EOMES and CDX2 positive.

Table 33: Percentage of colonies positive for GATA3, EOMES, TFAP2C and CDX2

	Percentage of all colonies
GATA3 positive colonies	80%
EOMES positive colonies	30%
TFAP2C positive colonies	30%
CDX2 positive colonies	5%

Furthermore, also clones iTFAP2C, iGETE and iGETT clones stained positive for GATA3 on day 30, however, not for other hTSC markers (Figure 44). Overall, the GATA3 positivity in these clones was reduced in comparison to iTETRA clones.

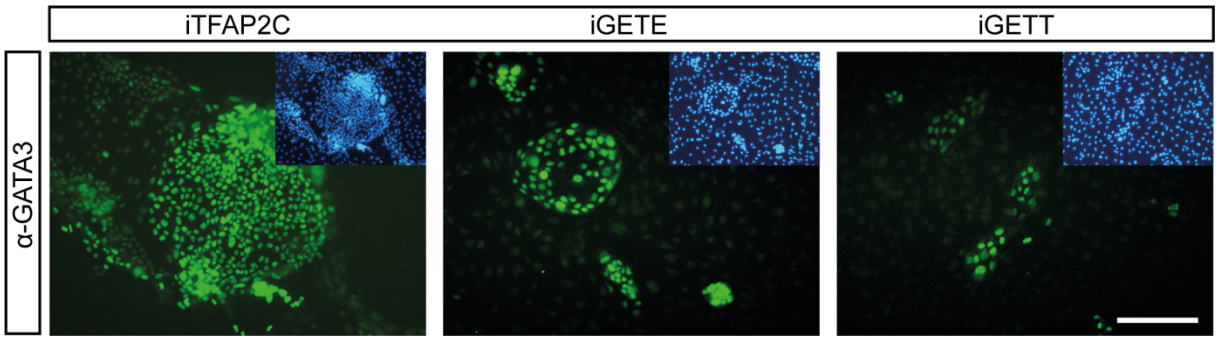

Figure 44: GATA3 positive colonies detected in iTFAP2C, iGETE and iGETT on day 30
Immunofluorescence staining against GATA3 in iTFAP2C, iGETE and iGETT clones on day 30 showing few GATA3-positive colonies. Insets display corresponding Hoechst stainings. Scale bar represents 250 µm.

Albeit limited in number of samples examined and scope of analyses conducted, this data suggests that an induction of hTSC fate in hiPSCs is indeed possible by overexpressing hTSC specific transcription factors. In this approach, combination of TFAP2A, TFAP2C, GATA2 and GATA3 proved most promising. Further experiments will show whether a full conversion can be achieved. Therefore, single colonies should be picked and extensively analyzed. Also, length of transgene induction and further transgene combination could be investigated.

8 Results III

Previously established data showed that the KIT^{D816V} autoactivating mutation resulted in an aberrant placental phenotype characterized by reduced proliferation resulting in severe growth retardation of the embryo (Kaiser et al., 2020b). The placental structure was immensely affected – demonstrated by a decreased labyrinth and spongiotrophoblast layer. Further, an excessive and premature differentiation into P-TGC subtypes was detected while other TGC-subtypes remained underrepresented (Kaiser et al., 2020b). TGCs possess various functions essential for correct placental development. Among others, these comprise secretion of placental hormones and proteins, attaching the blastocyst to the uterine wall and connecting maternal and fetal blood flow. To this end, TGCs are required to invade into the uterine wall (Simmons and Cross, 2005; Simmons et al., 2007). In order to assess the KIT^{D816V} effect on TGC capabilities more closely, it was tested whether KIT^{D816V}-TSCs demonstrate altered invasiveness and skewed differentiation in comparison to control TSCs.

8.1 Establishment of a TGC invasion assay

In a first step, an assay was established to investigate the invasive capacity of TGCs. A previous study applied the Boyden chamber for such approaches (Hemberger et al., 2004). Here, the authors monitored trophoblast migration and invasion through a Matrigel covered filter membrane of the Transwell insert. Cells adherent to the bottom side of the filter were stained using hematoxylin and the membrane was mounted onto microscope slides (Hemberger et al., 2004). While the experimental setup was easy to handle, the evaluation of this technique was challenging as visualization of invaded cells with hematoxylin did not yield clearly distinguishable cells and identification and quantification of TGCs remained difficult. Therefore, a protocol commonly used for cancer cells was adapted for TGC invasion assay approaches (Esser et al., 2022). Here, FluoroBlok Cell Culture Inserts were implemented which allow for DAPI or Hoechst staining of the migrated cells' nuclei. Interestingly, it was shown that cell densities and Matrigel concentration were crucial to the outcome of the invasion assay (Hemberger et al., 2004). Increased invasive capacity was observed for lower cell concentrations. Further, non-TGCs did not migrate through thick Matrigel layer, therefore, higher Matrigel concentration could serve as a preselection for TGCs (Hemberger et al., 2004). Thus, experimental conditions were adjusted by performing dilution series for the number of cells seeded onto the filter membrane and for Matrigel concentrations. Similarly, the duration of differentiation and invasion was customized. Final, optimized TGC invasion experiments were then performed by coating filter membranes of inserts with 0.8 mg/ml Matrigel which was dried at 37°C for two hours first, then overnight at RT (Figure 45 A). On the next day, Matrigel was rehydrated using supplemented RPMI. KIT^{D816V}-TSCs and control TSCs were harvested, and $2*10^4$ cells were seeded per well. Cells were kept under differentiating conditions for five

days (Figure 45 B). The lower chamber was filled with TS medium without CM, FGF4 or heparin and changed every day. On day 5, Matrigel in upper chamber and medium in lower chamber were discarded. Filter inserts were fixed and stained with Hoechst in methanol for 10 minutes (Figure 45 C). First attempts with TSC control cells yielded a clear visualization of invaded cells on the filter membrane after five days of growth factor removal. The stained nuclei strongly resembled TGC nuclei in structure and size indicating a successful identification of invasive TGC.

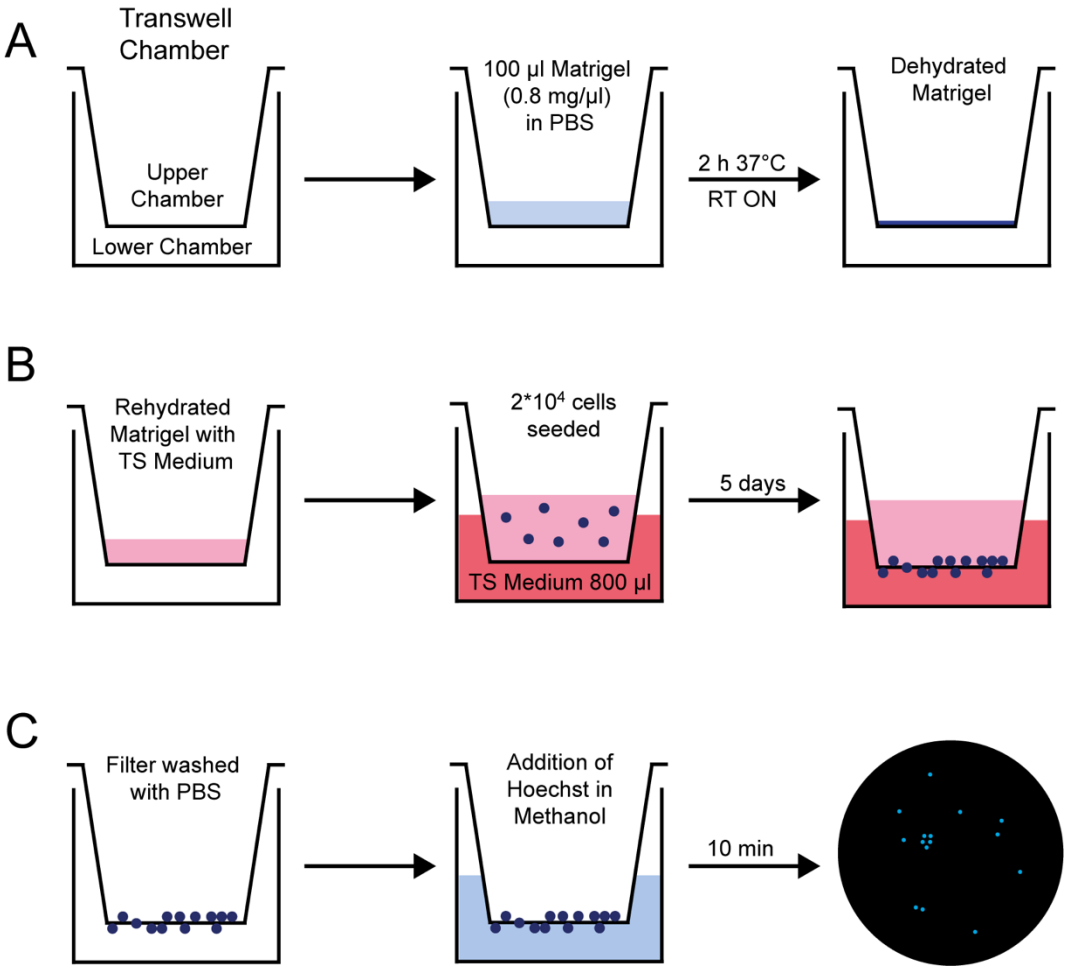

Figure 45: Schematic depicting invasion assay for TGCs
A. FluoroBlok Cell Culture Inserts were placed into 24 well plates. Filter membranes of inserts were coated with 100 µl of Matrigel diluted in PBS (0.8 mg/ml). Matrigel layer was dried at 37°C for two hours followed by incubation at RT overnight. **B.** Matrigel layer was rehydrated with supplemented RPMI medium. $2*10^4$ cells were seeded into the upper chamber and the lower chamber was filled with TS medium without CM, FGF4 and heparin. Cells were kept under differentiating conditions for five days to allow for migration and invasion. **C.** Next, the Matrigel layer and the medium in the lower chamber were discarded and filters were washed with PBS. Hoechst diluted in methanol was then added to the lower chamber to fix and stain cells' nuclei. Detection of TGC nuclei was carried out by fluorescence microscopy. Schematic depiction adapted from König and Runge, 2021.

8.2 KIT^{D816V}-TGCs are significantly more invasive than wildtype TGCs

The invasive capability of KIT^{D816V}-TGCs was assessed in comparison to wildtype (WT)-TGCs. After five days of culture under differentiation inducing conditions, invaded TGCs were detected by fluorescence microscopy and quantified per filter. Interestingly, the KIT^{D816V}-TSC

line showed significantly more invaded cells in comparison to the wildtype TSC line (Figure 46 A and B).

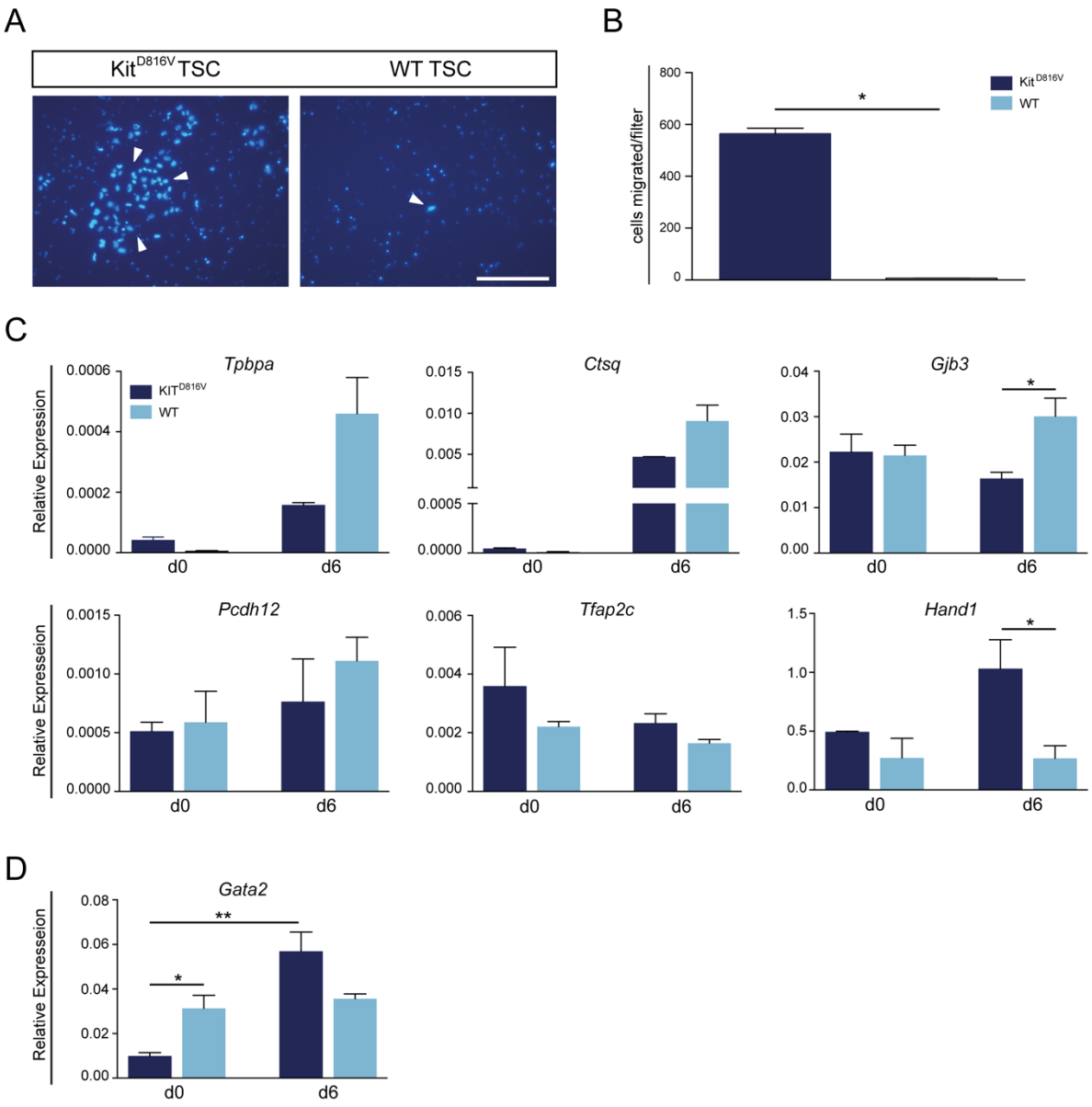

Figure 46: KIT^{D816V}-TGCs are significantly more invasive than control TGCs
A. Representative photomicrographs of nuclei of TGCs that invaded through Matrigel covered filter membrane due to five-day culture under differentiating conditions. Nuclei were stained by Hoechst and are indicated by white arrows. Scale bar represents 250 µm. **B.** Quantification of TGCs that invaded through the membrane per filter in KIT^{D816V}-TSC line and WT-TSC line. Data was obtained in two independent experiments and is represented by mean value ± SEM. Significance was determined by unpaired *t*-test and indicated with *p<0.05. **C.** qRT- PCR analysis of endogenous expression of *Tpbpa, Ctsq, Gjb3, Pcdh12, Tfap2c, Mash2* and *Hand1* in KIT^{D816V}-TSC line #4 and WT-TSC line 2.1 **D.** qRT- PCR analysis of endogenous expression of *Gata2* in KIT^{D816V}-TSC line #4 and WT-TSC line 2.1. RNA was obtained from three independent replicates at d0 in an undifferentiated state and after six days after culture under differentiation conditions. Expression was normalized to the housekeeping gene *Gapdh*; data is represented by mean value ± SEM; Significance was determined by unpaired *t*-test and indicated with *p < 0.05 and **p < 0.01. *In vitro* differentiation of TSCs and qRT-PCR were performed by Jan Langkabel. Modified from Kaiser et al., 2020b.

Next, markers *Tpbpa*, *Ctsq*, *Gjb3*, *Pcdh12*, *Tfap2c* and *Hand1* were investigated for their *in vitro* expression in KIT^{D816V}-TSCs after six days of differentiation. To this end, CM and growth

factors were withdrawn from culture medium and KIT^{D816V}-TSCs and wildtype TSCs were kept under differentiating conditions for six days. Upon growth factor withdrawal, spongiotrophoblast marker *Tpbpa*, labyrinth and S-TGC marker *Ctsq* and GlyT marker *Gjb3* and *Pcdh12* were downregulated in KIT^{D816V}-TSCs in comparison to wildtype TSCs (Figure 46 C). These findings were also confirmed by *in vivo* analyses which demonstrated increased levels of P-TGC markers as well as decreased levels of S-TGC, C-TGC and SpA-TGC markers in KIT^{D816V}-placentas (Kaiser et al., 2020b). Differentiation marker *Hand1* which is expressed in the ectoplacental cone and mediates TGC differentiation was also significantly upregulated in KIT^{D816V}-TSCs after six days of differentiation. Interestingly, both *Hand1* and TSC differentiation marker *Tfap2c* were already increased under stem cell culture conditions in KIT^{D816V}-TSCs, indicating premature differentiation in KIT^{D816V} placentas. As KIT^{D816V} was shown to increase *Gata2* expression in the hematopoietic system, *Gata2* was analyzed next in KIT^{D816V}-TSCs undergoing differentiation (Haas et al., 2015; Zeuner et al., 2011). After six days of growth factor withdrawal, KIT^{D816V}-TSCs demonstrated a significant increase in *Gata2* expression which remained unaltered in wildtype TSC (Figure 46 D). Also, *Gata2* levels were higher in KIT^{D816V}-TSCs than in wildtype TSCs on day 6. Taken together, these analyses suggest a premature differentiation in KIT^{D816V}-TSCs which favors differentiation to P-TGCs at the expense of other TGC subtypes and leads to earlier and increased gain of invasive capacity, thereby yielding a higher number of invasive cells.

Parts of this chapter have been published in:

Franziska Kaiser, Julia Hartweg, Selina Jansky, Natalie Pelusi, Carolina Kubaczka, Neha Sharma, Dominik Nitsche, Jan Langkabel and Hubert Schorle. “Persistent human KIT receptor signaling disposes murine placenta to premature differentiation resulting in severely disrupted placental structure and functionality.” International Journal of Molecular Sciences 21, 2020.

9 Discussion I

9.1 TX medium promotes ESC to TSC conversion

This part of the study set out to shed light on the first lineage decision in mammalian development by achieving complete conversion from murine ESC to TSC fate. *In vivo,* trophectoderm and epiblast are strictly separated by distinct transcription factor circuits and maintenance of an epigenetic barrier (Cockburn and Rossant, 2010; Hemberger et al., 2009; Rugg-Gunn et al., 2010; Senner et al., 2012). Previous studies could show that TSC-like cells can be obtained by individually overexpressing *Tfap2c*, *Gata3* or *Cdx2* (Kuckenberg et al., 2010; Niwa et al., 2005; Ralston et al., 2010). However, it was also reported that TSC-like cells retain an epigenetic memory of ESCs when e.g. overexpressing *Cdx2* or activating the MAPK pathway (Cambuli et al., 2014). Therefore, this study investigated the combination of TSC transcription factor activation required for ESC to TSC conversion, while at the same time examining the optimal culture conditions for this approach. Different culture media are commonly used for murine TSC culture. First, the conventional serum containing TS medium was developed which requires to be conditioned by fibroblasts (Tanaka et al., 1998). Then two chemically defined media compositions that forgo serum and yield homogenous, undifferentiated TSC colonies were introduced (Kubaczka et al., 2014; Ohinata and Tsukiyama, 2014).

Here, it was shown that a three-day overexpression of five factors *Tfap2c*, *Eomes*, *Gata3*, *Ets2* and *Cdx2* is sufficient to induce bona fide TSC fate in ESCs independent of culture medium. Interestingly, induction of 4F (*Tfap2c*, *Eomes*, *Gata3* and *Ets2*) or iCdx2 resulted in TSC fate only when clones were cultured in the chemically defined TX medium, indicating the importance of culture conditions in combination with transgene induction (Figure 47). Factors supplied with the TX medium are able to substitute for either four factors in the case of iCdx2 or for CDX2 in the case of 4F clones. The iTSC clones could be stably propagated for more than four months and presented with high levels of TSC specific cell surface markers and expression of TSC markers which was comparable to wildtype TSCs. Importantly, in all aforementioned approaches, the epigenetic barrier was overcome. Moreover, $5F2^{TX}$-iTSCs showed *in vivo* functionality as they contributed to placental chimerization upon blastocyst injection. As reported by Cambuli et al., $iCdx2^{TS}$ clones showed upregulation of TSC markers but the *Elf5* promoter remained methylated (Cambuli et al., 2014). Similarly, $4F^{TS}$ clones did not result in a conversion to iTSCs which confirmed previously published results (Kubaczka et al., 2015). Single factor lines iTfap2c, iGata3, iEomes and iEts2 did not achieve induction of TSC fate in both culture conditions: ESC methylation pattern was retained, and clones exhibited only low levels of TSC marker.

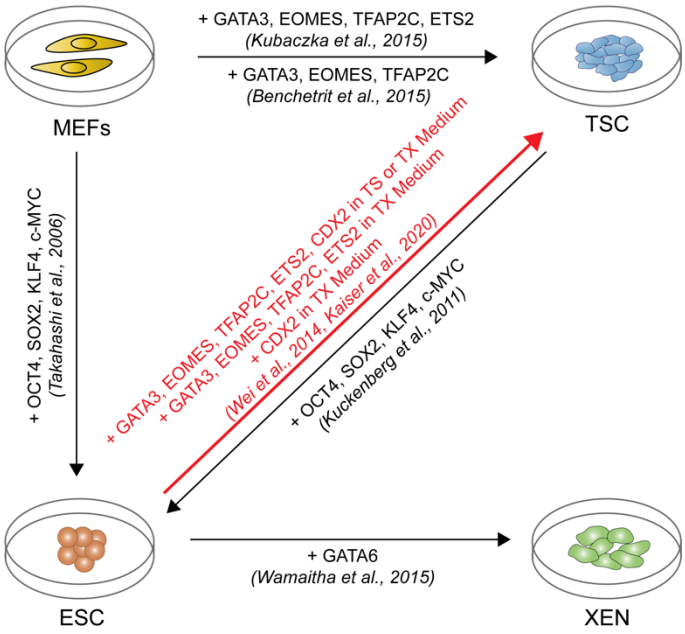

Figure 47: Complete murine ESC to TSC conversion put into the current state of research
Completion of schematic shown as figure 7 in 1.1.6.. This study could show that overexpression of *Gata3*, *Eomes*, *Tfap2c*, *Ets2* and *Cdx2* in TS or TX medium as well as overexpression of *Gata3*, *Eomes*, *Tfap2c* and *Ets2* or *Cdx2* in TX medium results in stable induction of bona fide TSC fate in murine ESCs. Wei et al. were also able to show conversion from ESC to TSC fate using CRISPR/Cas9 mediated overexpression of *Cdx2* in TX medium.

In the course of the study, the established clones were first verified for the presence of transgenes. Genotyping showed proper integration of transgenes in the genome and doxycycline administration induced transgene expression and protein transcription in clones after three days. Strikingly, transgene expression was higher in clones cultured in TX medium than in clones cultured in TS medium. This might be due to a technical problem since serum proteins included in TS medium were shown to bind small molecules such as doxycycline, thus a decreased number of molecules might be available for binding to transactivator rtTA (Riond and Riviere, 1989; Schmidt et al., 2008). TX medium on the other hand might result in higher concentrations of free doxycycline molecules and unimpaired binding, therefore reaching transgene expression levels required for successful ESC to TSC conversion. Analysis of transgene expression also showed that levels varied between the different 4F clones. Clone 4F3 showed lower transgene expression of *Eomes*, *Gata3* and *Ets2* but higher *Tfap2c* expression than 4F1 and 4F2 in both media conditions. Within the 5F clones, $5F2^{TX}$ showed the highest transgene expression of all factors. While *Tfap2c* was introduced into Col1A1 locus, the remaining factors were delivered into the genome by lentiviral transduction thereby being random in site and number of integrations. Further variations might result from methylation-induced transgene silencing which was shown to occur with transgenes delivered by lentiviral vectors albeit less frequently than following simple retrovirus transduction (Pfeifer et al., 2002; Wen et al., 2021).

After successful validation of ESC clones, transgenes were induced for three days in clones cultured in TS or TX medium, respectively. Interestingly, endogenous expression on day 3 depended directly on levels of transgene expression as 4F3 showed less CD40+/PLET1+ cells

and lower levels of *Elf5*, *Cdx2*, *Eomes* but not of *Tfap2c* than 4F1 and 4F2. As TFAP2C was shown to exhibit a self-reinforcing capacity, presence of transgenic *Tfap2c* resulted in high levels of endogenous *Tfap2c* expression (Kidder and Palmer, 2010). Similarly, high expression of all transgenes in $5F2^{TX}$ yielded the highest expression of *Elf5* on day 3. Still, TSC marker expression and protein levels were significantly lower compared to bona fide TSCs in all clones. With propagation from day 3 to passage 5, an increase in levels of CD40 and PLET1 as well as rising expression levels of *Elf5*, *Cdx2*, *Eomes* and *Tfap2c* were observed. This indicates a continuous conversion process independent of transgene induction. The reprogramming process from somatic cells to iPSCs is separated into three phases termed initiation, maturation and stabilization (Hawkins et al., 2014; Samavarchi-Tehrani et al., 2010). In our approach, three days of transgene induction represent the initiation stage of cell fate conversion which is followed by maturation with ongoing cultivation. Continuous passaging of clones resulted in stabilization of TSC fate at passage 5 which was then confirmed by methylation analyses.

In contrast to 5F clones, 4F and iCxd2 clones achieve a full conversion in TX medium only. These results are in line with two other publications. Cambuli et al. showed that *Cdx2* overexpression in ESCs cultured in TS medium yields only TSC-like cells with a methylation pattern reminiscent of ESCs while Wei et al. demonstrated a complete conversion by CRISPR/Cas9 mediated activation of *Cdx2* in TX medium (Cambuli et al., 2014; Wei et al., 2016). Besides implementing different methods for *Cdx2* induction, these two studies also differ in the culture medium used. There are two distinct qualities of TX medium presumably supporting the conversion. Firstly, TX medium was shown to be strictly selective for undifferentiated TSCs (Kubaczka et al., 2014). The extent of spontaneous differentiation was demonstrated to be reduced in TX medium due to cells eventually undergoing apoptosis upon differentiation (Kubaczka et al., 2014). Thus, TX medium yields a homogenous TSC population which is equivalent to E7.5 trophoblast (Kubaczka et al., 2014). As a result, ESC control cells and incompletely converted cells developing from single factor lines iTfap2c, iEomes, iGata3 and iEts2 could not be propagated in TX medium. Secondly, TX medium was reported to mimic the *in vivo* environment more closely than TS medium (Kubaczka et al., 2014). In this context, Cambuli et al. could show that blastocyst injections of incompletely converted TSC-like cells yielded chimeric placentas anyway (Cambuli et al., 2014). The authors propose that a completion of conversion occurs due to factors present in the *in vivo* environment (Cambuli et al., 2014; Lu et al., 2008). TX medium could be exhibiting a similar promoting effect on cells converting from ESC to TSC fate. However, it is important to note that TX medium alone is not sufficient to cause TSC fate induction in ESCs. Withdrawal of LIF and switch to TX medium resulted in ESCs undergoing apoptosis even when performing the medium change gradually

or after intermediate culture in TS medium. Therefore, the necessity for overexpression of TSC specific transcription factors is indispensable.

As previously shown, *Cdx2* expression results in downregulation of OCT4, while *Tfap2c* expression yields downregulation of NANOG (Kuckenberg et al., 2012; Niwa et al., 2005). The effect of *Cdx2* overexpression in ESCs was analyzed in detail and it was reported that CDX2 does not bind directly to regulatory regions of pluripotency genes but inhibits a pro-pluripotency complex (Nishiyama et al., 2009). When monitoring OCT4 levels during the first eight days of ESC to TSC conversion, Western Blotting analyses revealed the fastest downregulation of OCT4 in iCdx2^{TX} clones. Interestingly, all clones showed reduction in OCT4 levels faster when cultured in TX medium compared to culture in TS medium. 5F and iCdx2 clones trigger OCT4 downregulation directly by expression of transgenic *Cdx2*. 4F clones, however, are required to induce endogenous *Cdx2* expression first. That is the reason why for 4F3^{TS} and 4F3^{TX}, OCT4 downregulation was delayed and protein levels still detectable on day 8. Endogenous *Cdx2* expression was detected in 4F clones on day 3 in combination with consequential OCT4 downregulation starting from day 4 in TX medium and day 6 in TS medium. *Cdx2* expression can be induced by different transgenic TSC transcription factors: GATA3 was reported to regulate *Cdx2* transcription by binding to the *Cdx2* chromatin domain (Home et al., 2009). Also ETS2 was shown to regulate Cdx2 expression (Donnison et al., 2005). Summarized, the results confirm that downregulation of OCT4 and thereby loss of pluripotency is essential for ESC to TSC conversion as clones with a rapid and complete downregulation of OCT4 achieve a full conversion.

Besides OCT4 downregulation, the activation of the hierarchical, self-reinforcing TSC transcription factor network plays an important role during the conversion and in regulating TSC fate. *Cdx2* and the remaining factors *Eomes*, *Tfap2c*, *Gata3* and *Ets2* are involved in activating specific parts of the intrinsic network. *In vivo*, CDX2 is directly targeted and induced by TEAD4. CDX2 is regarded as determining factor of trophoblast fate, as it is not found in non-TE cells while TEAD4 is still present in all cells of morula (Nishioka et al., 2009). In TSCs, CDX2 was demonstrated to act upstream of TFAP2C and ETS2 (Beck et al., 1995; Niwa et al., 2005) as well as being able to induce *Eomes* and reinforce its own expression (Niwa et al., 2005). Interestingly, iCdx2^{TS} and iCdx2^{TX} clones show an equivalent upregulation of *Eomes* expression compared to 5F clones and higher than in 4F clones. This indicates that *Eomes* is most prominently induced by CDX2. Also, *Elf5*, *Tfap2c* and endogenous *Cdx2* expression was increased after the only short induction of transgenic *Cdx2* on day 3. In parallel to CDX2, GATA3 is activated by TEAD4. In iGata3 single factor clones, induction of *Eomes* was most striking after three days of transgene activation. In iEomes on the other hand, transgenic EOMES was capable of upregulating all markers examined – *Elf5*, *Cdx2* endogenous *Eomes*

and *Tfap2c*. Interestingly, induction of *Eomes* expression was most pronounced in all single factor clones indicating that EOMES plays a central role in the TSC transcription factor network. The strongest *Tfapc2* induction was detected in iTfap2c, strengthening the finding of its self-reinforcing capacity (Kidder and Palmer, 2010). Induction of transgenes in neither iTfap2c, iGata3 nor iEts2 caused upregulation of *Cdx2* or *Elf5* which could be an important reason as to why conversion to TSC fate failed in these clones. Several of previously described interactions in the TSC transcription factor network were detected in this study. On top of that, the data showed that also ETS2 and TFAP2C are capable of activating *Eomes* expression (Figure 48).

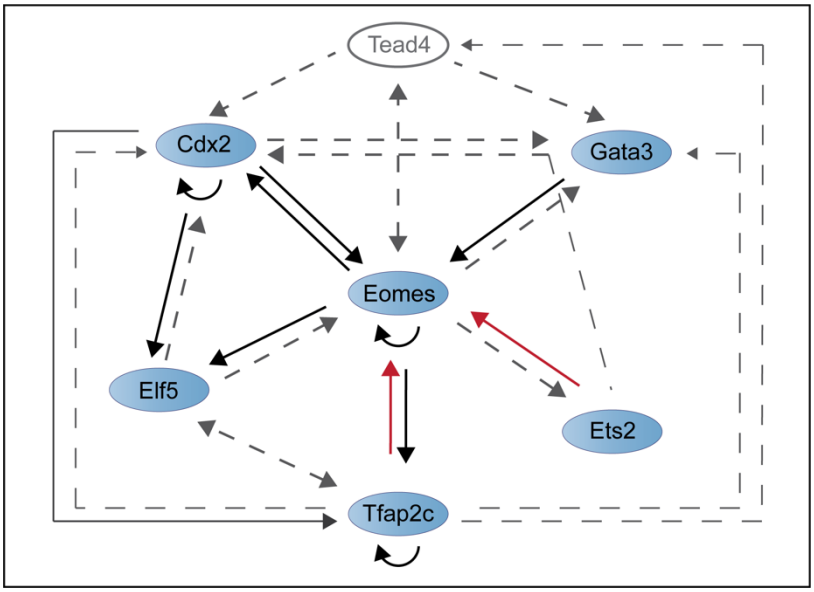

Figure 48: Additional interactions found in the murine TSC transcription factor network
The interactions between TSC transcription factors confirmed in this study are represented by black arrows. Those that were additionally described in previous publications are shown dashed and in grey (Kubaczka et al., 2016). In addition, the interactions that had not been described yet but were detected in this study are depicted by red arrows.

To summarize, 5F clones presented with the highest conversion efficiency since transgenic CDX2 caused downregulation of OCT4 while simultaneously transgenic TFAP2C downregulated NANOG. All five transgenes contributed to activating the innate transcription factor network. Thereby, 5F clones reproduced most of the interactions that take place in bona fide TSCs at the stage of the first lineage separation. 5F clones, however, do not require the presence of TEAD4 to initiate the regulative network. Even though single factor lines did not yield TSC fate, they were well suited for verifying the activation cascade within the transcription factor network.

Interestingly, $4F^{TS}$ and $iCdx2^{TS}$ at passage 5 present with a homogenous, proliferating population but are neither comparable to bona fide ESCs nor TSCs. $4F3^{TS}$ clones showed ESC-like morphology and only 2% of the cells were positive for CD40 and PLET1. $iCdx2^{TS}$ cells showed TSC-like morphology and 91% of the cells were CD40 and PLET1 positive. Both clones showed ESC-like methylation pattern but were OCT4 negative. For additional

investigation of these clones, they were continuously propagated up to passage 12. Here, clones cultured for 12 passages in TS medium remained with ESC methylation pattern of the *Elf5* promoter. 4F2$^{TS→TX}$ and iCdx2$^{TS→TX}$ clones that were switched to TX medium at passage 5 for an additional 5 passages in TX medium showed a demethylation of the *Elf5* promotor at passage 12. Morphological observations especially in 4F3$^{TS→TX}$ clones suggest that increased apoptosis and differentiation were co-occurring with the medium switch. Yet, neither of the clones showed extensive apoptosis comparable to ESC control cells cultured in TX medium. This suggests that a preliminary TSC fate was initiated even in 4F^{TS} and iCdx2^{TS} clones due to previous transgene induction that could be completed by TX culture. Schwarz et al. and other groups investigated the reprogramming process from murine somatic cells to iPSC including the reprogramming efficiency which is low under standard conditions. The authors could show, however, that it could be drastically increased if they sort for cells poised for reprogramming using distinct cell surface markers as they discovered that not all cells in a bulk population harbor the same potential for reprogramming (Brambrink et al., 2008; Schwarz et al., 2018; Stadtfeld et al., 2008). Correspondingly, the conversion efficiency in 4F^{TS} and iCdx2^{TS} clones might be particularly low. Poised or already converted cells are obscured by the majority of cells that did not initiate the conversion. Sorting for a subpopulation that is poised for conversion to TSC fate would be possible after identifying appropriate cell surface markers. Further experiments using techniques such as single cell RNAseq could help characterizing the incompletely converted cells that suggest being caught in an intermediate state between ESCs and TSCs.

The epigenetic barrier between ESCs and TSCs is maintained by several differentially methylated loci comprising *Elf5*, *Nanog*, *Oct4*, *Tead4*, *Ezrin*, *Hand1*, *Lasp1*, *Map3k8*, *Plet1*, *Rin3*, *Sh2d3c* and *Tinagl* (Cambuli et al., 2014; Kuckenberg et al., 2011; Ng et al., 2008). As Cambuli et al. showed that the epigenetic pattern remained ESC-like when e.g., overexpressing *Cdx2* in ESCs, the analysis of *Elf5*, *Oct4* and *Nanog* promoter methylation represented an important milestone in this study. 5F^{TS}, 5F^{TX}, 4F^{TX} and iCdx2^{TX} clones showed demethylation of the *Elf5* promoter and hypermethylation of the *Oct4* and *Nanog* promoter at passage 5. They also presented with high expression levels of the additional genes that were identified to have differentially methylated promoter regions in ESCs and TSCs. Therefore, a complete conversion to TSC fate could be successfully shown in these clones. Of note, ESC-like methylation patterns were still detected for all the clones on day 3 (data not shown) confirming the continuing conversion to TSC fate past transgene induction. And while primary upregulation of marker expression was achieved within three days, changes in methylation required more time. Additionally, the expression of *de novo* DNA methyltransferases *Dnmt3a* and *Dnmt3b* as well as expression of *Dnmt1*, the main maintenance DNMT were tested in 4F3,

5F2, iCdx2, ESC and TSC clones (Okano et al., 1999; Song et al., 2012). Interestingly, *Dnmt3a* and *Dnmt3b* were highly expressed in those clones that achieved a full conversion. It stands to reason that the high activity of these *de novo* DNMTs was required for establishing methylation in *Oct4* and *Nanog* promoter regions and additional genes that are repressed in TSCs but not in ESCs. Expression levels of *Dnmt1* were comparable for all clones tested – including wildtype ESCs and TSCs. Thus, the maintenance of methylation after cell replication was upheld in all clones tested. Interestingly, it was reported that inhibition of DNMTs or depletion of DNTM substrate SAM promotes conversion from somatic to iPSC cells by causing demethylation of silenced pluripotency genes (Hou et al., 2013; Mikkelsen et al., 2008; Qin et al., 2017; Shi et al., 2008).

As appropriate modulation of signaling pathways was shown to support and direct the reprogramming from somatic cells to iPSCs, cardiac cells and neural cells (Hawkins et al., 2014; Qin et al., 2017; Tanabe, 2015), it was investigated whether components of TX medium activate distinct TSC pathways to a greater extent than TS medium. In this context, it was shown for instance that altering the MAPK or Wnt/β-catenin pathway could promote reprogramming of somatic cells (Sanges and Cosma, 2011). The Ras-MAPK signaling was also demonstrated to be essential for pre-implantation development by controlling the establishment of the trophectoderm (Maekawa et al., 2005). Inhibition of Ras-MAPK signaling resulted in impaired cavity formation and adverse development and functionality of early extra-embryonic lineages *in vivo* as well as loss of *Cdx2* expression (Lu et al., 2008; Maekawa et al., 2005). By contrast, TSC fate could be induced in ESCs by Ras activation (Cambuli et al., 2014; Lu et al., 2008). Also, TGFβ was identified as an essential factor for maintenance of TSC fate and was able to support proliferation of TSCs in the absence of fibroblast conditioned medium (Erlebacher et al., 2004; Kubaczka et al., 2014). Inhibition of TGFβ signaling resulted in enhanced differentiation (Erlebacher et al., 2004). Greater activation of any one of these pathways could be a reason for faster and more efficient conversion to TSC fate in TX medium. Hence, the phosphorylation of proteins involved in MAPK pathway (AKT1, CREB, ERK1/2, GSK3A, GSK3B, HSP27, JNK, MEK, MKK3, MKK6, MSK2, mTOR, p38, p53, p70S6K, RSK1 and RSK2) as well as the levels of proteins involved in TGFβ signaling (Activin A, ActivinR1A, BAMBI, Beta-IG-H3, BMP2, BMP4, BMP6, BMP7, BMP8, BMP9, BMP15, BMPRIA, BMPRII, Follistatin, GDF11, GDF15, LeftyA, NOGGIN, SMAD3, SMAD4, TGFα, TGFβ1, TGFβ2, TGFβRII, TGFβRIII) were examined in cell lysates from clones iCdx2^{TS}, iCdx2^{TX}, TSC^{TS} and TSC^{TX} using specific microarrays. Yet, when comparing levels of said proteins in both pathways, no alteration could be detected between TS or TX culture conditions.

In this study, transgene induction in SF lines iTfap2c, iEomes, iGata3 and iEts2 did not result in stable induction or even transient upregulation of TSC markers. In contrast, other studies could show that also single factor activation in ESCs can result in induction of TSC fate. These studies, however, have only been conducted in TS medium and complete conversion was never assessed as methylation status remained unevaluated. *Tfap2c* overexpression for ten days resulted in TSC-like cells that were expressing *Elf5* (Kuckenberg et al., 2012). Six-day overexpression of *Eomes* yielded TSC-like cells that were morphologically comparable to bona-fide TSCs and expressed *Cdx2* and *Eomes* (Niwa et al., 2005). Overexpression of *Gata3* for six days was shown to lead to an induction TSC marker expression in ESC, but also here, stable TSC lines could not be established (Ralston et al., 2010). These approaches have in common that transgene induction was continued for more than three days. Transgene activation for only three days might be insufficient for individual transgenes *Tfap2c*, *Eomes*, *Ets2* or *Gata3* to induce TSC marker expression or even conversion to TSC fate.

In conclusion, complete conversion from ESC to TSC fate was achieved in $5F^{TS}$, $5F^{TX}$, $4F^{TX}$ and $iCdx2^{TX}$ clones. This was verified by TSC marker expression, protein levels and TSC methylation patterns. The clones also show long-term stability as well as the full potential to differentiate into trophoblast subtypes *in vitro*. $5F^{TX}$ also showed *in vivo* functionality upon blastocyst injection. This study also highlighted the importance of culture conditions for cell fate changes as components of the TX medium promoted ESC to TSC conversion. Today, there is a wide range of reprogramming techniques including pathway activation, transgene integration by lentiviral transduction or CRISPR/Cas9 mediated gene expression (Rao and Malik, 2012), but small molecule reprogramming is gaining increasingly more attention. It is caused by not-integrating viral vectors, microRNAs and non-viral and non-integrating chemical compounds approaches (Baranek et al., 2017; Chen et al., 2020; Ma et al., 2017). For instance, studies set out to identify chemical compounds which are capable of substituting the Yamanaka factors in murine fibroblast to iPSC reprogramming (Ma et al., 2017). Hou et al. and Zhao et al. could demonstrate reprogramming from murine somatic cells to iPSCs by using a cocktail of small-molecule compounds (Hou et al., 2013; Qin et al., 2017; Zhao et al., 2015). In that approach, inhibition of TGFβ signaling promoted mesenchymal to epithelial transition while induction of Wnt signaling promoted the expression of pluripotency genes. Late stage reprogramming was facilitated by MAPK/ERK inhibition (Chen et al., 2020; Qin et al., 2017). Also, derivation of neurons from hiPSCs was facilitated by appropriate cell culture environment and initial induction of hTSC fate can be triggered in hiPSCs by adding BMP4 to the culture medium (Amita et al., 2013; Castel et al., 2020; Cinkornpumin et al., 2020; Dong et al., 2020; Horii et al., 2020; Mischler et al., 2021). Deciphering the complex mechanisms that cause cell fate conversion, cell reprogramming or transdifferentiation is of great importance for modeling

of diseases and subsequent drug research (Ma et al., 2017). Small molecules have the advantage that they could be transformed into appropriate drugs with targeted delivery to the affected areas (Ma et al., 2017). Future studies will show whether cell reprogramming will eventually find implementation in therapeutic approaches to treat conditions such as cardiac failures or cancer.

Parts of this chapter have been published in:

Franziska Kaiser, Caroline Kubaczka, Monika Graf, Nina Langer, Jan Langkabel, Lena Arévalo, and Hubert Schorle. “Choice of Factors and Medium Impinge on Success of ESC to TSC Conversion.” Placenta 90, 2020.

10 Discussion II

10.1 Induction of hTSC fate in primed hiPSC

Human trophoblast stem cells are presumed to be a subset of villous cytotrophoblasts that proliferate, self-renew and differentiate along all human trophoblast lineages. As effects of aberrant hTSC development could manifest later in development in form of preeclampsia, fetal growth restriction, miscarriage or choriocarcinomas, it is of great interest to analyze the proper development of hTSCs and establish connections between them and the aforementioned malfunctions (Burton et al., 2016; Hemberger et al., 2020; Knöfler et al., 2019). While mouse TSCs were first derived in 1998, human TSCs still remain a relatively new field of research (Castel et al., 2020; Tanaka et al., 1998). And even though human ESCs were already derived from human blastocysts, stable hTSCs could first not be established *in vitro* (Castel et al., 2020; Thomson et al., 1998). Only in 2018, Okae et al. showed successful derivation of hTSC lines from blastocysts and first-trimester cytotrophoblasts (Okae et al., 2018). The obtained hTSCs proliferated stably in culture, showed cobblestone-like morphology and differentiated into EVT as well as STB lineages. Importantly, the authors developed a new medium for hTSC culture. This medium contains EGF, a Wnt pathway activator as well as NODAL/TGFß inhibitors (Okae et al., 2018). Human placental organoids that were established shortly before, rely on similar culture conditions (Haider et al., 2018; Turco et al., 2018). Interestingly, this is in contrast to murine TSC culture conditions which rely on administration of FGF4 and TGFß (Kubaczka et al., 2014; Tanaka et al., 1998).

Here, the cell lines newly established by Okae et al. were first expanded and further analyzed (Okae et al., 2018). The cell line CT27 derived from first-trimester cytotrophoblasts showed typical epithelial-like colonies which were positive for TFAP2C and GATA3, however, negative for CDX2, EOMES and ETS2. Furthermore, cells were expressing low levels of *GATA3* as well as high levels of *KRT7* and *HCG* which is in line with results shown by Okae et al. (Okae et al., 2018). An assessment of these derived hTSCs will be part of the ensuing discussion.

Next, this study set out to elucidate the combination of hTSC specific transcriptions factors that is sufficient to induce hTSC fate in hiPSCs. As of yet, several approaches for induction of hTSC fate have been conducted, all of which relied on cell fate conversion using chemical compounds. To this end, it was shown that BMP4 addition or medium switch to hTSC medium can result in an induction of a TSC-like state (Amita et al., 2013; Castel et al., 2020; Cinkornpumin et al., 2020; Dong et al., 2020; Horii et al., 2020; Mischler et al., 2021). Primed hPSCs which are equivalent to post-implantation epiblast were shown to adopt a trophoblast fate after being exposed to BMP4 or BAP treatment (Amita et al., 2013; Horii et al., 2020). While these cells showed conversion to trophoblast-like fate, they did not self-renew and rather

resembled differentiated trophoblasts. Other groups even claimed that hiPSCs did not undergo conversion to hTSC-like cells but rather differentiated to mesoderm- or amnion-like cells (Bernardo et al., 2011; Guo et al., 2021; Roberts et al., 2014).
Interestingly, naïve hiPSCs which represent the human pre-implantation epiblast harbor a capability to convert to hTSC fate that is distinct from primed iPSCs (Dong et al., 2020; Huang et al., 2014). To this end, Dong et al. could show that BMP4 addition to the medium resulted in induction of hTSC-like fate in primed but not in naïve hiPSCs. Naïve hiPSCs were required to be cultured in standard hiPSC medium first before responding to BMP4 treatment. Naïve hiPSCs, however, show a conversion to hTSC fate after switch to hTSC medium (Dong et al., 2020). This was even successful when reprogramming fibroblasts using OSKM factors under hTSC culture conditions (Castel et al., 2020; Takahashi et al., 2007). These obtained hiTSCs showed self-renewal, differentiation potential to STB and EVT and share expression profiles with hTSCs established by Okae et al. (Castel et al., 2020; Okae et al., 2018). For primed hiPSCs, however, a mere change to hTSC medium is not sufficient to induce hTSC fate. This is in line with results obtained in this study as primed hiPSCs control cells did not show induction of hTSC fate after culture in hTSC medium for several passages. It was suggested that hiPSCs' potential to convert to hTSCs is depending on their developmental stage with naive hiPSCs being most prone to the conversion (Castel et al., 2020). While murine ESCs do not form cells of the trophectoderm lineage without exogenous genetic or epigenetic modifications, recent results suggest more plasticity between cell fate lineages in the human system and that hNPSCs harbor an intrinsic capacity to generate trophectoderm cells (Guo et al. 2021; Posfal et al., 2021).

In this study, it took ten days for morphological changes towards hTSC fate to become apparent in iTETRA clones while the other clones remained unaltered in comparison to their respective control clone cultured without doxycycline. iTETRA clones also showed increased expression of *CDX2*, *TFAP2C*, *GATA3*, *HCG* and *KRT7* as well as presence of GATA3, TFAP2C and even CDX2 positive colonies. The hTSC medium itself was not selective for hTSC-like cells as also hiPSCs and transduced cells cultured without doxycycline could be stably propagated. Yet, iTETRA clones showed a selection for distinct colony structures, which were highly resembling hTSC colonies while unconverted cells were lost with further passages up to day 30. In 80% of all iTETRA colonies, all cells were now detected to be GATA3 positive indicating that GATA3 negative cells were not further supported or also converted to GATA3 positive cells. Also, there was an increase in transcript levels of *TFAP2C*, *GATA3*, *HCG* and *KRT7* detectable from day 10 to day 30 in iTETRA clones. *KRT7* levels of iTETRA even exceeded those of bona fide hTSCs (Okae et al., 2018). These findings suggest that there is a continuous conversion occurring further strengthening the hTSC-like fate. Interestingly, in a

few iTETRA colonies, cells were even CDX2 positive on day 30. In further experiments, it would be important to pick those single colonies in order to enrich for CDX2 positive cells. As clones were cultured under constant doxycycline administration, it cannot be distinguished between endogenous and transgenic GATA3 and TFAP2C positive cells. EOMES, CDX2 and HCG and KRT7, however, were activated through the intrinsic hTSC transcription factor network in iTETRA clones and expressed endogenously. In clones iGETE, iGETT and iTFAP2C, GATA3 positive colonies were detected, but to a lesser extent than in iTETRA clones. Further, no TFAP2C, EOMES, CDX2 positive colonies were detectable there. This indicates that these transcription factor combinations might not be sufficient for complete induction of hTSC fate. Even though limited to a single approach, iTETRA induction represents the most promising combination of hTSC transcription factors.

As TETRA factors were regarded as the earliest drivers of trophoblast fate, it is not unexpected that overexpression of these factors resulted in the most promising approach. When assessing the effect of BMP4-induced conversion from hiPSCs to hiTSCs, Krendl et al. discovered the circuit of TFAP2A, TFAP2C, GATA2 and GATA3 transcription factors and coined the expression trophectoderm four (TEtra) factors (Krendl et al., 2017). It was shown that these factors induce trophoblast specific gene expression while also suppressing the pluripotency network by binding to the first intron of *OCT4*. In this context, GATA3 was regarded as a pioneer factor (Krendl et al., 2017). TEAD4 was not found to be induced in the early stages of hiPSC to hiTSC conversion indicating a reason as to why iGETT clones did not achieve an induction of hTSC fate (Krendl et al., 2017). While CDX2, TFAP2C, GATA3 were found in human TE progenitors indicating their role in early trophoblast development, they were not sufficient for hTSC induction in this setting (Deglincerti et al., 2016; Niakan and Eggan, 2013).

Of note, the presence of CDX2 positive cells is the most striking difference between hTSC-like cells established in this study and hTSCs derived from blastocysts or first term placentas (Okae et al., 2018). The existence of both CDX2+ and CDX2- human trophoblast cells might result from different developmental stages *in vivo*, which these *in vitro* cultures correspond to. To this end, single cell RNA-seq of the human embryo during peri-implantation development from E3-E14 showed that primary, CDX2 negative hTSCs resemble E8-E10 cytotrophoblast cells. CDX2 positive cells, however, are found earlier in TE development – around E5-E6 (Castel et al., 2020; Okae et al., 2018). Therefore, hTSCs published by Okae et al. can be studied for early trophoblast lineage development but not pre-implantation TE (Cinkornpumin et al., 2020; Dong et al., 2020; Knöfler et al., 2019; Mischler et al., 2021). Recent data showed the parallel conversion of hESCs to both hiTSCs^{CXD2+} and hiTSCs^{CDX2-} (Mischler et al., 2021). Those two populations require distinct cell culture conditions and exhibit different gene expression

patterns. Similarly, the CDX2- population is comparable to placental derived hTSCs and villous cytotrophoblasts. The authors also suggest hiTSCs^{CXD2+} to be a more primitive cell type than hiTSCs^{CDX2-}. Therefore, CDX2+ hiTSC-like cells obtained in this study could represent early stages of human TE development and could be used for studies of the pre-implantation phase.

If preliminary results obtained in this study can be confirmed in the future, overexpression of hTSC specific transcription factors such as iTETRA factors could be introduced as a first method to convert primed hiPSCs to pre-implantation, CDX2 positive hiTSCs (Figure 49). Further experiments need to be performed investigating among others iTETRA-CDX2+ subclones, overexpression of additional transcription factors individually or in combinations and minimal length of transgene induction for sufficient induction of bona fide hTSC fate. When obtaining homogenous hiTSC cell lines, *ELF5* methylation status as well as *in vitro* differentiation potential to STB and EVT should be examined in addition to markers analyzed so far (Lee et al., 2016). Further, it would be worthwhile to verify if they are able to form trophoblast organoids to investigate 3D self-organization capacity (Haider et al., 2018; Turco et al., 2018).

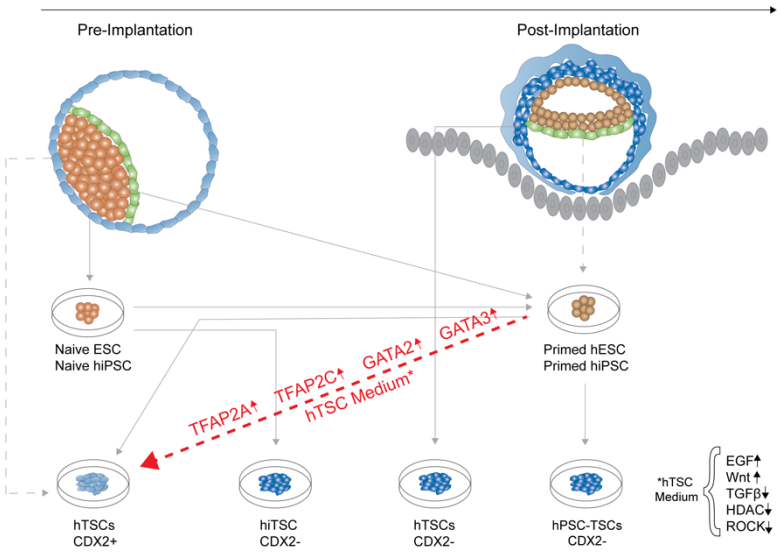

Figure 49: Initial hTSC fate induction integrated into current state of research
Extract from Figure 9, integrating the findings from this study into the network obtained from previous reprogramming and conversion approaches. Results from this study suggest that overexpression of TFAP2A, TFAP2C, GATA2 and GATA3 factors in hiPSCs in combination with culture in hTSC medium results in emerging CDX2 positive hTSC-like cells.

Generation of hiPSC-derived bona fide hiTSCs is of great interest as it offers the possibility to study diverse genetic backgrounds and allows for *in vitro* disease modeling. Thereby, regulators of early human placentation and pregnancy complications can be discovered. Development of *in vitro* blastoids or synthetic human embryos consisting of hiPSCs and hiTSCs would allow not only to analyze the stem cell types individually but also the crosstalk between them. This could lead to improving human embryo culture media with possible implementation in *in vitro* fertilization (Castel et al., 2020). In general, it would strengthen our understanding of early human development with implications for reproductive and regenerative medicine.

11 Discussion III

11.1 Activating mutation in KIT receptor causes increased invasiveness of TGCs

The effect of continuous KIT signaling on placental development due to activating mutation D816V was assessed in the final part of this study. It was shown by our group that the KIT^{D816V} mutation interferes with proper placental development (Kaiser et al., 2020b). Effects found in the placenta comprised decreased proliferation in combination with premature differentiation to P-TGCs. Further, specialized TGC subtypes were decreased in number and the placental structure was hallmarked by a reduced labyrinth and spongiotrophoblast layer. The embryo displayed growth retardation due to insufficient nourishment by the placenta (Kaiser et al., 2020b). The results obtained in this study demonstrated that spongiotrophoblast and S-TGC markers were downregulated in differentiating KIT^{D816V} TSCs whereas differentiation markers *Hand1* and *Tfap2c* were already expressed under stem cell conditions suggesting premature differentiation. Also, KIT^{D816V}-TGCs demonstrated significantly increased invasiveness in comparison to WT-TGCs. The invasive capacity of TGCs is of great importance for proper implantation of the blastocyst into the uterine wall and must be carefully controlled (Sharkey et al., 1994). Sharkey et al. postulated that pre-eclampsia and intrauterine growth retardation appear to be associated with inadequate invasion or premature differentiation of the invading trophoblast. Continued invasion through the uterine wall, as seen in placenta percreta, however, can be lethal to the mother (Sharkey et al., 1994). Interestingly, already in 1992, Sharkey et al. suspected that the KIT-receptor and SCF are involved in the regulation of trophoblast invasion (Sharkey et al., 1992). Taken together, these results suggest that KIT^{D816V} causes premature differentiation which entails aberrant structural development of the placenta as well as early and increased acquiring of invasiveness in TSCs (Kaiser et al., 2020b).

Chronic KIT activation resulted in increased differentiation into P-TGC subtypes at the expense of SpA-TGCs, S-TGCs and C-TGCs. However, these underrepresented TGCs contribute to distinct and essential processes in the placental development. These functions comprise apart from invasion into the uterine wall, also secretion of placental hormones and vasodilators, establishing the connection of the maternal blood flow to the placenta and remodeling of the maternal spiral arteries (Hu and Cross, 2010; Simmons et al., 2007). Reduction of any of these highly specialized cell types will have imminent effects on proper development of the embryo. For instance, insufficient blood flow between mother and fetus due to incorrectly formed blood vessels causes lack of exchange of gases and nutrients resulting in malnourishment of the embryo. This could be a reason for the observed growth retardation in embryos of the KIT^{D816V} mouse model. As KIT^{D816V} positive cells could not be detected in the embryo but in the placenta only, additive embryonic effects are unlikely to contribute to the phenotype (Kaiser et al., 2020b).

Moreover, it was shown here, that *Gata2* expression increased significantly in KIT^{D816V}-TSCs upon differentiation which was not the case in differentiating WT-TSCs. This is in line with previous results which showed that *Gata2* expression increased in cells of the hematopoietic system due to KIT^{D816V} (Haas et al., 2015; Zeuner et al., 2011). Interestingly, also increased levels of PL1 and PLF positive cells were detected in KIT^{D816V} placentas (Kaiser et al., 2020b). Both genes were shown to be transactivated by GATA2 in trophoblast cells (Ma et al., 1997; Ng et al., 1994). This indicates that in trophoblast as well as in hematopoietic cells, KIT signaling causes induction of *Gata2* expression. In trophoblast cells, GATA2 then induces transactivation of PL1 and PLF (Kaiser et al., 2020b).

Another publication could show that administration of retinoic acid (RA) to the mother resulted in a similar phenotype as observed for KIT^{D816V} placentas (Kaiser et al., 2020b; Yan et al., 2001). The RA phenotype was characterized by increased differentiation, higher number of invasive TGCs and severe decrease in proliferation (Hemberger et al., 2004; Yan et al., 2001). Also, comparable to the KIT^{D816V} phenotype, TPBPA levels were lower, PL1 levels higher and spongiotrophoblast layer smaller than in WT placentas (Yan et al., 2001). Like administration of RA, also deficiency of suppressor of cytokine signaling (SOCS) 3 resulted in an atypical placental phenotype comparable to the one caused by the expression of KIT^{D816V}. It is represented by e.g., a decreased spongiotrophoblast layer and augmented TGC differentiation (Takahashi et al., 2008). This indicates that KIT, RA and SOCS are involved in the same pathway (Kaiser et al., 2020b; Takahashi et al., 2003). In SOCS3 deficient mice, also STAT3 was reported to be constitutively activated (Takahashi et al., 2003). KIT^{D816V} placentas showed augmented presence of phosphorylated STAT3 upon differentiation of KIT^{D816V}-TSCs (Kaiser et al., 2020b). STAT3 is involved in cell migration and invasion which were found to be affected in KIT^{D816V}-TSCs (Huang, 2007). STAT3 is part of the LIF/JAK/STAT3 signaling and is involved in cell migration and invasion (Huang, 2007; Suman et al., 2013).

From all data collected, the following signaling cascades were proposed by us (Kaiser et al., 2020b): First, it was concluded that RA acts upstream of KIT and that independent of RA administration, RA signaling was activated in KIT^{D816V} placentas due to constant KIT signaling. It was further proposed that the KIT receptor plays a role in LIF/JAK/STAT3 signaling. LIF/JAK/STAT3 signaling is induced by binding of LIF to its receptor which results in activation of JAK. JAK phosphorylates STAT3 which in turn activates SOCS3. SOCS3 is part of a negative feedback loop that inhibits LIF (Suman et al., 2013). When KIT signaling is active, it represses SOCS3 which leads to the loss of the negative feedback loop, increased LIF levels and accumulation of phosphorylated STAT3 in the cytoplasm (Kaiser et al., 2020b). This in combination with active RA signaling and increase in PL1 and PLF due to *Gata2* expression results in the various effects detected in KIT^{D816V} placentas such as increased invasive capacity

and premature differentiation indicated by expression of differentiation markers already at the stem cell stage (Kaiser et al., 2020b). Our group hypothesized that under stem cell culture conditions, constant FGF4 signaling maintains a stem cell state in KIT^{D816V}-TSCs, albeit with differentiation already in place as seen by upregulation of *Tfap2c* and *Hand1* expression due to active KIT signaling (Kaiser et al., 2020b). Upon growth factor withdrawal, differentiation is then initiated prematurely and quicker than in WT-TSCs (Kaiser et al., 2020b).

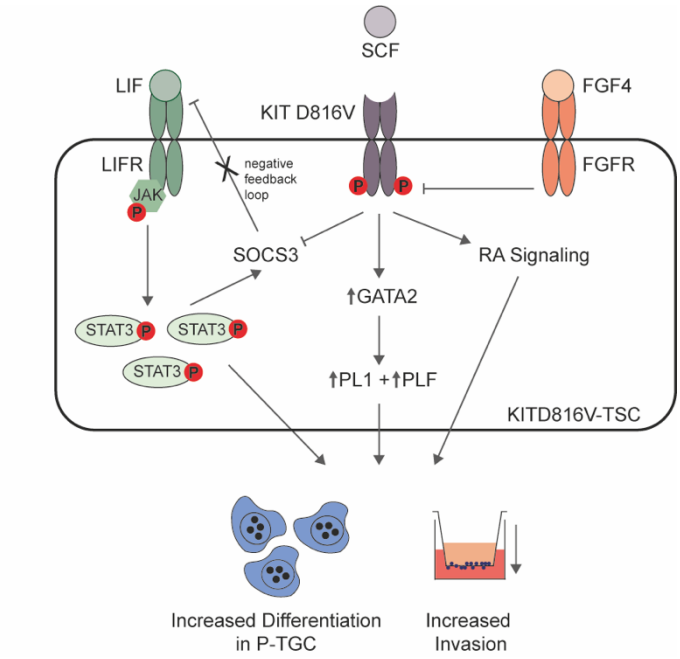

Figure 50: Proposed signaling cascades in KIT^{D816V}-TSCs
The KIT^{D816V} receptor is activated even without binding of its ligand SCF. LIF binds to its receptor LIFR, thereby causing initiation of LIF/JAK/STAT signaling which is controlled by a negative feedback loop including SOCS3. However, the active KIT^{D816V} receptor represses SOCS3 which results in accumulation of phosphorylated STAT3. Activated KIT signaling also results in RA signaling independent of RA presence and an increase in *Gata2* expression which in turn transactivates PL1 and PLF. In combination, this results among others in increased differentiation to P-TGCs and increased invasiveness of TGCs derived from KIT^{D816V}-TSCs. However, under stem cell culture conditions, FGF4 signaling is proposed to be capable of overruling KIT signaling. Modified from Kaiser et al., 2020b.

The understanding of the role that the KIT receptor plays in specific pathways is of great importance for finding appropriate drugs to treat diseases such as cancer that result from constitutively active receptor signaling. To this end, it was shown that inhibition of PI3K and MAPK pathways in combination with KIT inhibitors can serve as treatment for gastrointestinal stromal tumors (Gupta et al., 2021). Even though, it would be a long way to treating adverse placental development due to aberrant KIT signaling, these findings allow us to understand the mechanisms and pathway involvement of the receptor and might even be transferred onto other tissues.

Parts of this chapter have been published in:

Franziska Kaiser, Julia Hartweg, Selina Jansky, Natalie Pelusi, Carolina Kubaczka, Neha Sharma, Dominik Nitsche, Jan Langkabel and Hubert Schorle. “Persistent human KIT receptor signaling disposes murine placenta to premature differentiation resulting in severely disrupted placental structure and functionality.” International Journal of Molecular Sciences 21, 2020.

12 Bibliography

Allis, C.D., and Jenuwein, T. (2016). The molecular hallmarks of epigenetic control. Nat. Rev. Genet. *17*, 487–500.

Amita, M., Adachi, K., Alexenko, A.P., Sinha, S., Schust, D.J., Schulz, L.C., Roberts, R.M., and Ezashi, T. (2013). Complete and unidirectional conversion of human embryonic stem cells to trophoblast by BMP4. Proc. Natl. Acad. Sci. *110*, E1212 LP-E1221.

Ashman, L.K. (1999). The biology of stem cell factor and its receptor C-kit. Int. J. Biochem. Cell Biol. *31*, 1037–1051.

Azevedo Portilho, N., and Pelajo-Machado, M. (2018). Mechanism of hematopoiesis and vasculogenesis in mouse placenta. Placenta *69*, 140–145.

Baranek, M., Belter, A., Naskręt-Barciszewska, M.Z., Stobiecki, M., Markiewicz, W.T., and Barciszewski, J. (2017). Effect of small molecules on cell reprogramming. Mol. Biosyst. *13*, 277–313.

Beard, C., Hochedlinger, K., Plath, K., Wutz, A., and Jaenisch, R. (2006). Efficient method to generate single-copy transgenic mice by site-specific integration in embryonic stem cells. Genesis *44*, 23–28.

Beck, F., Erler, T., Russell, A., and James, R. (1995). Expression of Cdx-2 in the mouse embryo and placenta: Possible role in patterning of the extra-embryonic membranes. Dev. Dyn. *204*, 219–227.

Benchetrit, H., Herman, S., van Wietmarschen, N., Wu, T., Makedonski, K., Maoz, N., Yom Tov, N., Stave, D., Lasry, R., Zayat, V., et al. (2015). Extensive Nuclear Reprogramming Underlies Lineage Conversion into Functional Trophoblast Stem-like Cells. Cell Stem Cell *17*, 543–556.

Benchetrit, H., Jaber, M., Zayat, V., Sebban, S., Pushett, A., Makedonski, K., Zakheim, Z., Radwan, A., Maoz, N., Lasry, R., et al. (2019). Direct Induction of the Three Pre-implantation Blastocyst Cell Types from Fibroblasts. Cell Stem Cell *24*, 983-994.e7.

Bernardo, A.S., Faial, T., Gardner, L., Niakan, K.K., Ortmann, D., Senner, C.E., Callery, E.M., Trotter, M.W., Hemberger, M., Smith, J.C., et al. (2011). BRACHYURY and CDX2 Mediate BMP-Induced Differentiation of Human and Mouse Pluripotent Stem Cells into Embryonic and Extraembryonic Lineages. Cell Stem Cell *9*, 144–155.

Bestor, T.H. (2000). The DNA methyltransferases of mammals. Hum. Mol. Genet. *9*, 2395–2402.

Bodemer, C., Hermine, O., Palmérini, F., Yang, Y., Grandpeix-Guyodo, C., Leventhal, P.S., Hadj-Rabia, S., Nasca, L., Georgin-Lavialle, S., Cohen-Akenine, A., et al. (2010). Pediatric mastocytosis is a clonal disease associated with D 816 v and other activating c-KIT mutations. J. Invest. Dermatol. *130*, 804–815.

Brambrink, T., Foreman, R., Welstead, G.G., Lengner, C.J., Wernig, M., Suh, H., and Jaenisch, R. (2008). Sequential Expression of Pluripotency Markers during Direct Reprogramming of Mouse Somatic Cells. Cell Stem Cell *2*, 151–159.

Burton, G.J., and Jauniaux, E. (2015). What is the placenta? Am. J. Obstet. Gynecol. *213*, S6.e1, S6-8.

Burton, G.J., and Fowden, A.L. (2015). The placenta: a multifaceted, transient organ. Philos. Trans. R. Soc. Lond. B. Biol. Sci. *370*, 20140066.

Burton, G.J., Fowden, A.L., and Thornburg, K.L. (2016). Placental Origins of Chronic Disease. Physiol. Rev. *96*, 1509–1565.

Cambuli, F., Murray, A., Dean, W., Dudzinska, D., Krueger, F., Andrews, S., Senner, C.E., Cook, S.J., and Hemberger, M. (2014). Epigenetic memory of the first cell fate decision prevents complete ES cell reprogramming into trophoblast. Nat. Commun. *5*, 5538.

Cao, Z., Carey, T.S., Ganguly, A., Wilson, C.A., Paul, S., and Knott, J.G. (2015). Transcription factor AP-2γ induces early Cdx2 expression and represses HIPPO signaling to specify the trophectoderm lineage. Development *142*, 1606–1615.

Castel, G., Meistermann, D., Bretin, B., Firmin, J., Blin, J., Loubersac, S., Bruneau, A., Chevolleau, S., Kilens, S., Chariau, C., et al. (2020). Induction of Human Trophoblast Stem Cells from Somatic Cells and Pluripotent Stem Cells. Cell Rep. *33*, 108419.

Chabot, B., Stephenson, D.A., Chapman, V.M., Besmer, P., and Bernstein, A. (1988). The proto-oncogene c-kit encoding a transmembrane tyrosine kinase receptor maps to the mouse W locus. Nature *335*, 88–89.

Chen, G., Gulbranson, D.R., Hou, Z., Bolin, J.M., Ruotti, V., Probasco, M.D., Smuga-Otto, K., Howden, S.E., Diol, N.R., Propson, N.E., et al. (2011). Chemically defined conditions for human iPSC derivation and culture. Nat. Methods *8*, 424–429.

Chen, G., Guo, Y., Li, C., Li, S., and Wan, X. (2020). Small Molecules that Promote Self-Renewal of Stem Cells and Somatic Cell Reprogramming. Stem Cell Rev. Reports *16*, 511–523.

Chrysanthou, S., Senner, C.E., Woods, L., Fineberg, E., Okkenhaug, H., Burge, S., Perez-Garcia, V., and Hemberger, M. (2018). A Critical Role of TET1/2 Proteins in Cell-Cycle Progression of Trophoblast Stem Cells. Stem Cell Reports *10*, 1355–1368.

Cinkornpumin, J.K., Kwon, S.Y., Guo, Y., Hossain, I., Sirois, J., Russett, C.S., Tseng, H.-W., Okae, H., Arima, T., Duchaine, T.F., et al. (2020). Naive Human Embryonic Stem Cells Can Give Rise to Cells with a Trophoblast-like Transcriptome and Methylome. Stem Cell Reports *15*, 198–213.

Cockburn, K., and Rossant, J. (2010). Making the blastocyst: lessons from the mouse. J. Clin. Invest. *120*, 995–1003.

Copeland, N.G., Gilbert, D.J., Cho, B.C., Donovan, P.J., Jenkins, N.A., Cosman, D., Anderson, D., Lyman, S.D., and Williams, D.E. (1990). Mast cell growth factor maps near the steel locus on mouse chromosome 10 and is deleted in a number of steel alleles. Cell *63*, 175–183.

Deglincerti, A., Croft, G.F., Pietila, L.N., Zernicka-Goetz, M., Siggia, E.D., and Brivanlou, A.H. (2016). Self-organization of the in vitro attached human embryo. Nature *533*, 251–154.

Dellschaft, N.S., Hutchinson, G., Shah, S., Jones, N.W., Bradley, C., Leach, L., Platt, C., Bowtell, R., and Gowland, P.A. (2020). The haemodynamics of the human placenta in utero. PLoS Biol. *18*, e3000676–e3000676.

Dong, C., Beltcheva, M., Gontarz, P., Zhang, B., Popli, P., Fischer, L.A., Khan, S.A., Park, K., Yoon, E.-J., Xing, X., et al. (2020). Derivation of trophoblast stem cells from naïve human pluripotent stem cells. Elife *9*, e52504.

Dong, C., Fu, S., Karvas, R.M., Chew, B., Fischer, L.A., Xing, X., Harrison, J.K., Popli, P., Kommagani, R., Wang, T., et al. (2022). A genome-wide CRISPR-Cas9 knockout screen identifies essential and growth-restricting genes in human trophoblast stem cells. Nat. Commun. *13*, 2548.

Donnison, M., Beaton, A., Davey, H.W., Broadhurst, R., L'Huillier, P., and Pfeffer, P.L. (2005). Loss of the extraembryonic ectoderm in Elf5 mutants leads to defects in embryonic patterning. Development *132*, 2299–2308.

Edling, C.E., and Hallberg, B. (2007). c-Kit—A hematopoietic cell essential receptor tyrosine kinase. Int. J. Biochem. Cell Biol. *39*, 1995–1998.

Erlebacher, A., Price, K.A., and Glimcher, L.H. (2004). Maintenance of mouse trophoblast stem cell proliferation by TGF-β/activin. Dev. Biol. *275*, 158–169.

Esser, L.K., Branchi, V., Shakeri, F., Simon, A.G., Stephan, C., Kristiansen, G., Buness, A., Schorle, H., and Toma, M.I. (2022). Overexpression of Parkin in clear cell renal cell carcinoma decreases tumor aggressiveness by regulating CKS2 levels. Int. J. Oncol. *60*.

Evans, M.J., and Kaufman, M.H. (1981). Establishment in culture of pluripotential cells from mouse embryos. Nature *292*, 154–156.

Fock, V., Plessl, K., Draxler, P., Otti, G.R., Fiala, C., Knöfler, M., and Pollheimer, J. (2015). Neuregulin-1-mediated ErbB2–ErbB3 signalling protects human trophoblasts against apoptosis to preserve differentiation. J. Cell Sci. *128*, 4306–4316.

Gao, X., Nowak-Imialek, M., Chen, X., Chen, D., Herrmann, D., Ruan, D., Chen, A.C.H., Eckersley-Maslin, M.A., Ahmad, S., Lee, Y.L., et al. (2019). Establishment of porcine and human expanded potential stem cells. Nat. Cell Biol. *21*, 687–699.

Ghimire, S., Van der Jeught, M., Neupane, J., Roost, M.S., Anckaert, J., Popovic, M., Van Nieuwerburgh, F., Mestdagh, P., Vandesompele, J., Deforce, D., et al. (2018). Comparative analysis of naive, primed and ground state pluripotency in mouse embryonic stem cells originating from the same genetic background. Sci. Rep. *8*, 5884.

Greenberg, M.V.C., and Bourc'his, D. (2019). The diverse roles of DNA methylation in mammalian development and disease. Nat. Rev. Mol. Cell Biol. *20*, 590–607.

Guo, G., Stirparo, G.G., Strawbridge, S.E., Spindlow, D., Yang, J., Clarke, J., Dattani, A., Yanagida, A., Li, M.A., Myers, S., et al. (2021). Human naive epiblast cells possess unrestricted lineage potential. Cell Stem Cell *28*, 1040–1056.

Gupta, A., Ma, S., Che, K., Pobbati, A. V, and Rubin, B.P. (2021). Inhibition of PI3K and MAPK pathways along with KIT inhibitors as a strategy to overcome drug resistance in gastrointestinal stromal tumors. PLoS One *16*, e0252689–e0252689.

Haas, N., Riedt, T., Labbaf, Z., Baßler, K., Gergis, D., Fröhlich, H., Gütgemann, I., Janzen, V., and Schorle, H. (2015). Kit transduced signals counteract erythroid maturation by MAPK-dependent modulation of erythropoietin signaling and apoptosis induction in mouse fetal liver. Cell Death Differ. *22*, 790–800.

Haider, S., Meinhardt, G., Saleh, L., Kunihs, V., Gamperl, M., Kaindl, U., Ellinger, A., Burkard, T.R., Fiala, C., Pollheimer, J., et al. (2018). Self-Renewing Trophoblast Organoids Recapitulate the Developmental Program of the Early Human Placenta. Stem Cell Reports *11*, 537–551.

Hamilton, W.J., and Boyd, J.D. (1960). Development of the human placenta in the first three months of gestation. J. Anat. *94*, 297–328.

Hata, K., Okano, M., Lei, H., and Li, E. (2002). Dnmt3L cooperates with the Dnmt3 family of de novo DNA methyltransferases to establish maternal imprints in mice. Development *129*, 1983–1993.

Hawkins, K., Joy, S., and McKay, T. (2014). Cell signalling pathways underlying induced pluripotent stem cell reprogramming. World J. Stem Cells *6*, 620–628.

Hemberger, M., Nozaki, T., Masutani, M., and Cross, J.C. (2003). Differential expression of angiogenic and vasodilatory factors by invasive trophoblast giant cells depending on depth of invasion. Dev. Dyn. *227*, 185–191.

Hemberger, M., Hughes, M., and Cross, J.C. (2004). Trophoblast stem cells differentiate in vitro into invasive trophoblast giant cells. Dev. Biol. *271*, 362–371.

Hemberger, M., Dean, W., and Reik, W. (2009). Epigenetic dynamics of stem cells and cell lineage commitment: digging Waddington's canal. Nat. Rev. Mol. Cell Biol. *10*, 526–537.

Hemberger, M., Hanna, C.W., and Dean, W. (2020). Mechanisms of early placental development in mouse and humans. Nat. Rev. Genet. *21(1)*, 27–43.

Hertig, A.T., Rock, J., and Adams, E.C. (1956). A description of 34 human ova within the first 17 days of development. Am. J. Anat. *98*, 435–493.

Home, P., Ray, S., Dutta, D., Bronshteyn, I., Larson, M., and Paul, S. (2009). GATA3 Is Selectively Expressed in the Trophectoderm of Peri-implantation Embryo and Directly Regulates Cdx2 Gene Expression. J. Biol. Chem. *284*, 28729–28737.

Home, P., Saha, B., Ray, S., Dutta, D., Gunewardena, S., Yoo, B., Pal, A., Vivian, J.L., Larson, M., Petroff, M., et al. (2012). Altered subcellular localization of transcription factor TEAD4 regulates first mammalian cell lineage commitment. Proc. Natl. Acad. Sci. *109*, 7362 LP – 7367.

Horie, K., Fujita, J., Takakura, K., Kanzaki, H., Kaneko, Y., Iwai, M., Nakayama, H., and Mori, T. (1992). Expression of C-Kit Protein during Placental Development1. Biol. Reprod. *47*, 614–620.

Horii, M., Touma, O., Bui, T., and Parast, M.M. (2020). Modeling human trophoblast, the placental epithelium at the maternal fetal interface. Reproduction *160*, R1–R11.

Hou, P., Li, Y., Zhang, X., Liu, C., Guan, J., Li, H., Zhao, T., Ye, J., Yang, W., Liu, K., et al. (2013). Pluripotent Stem Cells Induced from Mouse Somatic Cells by Small-Molecule Compounds. Science *341*, 651 LP – 654.

Hu, D., and Cross, J.C. (2010). Development and function of trophoblast giant cells in the rodent placenta. Int. J. Dev. Biol. *54*, 341–354.

Huang, S. (2007). Regulation of Metastases by Signal Transducer and Activator of Transcription 3 Signaling Pathway: Clinical Implications. Clin. Cancer Res. *13*, 1362 LP – 1366.

Huang, K., Maruyama, T., and Fan, G. (2014). The naive state of human pluripotent stem cells: a synthesis of stem cell and preimplantation embryo transcriptome analyses. Cell Stem Cell *15*, 410–415.

Io, S., Kabata, M., Iemura, Y., Semi, K., Morone, N., Minagawa, A., Wang, B., Okamoto, I., Nakamura, T., Kojima, Y., et al. (2021). Capturing human trophoblast development with naive pluripotent stem cells in vitro. Cell Stem Cell *28*, 1023-1039.e13.

Jedrusik, A., Cox, A., Wicher, K.B., Glover, D.M., and Zernicka-Goetz, M. (2015). Maternal-zygotic knockout reveals a critical role of Cdx2 in the morula to blastocyst transition. Dev. Biol. *398*, 147–152.

Jeong, M., and Goodell, M. a. (2014). New answers to old questions from genome-wide maps of DNA methylation in hematopoietic cells. Exp. Hematol. *42*, 609–617.

Kaiser, F., Kubaczka, C., Graf, M., Langer, N., Langkabel, J., Arévalo, L., and Schorle, H. (2020a). Choice of factors and medium impinge on success of ESC to TSC conversion. Placenta *90*, 128–137.

Kaiser, F., Hartweg, J., Jansky, S., Pelusi, N., Kubaczka, C., Sharma, N., Nitsche, D., Langkabel, J., and Schorle, H. (2020b). Persistent Human KIT Receptor Signaling Disposes Murine Placenta to Premature Differentiation Resulting in Severely Disrupted Placental Structure and Functionality. Int. J. Mol. Sci. *21*, 5503.

Kauma, S., Huff, T., Krystal, G., Ryan, J., Takacs, P., and Turner, T. (1996). The expression of stem cell factor and its receptor, c-kit in human endometrium and placental tissues during pregnancy. J. Clin. Endocrinol. Metab. *81*, 1261–1266.

Kemmer, K., Corless, C.L., Fletcher, J.A., McGreevey, L., Haley, A., Griffith, D., Cummings, O.W., Wait, C., Town, A., and Heinrich, M.C. (2004). KIT mutations are common in testicular seminomas. Am. J. Pathol. *164*, 305–313.

Kidder, B.L., and Palmer, S. (2010). Examination of transcriptional networks reveals an important role for TCFAP2C, SMARCA4, and EOMES in trophoblast stem cell maintenance. Genome Res. *20*, 458–472.

Kissel, H., Timokhina, I., Hardy, M.P., Rothschild, G., Tajima, Y., Soares, V., Angeles, M., Whitlow, S.R., Manova, K., and Besmer, P. (2000). Point mutation in Kit receptor tyrosine kinase reveals essential roles for Kit signaling in spermatogenesis and oogenesis without affecting other Kit responses. EMBO J. *19*, 1312–1326.

Knöfler, M., Haider, S., Saleh, L., Pollheimer, J., Gamage, T.K.J.B., and James, J. (2019). Human placenta and trophoblast development: key molecular mechanisms and model systems. Cell. Mol. Life Sci. *76*, 3479–3496.

König, C., and Runge, A. (2021). Metastatic Dissemination Mimicked in a Multicellular Transwell Assay BT - Pericytes: Methods and Protocols. B.M. Péault, ed. (New York, NY: Springer US), pp. 181–190.

Krendl, C., Shaposhnikov, D., Rishko, V., Ori, C., Ziegenhain, C., Sass, S., Simon, L., Müller, N.S., Straub, T., Brooks, K.E., et al. (2017). GATA2/3-TFAP2A/C transcription factor network couples human pluripotent stem cell differentiation to trophectoderm with repression of pluripotency. Proc. Natl. Acad. Sci. *114*, E9579 LP-E9588.

Kubaczka, C., Senner, C., Araúzo-Bravo, M.J., Sharma, N., Kuckenberg, P., Becker, A., Zimmer, A., Brüstle, O., Peitz, M., Hemberger, M., et al. (2014). Derivation and maintenance of murine trophoblast stem cells under defined conditions. Stem Cell Reports *2*, 232–242.

Kubaczka, C., Senner, C.E., Cierlitza, M., Araúzo-Bravo, M.J., Kuckenberg, P., Peitz, M., Hemberger, M., and Schorle, H. (2015). Direct Induction of Trophoblast Stem Cells from Murine Fibroblasts. Cell Stem Cell *17*, 557–568.

Kubaczka, C., Kaiser, F., and Schorle, H. (2016). Breaking the first lineage barrier – many roads to trophoblast stem cell fate. Placenta *60*, S52–S56.

Kuckenberg, P., Buhl, S., Woynecki, T., Fürden, B. van, Tolkunova, E., Seiffe, F., Moser, M., Tomilin, A., Winterhager, E., and Schorle, H. (2010). The Transcription Factor TCFAP2C/AP-2γ Cooperates with CDX2 To Maintain Trophectoderm Formation. Mol. Cell. Biol. *30*, 3310–3320.

Kuckenberg, P., Peitz, M., Kubaczka, C., Becker, A., Egert, A., Wardelmann, E., Zimmer, A., Brüstle, O., and Schorle, H. (2011). Lineage Conversion of Murine Extraembryonic Trophoblast Stem Cells to Pluripotent Stem Cells. Mol. Cell. Biol. *31*, 1748 LP – 1756.

Kuckenberg, P., Kubaczka, C., and Schorle, H. (2012). The role of transcription factor Tcfap2c/TFAP2C in trophectoderm development. Reprod. Biomed. Online *25*, 12–20.

Langkabel, J., Horne, A., Bonaguro, L., Holsten, L., Hesse, T., Knaus, A., Riedel, Y., Becker, M., Händler, K., Elmzzahi, T., et al. (2021). Induction of Rosette-to-Lumen stage embryoids using reprogramming paradigms in ESCs. Nat. Commun. *12*, 7322.

Lasota, J., Jasinski, M., Sarlomo-Rikala, M., and Miettinen, M. (1999). Mutations in exon 11 of c-Kit occur preferentially in malignant versus benign gastrointestinal stromal tumors and do not occur in leiomyomas or leiomyosarcomas. Am. J. Pathol. *154*, 53–60.

Latos, P.A., and Hemberger, M. (2013). Review: The transcriptional and signalling networks of mouse trophoblast stem cells. Placenta *35*, S81–S85.

Latos, P.A., Sienerth, A.R., Murray, A., Senner, C.E., Muto, M., Ikawa, M., Oxley, D., Burge, S., Cox, B.J., and Hemberger, M. (2015a). Elf5-centered transcription factor hub controls trophoblast stem cell self-renewal and differentiation through stoichiometry-sensitive shifts in target gene networks. Genes Dev. *29*, 2435–2448.

Latos, P.A., Goncalves, A., Oxley, D., Mohammed, H., Turro, E., and Hemberger, M. (2015b). Fgf and Esrrb integrate epigenetic and transcriptional networks that regulate self-renewal of trophoblast stem cells. Nat. Commun. *6*, 7776.

Latos, P.A., and Hemberger, M. (2016). From the stem of the placental tree: trophoblast stem cells and their progeny. Development *143*, 3650 LP – 3660.

Lee, C.Q.E., Gardner, L., Turco, M., Zhao, N., Murray, M.J., Coleman, N., Rossant, J., Hemberger, M., and Moffett, A. (2016). What Is Trophoblast? A Combination of Criteria Define Human First-Trimester Trophoblast. Stem Cell Reports *6*, 257–272.

Liang, J., Wu, Y.-L., Chen, B.-J., Zhang, W., Tanaka, Y., and Sugiyama, H. (2013). The C-kit receptor-mediated signal transduction and tumor-related diseases. Int. J. Biol. Sci. *9*, 435–443.

Linnekin, D. (1999). Early signaling pathways activated by c-Kit in hematopoietic cells. Int. J. Biochem. Cell Biol. *31*, 1053–1074.

Lois, C., Hong, E.J., Pease, S., Brown, E.J., and Baltimore, D. (2002). Germline Transmission and Tissue-Specific Expression of Transgenes Delivered by Lentiviral Vectors. Science *295*, 868 LP – 872.

Lu, C.-W., Yabuuchi, A., Chen, L., Viswanathan, S., Kim, K., and Daley, G.Q. (2008). Ras-MAPK signaling promotes trophectoderm formation from embryonic stem cells and mouse embryos. Nat. Genet. *40*, 921–926.

Luo, J., Sladek, R., Bader, J.-A., Matthyssen, A., Rossant, J., and Giguère, V. (1997). Placental abnormalities in mouse embryos lacking the orphan nuclear receptor ERR-β. Nature *388*, 778–782.

Ma, G.T., Roth, M.E., Groskopf, J.C., Tsai, F.Y., Orkin, S.H., Grosveld, F., Engel, J.D., and Linzer, D.I. (1997). GATA-2 and GATA-3 regulate trophoblast-specific gene expression in vivo. Development *124*, 907 LP – 914.

Ma, X., Kong, L., and Zhu, S. (2017). Reprogramming cell fates by small molecules. Protein Cell *8*, 328–348.

Maekawa, M., Yamamoto, T., Tanoue, T., Yuasa, Y., Chisaka, O., and Nishida, E. (2005). Requirement of the MAP kinase signaling pathways for mouse preimplantation development. Development *132*, 1773–1783.

Malaise, M., Steinbach, D., and Corbacioglu, S. (2009). Clinical implications of c-Kit mutations in acute myelogenous leukemia. Curr. Hematol. Malig. Rep. *4*, 77–82.

McConnell, J., Petrie, L., Stennard, F., Ryan, K., and Nichols, J. (2005). Eomesodermin is expressed in mouse oocytes and pre-implantation embryos. Mol. Reprod. Dev. *71*, 399–404.

McDole, K., Xiong, Y., Iglesias, P.A., and Zheng, Y. (2011). Lineage mapping the pre-implantation mouse embryo by two-photon microscopy, new insights into the segregation of cell fates. Dev. Biol. *355*, 239–249.

Meinhardt, G., Haider, S., Kunihs, V., Saleh, L., Pollheimer, J., Fiala, C., Hetey, S., Feher, Z., Szilagyi, A., Than, N.G., et al. (2020). Pivotal role of the transcriptional co-activator YAP in trophoblast stemness of the developing human placenta. Proc. Natl. Acad. Sci. *117*, 13562 LP – 13570.

Miettinen, M., and Lasota, J. (2005). KIT (CD117): A Review on Expression in Normal and Neoplastic Tissues, and Mutations and Their Clinicopathologic Correlation. Appl. Immunohistochem. Mol. Morphol. *13*, 205–220.

Mikkelsen, T.S., Hanna, J., Zhang, X., Ku, M., Wernig, M., Schorderet, P., Bernstein, B.E., Jaenisch, R., Lander, E.S., and Meissner, A. (2008). Dissecting direct reprogramming through integrative genomic analysis. Nature *454*, 49–55.

Miller, R.K., Genbacev, O., Turner, M.A., Aplin, J.D., Caniggia, I., and Huppertz, B. (2005). Human placental explants in culture: Approaches and assessments. Placenta *26*, 439–448.

Mischler, A., Karakis, V., Mahinthakumar, J., Carberry, C.K., San Miguel, A., Rager, J.E., Fry, R.C., and Rao, B.M. (2021). Two distinct trophectoderm lineage stem cells from human pluripotent stem cells. J. Biol. Chem. *296*, 100386.

Motro, B., van der Kooy, D., Rossant, J., Reith, A., and Bernstein, A. (1991). Contiguous patterns of c-kit and steel expression: analysis of mutations at the W and Sl loci. Development *113*, 1207 LP – 1221.

Murray, A., Sienerth, A.R., and Hemberger, M. (2016). Plet1 is an epigenetically regulated cell surface protein that provides essential cues to direct trophoblast stem cell differentiation. Sci. Rep. *6*, 25112.

Nakamura, T., Okamoto, I., Sasaki, K., Yabuta, Y., Iwatani, C., Tsuchiya, H., Seita, Y., Nakamura, S., Yamamoto, T., and Saitou, M. (2016). A developmental coordinate of pluripotency among mice, monkeys and humans. Nature *537*, 57–62.

Natale, B. V, Schweitzer, C., Hughes, M., Globisch, M.A., Kotadia, R., Tremblay, E., Vu, P., Cross, J.C., and Natale, D.R.C. (2017). Sca-1 identifies a trophoblast population with multipotent potential in the mid-gestation mouse placenta. Sci. Rep. *7*, 5575.

Ng, Y.K., George, K.M., Engel, J.D., and Linzer, D.I. (1994). GATA factor activity is required for the trophoblast-specific transcriptional regulation of the mouse placental lactogen I gene. Development *120*, 3257 LP – 3266.

Ng, R.K., Dean, W., Dawson, C., Lucifero, D., Madeja, Z., Reik, W., and Hemberger, M. (2008). Epigenetic restriction of embryonic cell lineage fate by methylation of Elf5. Nat. Cell Biol. *10*, 1280–1290.

Niakan, K.K., and Eggan, K. (2013). Analysis of human embryos from zygote to blastocyst reveals distinct gene expression patterns relative to the mouse. Dev. Biol. *375*, 54–64.

Niakan, K.K., Schrode, N., Cho, L.T.Y., and Hadjantonakis, A.-K. (2013). Derivation of extraembryonic endoderm stem (XEN) cells from mouse embryos and embryonic stem cells. Nat. Protoc. *8*, 1028–1041.

Nichols, J., and Smith, A. (2009). Naive and Primed Pluripotent States. Cell Stem Cell *4*, 487–492.

Nishioka, N., Yamamoto, S., Kiyonari, H., Sato, H., Sawada, A., Ota, M., Nakao, K., and Sasaki, H. (2008). Tead4 is required for specification of trophectoderm in pre-implantation mouse embryos. Mech. Dev. *125*, 270–283.

Nishioka, N., Inoue, K., Adachi, K., Kiyonari, H., Ota, M., Ralston, A., Yabuta, N., Hirahara, S., Stephenson, R.O., Ogonuki, N., et al. (2009). The Hippo Signaling Pathway Components Lats and Yap Pattern Tead4 Activity to Distinguish Mouse Trophectoderm from Inner Cell Mass. Dev. Cell *16*, 398–410.

Nishiyama, A., Xin, L., Sharov, A.A., Thomas, M., Mowrer, G., Meyers, E., Piao, Y., Mehta, S., Yee, S., Nakatake, Y., et al. (2009). Uncovering Early Response of Gene Regulatory Networks in ESCs by Systematic Induction of Transcription Factors. Cell Stem Cell *5*, 420–433.

Niwa, H., Toyooka, Y., Shimosato, D., Strumpf, D., Takahashi, K., Yagi, R., and Rossant, J. (2005). Interaction between Oct3/4 and Cdx2 determines trophectoderm differentiation. Cell *123*, 917–929.

Nosi, U., Lanner, F., Huang, T., and Cox, B. (2017). Overexpression of Trophoblast Stem Cell-Enriched MicroRNAs Promotes Trophoblast Fate in Embryonic Stem Cells. Cell Rep. *19*, 1101–1109.

Odiatis, C., and Georgiades, P. (2010). New Insights for Ets2 Function in Trophoblast using Lentivirus-Mediated Gene Knockdown in Trophoblast Stem Cells. Placenta *31*, 630–640.

Ohinata, Y., and Tsukiyama, T. (2014). Establishment of Trophoblast Stem Cells under Defined Culture Conditions in Mice. PLoS One *9*, e107308.

Okae, H., Toh, H., Sato, T., Hiura, H., Takahashi, S., Shirane, K., Kabayama, Y., Suyama, M., Sasaki, H., and Arima, T. (2018). Derivation of Human Trophoblast Stem Cells. Cell Stem Cell *22*, 50-63.e6.

Okano, M., Bell, D.W., Haber, D. a., and Li, E. (1999). DNA methyltransferases Dnmt3a and Dnmt3b are essential for de novo methylation and mammalian development. Cell *99*, 247–257.

Ottersbach, K., and Dzierzak, E. (2005). The Murine Placenta Contains Hematopoietic Stem Cells within the Vascular Labyrinth Region. Dev. Cell *8*, 377–387.

De Paepe, C., Cauffman, G., Verloes, A., Sterckx, J., Devroey, P., Tournaye, H., Liebaers, I., and Van de Velde, H. (2013). Human trophectoderm cells are not yet committed. Hum. Reprod. *28*, 740–749.

Parry, A., Rulands, S., and Reik, W. (2021). Active turnover of DNA methylation during cell fate decisions. Nat. Rev. Genet. *22*, 59–66.

Pastor, W.A., Liu, W., Chen, D., Ho, J., Kim, R., Hunt, T.J., Lukianchikov, A., Liu, X., Polo, J.M., Jacobsen, S.E., et al. (2018). TFAP2C regulates transcription in human naive pluripotency by opening enhancers. Nat. Cell Biol. *20*, 553–564.

Pathania, S., Pentikäinen, O.T., and Singh, P.K. (2021). A holistic view on c-Kit in cancer: Structure, signaling, pathophysiology and its inhibitors. Biochim. Biophys. Acta - Rev. Cancer *1876*, 188631.

Pelusi, N., Kosanke, M., Riedt, T., Rösseler, C., Seré, K., Li, J., Gütgemann, I., Zenke, M., Janzen, V., and Schorle, H. (2017). The spleen microenvironment influences disease transformation in a mouse model of KITD816V-dependent myeloproliferative neoplasm. Sci. Rep. *7*, 41427.

Pfeifer, A., Ikawa, M., Dayn, Y., and Verma, I.M. (2002). Transgenesis by lentiviral vectors: lack of gene silencing in mammalian embryonic stem cells and preimplantation embryos. Proc. Natl. Acad. Sci. U. S. A. *99*, 2140–2145.

Qin, H., Zhao, A., and Fu, X. (2017). Small molecules for reprogramming and transdifferentiation. Cell. Mol. Life Sci. *74*, 3553–3575.

Ralston, A., Cox, B.J., Nishioka, N., Sasaki, H., Chea, E., Rugg-Gunn, P., Guo, G., Robson, P., Draper, J.S., and Rossant, J. (2010). Gata3 regulates trophoblast development downstream of Tead4 and in parallel to Cdx2. Development *137*, 395 LP – 403.

Rao, M.S., and Malik, N. (2012). Assessing iPSC reprogramming methods for their suitability in translational medicine. J. Cell. Biochem. *113*, 3061–3068.

Reik, W., Dean, W., and Walter, J. (2001). Epigenetic Reprogramming in Mammalian Development. *293*, 1089–1094.

Riley, P., Anaon-Cartwight, L., and Cross, J.C. (1998). The Hand1 bHLH transcription factor is essential for placentation and cardiac morphogenesis. Nat. Genet. *18*, 271–275.

Riond, J.L., and Riviere, J.E. (1989). Doxycycline binding to plasma albumin of several species. J. Vet. Pharmacol. Ther. *12*, 253–260.

Roberts, R.M., Loh, K.M., Amita, M., Bernardo, A.S., Adachi, K., Alexenko, A.P., Schust, D.J., Schulz, L.C., Telugu, B.P.V.L., Ezashi, T., et al. (2014). Differentiation of trophoblast cells from human embryonic stem cells: to be or not to be? Reproduction *147*, D1–D12.

Rose, C.M., van den Driesche, S., Meehan, R.R., and Drake, A.J. (2013). Epigenetic reprogramming: preparing the epigenome for the next generation. Biochem. Soc. Trans. *41*, 809–814.

Roskoski, R. (2005). Signaling by Kit protein-tyrosine kinase - The stem cell factor receptor. Biochem. Biophys. Res. Commun. 1–13.

Rossant, J., and Cross, J.C. (2001). Placental development: Lessons from mouse mutants. Nat. Rev. Genet. *2*, 538–548.

Rugg-Gunn, P.J., Cox, B.J., Ralston, A., and Rossant, J. (2010). Distinct histone modifications in stem cell lines and tissue lineages from the early mouse embryo. Proc. Natl. Acad. Sci. *107*, 10783–10790.

Rugg-Gunn, P.J., Cox, B.J., Lanner, F., Sharma, P., Ignatchenko, V., McDonald, A.C.H., Garner, J., Gramolini, A.O., Rossant, J., and Kislinger, T. (2012). Cell-surface proteomics identifies lineage-specific markers of embryo-derived stem cells. Dev. Cell *22*, 887–901.

Russ, A.P., Wattler, S., Colledge, W.H., Aparicio, S.A.J.R., Carlton, M.B.L., Pearce, J.J., Barton, S.C., Surani, M.A., Ryan, K., Nehls, M.C., et al. (2000). Eomesodermin is required for mouse trophoblast development and mesoderm formation. Nature *404*, 95–99.

Saha, B., Ganguly, A., Home, P., Bhattacharya, B., Ray, S., Ghosh, A., Rumi, M.A.K., Marsh, C., French, V.A., Gunewardena, S., et al. (2020). TEAD4 ensures postimplantation development by promoting trophoblast self-renewal: An implication in early human pregnancy loss. Proc. Natl. Acad. Sci. *117*, 17864–17875.

Samavarchi-Tehrani, P., Golipour, A., David, L., Sung, H., Beyer, T.A., Datti, A., Woltjen, K., Nagy, A., and Wrana, J.L. (2010). Functional Genomics Reveals a BMP-Driven Mesenchymal-to-Epithelial Transition in the Initiation of Somatic Cell Reprogramming. Cell Stem Cell *7*, 64–77.

Sanges, D., and Cosma, M.-P. (2011). Reprogramming cell fate to pluripotency: the decision-making signalling pathways. Int. J. Dev. Biol. *54*, 1575–1587.

Sasaki, T., Mizuochi, C., Horio, Y., Nakao, K., Akashi, K., and Sugiyama, D. (2010). Regulation of hematopoietic cell clusters in the placental niche through SCF/Kit signaling in embryonic mouse. Development *137*, 3941 LP – 3952.

Schmidt, S., Röck, K., Sahre, M., Burkhardt, O., Brunner, M., Lobmeyer, M.T., and Derendorf, H. (2008). Effect of protein binding on the pharmacological activity of highly bound antibiotics. Antimicrob. Agents Chemother. *52*, 3994–4000.

Schübeler, D. (2015). Function and information content of DNA methylation. Nature *517*, 321–326.

Schwarz, B.A., Cetinbas, M., Clement, K., Walsh, R.M., Cheloufi, S., Gu, H., Langkabel, J., Kamiya, A., Schorle, H., Meissner, A., et al. (2018). Prospective Isolation of Poised iPSC Intermediates Reveals Principles of Cellular Reprogramming. Cell Stem Cell *23*, 289-305.e5.

Schwenk, F., Baron, U., and Rajewsky, K. (1995). A cre -transgenic mouse strain for the ubiquitous deletion of loxP -flanked gene segments including deletion in germ cells . Nucleic Acids Res. *23*, 5080–5081.

Scott, I.C., Anson-Cartwright, L., Riley, P., Reda, D., and Cross, J.C. (2000). The HAND1 Basic Helix-Loop-Helix Transcription Factor Regulates Trophoblast Differentiation via Multiple Mechanisms. Mol. Cell. Biol. *20*, 530 LP – 541.

Senner, C.E., and Hemberger, M. (2010). Regulation of early trophoblast differentiation – Lessons from the mouse. Placenta *31*, 944–950.

Senner, C.E., Krueger, F., Oxley, D., Andrews, S., and Hemberger, M. (2012). DNA Methylation Profiles Define Stem Cell Identity and Reveal a Tight Embryonic–Extraembryonic Lineage Boundary. Stem Cells *30*, 2732–2745.

Senner, C.E., Chrysanthou, S., Burge, S., Lin, H.-Y., Branco, M.R., and Hemberger, M. (2020). TET1 and 5-Hydroxymethylation Preserve the Stem Cell State of Mouse Trophoblast. Stem Cell Reports *15*, 1301–1316.

Sharkey, A., Jones, D.S., Brown, K.D., and Smith, S.K. (1992). Expression of messenger RNA for kit-ligand in human placenta: localization by in situ hybridization and identification of alternatively spliced variants. Mol. Endocrinol. *6*, 1235–1241.

Sharkey, A.M., Jokhi, P.P., King, A., Loke, Y.W., Brown, K.D., and Smith, S.K. (1994). Expression of C-kit and kit ligand at the human maternofetal interface. Cytokine *6*, 195–205.

Shi, Y., Desponts, C., Do, J.T., Hahm, H.S., Schöler, H.R., and Ding, S. (2008). Induction of Pluripotent Stem Cells from Mouse Embryonic Fibroblasts by Oct4 and Klf4 with Small-Molecule Compounds. Cell Stem Cell *3*, 568–574.

Silva, J., Barrandon, O., Nichols, J., Kawaguchi, J., Theunissen, T.W., and Smith, A. (2008). Promotion of reprogramming to ground state pluripotency by signal inhibition. PLoS Biol. *6*, e253.

Sim, Y.-J., Kim, M.-S., Nayfeh, A., Yun, Y.-J., Kim, S.-J., Park, K.-T., Kim, C.-H., and Kim, K.-S. (2017). 2i Maintains a Naive Ground State in ESCs through Two Distinct Epigenetic Mechanisms. Stem Cell Reports *8*, 1312–1328.

Simmons, D.G., and Cross, J.C. (2005). Determinants of trophoblast lineage and cell subtype specification in the mouse placenta. Dev. Biol. *284*, 12–24.

Simmons, D.G., Fortier, A.L., and Cross, J.C. (2007). Diverse subtypes and developmental origins of trophoblast giant cells in the mouse placenta. Dev. Biol. *304*, 567–578.

Soncin, F., and Parast, M.M. (2020). Role of Hippo signaling pathway in early placental development. Proc. Natl. Acad. Sci. *117*, 20354 LP – 20356.

Song, J., Teplova, M., Ishibe-Murakami, S., and Patel, D.J. (2012). Structure-based mechanistic insights into DNMT1-mediated maintenance DNA methylation. Science *335*, 709–712.

Sozen, B., Cox, A.L., De Jonghe, J., Bao, M., Hollfelder, F., Glover, D.M., and Zernicka-Goetz, M. (2019). Self-Organization of Mouse Stem Cells into an Extended Potential Blastoid. Dev. Cell *51*, 698-712.e8.

Stadtfeld, M., Maherali, N., Breault, D.T., and Hochedlinger, K. (2008). Defining Molecular Cornerstones during Fibroblast to iPS Cell Reprogramming in Mouse. Cell Stem Cell *2*, 230–240.

Strauss, J.F., Kido, S., Sayegh, R., Sakuragi, N., and Gåfvels, M.E. (1992). The cAMP signalling system and human trophoblast function. Placenta *13*, 389–403.

Suetake, I., Shinozaki, F., Miyagawa, J., Takeshima, H., and Tajima, S. (2004). DNMT3L Stimulates the DNA Methylation Activity of Dnmt3a and Dnmt3b through a Direct Interaction *. J. Biol. Chem. *279*, 27816–27823.

Suman, P., Malhotra, S.S., and Gupta, S.K. (2013). LIF-STAT signaling and trophoblast biology. JAK-STAT *2*, e25155.

Sun, J., Pedersen, M., and Rönnstrand, L. (2009). The D816V mutation of c-Kit circumvents a requirement for Src family kinases in c-Kit signal transduction. J. Biol. Chem. *284*, 11039–11047.

Takahashi, Y., Carpino, N., Cross, J.C., Torres, M., Parganas, E., and Ihle, J.N. (2003). SOCS3: an essential regulator of LIF receptor signaling in trophoblast giant cell differentiation. EMBO J. *22*, 372–384.

Takahashi, K., Tanabe, K., Ohnuki, M., Narita, M., Ichisaka, T., Tomoda, K., and Yamanaka, S. (2007). Induction of Pluripotent Stem Cells from Adult Human Fibroblasts by Defined Factors. Cell *131*, 861–872.

Takahashi, Y., Takahashi, M., Carpino, N., Jou, S.-T., Chao, J.-R., Tanaka, S., Shigeyoshi, Y., Parganas, E., and Ihle, J.N. (2008). Leukemia Inhibitory Factor Regulates Trophoblast Giant Cell Differentiation via Janus Kinase 1-Signal Transducer and Activator of Transcription 3-Suppressor of Cytokine Signaling 3 Pathway. Mol. Endocrinol. *22*, 1673–1681.

Takashima, Y., Guo, G., Loos, R., Nichols, J., Ficz, G., Krueger, F., Oxley, D., Santos, F., Clarke, J., Mansfield, W., et al. (2014). Resetting Transcription Factor Control Circuitry toward Ground-State Pluripotency in Human. Cell *158*, 1254–1269.

Tanabe, S. (2015). Signaling involved in stem cell reprogramming and differentiation. World J. Stem Cells *7*, 992–998.

Tanaka, S., Kunath, T., Hadjantonakis, A.-K., Nagy, A., and Rossant, J. (1998). Promotion of Trophoblast Stem Cell Proliferation by FGF4. Science *282*, 2072 LP – 2075.

Theunissen, T.W., Powell, B.E., Wang, H., Mitalipova, M., Faddah, D.A., Reddy, J., Fan, Z.P., Maetzel, D., Ganz, K., Shi, L., et al. (2014). Systematic Identification of Culture Conditions for Induction and Maintenance of Naive Human Pluripotency. Cell Stem Cell *15*, 471–487.

Thomson, J.A., Itskovitz-Eldor, J., Shapiro, S.S., Waknitz, M.A., Swiergiel, J.J., Marshall, V.S., and Jones, J.M. (1998). Embryonic Stem Cell Lines Derived from Human Blastocysts. Science *282*, 1145 LP – 1147.

Tian, Q., Frierson, H.F., Krystal, G.W., and Moskaluk, C.A. (1999). Activating c-kit gene mutations in human germ cell tumors. Am. J. Pathol. *154*, 1643–1647.

Tucker, K.L., Wang, Y., Dausman, J., and Jaenisch, R. (1997). A transgenic mouse strain expressing four drug-selectable marker genes. Nucleic Acids Res. *25*, 3745–3746.

Turco, M.Y., Gardner, L., Kay, R.G., Hamilton, R.S., Prater, M., Hollinshead, M.S., McWhinnie, A., Esposito, L., Fernando, R., Skelton, H., et al. (2018). Trophoblast organoids as a model for maternal–fetal interactions during human placentation. Nature *564*, 263–281.

Turco, M.Y., and Moffett, A. (2019). Development of the human placenta. Dev. *146*, dev164328.

Waddington, C.H. (2012). The epigenotype. 1942. Int. J. Epidemiol. *41*, 10–13.

Wamaitha, S.E., del Valle, I., Cho, L.T.Y., Wei, Y., Fogarty, N.M.E., Blakeley, P., Sherwood, R.I., Ji, H., and Niakan, K.K. (2015). Gata6 potently initiates reprograming of pluripotent and differentiated cells to extraembryonic endoderm stem cells. Genes Dev. *29*, 1239–1255.

Ware, C.B., Nelson, A.M., Mecham, B., Hesson, J., Zhou, W., Jonlin, E.C., Jimenez-Caliani, A.J., Deng, X., Cavanaugh, C., Cook, S., et al. (2014). Derivation of naive human embryonic stem cells. Proc. Natl. Acad. Sci. U. S. A. *111*, 4484–4489.

Wei, S., Zou, Q., Lai, S., Zhang, Q., Li, L., Yan, Q., Zhou, X., Zhong, H., and Lai, L. (2016). Conversion of embryonic stem cells into extraembryonic lineages by CRISPR-mediated activators. Sci. Rep. *6*, 19648.

Wen, F., Tynan, J.A., Cecena, G., Williams, R., Múnera, J., Mavrothalassitis, G., and Oshima, R.G. (2007). Ets2 is required for trophoblast stem cell self-renewal. Dev. Biol. *312*, 284–299.

Wen, J., Wu, J., Cao, T., Zhi, S., Chen, Y., Aagaard, L., Zhen, P., Huang, Y., Zhong, J., and Huang, J. (2021). Methylation silencing and reactivation of exogenous genes in lentivirus-mediated transgenic mice. Transgenic Res. *30*, 63–76.

Werling, U., and Schorle, H. (2002). Transcription factor gene AP-2 gamma essential for early murine development. Mol. Cell. Biol. *22*, 3149–3156.

Whigham, C.-A., MacDonald, T.M., Walker, S.P., Pritchard, N., Hannan, N.J., Cannon, P., Nguyen, T.V., Hastie, R., Tong, S., and Kaitu'u-Lino, T.J. (2019). Circulating GATA2 mRNA is decreased among women destined to develop preeclampsia and may be of endothelial origin. Sci. Rep. *9*, 235.

Xiang, Z., Kreisel, F., Cain, J., Colson, A., and Tomasson, M.H. (2007). Neoplasia driven by mutant c-KIT is mediated by intracellular, not plasma membrane, receptor signaling. Mol. Cell. Biol. *27*, 267–282.

Yagi, R., Kohn, M.J., Karavanova, I., Kaneko, K.J., Vullhorst, D., DePamphilis, M.L., and Buonanno, A. (2007). Transcription factor TEAD4 specifies the trophectoderm lineage at the beginning of mammalian development. Development *134*, 3827–3836.

Yamanaka, S. (2020). Pluripotent Stem Cell-Based Cell Therapy - Promise and Challenges. Cell Stem Cell *27*, 523-531.

Yan, J., Tanaka, S., Oda, M., Makino, T., Ohgane, J., and Shiota, K. (2001). Retinoic acid promotes differentiation of trophoblast stem cells to a giant cell fate. Dev. Biol. *235*, 422–432.

Yang, Y., Liu, B., Xu, J., Wang, J., Wu, J., Shi, C., Xu, Y., Dong, J., Wang, C., Lai, W., et al. (2017). Derivation of Pluripotent Stem Cells with In Vivo Embryonic and Extraembryonic Potency. Cell *169*, 243-257.e25.

Yasuda, T., and Kurosaki, T. (2008). Regulation of lymphocyte fate by Ras/ERK signals. Cell Cycle *7*, 3634–3640.

Ying, Q.-L., Wray, J., Nichols, J., Batlle-Morera, L., Doble, B., Woodgett, J., Cohen, P., and Smith, A. (2008). The ground state of embryonic stem cell self-renewal. Nature *453*, 519–523.

Zeuner, A., Francescangeli, F., Signore, M., Venneri, M.A., Pedini, F., Felli, N., Pagliuca, A., Conticello, C., and De Maria, R. (2011). The Notch2-Jagged1 interaction mediates stem cell factor signaling in erythropoiesis. Cell Death Differ. *18*, 371–380.

Zhang, S., Chen, T., Chen, N., Gao, D., Shi, B., Kong, S., West, R.C., Yuan, Y., Zhi, M., Wei, Q., et al. (2019). Implantation initiation of self-assembled embryo-like structures generated using three types of mouse blastocyst-derived stem cells. Nat. Commun. *10*, 496.

Zhao, Y., Zhao, T., Guan, J., Zhang, X., Fu, Y., Ye, J., Zhu, J., Meng, G., Ge, J., Yang, S., et al. (2015). A XEN-like State Bridges Somatic Cells to Pluripotency during Chemical Reprogramming. Cell *163*, 1678–1691.